The Role of Cell Type-Specific Tumour Necrosis Factor in Protective Immunity against Neurotuberculosis

NGIAMBUDULU MBANDU FRANCISCO

Thesis Presented for the Degree of

DOCTOR OF PHILOSOPHY

In the Division of Immunology

Department of Clinical Laboratory Sciences

Faculty of Health Sciences

UNIVERSITY OF CAPE TOWN

November - 2013

DECLARATION

I, **Ngiambudulu Mbandu Francisco** hereby declare that the work on which this thesis is based is my own unaided work, both in concept and execution, and that apart from the normal guidance from my supervisor. I have received no assistance except as stated below, and neither the substance nor any part of the above thesis has been submitted in the past, or is to be submitted for a degree at this University or at any other university, except as stated below.

I empower the university to reproduce for the purpose of research either the whole or any portion of the contents in any manner whatsoever.

Signature: Signed by candidate ……..…….

Date: …….……..……

DEDICATION

To my parents for raising me

What God out of His mercy does bestow on mankind there is none can withhold: what He does withhold there is none can grant apart from Him: and He is the Exalted in power, Full of wisdom. Qur'an 35:2

ACKNOWLEDGEMENTS

It is my pleasant duty to express gratitude to all those who have made it possible in many ways for me to complete this thesis.

First and foremost I am grateful to the **almighty God** for his blessings, and to my **family members** for their love.

I sincere acknowledge with deep gratitude the motivation and help I received from my Supervisor, **Dr. Muazzam Jacobs, Ph.D**, Associate Professor in the Division of Immunology, University of Cape Town. His experience coupled with up-to-date knowledge in the field was a great source of motivation for the progress of the thesis.

It is with a deep sense of gratitude and indebtedness I acknowledge the valuable help from my darling friend **Diana Kangwa**.

I wish to record my sincere thanks to **Dr. Roanne Keeton, Ph.D**, post-doctorate fellow in the Division of Immunology for the manuscript review. I am indeed grateful to **Dr. Nasiema Allie, Ph.D** and **Dr. Nai-Jen Hsu, Ph.D**, post-doctorate fellows, **Ms. Boipelo Sebesho** and **Ms. Philippa Randall**, PhD students in the Division of Immunology for their helps and motivations.

My sincere thanks to **Dr. Lauriston Kellaway, Ph.D**, Professor and Head in the Department of Human biology for his advices and motivations, and **Dr. Dhiren Govender, M.Med,** Professor and Head of Division of Anatomical Pathology for his histopathology expertise.

I am indebted to the **staffs** of Research Animal Facility of the Faculty of Health Sciences at the University of Cape for their assistances in breeding mice strains used in this study, and **Dr. Berth Mohr, Ph.D**, Director of Research Animal Facility for reviewing my animal ethics application before submitting to the animal ethics committee.

I extend my gratitude to **Mrs Lizette Fick** and **Mrs Marilyn Tyler** for their skilful assistance with histology, to **Mr. Faried Abbass** for his technical support, and to my **colleagues** in the Division of Immunology for their endless assistance.

TABLE OF CONTENT

LIST OF FIGURES

LIST OF TABLES

LIST OF ABBREVIATIONS

AFB	Acid Fast Bacilli
ANOVA	Analysis of Variance
APC	Antigen Presenting Cell
APES 3-	Aminopropyltriethoxysilane
BBB	Blood-Brain Barrier
B220	B-cell isoform of 220 kDa
BCG	Bacille Calmette-Guérin
BD	Beckon and Dickinson
BSA	bovine Serum Albumin
bp	Base pair
CD	Cluster of Differentiation
CDC	Centres for Disease Control and prevention
cfu	Colony-forming units
CNS	Central Nervous System
Cre	Cyclization recombination
CSF	Cerebrospinal fluid
DCs	Dendritic cells
DD	Death domaine
DNA	Deoxyribonucleic acid
dNTP	Deoxyribonucleotide triphosphate
EDTA	Ethylenediaminetetraacetic acid
ELISA	Enzyme-linked immunosorbent assay
ESAT-6	Early secreted antigen 6
FACS	Fluorescence activated cell sorting
FCS	Fetal calf serum
FcR	Receptor for Fc portion of immunoglobulin
FITC	Flourescein isothiocyanat
Fo B	Follicular B cell
HEPES	(2-hydroxyethyl)-1-piperazineethanesulfonic acid
HIV	Human immunodeficiency virus
IFN-γ	Interferon gamma

IgM	Immunoglobulin M
IL	Interleukin
iNOS	Inducible nitric oxide synthase
JNKs	c-Jun N-terminal kinases
LAM	Leukocyte adhesion molecule
LTBI	Latent tuberculosis infection
MCP-1	Monocyte chemoattractant protein-1
MDR	Multidrug resistant
MFI	Mean fluorescence intensity
MHC	Major histocompatibility complex
MIP-1α	Macrophage inflammatory protein-1 alpha
MRC	Medical Research Council
M. tuberculosis	*Mycobacterium tuberculosis*
MyD88	Myeloid differentiation primary response 88
Na_2EDTA	Ethylenediaminetetra-acetic acid disodium salt
ND	Not detected
NF-κb	Nuclear factor-kappa B
NK	Natural Killer
NO	Nitric oxide
n	Sample number
NOS	Nitric oxide synthase
OADC	Oleic-acid-albumin dextrose catalase
PAMPs	Pathogen-associated molecular patterns
PBS	Phosphate-buffered saline
PCR	Polymerase chain reaction
PE	R-phycoerythrin
p.i	Post-infection
PNPP	P-Nitrophenol-phosphate
PRRs	Pattern recognition receptors
RANTES	Regulated on activation, normal, T cell expressed and secreted
RBC	Red blood cells
RNI	Reactive nitrogen intermediates
SD	Standard deviation

SDS	Sodium dodecyl sulfate
SPF	Specific pathogen free
sTNF	Soluble tumour necrosis factor
Syn	Synapsin
TACE	Tumour necrosis factor alpha converting enzyme
TB	Tuberculosis
TBE	Tris borate ethylene diamino tetra acetic acid
TBM	Tuberculous meningitis
TCR	T-cell receptor
tmTNF	Transmembrane tumour necrosis factor
TNF	Tumour necrosis factor
TNFR	Tumour necrosis factor receptor
USA	United Stated of America
VCAM	Vascular cell adhesion molecule
WHO	World Health Organization
WT	Wild type

UNITS OF MEASUREMENT

%	Percentage
°C	Degree celsius
µl	Microlitre
µM	Micromolar
bp	Basepair
cfu/ml	Colony forming unit per Millilitre
g	Gram
h	Hour
max	Maximum
mg/l	Milligram per litre
ml	Millilitre
mM	Millimolar
ng	Nanogram
pg	Picogram
pH	Negative logarithm of hydrogen ion concentration

ABSTRACT

Neurotuberculosis is the most severe form of extra-pulmonary tuberculosis, characterised by the formation of rich foci a brain form of granulomas, and tuberculous meningitis. Granulomas contain mycobacteria by recruitment of immune cells that surround the bacteria. The cytokine tumour necrosis factor has been found to be involved in the recruitment of the immune cells and structure maintenance of granulomas. Tumour necrosis factor is a multifunctional proinflammatory cytokine which play a critical role in the initial and long-term host immune protection against *Mycobacterium tuberculosis* (*M. tuberculosis*) infection. This cytokine is synthesised by several cell types of hematopoetic origin, such as microglia/macrophages, neutrophils, dendritic cells and lymphocytes, and non-hematopoetic origin such as astrocytes and neurons. During neurotuberculosis, excess of tumour necrosis factor has been implicated in persisting hyperinflammation, however, deficiency of tumour necrosis factor lead to uncontrolled bacterial growth; both phenomena causing necrotic lysis. Thus, a need exists to investigate the contribution of tumour necrosis factor by specific cell types in the control of cerebral *M. tuberculosis* infection and its protective immune response. In this study, we investigated the role of tumour necrosis factor derived from neurons, microglia/macrophages, neutrophils, $CD4^+$ and $CD8^+$ T cells in host immunity against *M. tuberculosis;* using an experimental murine model with cell type-specific gene targeting. We found that mice deficient for tumour necrosis factor in neurons ($NsTNF^{-/-}$), as well as from microglia/macrophages and neutrophils ($M\text{-}TNF^{-/-}$) are not susceptible to *M. tuberculosis* infection with a phenotype similar to wild type mice. Interestingly, mice with ablation of tumour necrosis factor in myeloid (microglia/macrophages, neutrophils) and $CD4^+$ and $CD8^+$ T cells ($MT\text{-}TNF^{-/-}$) were highly susceptible to *M. tuberculosis* infection with a phenotype similar to that of complete deficient tumour necrosis factor ($TNF^{-/-}$) mice, which succumbed by 21 days post-infection. Thus, it seems that the resistance observed in $M\text{-}TNF^{-/-}$ mice may be caused by the compensation of T cell-derived TNF whose function appeared as non-redundant. Impaired protective immunity observed in $MT\text{-}TNF^{-/-}$ and $TNF^{-/-}$ mice were related to alteration of cytokines and chemokines, and also to reduce antigen response and B cells IgM secretion. Our data suggest that neurons as well as microglia/macrophages and neutrophils derived tumor necrosis factor have a very limited role in protective cerebral immune responses. In $MT\text{-}TNF^{-/-}$ mice, TNF mediated protective immunity against cerebral *M. tuberculosis* infection requires primarily T cell-derived TNF as opposed to macrophage/neutrophil derived TNF. These findings may inform the development of immunomodulatory therapy strategies against neurotuberculosis.

CHAPTER I

INTRODUCTION

1.1 *Mycobacterium tuberculosis* complex

1.1.1 Morphology and physiology

Mycobacterium tuberculosis (*M. tuberculosis*), previously known as the *tubercle bacillus,* was first discovered by Robert Koch on 24th March 1882. *M. tuberculosis* is an intracellular rod shaped bacteria. This gram-positive bacterial species is found in the genus *Mycobacterium* and demonstrates the acid-fast staining characteristic. It is the causative agent of most cases of human tuberculosis, including neurotuberculosis (Springer *et al.,* 2001). Tuberculosis is a primary infectious disease caused by the members of *M. tuberculosis* complex (*Mycobacterium africanum, Dassie bacillus, Oryx bacillus, Seal bacillus, Mycobacterium microti, Mycobacterium caprae and Mycobacterium bovis*). *Mycobacterium bovis,* is the causal agent of TB in cattle, while the *Mycobacterium africanum* cause human pulmonary tuberculosis in West and Central Africa, and has been prevalent since ancient times (Girard *et al.,* 2005 and Demers *et al.,* 2010). *Mycobacterium tuberculosis* is nonmotile, obligate aerobe that does not form spores. The cell wall of *M. tuberculosis* contains peptidoglycan similar to that of other Gram-positive organisms, to which many branched-chain polysaccharides, proteins, and lipids are attached (Ryan *et al.,* 2010). Porins and other proteins are found through the cell wall (Kartmann, 1999). Of particular importance is the presence of long-chain fatty acids called mycolic acids (for which the mycobacteria are named) and arabinogalactan, a lipid polysaccharide complex extending from the plasma membrane to the surface. These elements give the mycobacteria a cell wall with unusually high lipid content (more than 60% of the total cell wall mass), which accounts for many of their biological characteristics (Ryan *et al.,* 2010). A schematic representation of the *M. tuberculosis* cell wall is illustrated in Figure 1.1. The acid-fast staining characteristic is the most frequently observed of these features. It does not retain any bacteriological stain due to high lipid content in its cell wall.

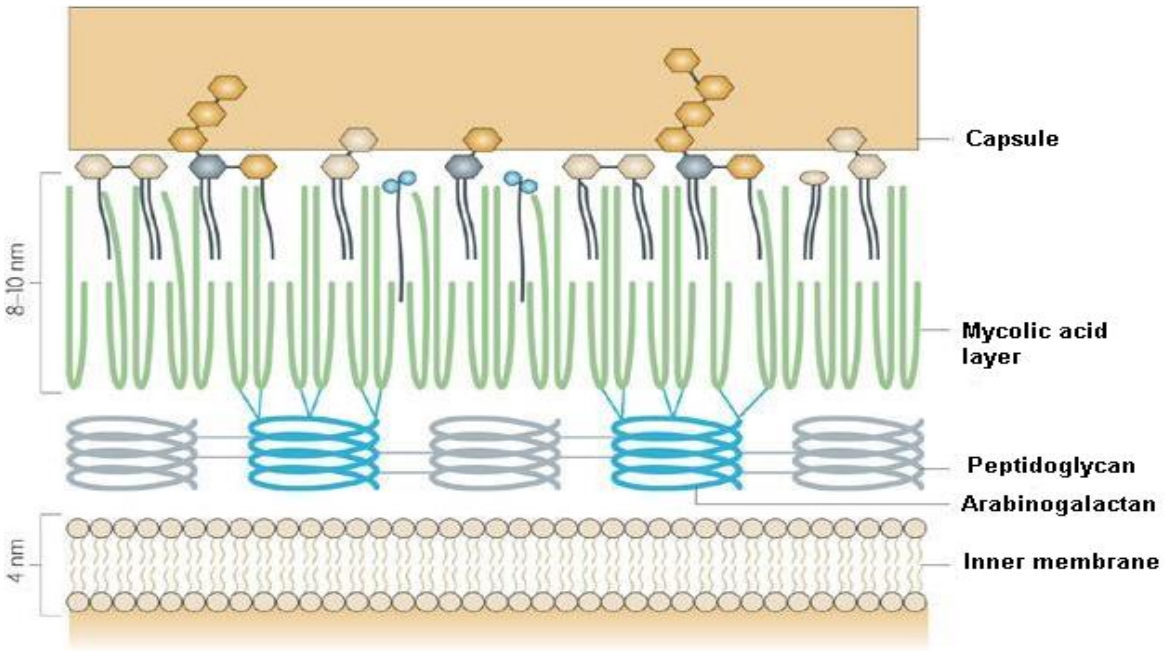

Figure 1.1: Schematic representation of the *M. tuberculosis* cell wall (adapted from Abdallah *et al.*, 2007).

The *M. tuberculosis* bacillus divides approximately every 15-20 hours, This is extremely slow compared to other bacteria, which tend to have division times measured in minutes (such as *Escherichia coli*, which can divide every 20 minutes). Their slow growth is due to the fact that they have a hydrophobic cell surface, which causes them to clump and limits permeability of nutrients into the cell (Ryan *et al.,* 2010). When in the lungs, *M. tuberculosis* are taken up by the alveolar macrophages. These, after activation, produce effector molecules such as TNF and NO which restricts the growth of *M. tuberculosis*. Despite the antimicrobial effects produced by the host (macrophage), in most cases, they are unable to digest *M. tuberculosis*. Nitrate can be produced by oxidation of nitric oxide and has been found to be the source of nitrogen for bacteria within the human host (Niederweis, 2008). Nitrate reduction by *M. tuberculosis* is regulated by controlling the transport of nitrate into the cell by the NarK2 gene (Niederweis, 2008). It is therefore proposed that the NarK2 gene senses the redox state of the cell, probably by monitoring the flow of electrons to cytochrome oxidase, and adjusts its activity so that nitrate is transported under reducing form, but not under oxidizing (Sohaskey, 2003). Inhibition of nitrate transport by oxygen has been demonstrated in other bacteria model (Moir & Wood, 2001).

It also has been suggested that the fusion of the phagosome with a lysosome may be prevented by the *M. tuberculosis* cell wall, which blocks the bridging of endosomal and phagosomal membrane-tethering molecule, called early endosomal autoantigen 1 (Fratti *et al.,* 2001 and Fratti *et al.,* 2003). However, this blockage does not prevent the fusion of vesicles filed with nutrients. As a consequence, the *M. tuberculosis* multiplies unchecked inside the macrophage (Li *et al.,* 2010). *M. tuberculosis* carries the UreC gene, which prevents the phagosome from acidifying (Reyrat *et al.,* 1995). It produces an enzyme called alkyl hydroperoxide reductase, which is believed to be involved in protecting the organism against the oxidative stress induced by reactive oxygen species and reactive nitrogen species, encountered within the infected macrophage (Springer *et al.,* 2001). In addition, *M. tuberculosis* secrete early secretory antigenic target (ESAT-6) (Tsolaki *et al.,* 2013), which helps the mycobacterium to escape from the phagosome into cytosol. Also, it may inhibit the activation of NF-κB (nuclear factor kappa-light-chain-enhancer of activated B cells) through preventing interaction between MyD88 (myeloid differentiation primary response gene 88) and the downstream kinase of interleukin-1 receptor-associated kinase 4 (Pathak *et al.,* 2007 and Yu & Xie, 2012).

1.1.2 *Mycobacterium tuberculosis* genotype

The genome sequences of two virulent strains, *M. tuberculosis* H37Rv (a commonly used laboratory strain which has been subjected to *in vitro* passage) and the clinical strains such as CDC 1551, Beijing clinical isolates (CCDC5180 and CCDC5079) and Colombian clinical isolate UT205 are now publicly available (Cole *et al*., 1998; Valway *et al*., 1998; Zhang *et al.,* 2011 and Isaza *et al.,* 2012). One study has shown that the *M. tuberculosis* genotype influences the clinical disease phenotype, and that a significant interaction exists between host and mycobacterial genotypes for the development of tuberculosis disease (Nahid *et al.,* 2010). The *M. tuberculosis* CDC 1551 strain was clinical isolated, and was responsible for an outbreak of TB in a rural area of the USA in 1995 (Valway *et al*., 1998). The Beijing clinical isolates CCDC5180 and CCDC5079, and the recently isolated Colombian clinical isolate UT205 are associated with drug resistant-TB (Zhang *et al.,* 2011 and Saza *et al.,* 2012). The *M. tuberculosis* H37Rv strain was first isolated in 1905, and is used as reference strain. It is currently the most used strain in tuberculosis research. In addition, research has shown that this strain still maintains its virulence in animal models (Betts *et al.,* 2000). The two genomes

(the *M. tuberculosis* clinical strains and *M. tuberculosis* H37Rv strain) show 99% identity at the nucleotide level, but the strains display phenotypic differences which might be explained by changes at the protein expression level (Delcher *et al*., 1999). The strain size of the genome H37Rv comprises 4,411,529 base pairs, with 3959 genes of high guanine and cytosine content that is reflected in the biased amino-acid content of the proteins (Cole *et al.,* 1998). The difference between *M. tuberculosis* and other bacteria are in a large portion of coding capacity found in *M. tuberculosis*, which are dedicated to the production of enzymes that usually participate in lipolysis and lipogenesis and also to the newly found two families of glycine-rich proteins (Cole *et al.,* 1998).

1.1.3 Epidemiology of tuberculosis and neurotuberculosis

Neurotuberculosis will exist as long as the primary pulmonary infection exists and it is imperative to consider the epidemiology of TB. Global control of tuberculosis is far from complete (Lönnroth *et al.,* 2010). Important to consider is that TB also exists in a latent form, latent TB infection (LTBI) is the presence of *M. tuberculosis* in an individual without clinical, imaging, or microbiologic evidence of active disease (Sharma *et al.,* 2012). This burden is distributed largely among under-resourced countries (Sharma *et al.,* 2012). Latent TB prevalence rates have been noted for up to 79%, with an annual risk of developing TB infection ranging from 0.5% to 14.3% among healthcare workers in resource limited countries (WHO, 2012). In the general population, the lifetime risk of progression from LTBI to active disease is about 5% to 10%; in the immunocompromised individuals (e.g. those with HIV), this rises to 30% (annual risk, 10%) (Selwyn *et al.,* 1989). The pathogenic state of bacterial infection and probability of reactivation depend on the balance between host immunity (Sharma *et al.,* 2012). Research has shown that primates, mouse, rabbit and guinea pig are also susceptible to *M. tuberculosis* infection (Lurie *et al.,* 1952; Riley, 1957; Riley *et al.,* 1959; Rhoades *et al.,* 1997; Flynn *et al.,* 2003 and Dannenberg, 2006). Research has also shown that *Mycobacterium bovis (M. bovis)* may cause bovine tuberculosis, a highly infectious disease in cattle, and one of the biggest challenges facing the cattle farming industry today (O'Reilly & Daborn, 1995). *M. bovis* may also infect and cause TB in goats, pigs, deer, badgers, camelids (llamas and alpacas), dogs and cats, as well as many other mammals (O'Reilly & Daborn, 1995; Smith *et al.,* 2009 and Brooks-Pollock *et al.* 2013). Transmission of infection within and between species is mainly by the airborne route (O'Reilly & Daborn, 1995).

Study has also shown that other form bacterium Mycobacterium such as *Mycobacterium bovis* (*M. bovis*) may cause Bovine tuberculosis, which is an highly infectious disease of cattle, and one of the biggest challenges facing the cattle farming industry today (O'Reilly & Daborn,1995). *M. bovis* may also infect and cause TB in goats, pigs, deer, badgers, camelids (llamas and alpacas), dogs and cats, as well as many other mammals (O'Reilly & Daborn 1995; Smith *et al.,* 2009 and Brooks-Pollock *et al.* 2013). Transmission of infection within and between species is mainly by the airborne route (O'Reilly & Daborn 1995).

The ambiguity about the eradication of the burden of TB is supported by an analysis of predictors of TB case notification trends during the past few years (Dye, 2006). This analysis suggests that the variation in TB trends is more strongly associated with social, economic and biological factors. Social determinants of TB, such as food insecurity and malnutrition, poor housing and environmental conditions, and financial, geographic, and cultural barriers to health care access (Hargreaves *et al.,* 2011) are factor that increases susceptibility to TB. For example, poor ventilation and overcrowding in homes, workplaces, and communities increase the likelihood of uninfected individuals being exposed to TB infection (Hill *et al.,* 2006; Baker *et al.,* 2008 and Boccia *et al.,* 2009); poverty, malnutrition, and hunger may increase susceptibility to infection (Boccia *et al.,* 2009), disease (Pakasi *et al.,* 2009), and severity of clinical outcome (Van Lettow *et al.,* 2004).

Although rates of prevalence and death are falling globally, the rate of decline is not fast enough to meet the millennium development goal estimated targets to cut in half, TB prevalence and death rates by 2015 compared to 1990 levels (WHO, 2009; Lönnroth *et al.,* 2010). The World Health Organization (WHO), has reported the highest estimated incidence rate (356 per 100 000 population per year), but the majority of patients with tuberculosis live in the most populous countries of Asia such as Bangladesh, China, India, Indonesia, and Pakistan; which together account for almost half (48%) of the new cases that arise every year (Lönnroth *et al.,* 2010).

In the year 2007, South Africa was classified as the world's highest prevalence of human immunodeficiency virus (HIV) in incident TB cases (73%) and the second-highest prevalence of TB with 692/100,000 (WHO, 2009). In 2008, around 9.4 million new cases of tuberculosis have been reported, amongst these, 1.2 million of MDR-TB, and HIV continues to reinforce the epidemic, especially in Africa (Corbett *et al.,* 2003; Cheng, 2009; WHO, 2009 and Wright *et al.,* 2009). However, the long-term elimination target to reduce incidence of TB to less than one case per million by 2050, may not be achieved with existing technologies and factors (Lönnroth

et al., 2010). Recently, the emergence and spread of totally drug-resistant TB was reported in South Africa (Klopper *et al.,* 2013).

Some of these important factors are poor living and working conditions. These could be associated with high risk of TB transmission. In addition, other factors that are included in the host's defence impairment against TB infection are HIV infection, malnutrition, diabetes, smoking, indoor air pollution and alcohol abuse (Lönnroth *et al.,* 2009). Despite the 2.2% decrease reported in previous years, in 2011, approximately 8.7 million cases of new pulmonary TB cases were reported globally (Figure: 1.2) (WHO, 2012). In 2009, the Centres for Disease Control (CDC), USA, recorded that 4.7% of all TB were meningeal (CDC, 2010). Phypers *et al.,* (2006) reported that 1% of Canadian TB patients will develop neurotuberculosis. In Taiwan 1.5% of TB deaths were reported due to neurotuberculosis (Lu *et al.,* 2005). In countries with high TB prevalence children are most at risk of developing neurotuberculosis, however, in countries with low TB prevalence, it is immigrants from high prevalence areas who are most at risk (Katti, 2004 and Thwaites *et al.,* 2009).

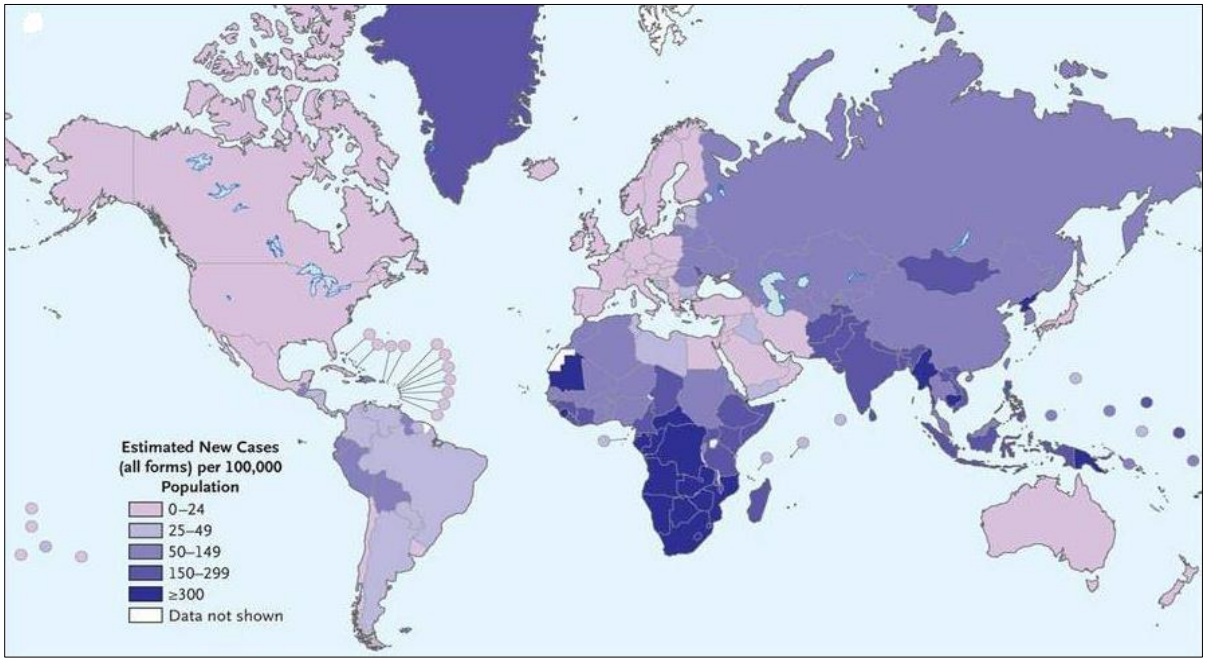

Figure 1.2: Estimated global incidence of tuberculosis in 2011 (Zumla *et al.,* 2013).

In 2009, 53 411 new cases were reported, and the South African Department of Health reported that tuberculosis meningitis (TBM) had the highest number of cases among all extrapulmonary TB cases (Department: Health, Republic of South Africa: "National tuberculosis management guidelines 2009" and http://www.doh.gov.za/docs/stats/2011/ SouthAfrican Tuberculosis Profile 2011 WHO.pdf). A recent study from Cameroon showed that 8% of patients with HIV infection developed neurotuberculosis, and 80% of these patients died (Luma *et al.,* 2013). Neurotuberculosis occurs in 1 to 10% of all cases of TB (Rock *et al.,* 2004 and Nelson & Zunt, 2011). Accurate figures for incidence and prevalence of neurotuberculosis are difficult to ascertain because the diagnosis is usually missed and data are largely unreported (WHO, 2010).

1.2 Neurotuberculosis

Neurotuberculosis is extrapulmonary tuberculosis caused by *M. tuberculosis*. Neurotuberculosis occurs when the immune response is weakened, mycobacteria disseminate from the primary site of infection, with continuous enlargement of the caseating granulomas in the lymph nodes. This phenomenon is referred to as progressive primary tuberculosis (TB) (Davis & Ramakrishnan, 2009). However, the enlarging nodes spread the infection progressively in two different ways: (i) Bronchus: occurs when there is creation of tuberculous bronchopneumonia, due to the erosion on an infected lymph node into a bronchus. Infection can spread by passing the bacilli from the bronchi of one lung into the opposite lung. This condition is known as galloping consumption. (ii) Blood vessel: occurs when the erosion of an infected lymph node into a blood vessel leads to lympho-heamatogenous spread of mycobacteria into many parts of the mammalian body, including the central nervous system (CNS) and leading to neurotuberculosis.

Neurotuberculosis is a devastating complication of disease caused by *M. tuberculosis*, it carries a high mortality with a high distressing level of neurological morbidity. It disproportionately affects children, especially in the developing world and immunocompromised individuals (Rock *et al.,* 2008). The mortality rate of neurotuberculosis is ~50%, and the majority of the survivors suffer permanent neurologic sequelae (Girgis *et al.,* 1991; Joosten *et al.,* 2000; Hosoglu *et al.,* 2002; Thwaites & Hien, 2005; Gijs *et al.,* 2009; Anderson *et al.,* 2010; Donald, 2010 and Pan *et al.,* 2012). Neurotuberculosis continues to exert a disturbing toll in developed and developing countries, despite the availability of anti-tuberculosis treatment (Thwaites & Hien, 2005). Current World Health Organization guidelines recommend a four-drug regimen for

an initial 2-month treatment period, followed by a two-drug regimen for 10 months. The total duration of treatment for neurotuberculosis is 12 months, which makes it more difficult for patients to adhere. In sub-Saharan African countries, due to the effects of HIV, tuberculosis is now the most common form of bacterial meningitis (Vinnard *&* Macgregor, 2009). However, in countries where a high incidence of tuberculosis is declared, tuberculosis meningitis is usually a disease of young children that develops three to six months after primary pulmonary infection with *M. tuberculosis* (Thwaites & Hien, 2005).

1.2.1 Pathogenesis of neurotuberculosis

Neurotuberculosis results from a rupture of subpial or subependymal foci which has been deposited earlier following lympho-hematogenous dissemination of *M. tuberculosis* from the primary pulmonary infection (Gijs *et al.,* 2009 and Misra *et al.,* 2010), or rupture of an adjacent parenchymal focus as suggested by Leonard & Des Prez (1990). It is now believed that the dissemination to the CNS is directly related to the pattern of blood flow, which usually spreads to the basal ganglia and cerebral hemispheres in adults, and to the cerebellum in children (Harris & Morris, 2007). The widely accepted hypothesis of Rich & McCordock (1933) reported that bacilli reach the CNS by a haematogenous route secondary to disease elsewhere in the body. Since the brain parenchyma and the meninges are physiologically and anatomically protected from the systemic circulation system by the blood brain barrier (BBB), the mechanisms by which the bacilli initially invade this barrier are not clear. It is believed that *M. tuberculosis* can cross the BBB as a free organism or *via* infected peripheral myeloid cells. However the latter hypothesis seems controversial, as myeloid cellular traffic is severely restricted into the CNS prior to invasion by the offending pathogen (Ransohoff *et al.,* 2003), however according to the proposed statement by Kivisäkk *et al.,* (2003) and Krumbholz *et al.,* (2007) lymphoid cells can in physiological state bypass the BBB by entering the subarachnoid space via the meningeal veins or the choroid plexus. The BBB poses a challenge for the treatment of neurotuberculosis. Isoniazid, the bactericidal agent easily crosses the BBB and achieves concentrations in the CSF similar to those in serum (Shin *et al.,* 1990). Although pyrazinamide can cross the BBB, its role in neurotuberculosis is uncertain given its bacteriostatic activity, is thought to be directed against older, resting bacilli (Phuapradit *et al.,* 1990). However, many other drugs such as rifampicin, ethambutol, and streptomycin cross the BBB poorly (Girgis *et al.,* 1976; Girgis *et al.,* 1978 and Nau *et al.,* 1992).

Rich & McCordock, (1933) proposed that CNS tuberculosis develops in two stages, at first, small tuberculous lesions (Rich's foci) develop in the CNS, either during the stage of bacteremia of the primary tuberculous infection or shortly afterwards. These initial tuberculous lesions localise either in the meninges, the subpial or subependymal surface of the brain or the spinal cord and may remain dormant for years after initial infection (Cambrea *et al.,* 2009). Second, rupture or growth of one or more of these small tuberculous lesions produces the development of various types of CNS tuberculosis (Dastur *et al.,* 1995 and Berger *et al.,* 1996). However, the specific incentive for rupture or the growth of Rich's foci is not yet well understood. It is suggested that immunological mechanisms also play a significant role (Cambrea *et al.,* 2009). Yet the type and size of lesions that result from the discharge of tuberculous bacilli into the cerebro-spinal fluid (CSF) depend on the number and virulence of the bacilli, as well as the immune response of the host (Garg, 1999). Studies have suggested that with a considerable inoculation or in the absence of an adequate cell-mediated immune response, the parenchymal cerebral tuberculous foci may develop into tuberculoma or tuberculous brain abscess (Dastur *et al.,* 1995). The parenchymal cerebral tuberculous foci, may lead to various pathogenesis, including hydrocephalus (Figure: 1.3). Which usually occur as a consequence of the obstruction of the basal cisterns, outflow of the fourth ventricle, or occlusion of the cerebral aqueduct. Hydrocephalus may lead to atrophy of the brain parenchyma (Trivedi *et al.,* 2009).

Neurotuberculosis is mainly characterized as a meningoencephalitis, as it affects both the meninges and the brain parenchyma together with its vasculature. Granulomatous inflammatory reaction in CNS caused by *M. tuberculosis* may involve the meninges, brain, spinal cord, and the bones covering the brain and spinal cord, and may manifest clinically depending on the specific location of the disease process as shown in Table: 1.1 (Trivedi *et al.,* 2009). During neurotuberculosis, there is a presence of thick, gelatinous exudates around the Sylvian fissures, basal cisterns, brainstem, and cerebellum. The basal gelatinous exudates of neurotuberculosis are more severe in the vicinity of the circle of Willis, and usually produce a vasculitis-like syndrome (Garg, 1999). These gelatinous exudates may contain leukocytes such as infiltrating macrophages, dendritic cells and lymphocytes, and also some erythrocytes. As the pathology progresses, lymphocytes and connective tissue elements predominate (Dastur *et al.,* 1995).

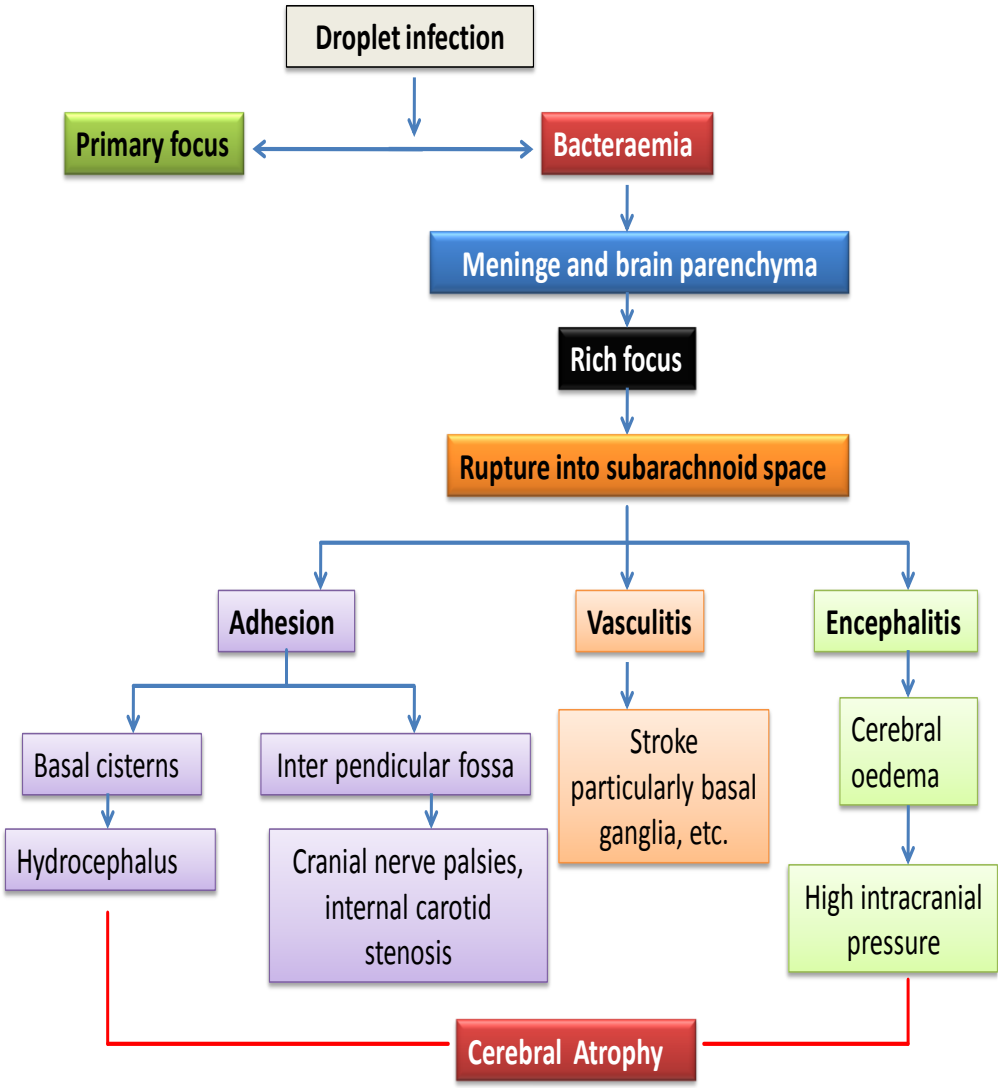

Figure 1.3: Pathogenesis of CNS lesions in neurotuberculosis (adapted from Rich & McCordock, 1933).

Table 1.1: Variable presentation of neurotuberculosis (adapted from Bano *et al.,* 2012)

Tubercular meningitis (TBM) & its complications ➢ Hydrocephalus ➢ Vasculitis causing infarction ➢ Cranial neuropathies
Pachymeningitis
Granulomatous basal meningitis
Parenchymal tuberculosis ➢ Parenchymal tuberculomas ➢ Tubercular abscesses ➢ Miliary tuberculomas ➢ Tubercular encephalopathy ➢ Focal tubercular cerebritis ➢ Tuberculoma en plaque
Spinal tuberculosis ➢ Tubercular Spondylitis (Pott's spine) ➢ Non-osseous spinal tuberculomas ➢ Tubercular arachnoiditis (myeloradiculopathy) ➢ Tubercular myelitis
CNS tuberculosis in HIV patients
Tubercular hypophysitis
Tuberculosis of calvarium and base of skull
Orbital tuberculosis
Tubercular otitis media & temporal bone tuberculosis

1.2.2 Immunobiology of neurotuberculosis

The majority of individuals in the general population who come in contact with *M. tuberculosis* never develop clinical disease (Comstock, 1982). This shows that the innate and adaptive immune response of the host in controlling *M. tuberculosis* infection is effective. Neuroturbeculosis often affects children and immunocompromised individuals due to the weakness of immune response in these individuals. The CNS was previously known as immunoprivileged. This vital system has a structure and function that is unique but, in common with all other systems. The CNS requires effective immune mechanisms to protect against

inflammation/infection. Failure to control these immune responses in the CNS can result in immunopathological disorders (Ransohoff & Engelhardt, 2012). Microglia cells are the resident myeloid cells of the CNS (Saijo & Glass, 2011). They constitute 5-20% of total glial cells in rodents, depending on the specific region of the CNS (Lawson *et al.,* 1990 and Perry *et al.,* 1991), In the human brain, microglia constitute 20% of all glial cells which comprises approximately 10% of all brain cells (Lawson *et al.,* 1990). Human microglial cells are effectively infected with *M. tuberculosis* and are possibly the principal cells target in the CNS (Peterson *et al.,* 1995 and Curto *et al.,* 2004). They are thought to be the first line of defence during neurotuberculosis (Curto *et al.,* 2004 and Rock *et al.,* 2004). The innate immune cells during *M. tuberculosis* infection expresses pattern recognition receptors (PRRs) that recognize various pathogens-associated molecular patterns (PAMPS) found on mycobacteria (Kleinnijenhuis *et al.,* 2011). Antigen presenting cells (APCs), including microglia as well as other myeloid cells, express these PRRs (Kratky *et al.,* 2011; Saijo & Glass, 2011 and Saijo *et al.,* 2013). Upon activation, they acquire an amoeboid-like morphologic condition (Kozlowski & Weimer, 2012). Following the recognition of PAMPs by microglia, PRR-mediated signalling induces the production of antimicrobial peptides (such as cathelicidin-related antimicrobial peptide (CRAMP)), cytokines (such as TNF and interleukin-1β (IL-1β)), chemokines (such as CCL2 also referred to as monocyte chemotactic protein-1 (MCP-1) that recruits cells of the immune response to the site of mycobacterial infection (Möller & Hoal, 2010), CCL3 also referred to as macrophage inflammatory protein 1 alpha (MIP-1 alpha) and CCL5 also referred to as regulated on activation, normal T cell expressed and secreted (RANTES)) and the production of reactive oxygen/nitrogen species (Male, 1996; Hasan *et al.,* 2005; Korbel *et al.,* 2008; Liu & Modlin, 2008 and Saijo & Glass, 2011). These molecules play key roles in innate immunity. Chemokines expressed by resident CNS cells during infection, enhance leukocyte trafficking into the CNS (Nygårdas *et al.,* 2000; Cardona *et al.,* 2003; Wilson *et al.,* 2010 and Ransohoff & Brown, 2012). Like peripheral antigen presenting cells (macrophages/neutrophils or DCs), activated microglia also up-regulate the expression of major histocompatibility class II (MHCII) molecules, to enable them to present antigens to T cells through the T cell receptor (TCR) (Rock *et al.,* 2004). In addition, activated microglia produce proinflammatory cytokines (such as IL-12) (Becher *et al.,* 1996; Park & Shin, 1996; Aloisi *et al.,* 1997 and Stalder *et al.,* 1997) to skew $CD4^+$ T cells into T helper 1 (Th1) cell. During this synapse, APCs (including microglia) produces various molecular markers of antigen presentation and activation such as MHCII as well as co-stimulatory molecules CD80 and CD86, also known as B7-1 and B7-2 respectively, and T cells upregulate stimulatory molecules such as IL-2, IL-6 or IFN-γ (Akiyama & McGeer, 1990 and Shrikant &

Benveniste, 1996). The above mentioned markers may also have both neurodegenerative and neuroprotective effects, through interactions with other cell types, including lymphocytes, astrocytes, and neurons (Rock *et al.,* 2004, 2008). Like other APCs, classically activated microglia contributes to both innate and adaptive immunity during neurotuberculosis.

The cytokine TNF has been shown to be critical in the neuropathogenesis of *M. tuberculosis* (Mardh *et al.,* 1983; Mastroianni *et al.,* 1997; Tsenova *et al.,* 1999; Curto *et al.,* 2004 and Tobin *et al.,* 2012). It also has been shown that TNF plays a major role in granuloma formation and the containment of mycobacterial infections (Kindler *et al.,* 1989 and Flynn *et al.,* 1995). The production of this pivotal cytokine in the CNS has been found to alter the BBB permeability and CSF leukocytosis in experimental bacterial meningitis (Ramilo *et al.,* 1990; Saez-Llorens *et al.,* 1990 and Saukkonen *et al.,* 1990). In addition, it has been implicated in fostering the progression of neurotuberculosis in a murine model (Tsenova *et al.,* 1999). However, Tobin *et al.,* (2012) show that TNF deficiency or TNF excess can both cause macrophage lysis, therefore placing *M. tuberculosis* in a permissive extracellular niche. It is therefore urgent and important to identify the cellular sources of TNF that contribute to the immunopathology, and the mechanisms by which TNF produces necrosis of infected cells or tissues. Cellular sources lineages are shown in (Figure 1.4).

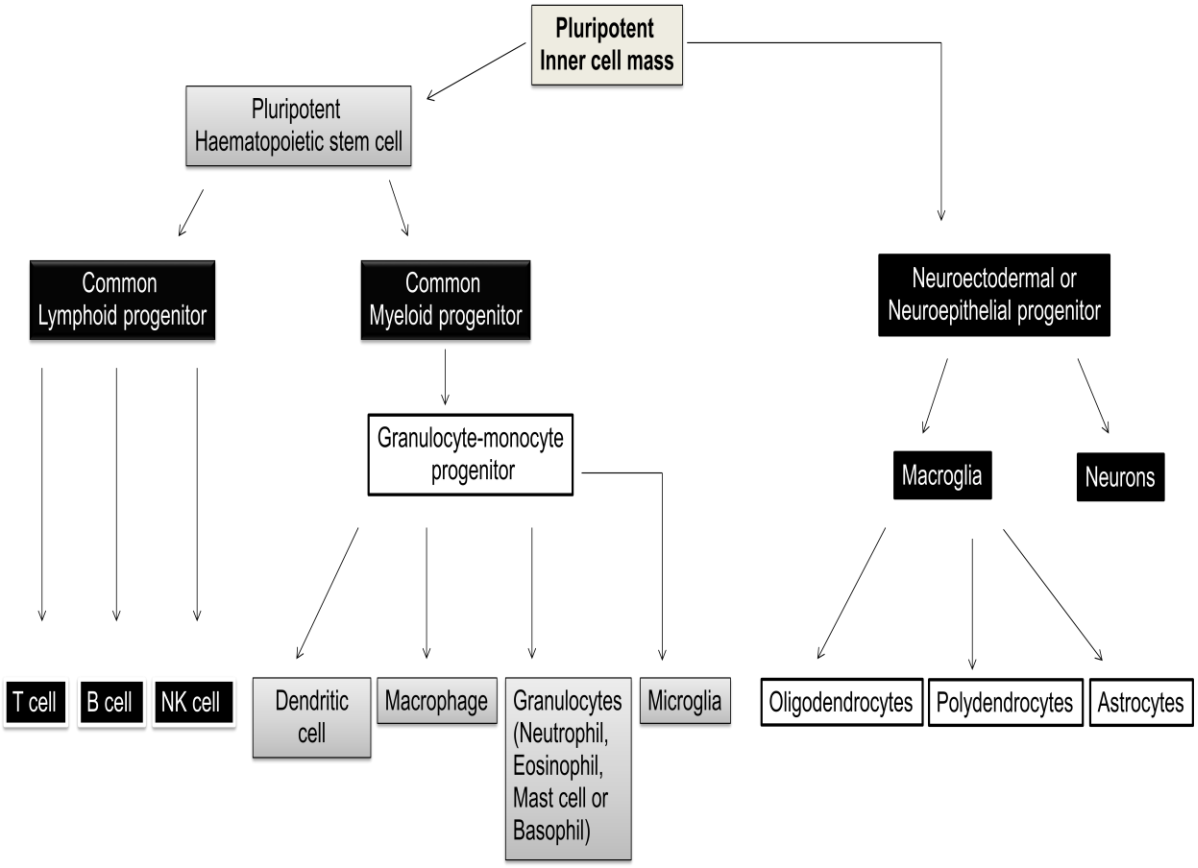

Figure 1.4: Lymphoid, myeloid and neuronal lineage. T cells, B cells and NK cells comprise lymphoid lineage. Only T cells and B cells are involved in adaptive immunity. Cells of the other progenitors take part in innate immunity.

1.3 Tumour necrosis factor

TNF is a pleiotropic cytokine that has been found to play a critical but incompletely understood role in immune response against intracellular bacterial pathogens including *M. tuberculosis* (Miller & Ernst, 2009). There are two types of TNF, alpha (α) and beta (β), but since the 1998 TNF congress, the names of TNF-α and TNF-β were changed to TNF and Lymphotoxin-α respectively (Tracey *et al.,* 2008 and Watanabe *et al.,* 2010). However, the nomenclature of TNF-α is still widely used and is synonymous with the term TNF used in this thesis. TNF occurs in two forms: (i) a type II transmembrane protein (tmTNF) and (ii) a soluble protein form (sTNF) (Locksley *et al.,* 1987; Birland *et al.,* 1992 and Tracey *et al.,* 2008). The

biology of tmTNF and sTNF is shown in Figure 1.5. The tmTNF is a precursor form of soluble TNF, and is initially expressed as a homotrimer of 26-kDa monomers tmTNF (Horiuchi *et al.,* 2010). Cleavage of the membrane form of TNF by the metalloproteinase TNF-alpha converting enzyme (TACE) (Itai *et al.,* 2001 and Mohan *et al.,* 2002), and by the protease cathepsin B (Guicciardi *et al.,* 2000 and Foghsgaard *et al.,* 2001) results in the generation of soluble TNF.

Thus, both mTNF and sTNF are biologically active (Horiuchi *et al.,* 2010). However, the relative amounts of each protein are collectively determined by the cell types involved, the inducing stimuli, the amounts of active TACE, the activation status of the cells, and the amounts of natural TACE inhibitors (Smookler *et al.,* 2006). The remaining tmTNF after cleavage with the metalloproteinase TACE is then, further processed by signal peptide peptidase-like 2B (SPPL2B), thereafter the intracellular domain is translocated into the nucleus and is thought to mediate cytokine production (Horiuchi *et al.,* 2010).

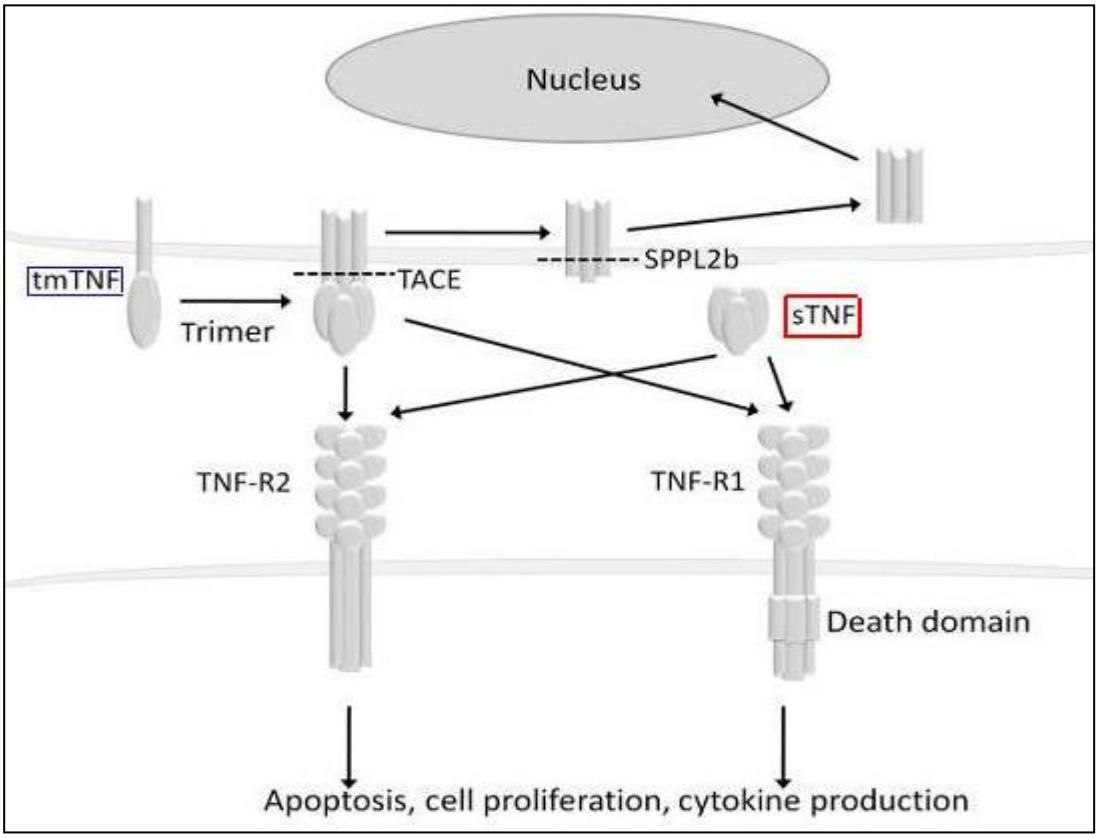

Figure 1.5: Biology of tmTNF and sTNF (adapted from Horiuchi *et al.,* 2010)

1.3.1 Tumour necrosis factor cell signalling in the CNS

Although this cytokine is mainly produced by macrophages, TNF is also produced by other cell types including adipose tissue, cardiac myocytes, endothelial cells, fibroblasts, neutrophils, dendritic cells, lymphoid cells, mast cells, and CNS cells (Ware *et al.,* 1992; Zhou & Tedder, 1995; Tracey *et al.,* 2008 and Chatzidakis & Mamalaki, 2010). In the CNS, the levels of TNF are approximately 100 pM (Santello *et al.*, 2011), and are thought to depend on local production mainly by microglia, astrocytes and neurons cells (Lee *et al.*,1993; Tchelingerian *et al.,* 1996; Bezzi *et al*., 2001; Bailey *et al.,* 2006; Stellwagen *et al.,* 2006 and Ransohoff & Cardona, 2010). However in pathological conditions, these cells undergo complex changes and significantly increase their capacity to synthesize proinflammatory TNF cytokines (Lue *et al.,* 2001 and Vezzani *et al.,* 2002). With the increased presence of infiltrating leukocytes in the CNS, the levels of TNF (tmTNF and sTNF) are further enhanced (Gregersen *et al.,* 2000). So far, the biological functions of tmTNF elicited by an outside-to-inside (reverse) signal have not completely been understood (Pattacini *et al.,* 2010). However, it has been proposed that outside-to-inside signalling mediated by tmTNF may have a great contribution to the pleiotropy of this proinflammatory cytokine and its enhancement of immune response (Eissner *et al,* 2004).

Currently, two types of TNF receptors (TNFRs) have been cloned and characterised, TNF receptor type 1 (TNFR1; CD120a; p55/60) and TNF receptor type 2 (TNFR2; CD120b; p75/80) with molecular weights of 55 kDa and 75 kDa respectively (Jacobsen *et al.,* 1994 and Ryan & Aksentijevich, 2009). These TNFRs are belonging to the TNF super family of receptors, they are structurally related and are present on the surface of numerous cells (Cubillas *et al.,* 2010).

TNF acts via either the low-affinity TNFR1 or high-affinity TNFR2 (Tartaglia & Goeddel, 1992). Binding of TNF to its two receptors, TNFR1 and TNFR2, results in recruitment of signal transducers that activate at least three distinct effectors. Via the complex signaling cascades and networks, these effectors lead to the activation of caspases and two transcription factors, activation Protein-1 and NF-KappaB (Nuclear Factor-Kappa B) (Baud & Karin, 2001). For TNFR 1, TRADD (TNFR-Associated Death Domain) protein, binds to TNFR1 and recruits FADD (Fas-Associated Death Domain), RAIDD (RIP-Associated ICH-1/CED-3-homologous protein with a Death Domain), MADD (MAPK Activating Death Domain) and RIP (Receptor-Interacting Protein) (Haider & Knöfler, 2009). The binding of TRADD and FADD to TNFR1 may lead to the recruitment, oligomerization, and activation of caspase 8. Activated caspase 8 subsequently initiates a proteolytic cascade that includes other caspases (caspases 3, 6 and 7)

and ultimately induces apoptosis. Caspase 8 also cleaves BID (BH3 Interacting Death Domain). The tBID (Truncated BID) disrupts the outer mitochondrial membrane to cause release of the pro-apoptotic factors CytoC (Cytochrome-C). CytoC that is released from the intermembrane space binds to APAF1 (Apoptotic Protease Activating Factor-1), which recruits caspase 9 and in turn can proteolytically activate caspase 3. The protein kinase RIP2 is related to RIP that is a component of TNFR1 which mediates the recruitment of caspase death proteases. It has been also found that TRAF2 (TNF Receptor-Associated Factor-2) is implicated in the activation of two distinct pathways that leads to the activation of activation protein-1 via the JNK (Jun NH2-terminal Kinase), MEKK (MEK Kinase), p38 and, together with RIP, NF-KappaB activation, via the NIK (NF-Kappa B-Inducing Kinase) (Baud *et al.,* 2001; Micheau *et al.,* 2003; Varfolomeev *et al.,* 2004 and Blackwell *et al.,* 2009). TNF has been shown to activate MAPKs (Mitogen Activated Protein Kinases). The TNF superfamily receptors typically induce both NF-κB and JNK activation by recruiting the TRAF2 signal transduction protein to their cytoplasmic domain (Adrian *et al.,* 2005). TNFR2 however, is a poor activator of these signaling pathways despite its high TRAF2 binding capability (Adrian *et al.,* 2005). Although, TNFR2 does not have a death domain (DD), it can mediate signalling through TRAFs, by sharing its signal effects with activated c-Jun N-terminal kinase (JNKs) molecules (Haider & Knöfler, 2009). TNFR2 expression is highly regulated and primarily found on cells of the immune system,nonetheless it is also expressed on endothelial and neurological tissues (Beltinger *et al.,* 1996 and Richter *et al.,* 2012). TNFR2 is efficiently activated only by mTNF, despite binding sTNF with high affinity (Grell *et al.,* 1995 and Brambilla *et al.,* 2011). Thus, mTNF-mediated signaling occurs in a juxtacrine fashion through intercellular signaling, typical of TNF responses such as cytotoxicity (Perez *et al.,* 1990) or lymphoïd T cell activation (Aversa *et al.,* 1993), while sTNF is able of promoting paracrine and systemic functions through TNFR1 (Grell *et al.,* 1995; Brambilla *et al.,* 2011 and Richter *et al.,* 2012).

TNFR1 is a large polypeptide with an extracellular domain, expressed on the cell surface of most cells and tissues. It consists of 4 cysteine-rich domains, an intracellular DD, and a transmembrane domain (Ryan & Aksentijevich, 2009). When, TNF binds to TNFR1, the receptor death domain recruits numerous adaptor proteins that form a signaling complex (Wang *et al.,* 2000). This signaling complex may then result in the activation of various transcription factors, such as c- Jun or nuclear factor kappaB (NF-kB), as well as expression of genes that are critical for physiological processes such as cell growth, apoptosis, and immunopathology (Santello & Volterra, 2012). The activation of each of these processes may be influenced by several factors, such as the type of adaptor proteins and downstream

molecules that are expressed in a given cell, which in turn may depend on the cell history and metabolic state (Shen *et al.,* 2006 and Zhang *et al.,* 2009). The signalling may be amplified or dampened by many complex feedback mechanisms (Wajant *et al.,* 2003). One may like to limit the TNFR1 signalling by proteolytically cleaving its extracellular domain with TACE, thereafter releasing a soluble fragment of TNFR1 (Ryan & Aksentijevich, 2009). TNFR1 and TNFR2, both have proteolytic effects (Ware *et al.,* 1995). Although, TNFR1 and TNFR2 do not share significant homology in their intracytoplasmic domains, they are characterised by four repeated cysteine-rich motifs, with significant intersubunit sequence homology (Tartaglia & Goeddel, 1992 and Wallach *et al.,* 1999). Signalling of TNF through TNFR1 either results in the formation of complex I and activation of NFkB (pathway 1) promoting inflammation, survival and differentiation or provokes cell death through complex II and activation of caspases (pathway 2) (Haider & Knöfler, 2009). Recruitment of the apoptosis signal-regulating kinase 1 (ASK-1) (pathway 3) induces JNK and activator protein 1 (AP-1) which in turn may initiate apoptosis or survival (Haider & Knöfler, 2009). TNFR2-dependent signalling may also promote cell death or survival through pathways 1 and 2 respectively, but also activate phosphatidylinositol-3-kinase/AKT (PI3K/AKT), suppressing apoptosis and promoting proliferation, migration and survival (Haider & Knöfler, 2009). The TNF signaling pathway through TNFR1 and TNFR2 is shown in Figure 1.6.

It is important to note that TNF action is more complex than previously thought and can produce reverse effects, protective or deleterious, depending on several factors, including: (i) the type of cells or organ in which the process of activation is taking place; (ii) the type of receptor predominantly activated by TNF; (iii) the concentration at which the cytokine acts (iv) and lastly the duration of its action (Santello & Volterra, 2012).

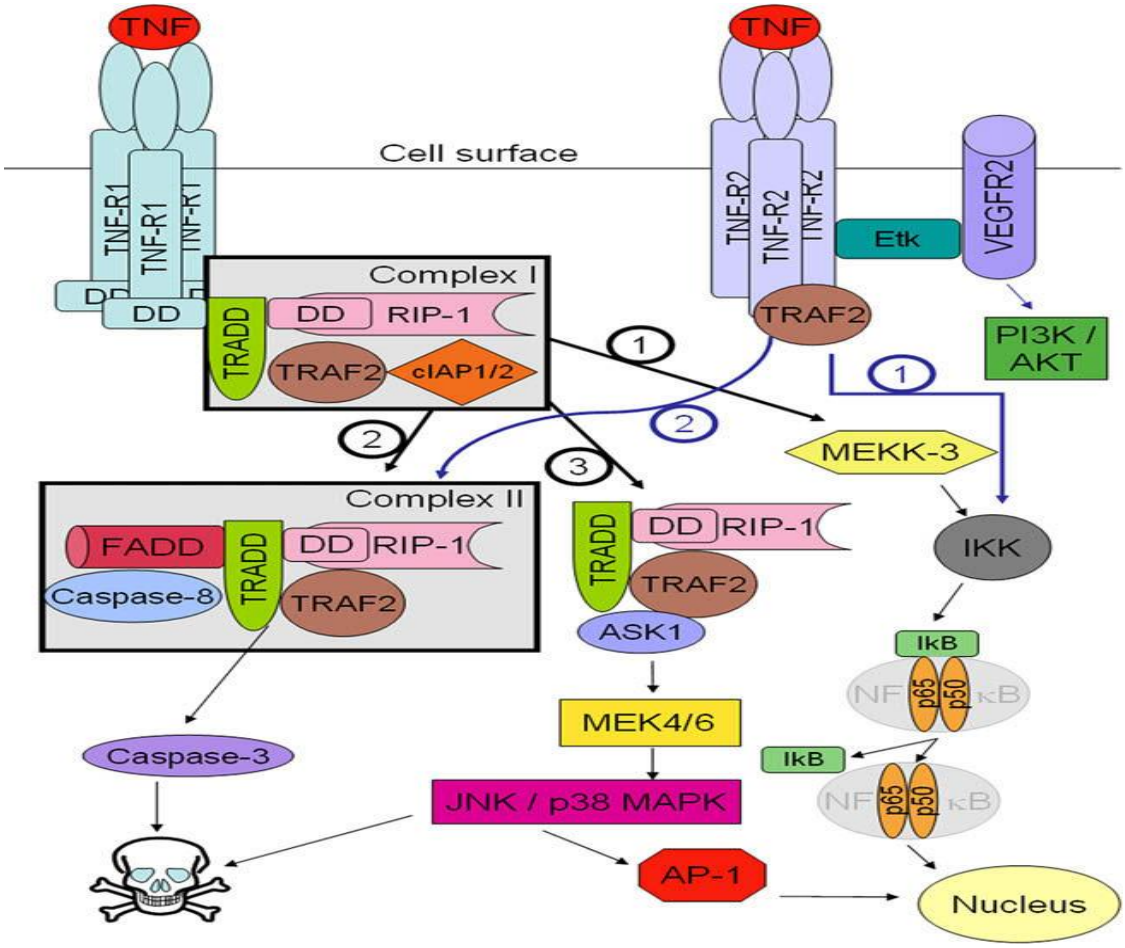

Figure 1.6: TNF-dependent signalling pathways mediated via TNFR1 and TNFR2 (Adapted from Haider & Knöfler, 2009).

1.3.2 Tumour necrosis factor involvement in neurotuberculosis

The cytokine TNF plays four major actions during TB: (i) It is involved in the activation of macrophages, affecting their phagocytic and killing abilities; (ii) participate in the recruitment of many inflammatory cells (key to proper granuloma formation); (iii) regulate the induction of cytokine and chemokine production; and (iv) induction of apoptosis of macrophages and T cells (Marino *et al.,* 2012). TNF plays a critical role in response to *M. tuberculosis* during neurotuberculosis (Buonsenso *et al.,* 2010). The effects triggered by TNF are not only quantitatively, but also qualitatively distinct from those exerted at normal levels. Studies have shown that excess TNF production can lead to neuronal and oligodendrocyte cell death (Akassoglou *et al.,* 1998 and Li *et al.,* 2004). The expression of TNF increases

intercellular adhesion molecule-1 (ICAM-1), leukocyte adhesion molecule-1 (LAM-1), and vascular cell adhesion molecule-1 (VCAM-1) via astrocyte-microglia interaction (Hurwitz et al., 1992; Kyrkanides *et al.,* 1999 and Tang *et al.,* 2011). TNF is involved in activation of the hypothalamus pituitary–adrenal axis, induction of a fever response, and triggers the release of other proinflammatory cytokines (Ramilo *et al.,* 1990; Saukkonen *et al.,* 1990; Hashimoto *et al.,* 1991 and De Vries *et al.,* 1997). TNF also influences the trafficking of compounds into the brain by affecting the BBB permeability (De Vries *et al.,* 1997). In patients with neurotuberculosis, high TNF levels in the CSF correlate with increased levels of IL-6 and protein, as well as low glucose levels (Low *et al.,* 1995). In addition, TNF and IL-1β levels are associated with prolonged fever, seizures, spasticity, and death (Low *et al.,* 1995 and Sharief *et al.,* 1992). Due to the pleiotropic mode of action of these cytokines, they can potentially influence an immense variety of CNS signals and processes (Carpentier & Palmerv, 2009). During CNS infection, specific attention has been attributed to the proinflammatory cytokines such as IL-1β, IL-6, IL-12 and TNF (Santello & Volterra, 2012). Cytokine such as TNF and IL-12, and chemokines with their receptors are secreted by various *M. tuberculosis* infected antigen presenting cells (Henderson *et al.,* 1997; Kim *et al.,* 1999; Giacomini *et al.,* 2001 and Hickman *et al.,* 2002). The detrimental effects of TNF in the CNS may also depend on the presence of other cytokines produced by either resident populations of CNS cells or infiltrating leukocytes, such as T cells. T cells have the ability to produce TNF along with interferon-γ (IFN-γ) that acts in both innate and specific cell-mediated immunities (Moser & Murphy, 2000). The effects produced by these cytokines may induce macrophage antimicrobicidal actions such as the production of nitric oxide (NO) and reactive nitrogen intermediates (RNI) mediated by nitric oxide sythase (NOS2) (Nathan, 1997 and Cooper *et al.,* 2002). Babu *et al.,* (2008) confirmed that TNF, IFN-γ and NO are involved in the immunopathology of neurotuberculosis. The combined effects of both TNF and IFN-γ may be harmful to neuronal elements (Babu *et al.,* 2008).

1.4 Genetically modified mice

All disease pathology, be they inherited, infectious or environmentally induced, is affected or influenced directly or indirectly by an individual genome. The use of genetic modified mice may help us to understand these fundamental interactions. Sequencing of the mouse and human genomes has revealed outstanding similarities. Most human genes have a related mouse version analogue and are ideal to provide insight into human diseases. Due to these

similarities and to the practical considerations (mice breed rapidly, and methods of genetic modification are more effective, when compared with other mammals), the mouse model is widely used as a tool, for research in investigating immune mechanisms to unravel biological systems, and in the development of new drug therapies. Neurotuberculosis is a complicated disease, until today, the immunopathologly of this devastating disease is still not well understood. Previous studies using mice infected with laboratory or clinical mycobacterial strains, using different infection routes have shown mice to develop CNS pathology similar to human (Thwaites *et al.,* 2003 and van Well *et al.,* 2007).

Gene targeting manipulation has been used widely. The method can be used to remove exons, add a gene, delete a gene of interest and introduce point mutations. Targeted gene mutations have allowed the generation of specific gene knockout mice where a specific gene of interest is rendered non-functional. Typically, mutations have been designed to eliminate gene function, resulting in the generation of null mutant or knockout mice. The first consists of the cloning of the specific gene of interest and modification by removing some sequences from the specific gene (Mak *et al.,* 2001). A targeting construct is then produced in which an exon of the gene of interest is replaced by a neomycin resistance cassette (Neo). A thymidine kinase (TK) cassette is included for negative selection. Homologous recombination results in the incorporation of the engineered mutation into the endogenous gene locus. Beside the above conditional mentioned approach, many approaches are routinely used for manipulating the mouse genome and generating new genetically modified mice; some of them are based on the Cre/loxP recombination system (Kuhn & Schwenk, 1997 and Bergqvist *et al.,* 1998).

Since 1998, at the workshop for “Conditional Genome Alterations” in Cold Spring Harbor; where it was announced by Rossant & McMahon, (1999) that “Cre (cyclisation recombination) works”. After several years of investigations, scientists are now certain that the Cre recombinase of the P1 bacteriophage efficiently catalyzes recombination between two of its consensus 34 base pair DNA recognition sites (*loxP* sites) in any cellular environment and on any kind of DNA (Nagy, 2000). The Cre/loxP recombination system is a site-specific recombinase technology widely used to elegantly carry out insertions, translocations, deletions and inversions in the DNA of cells. The system allows for organs/tissue or cell specific deletion of the gene of interest and can be expressed under the control of a tissue or cell specific promoter (Mak *et al.,* 2001 and Zhu *et al.,* 2001). Elimination of the gene by the Cre/loxP recombination system removes the problem of early embryonic fatality of mice, especially when the gene is important during the early development of the embryo (Bergqvist *et al.,* 1998). Cre

enzyme originates from the bacteriophage P1 and is a site specific recombinase that recombines DNA fragments only at loxP sites (Kuhn & Schwenk, 1997 and Mak *et al.,* 2001). The Cre recombinase of the P1 bacteriophage is a member of the integrase family of site-specific recombinases. It is a 38 kD protein that catalyzes the recombination between two of its recognition sites, called loxP (Hamilton & Abremski, 1984). This is a 34 bp consensus sequence, consisting of a core spacer sequence of 8 bp and two 13 bp palindromic flanking sequences. First, a pair of loxP sites repeats flanks the target DNA to be deleted (Figure 1.7). Thereafter, the mouse expressing Cre enzyme (under the control of an inducible promoter in the transgenic mice, so that it can delete the target DNA inside the selected cells) is generated. One loxP site is left behind and the two flanking fragments of DNA are spliced together. In a cell type-specific manner, the target DNA is excised and degraded. While other cell types, where the Cre enzyme is not directed still have their intact genes. Mating of these two lines will result in Cre-mediated deletion of the gene of interest only in the cells or tissue expressing Cre recombinase. Thereafter the strains are screened for homologous recombination by PCR or Southern blot analysis. One of the advantages of the Cre/loxP recombination system is that there is no need for additional sequence elements or co-factors for efficient recombination regardless of the cellular environment (Nagy, 2000). Concerning the molecular mechanism of recombination, a single recombinase molecule binds to each palindromic half of a loxP site, then the recombinase molecules form a tetramer, thus bringing two loxP sites together (Voziyanov *et al.,* 1999).

Many studies using mouse models of complete TNF deletion have demonstrated that TNF has numerous effects and functions during pulmonary tuberculosis (Flynn *et al.,* 1995; Botha *et al.,* 2003; Allie *et al.,* 2008 and Allie *et al.,* 2010). These studies demonstrated that TNF is involved in immune cell trafficking into the site of infection, controlling bacterial replication and in the instruction of granuloma formation and its maintenance.

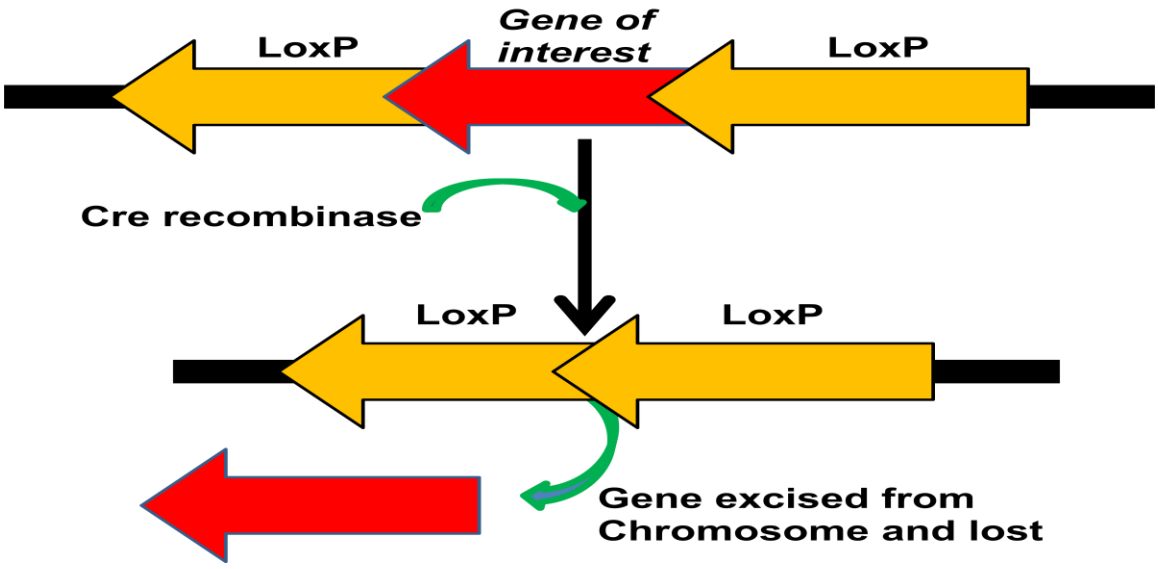

Figure 1.7: Cre/loxP mediated gene targeting only in the cells or tissue expressing Cre recombinase. The targeted gene is flanked by two loxP sites (floxed gene). The foxed gene is removed by the recombinase, and become non-functional.

1.5 Aims and objectives of the study

To our knowledge, no study has yet investigated the immunopathology of neurotuberculosis using complete TNF deficient or cell type-specific TNF deficient mice. In this thesis, we independently investigated the role of neurons as a basic functional cell of the brain, the myeloid (microglia-macrophages and neutrophils) cell subset, and lymphoid ($CD4^+$- and $CD8^+$) T cell subsets as cellular sources of TNF in protective immunity against cerebral *M. tuberculosis* infection. In this study we aimed: (i) to investigate the contribution of neuronal, microglia/macrophage, neutrophil, $CD4^+$- and $CD8^+$ T cell-derived TNF in the host's immune function against cerebral *M. tuberculosis* infection, and (ii) to assess the relative roles of each cell type and potential co-operativity in immune function during cerebral *M. tuberculosis* infection.

To achieve our aim we have designed the following objectives: (i) to evaluate the recruitment of immune cells such as antigen presenting cells, and T and B lymphoid cells into the central nervous system during *M. tuberculosis* infection as a function of TNF; (ii) to evaluate the activation status of recruiting immune cells in protective immunity against cerebral *M. tuberculosis* infection; (iii) to evaluate the mortality, bacilli burden as the primary indicator of TNF mediated immune protection and organ pathology in response to cerebral *M. tuberculosis* infection; (iv) to examine whether lymphocytic infiltration of the brain is regulated by neuronal, myeloid or lymphoid cell-derived TNF; (v) to assess whether the role of brain neuronal cell, as well as immune cells subsets such as microglia, macrophages, neutrophils, $CD4^+$ and $CD8^+$ T cell-derived TNF influence the expression of cytokine and chemokine levels during experimental neurotuberculosis, and (vi) to investigate whether TNF synthesised by neurons, microglia, macrophages, neutrophils or T cells regulate TNF cytokine and chemokine expression during experimental neurotuberculosis.

We therefore hypothesised that neuronal derived TNF, as well as myeloid or T cell-derived TNF is required to generate host protective immune responses against cerebral *M. tuberculosis* infection.

CHAPTER II

MATERIALS AND METHODS

2.1 Animals and development of conditional NsTNF$^{-/-}$ mice

Mice 8-12 week-old male or female (all on a C57BL/6 genetic background) were used in experiments. All mice were bred and maintained under specific pathogen free (SPF) conditions in the Research Animal Facility at the University of Cape Town. Experimental mice were housed in an individually ventilated cage (IVC) system and supplied with sterile water and food *ad libitum*. Tail biopsies of experimental mice were obtained to extract genomic DNA and confirm strain genotypes. All experimental procedures were performed in a biocontainment level 3 facility. Mouse strains used and generated in this study were: (i) Knockin transgenic Syn1-Cre mice obtained from Jackson Laboratories (Bar Harbor, Maine, USA), in which Cre expression is controlled by the rat Synapsin I promoter, and has been shown to drive transgene expression specifically in neuronal cells (Hoesche *et al.,* 1993 and Zhu *et al.,* 2001). (ii) The knockin TNF floxed mice (TNF$^{f/f}$, wild type (WT) used as control positive) in which the TNF gene was modified by the insertion of synthetic loxP sites flanking the coding region of interest. Briefly, three loxP sites were introduced into the targeting vector; where two loxP sites were flanked by the neo selection cassette and then placed approximately 1kb downstream of the TNF gene, and then the third loxP site was inserted into the third intron (Grivennikov *et al.,* 2005). (iii) In order to generate novel mice with specific deletion of the TNF gene in neurons (NsTNF$^{-/-}$ mice), we crossed the TNF$^{f/f}$ mice with Syn1-Cre mice. (iv) Microglia/macrophages and neutrophils specific TNF deficient mice (M-TNF$^{-/-}$ mice) generated by Grivennikov *et al.,* (2005). (v) Myeloid (microglia/macrophage and neutrophils) and lymphoid (CD4^{+}- and CD8^{+} T cells) cell type-specific TNF deficient mice (MT-TNF$^{-/-}$ mice) were generated by Allie *et al.,* (2013), by cross breeding the M-TNF$^{-/-}$ mice with the CD4/CD8TNF$^{-/-}$ mice (T-TNF$^{-/-}$) (Grivennikov *et al.,* 2005). (vi) and the complete TNF deficiency mice (TNF$^{-/-}$) were previously generated by Kuprash *et al.,* (2005). Our TNF$^{-/-}$ strain was originally generated from TNF$^{f/f}$ mice, we therefore opted to use this strain as our negative control for the entire study. All studies and procedures were approved by the University of Cape Town, Animal Ethics Committee (HSFAEC No: 010/018).

2.1.1 Genotyping of mice

The mice used in all experiments were first genotypes and phenotypes of matting, breeding stocks and litters used were confirmed by polymerase chain reaction (PCR). Mice were genotyped for the presence of either Cre or TNF using a Peltier Thermal Cycler (model PTC-200) from MJ research (Biozym, Hessissch Olderdorf, Germany). Primers were purchased

from The Department of Biochemistry, Faculty of Science, University of Cape Town.

2.1.1.1 Extraction of genomic DNA and PCR analysis

Mice tail tip biopsies (approximately 1 cm) were obtained under anaesthetic. Genomic DNA was extracted by lysing tails overnight with rotation at 56°C in lysing buffer containing 50mM Tris-HCl pH 8, 100mM EDTA pH 8, 100mM NaCl, 1% SDS and 0.5mg/ml Proteinase K (Sigma, St. Louis, MO). A volume of 250µl of saturated NaCl was added and the solution was vortexed for ± 15 seconds, before centrifugation for 10 minutes at 10,000 rpm. 750µl of supernatant was transferred to a tube containing 450µl of ice-cold isopropanol. DNA was precipitated by gently inverting the tube. The solution was then centrifuged for 5 minutes at 13000 rpm to sediment the DNA. The DNA was then washed with 70% ethanol, sedimented again by centrifugation and the pellet dried at 37°C using a Digital Dry Bath (Labnet international, inc Woodbridge, NJ 07095). The dried DNA pellet was resuspended in 200µl of distilled water for 3 hours at room temperature, and a volume of 2µl of DNA solution was used per PCR reaction. The standard PCR reaction mix (Table 2.1) was used in all PCR analysis, and PCR reagent preparation is further detailed in appendix A.

Table 2.1: Standard PCR reaction mix

Stock concentration	**Volume**	**Final concentration**
10 x PCR buffer	5 µl	1 x PCR Buffer
MgCL (25mM)	3 µl	1.5mM
dNTNP (10 µl)	1 µl	0.2mM
Primer 1 (10 µl)	1 µl	0.2mM
Primer 2 (10 µl)	1 µl	0.2mM
Taq (5U/µl)	0.125 µl	0.625U
DNA sample	2 µl	
H_2O	36.875 µl	
Total volume	**50 µl**	

2.1.1.2 Primer sequences used for screening of Syn1-Cre and TNF genes

Amplification of Syn1-Cre and TNF genes were performed by PCR, according to the conditions set out in tables 1, 2, 3 and 4. Magnesium chloride, 10x PCR buffer and *Taq* polymerase were purchased from Vector Laboratories, (UK) and the dNTP stocks were obtained from Promega, Madison, United states.

2.1.1.2.1 Primers used for screening Syn1-Cre and NsTNF$^{-/-}$ mice were as follows:

IMR1084: 5' GCG GTC TGG CAG TAA AAA CTA TC 3'
IMR1085: 5' GTG AAA CAG CAT TGC TGT CAC TT 3'
IMR7338: 5' CTA GGC CAC AGA ATT GAA AGA TCT 3'
IMR7339: 5' GTA GGT GGA AAT TCT AGC ATC ATC C 3'

Table 2.2: Amplification conditions for the Syn1-Cre gene

Cycling steps	Temperature (ºC)	Time (seconds)
1. Initial denaturation	94	180
2. Denaturation	94	30
3. Primer annealing	51.7	60
4. Extension	72	60
5. Final extension	72	120
Steps 2-4 was repeated for 35 cycles		

Amplification products:

Wild type gene: 324bp (IMR7338 and IMR7339)
Syn1-Cre gene transgene: ~100bp (IMR1084 and IMR1085)

2.1.1.2.2 Primer sequences used for screening TNF$^{f/f}$ mice were as follows:

KO41: 5' TGA GTC TGT CTT AAC TAA CC 3'
KO42: 5' CCC TTC ATT CTC AAG GCA CA 3'

Table 2.3: Amplification conditions for the TNF floxed gene

Cycling steps	Temperature (ºC)	Time (seconds)
1. Initial denaturation	94	120
2. Denaturation	94	40
3. Primer annealing	55	45
4. Extension	72	60
5. Final extension	72	300
Steps 2-4 was repeated for 35 cycles		

Amplification products:

Wild type TNF gene: 350bp
Floxed TNF gene: 400bp

2.1.1.2.3 Primer sequences used for screening of M-TNF$^{-/-}$ mice were as follows:

Mlys1: 5' CTT GGG CTG CCA GAA TTT CTC 3'
Mlys2: 5' TTA CAG TCG GCC AGG CTG AC 3
Cre8: 5' CCC AGA AAT GCC AGA TTA CG 3'

Table 2.4: Amplification conditions for the Mlys Cre gene

Cycling steps	Temperature (ºC)	Time (seconds)
1. Initial denaturation	94	300
2. Denaturation	94	30
3. Primer annealing	55	30
4. Extension	72	90
5. Final extension	72	420
Steps 2-4 was repeated for 34 cycles		

Amplification products:

Mlys gene (WT): 350bp (Mlys1 and Mlys2)
Mlys Cre transgene: ~700bp (primers Cre8 and Mlys1)

2.1.1.2.4 Primer sequences used for screening of MT-TNF$^{-/-}$ mice were as follows:

Mlys 1: 5' CTT GGG CTG CCA GAA TTT CTC 3'
Mlys 2: 5' TTA CAG TCG GCC AGG CTG AC 3
Cre 8: 5' CCC AGA AAT GCC AGA TTA CG 3'

Table 2.5: Amplification conditions for the Mlys Cre gene

Cycling steps	Temperature (ºC)	Time (seconds)
1. Initial denaturation	94	300
2. Denaturation	94	30
3. Primer annealing	55	30
4. Extension	72	90
5. Final extension	72	420
Steps 2-4 was repeated for 34 cycles		

Amplification products:

Mlys gene (WT): 350bp (Mlys1 and Mlys2)
Mlys Cre transgene: ~700bp (primers Cre8 and Mlys1)

CD4 Cre1: 5' ATC AAG GTC CTG AGG AAG AG 3'
CD4 Cre2: 5' ACC TCA TCA CTC GTT GCA TC 3'
CD4 Cre3: 5' CTA GGA GTT GTG CTG CAC AG 3'

Table 2.6: Amplification conditions for the CD4 Cre gene

Cycling steps	Temperature (ºC)	Time (seconds)
1. Initial denaturation	94	600
2. Denaturation	94	30
3. Primer annealing	55	60
4. Extension	72	120
5. Final extension	72	300
Steps 2-4 was repeated for 35 cycles		

Amplification products:

CD4 gene (WT): 350bp (CD4 Cre1 and CD4 Cre3)
CD4 Cre transgene: 242bp (CD4 Cre1 and CD4 Cre2)

2.1.1.2.5 Primer sequences used for screening $TNF^{-/-}$ mice were as follows:

KO 41: 5' TGA GTC TGT CTT AAC TAA CC 3'
KO 49: 5' CTC TTA AGA CCC ACT TGC TC 3'
MTNFRTP 81: 5' GTC TAC TTT GGA GTC ATT GC 3'
MTNFRTP 82: 5' GAC ATT CGA GGC TCC AGT 3'

Table 2.7: Amplification conditions for the $TNF^{-/-}$ gene

Cycling steps	Temperature (ºC)	Time (seconds)
1. Initial denaturation	94	180
2. Denaturation	94	30
3. Primer annealing	56	60
4. Extension	72	120
5. Final extension	72	300
Steps 2-4 was repeated for 35 cycles		

Amplification products:

TNF gene: 350bp (MTNFRTP81 and MTNFRTP82)
TNF Knockout gene: 450bp (KO41 and KO49)

Amplification reaction products were electrophoresed on 1.5% agarose gels (Appendix A) with ethidium bromide at 160 volts for 90 minutes using 0.5 x Tris borate ethylene diamino tetra acetic acid (TBE) (Appendix A) as the electrophoresis buffer. A 1.5kb DNA ladder (Promega, Madison, United States) was used as a molecular weight marker to determine amplification product size.

2.1.2 Characterisation of Neuron specific TNF Knockout mice

$TNF^{f/f}$, $NsTNF^{-/-}$ and $TNF^{-/-}$ mice were intracerebraly stimulated with 5µg/ml of LPS, for 90 minutes. Mice were transcardially perfused with 4% paraformaldehyde in PBS. Brains were collected in 1xPBS and kept on ice. Brain cells were harvested by passing brain through a 70 µm cell strainer (Beckton Dickinson (BD) Biosciences Discovery Labware, Bedford, MA, USA) to generate a single cell suspension. Harvested single cells were fixed with fixation buffer and thereafter incubated in permeabilisation buffer containing saponin before being intracellularly labelled with neuron-specific Beta III Tubulin antibody (unlabelled), as well as PE-conjugated secondary IgG and TNF-specific (TNF-Alexa Fluor 647) markers (Table 2.8). Samples were then resuspended in fixation assay buffer overnight before analysis on a multi-colour FACSAria flow cytometer (BD Biosciences, Erembodegem Belgium). Unstained as well as IgG-PE and IgG-Alexa Fluor 647 stained controls were used to set Beta-tubulin$^+$ and TNF^+ gates. Reagent preparation is further detailed in appendix E.

Table 2.8: Antibodies used for flow cytometry analysis of intracellular cytokine staining

Antibodies	Dilution used	Clone	Source
Neuron specific Beta III Tubulin	1:50	-	abcam®
anti-rabbit IgG:R-PE	1:20	711-116-152	Jackson ImmunoResearch
anti-mouse TNF:Alexa Fluor 647	1:50	MP6-XT22	BD Pharmingen™

2.2 *M. tuberculosis* strain

The *M. tuberculosis* H37Rv strain was obtained from the Trudeau Mycobacterial Culture Collection (Trudeau Institute, Saranac Lake, NY), and grown at 37°C until mid log phase in Middlebrook 7H9 broth (Difco™ BD Becton, Dickinson and Company, Sparks, MD 21152, USA) containing 0.5% glycerol and 10% oleic acid-albumin-dextrose-catalase (OADC) (BBLTM Becton Dickinson and Company Sparks, MD 21152, USA), culture aliquots were stored at -80°C in 2ml cryovials (Nalge Nunc International, Naperville, IL, USA) after adding 10% (v/v)glycerol

(Sigma, St Louis, MO). Colony forming units per milliliter were determined by passing the mycobacterial suspension 30x through a 29,5G needle fitted with a 1 ml syringe (Omnican®, B.Braun, Melsungen, Germany) to disperse clumps and plating 100µl of 10 fold serial dilutions on Middlebrook 7H10 agar (Difco™ BD Becton, Dickinson and Company, Sparks, MD 21152, USA) supplemented with 10% (v/v) OADC and 0.5% (v/v) glycerol. Plates were sealed in a plastic bag and incubated at 37°C for 18-21 days, thereafter colonies were counted using a colony counter (MRC Model 570, MRC Ltd, Israel) and the concentration of mycobacteria calculated.

2.3 Mycobacterial preparation for infection

A 1ml aliquot of *M. tuberculosis* H37Rv was thawed at room temperature and clumps were disrupted by aspirating the mycobacterial suspension 30 times through a 29,5G needle fitted with a 1ml syringe (Omnican®, B.Braun, Melsungen, AG, Germany). An inoculum volume of 2.5 ml at a concentration of 1 x 10^5 cfu/ml was prepared, thereafter 10-fold serial dilutions of inoculums were plated on Middlebrook 7H10 agar (Difco™ BD Becton, Dickinson and Company, Sparks, MD 21152, USA) supplemented with 10% (v/v) OADC (BBL™ BD Microbiology systems, and Company, Sparks,MD 21152, USA) and 0.5% (v/v) glycerol in 90mm compartmentalized plates (Sterilin, Bibby Sterilin Ltd., Stone, Staffs, UK). The culture plates were sealed in a plastic bag and incubated at 37°C for 18-21 days. The colonies were then counted using a colony counter (MRC Model 570, MRC Ltd, Israel) and the concentration of mycobacteria calculated. Middlebrook 7H10 agar preparation is detailed in appendix B.

2.4 Stereotaxic infection

Intracranial infection was performed using stereotaxic frame. Mice were anaesthetised by intraperitoneal injection with appropriate doses of ketamine hydrochloride (100mg/kg Bayer Pty Ltd, Germany) and Xylazine (10mg/kg Intervet, Zurich-Switzerland). After the animal has reached full anaesthesia, furs were removed from the top of the skull with the shaver. The anaesthetised mice were mounted to the stereotaxic frame. Mouse's ears were locked firmly with ear bars into ear sockets of the stereotactic frame, and slide the incisor bar into place and tighten nose clamp firmly on the bridge of the nose. The scalp was disinfected with 70%

ethanol, and an incision was made along a midline and extended forward to the back of the eyes and backward to between the ears, avoiding damage to the muscles. Animals were stereotaxically injected with a dose of $1x10^5$ CFU *M. tuberculosis*. Using single needle insertion (coordinates: +0.2 mm relative to bregma, 2.0mm from midline) to a depth of 2.0mm into the cortex. The solution was injected with a Hamilton syringe (Gastight no.1701, Hamilton, Bonaduz, Switzerland) at a rate of 0.1µl per minute and delivered in 3µl of saline keeping the needle in place for 10 minutes in order to allow absorption of the solution. The hole was sealed with bone wax, the incision was sutured and the animal was removed from the stereotaxic frame. Animals received subcutaneous analgesic Meloxicam (1 mg/kg; Boehringer Ingelheim Pharmaceuticals, Germany) as a prophylactic pain killer at the time of infection, followed by subsequent administration at 24h intervals for a two day period thereafter. The animals were kept warm during the recovery. Mice were monitored twice daily and sacrificed a various predetermined time points by either inhalation with 0.01% halothane (Safeline Pharmaceuticals Pty Ltd, South Africa) or overdose with ketamine/xylazine cocktail. Specific anaesthetic doses preparation is detailed in appendix C.

2.5 Clinical severity scoring system for mice

To evaluate the clinical course of neurotuberculosis in mice, we adapted the previously described scoring system according to the clinical manifestations presented in our animals (Tsenova *et al.,* 2005). Animals were intracerebrally infected with *M. tuberculosis* at a dose of $1x10^5$ cfu/brain. Mice were scored daily for neurologic manifestations during the course of infection as follows: Normal (no detectable signs) = 0; head tilt = 1; motility or decrease activity = 2; behaviour depression = 3; and moribund state = 4.

2.6 Colony forming units

Animals were euthanised by acute exposure to halothane (2-bromo-2-chloro-1,1,1-trifluoro-ethane) 0.01%. The abdomen and the thoracic cavity were opened and brain, lung, spleen and liver were aseptically collected, weighed and then put in 1ml 0.9% NaCl/ 0.04% (v/v) Tween 80 solution. Organs were homogenised using a glass tissue Grinder-homogeniser (Kimix - Chemicals and Laboratory Suppliers, Cape Town - South Africa), and 100µl solution of

ten-fold serial dilutions of organ homogenates were plated in duplicate onto Middlebrook 7H10 agar (Difco™ BD and Company, Sparks, MD 21152, USA) supplemented with10% OADC (v/v) (BBL™ Beckton Dickinson Microbiology systems, BD and Company, Sparks, MD 21152, USA) and 0.5% (v/v) glycerol in 90mm compartmentalised plates (Bibby Sterilin Ltd, Stone, Staffs, UK). Culture plates were sealed in plastic bags and incubated at 37°C for 18-21 days. Mycobacterial colonies were counted using a colony counter (MRC Model 570, MRC Ltd, Israel) and the final cerebral, pulmonary and splenic dose calculated. Cerebral, pulmonary and splenic bacterial burden of infected mice was assessed at various predetermined time points post-infection.

2.7 Organs and tissue preparation for histology

Brains, lungs and spleens were collected from euthanised mice at defined time points and immersed in a volume of 10% formalin (10% formaldehyde in PBS pH 7.4) at least 10x that of the tissue. Organs were processed and embedded in paraffin wax overnight (Histosec Pastilles, Merck). All fixed tissues were dehydrated in an automated tissue processor (Shandon Elliot, Shandon Southern Instruments, Ltd, Camberly, Surrey, UK) for paraffin wax embedding. Dehydration was completed after immersing the tissues in 1 x 70% ethanol for 2hrs, thereafter in 2 x in 96% ethanol for 2hrs each, following in 4 x 2hrs in absolute alcohol and 2 x 2hrs in Xylol. Sections 4 µm thick were cut from the paraffin blocks using a microtone (Leica, model RM-2125, Wetzlar, Germany), and labelled for haematoxylin and eosin (H&E), Ziehl Neelsen, or inducible-nitric oxide synthase (iNOS) and thereafter mounted on aminopropyltriethoxysilane (APES 99%) coated slides. Sections for H&E was used to reveal brain morphology and pathology, Ziehl Neelsen was to assess the presence of acid fast bacilli, and the inducible-nitric oxide synthase was used to assess the activation of antigen presenting cells.

2.7.1 Haematoxilin and eosin staining

After dewaxing tissues sections at 56°C overnight, each brain section was washed twice with absolute ethanol for 1 minute, twice in 96% alcohol for 1 minute, followed by 1 minute in 70% alcohol and rinsed in tap H_20. Sections were incubated for 8 minutes in haemotoxylin and rinsed with water. Thereafter they were washed for 30 - 60 minutes with water and directly

counter stained for 2 minutes in 1% eosin solution. Tissue sections were washed again with water, dehydrated in different alcohol concentrations (70% and 96% alcohol), and then Xylol and mounted with Canada Balsam (Sigma-Aldrich, Kempton Park, South Africa). Reagent preparation is further described in appendix D.

2.7.2 Ziehl-Neelsen staining

Following dewaxing tissues sections at 56°C overnight, slide sections were covered with a filtered carbol fuchsin solution and heated gently until fumes appeared. Slides were allowed to stand for 5 minutes, and then rinsed gently under a stream of running tap water. Excess stain was removed by rinsing in 1% acid alcohol containing 1% HCl in 70% alcohol. This procedure was followed by covering the slides with 20% sulphuric acid for 20 minutes. Thereafter, slides were rinsed gently under a stream of running tap water for 10 minutes. Sections were covered with drops of Loeffler's methylene blue for 1 minute. Slide sections were washed prior to dehydration with alcohol (70%, 90%, and 96%, absolute). All slides were dipped in xylol for a minute and mounted in Entellan (Merck, Darmstadt, Germany). Reagent preparation is further described in appendix D.

2.7.3 Brain inducible nitric oxide synthase staining

The inducible-nitric oxide synthase (iNOS) staining was used to assess the activation of antigen presenting cells. Formalin-fixed paraffin-embedded brain sections were deparaffinised and rehydrated followed by staining with rabbit anti-mouse specific inducible nitric oxide synthase as described by Garcia *et al.,* 2000.

2.8 Flow cytometry analysis

2.8.1 Brain single cells staining for flow cytometric analysis

Animals were euthanised with a lethal dose of Ketamine/xylazine. Thereafter, mice were disinfected with Ethanol (70%). The thoracic cavities of mice under aneasthesia were opened for transcardial perfusion with 10ml of 1x PBS. After the perfusion, the heads of the mice were removed and the brain aseptically collected into a tube containing 2ml of 1x PBS and kept on ice.

Brains were passed through a 70µm cell strainer (BD Biosciences Discovery Labware, Bedford, MA, USA) to generate a single cell suspension. Cells ($1x10^8$ cells/brain) were pelleted by centrifugation at 2000 rpm for 5 minutes.

2.8.2 Cell surface staining for flow cytometry analysis

Individual mice whole brain tissues were harvested at 0 (naïve), 1, 2 and 3 weeks post infection to generate single cell suspensions. For surface marker staining, 1 x 10^6 cells were used and non-specific binding to cells was prevented through incubation in 25µl of blocking solution containing αFcγRIII (1mg/ml of rat α-mouse CD32/16c in normal rat serum (heat inactivated) and normal mouse serum (heat inactivated), and diluted in 141.56µl FACS buffer (containing 0.1% (v/v) BSA and 0.01% (v/v) NaN_3 in PBS, pH 7.4) for 20 minutes at 4°C. The brain cells were thereafter washed by adding 1ml FACS buffer and then centrifuged at 2000 rpm for 5 minutes at 4°C. Diluted antibody combinations (25µl of each diluted antibody) at a final concentration of 2µg/ml were added to the cells and incubated for 20 minutes at 4°C in the dark. After washing the cells, a volume of 200µl of fixation buffer (2% paraformaldehyde (PFA) and 0.4% NaOH in PBS, pH 7.2) was added into each well and the cells fixed overnight at 4°C. Flow cytometric analysis was done on multi-colour FACS LSRFortesa cell analyser (BD Biosciences, San Jose, California, USA) using Flowjo software.

To identify the CD11b, CD11c and CD45 expression, isolated single cells were labelled with specific markers (CD11b:PerCP-Cy5-5, CD11c:Alexa 700 and CD45:APC) for flow cytometric analysis to examine CD11b, CD11c and CD45 expression. We confirmed the $CD11c^{+}CD45^{high}$ population by measuring CD11c expression after gating the $CD11b^{low}CD45^{high}$ population. Cell body or live cells were identified and gated according to the previously

published strategy (Guez-Barber *et al.,* 2012), and its application in these studies is shown in Figure 2.1. Microglia phenotype was defined as $CD11b^{+}$ and $CD45^{low}$ as previously reported (Sedgwick *et al.,* 1991; Ford *et al.,* 1995 and Nikodemova & Watters, 2012). In addition, the macrophage population was also identified as $CD11b^{+}$ cells, but showed to express $CD45^{high}$ (Sedgwick *et al.,* 1991 and Ford *et al.,* 1995). Distinct population was displayed, expressing $CD45^{high}$ cells, but expressed $CD11b^{low}$ which we referred to as dendritic cells (DCs), this population was later confirmed for the $CD11c^{+}$ in mice, expression of $CD11c^{+}$ determines DCs phenotype (Wildenberg *et al.,* 2009 and Fischer & Reichmann, 2001). The antibodies and initial concentrations used are listed in Table 2.9, and the gating strategy as described by Ford *et al.,* (1995); Carson *et al* (1998); Campanella *et al.,* (2002); Kruglov *et al.,* (2011) and Nimer *et al.,* (2013) was used.

To identify the Follicular B cells population, isolated single cells were labelled with specific B-cell markers (CD1d:PE, CD93(AA4.1):PerCP-Cy5-5 and B200:Horizon V500), and Figure 2.2 shows the gating strategy used to identify the $CD1d^{low}B220^{+}AA4.1^{-}$ (Follicular B cells) population. The follicular B cells were gated and identified according to Castillo-Méndez *et al.,* (2007) previously described method, and antibodies and initial concentrations used are described in Table 2.10.

In order to identify the plasmablast and plasma cells, isolated single cells were labelled with specific B-cell (CD1d:PE, CD93(AA4.1):PerCP-Cy5-5-A, CD138:APC and B200:Horizon V500) markers. Figure 2.3 shows the gating strategy used to identify the plasmablast and plasma cell populations. Plasmablast and plasma cells were identified and analysed using antibodies and their initial concentrations in Table 2.10 (Radwanska *et al.,* 2008).

The $CD4^{+}$- and $CD8^{+}$ T cells were identified and analysed after the isolated single cells were labelled with specific T cells (CD3e: Pacific Blue, CD4:Alexa 700 and CD8:PerCP-Cy5.5) for analysis of $CD4^{+}$- and $CD8^{+}$ T cell populations by flow cytometry (Figure 2.4). The antibodies and initial concentrations used ared described in Table 2.11, and the previously described gating strategy (Friberg *et al.,* 2011 and Schmetterer *et al.,* 2011). Reagents preparation is further described in appendix E.

2.8.3 Total cell number or absolute number calculation

The absolute numbers of each population gated were calculated using the following fomula:

Total cell number = Total cell count for the organ X Percentage of total cells which are positive.

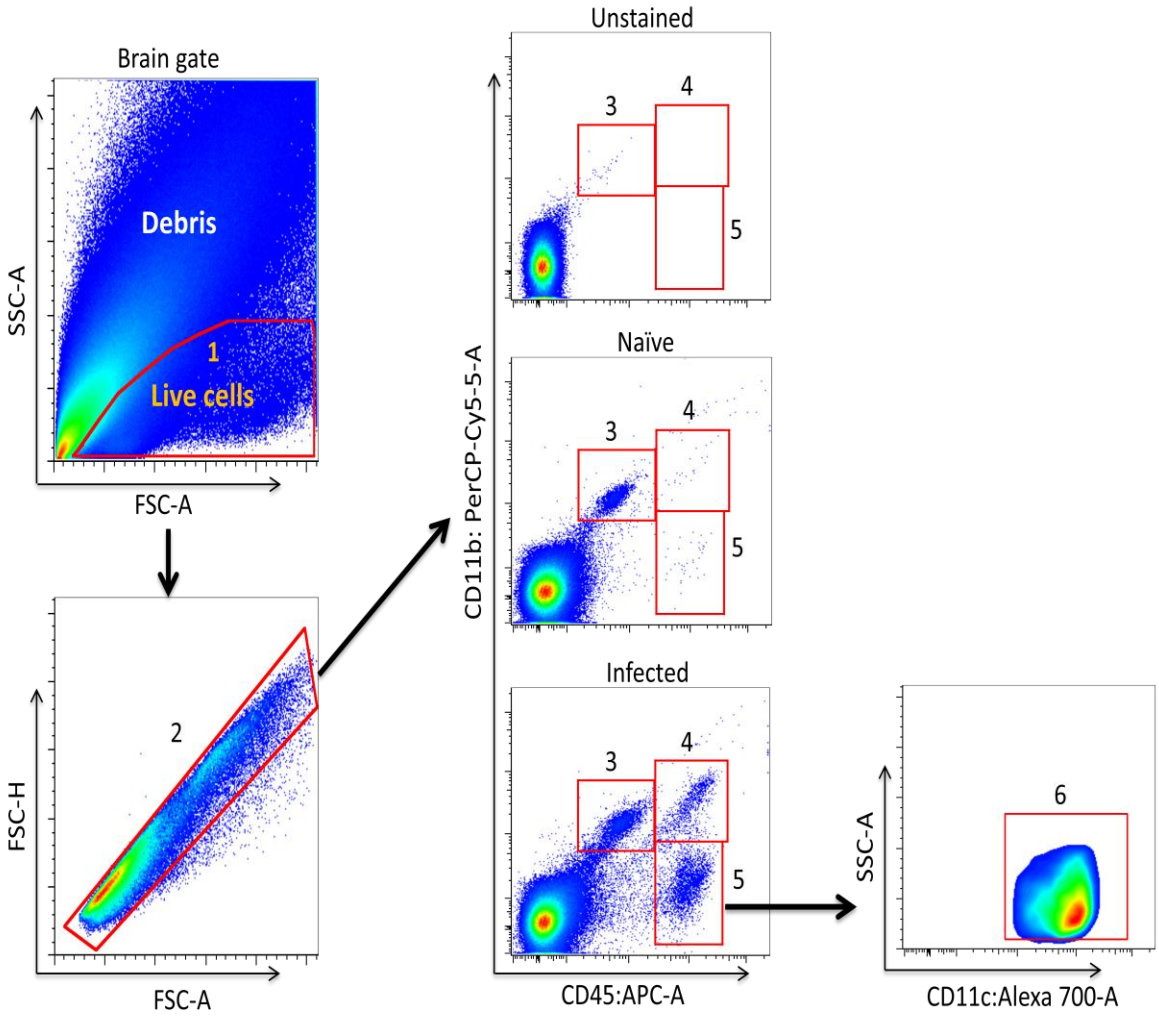

Figure 2.1: Gating strategy of myeloid derived APCs used during neurotuberculosis. $TNF^{f/f}$, $NsTNF^{-/-}$ and $TNF^{-/-}$ mice were intracerebrally infected with *M. tuberculosis* ($1x10^5$ cfu/brain). Brains were collected at week 0 (naïve), 1, 2 and 3 post-infection, and immediately harvested. To identify microglia and infiltrating myeloid populations, isolated cells labelled with CD11b:PerCP-Cy5-5, CD11c:Alexa 700 and CD45:APC as myeloid antigen presenting cell markers and analysed by flow cytometry. Live brain cells were first gated on a forward scatter/side scatter (FSC-A/SSC-A) dot plot showing distinct clusters for debris and live cells, using unstained, naïve and infected samples (1), and brain live cells were gated on FSC-A/FSC-H to generate singlets (2). Cells were thereafter labelled with CD11b:PerCP-Cy5-5 or CD11c:Alexa 700 and CD45:APC to gate for APCs. Microglia ($CD11b^+CD45^{low}$) (population 3), macrophages ($CD11b^+CD45^{high}$) (population 4), DCs ($CD11b^{low}CD45^{high}$) (population 5), were identified. To confirm the dendritic cell population ($CD11c^+CD45^{high}$) phenotype, we evaluated SSC-A/CD11c:Alexa 700 marker (6) expression after gating on $CD11b^{low}CD45^{high}$ population. Flow cytometry data of controls (wild type and $TNF^{-/-}$) used in result section 1 were the same data used as control in result section 2.

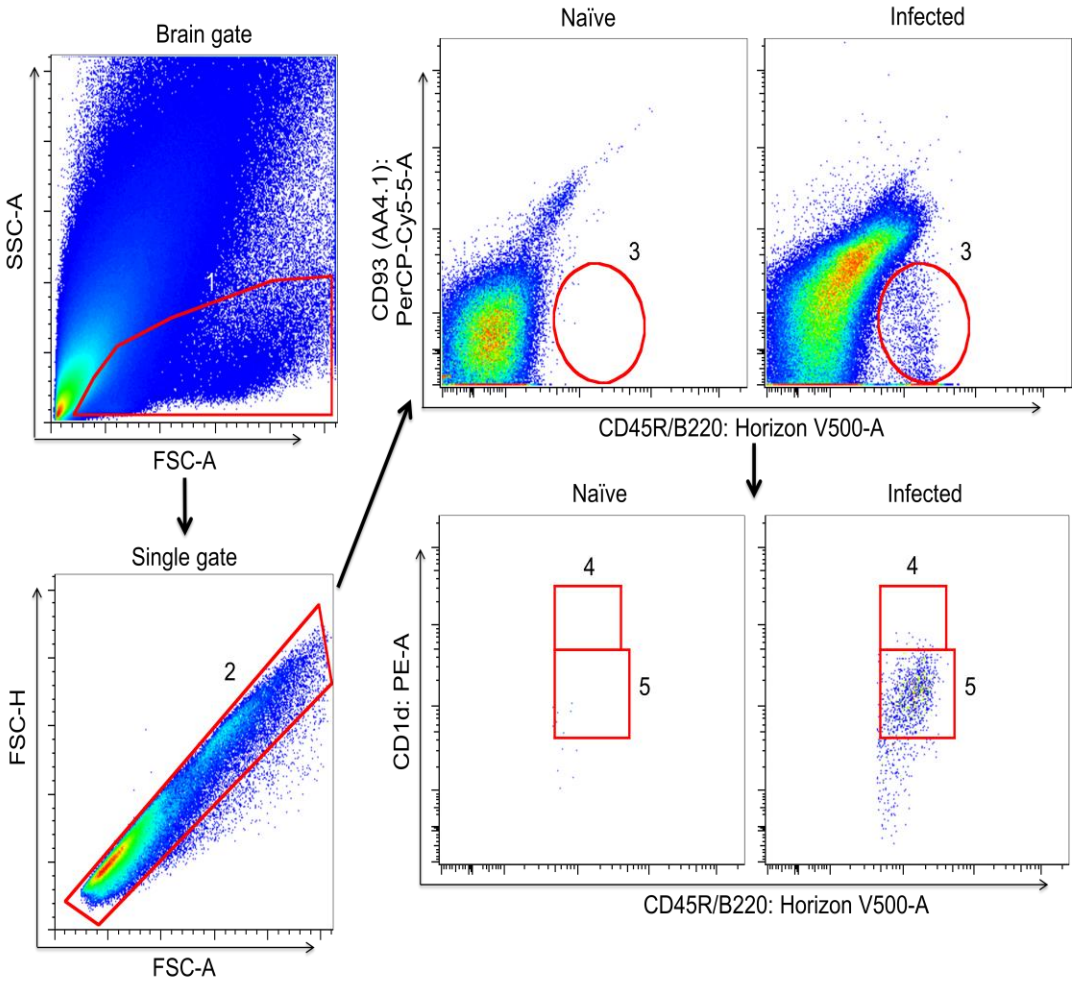

Figure 2.2: Fo B cells gating strategy used during neurotuberculosis. $TNF^{f/f}$, $NsTNF^{-/-}$ and $TNF^{-/-}$ mice were intracerebrally infected with *M. tuberculosis* at a dose of $1x10^5$ cfu/brain. Brains were harvested at week 0 (naïve), 1, 2 and 3 post-infection, and single cells labelled and analysed using the BD LSRFortessa flow cytometer analyzer. In order to identify Fo B cells population, isolated single brain cells were labelled with CD1d:PE-A, CD93(AA4.1):PerCP-Cy5-5-A and B220:V500-A markers. Brain live cells are first gated on a FSC-A/SSC-A dot plot using naïve and infected (1). The gate 1 event is visualised using an FSC-A/SSC-A dot plot and the singlets (single cells) were gated on FSC-A/FSC-H (2). Cells on gate 2 were simultaneously displayed on both CD93(AA4.1):PerCP-Cy5-5-A/B220:V500-A in order to discriminate the immature cells, and yielded to $AA4.1^+B220^+$ population and (3). The $AA4.1^-$ $B220^+$ population were then gated using CD1d:PE-A versus B220:Horizon V500-A markers to discriminate the marginal zone cells (4) and Fo B cells detected as $CD1d^{low}B220^+AA4.1^-$ cells (5) were mapped in a CD1d:PE/B220:V500 dot plots using gate 3. Flow cytometry data of controls (wild type and $TNF^{-/-}$) used in result section 1 were the same data used as control in result section 2.

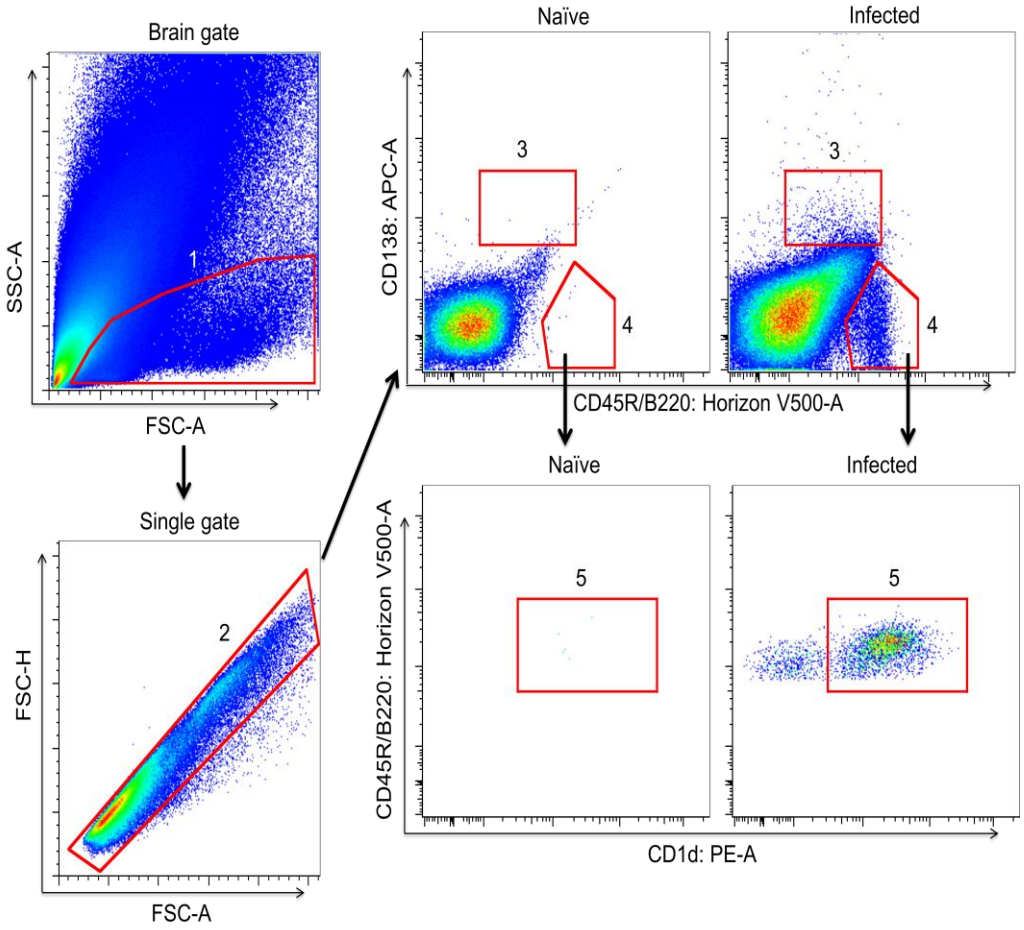

Figure 2.3: Flow cytometry gating strategy for plasmablast and plasma cells. Brains were harvested at week 0 (naïve), 1, 2 and 3 post-infection, and cells isolated from naïve and the intracerebrally infected $TNF^{f/f}$, $NsTNF^{-/-}$ and $TNF^{-/-}$ mice with *M. tuberculosis* at a dose of $1x10^5$ cfu/brain. Isolated single cells were labelled with CD1d:PE-A, AA4.1:PerCP-Cy5-5-A, CD138:APC-A and CD45R/B220:V500-A. From top left: Brain live cells are gated on FSC-A/SSC-A using naïve and infected samples (1), and singlets were gated on FSC-A/FSC-H (2). Thereafter gated with CD138:APC-A and B220 V500-A. Two B-cell subsets are identified: the plasma cells ($B220^{low}CD138^{+}$) (3), and plasmablast cells (4). The identified plasmablast population in 4, was further gated for B220 V500-A with CD1d:PE-A to discriminate the $CD1d^{low}$ cells, and the plasmablasts population yield as $CD1d^{high}B220^{high}CD138^{-}$ (5). Flow cytometry data of controls (wild type and $TNF^{-/-}$) used in result section 1 were the same data used as control in result section 2.

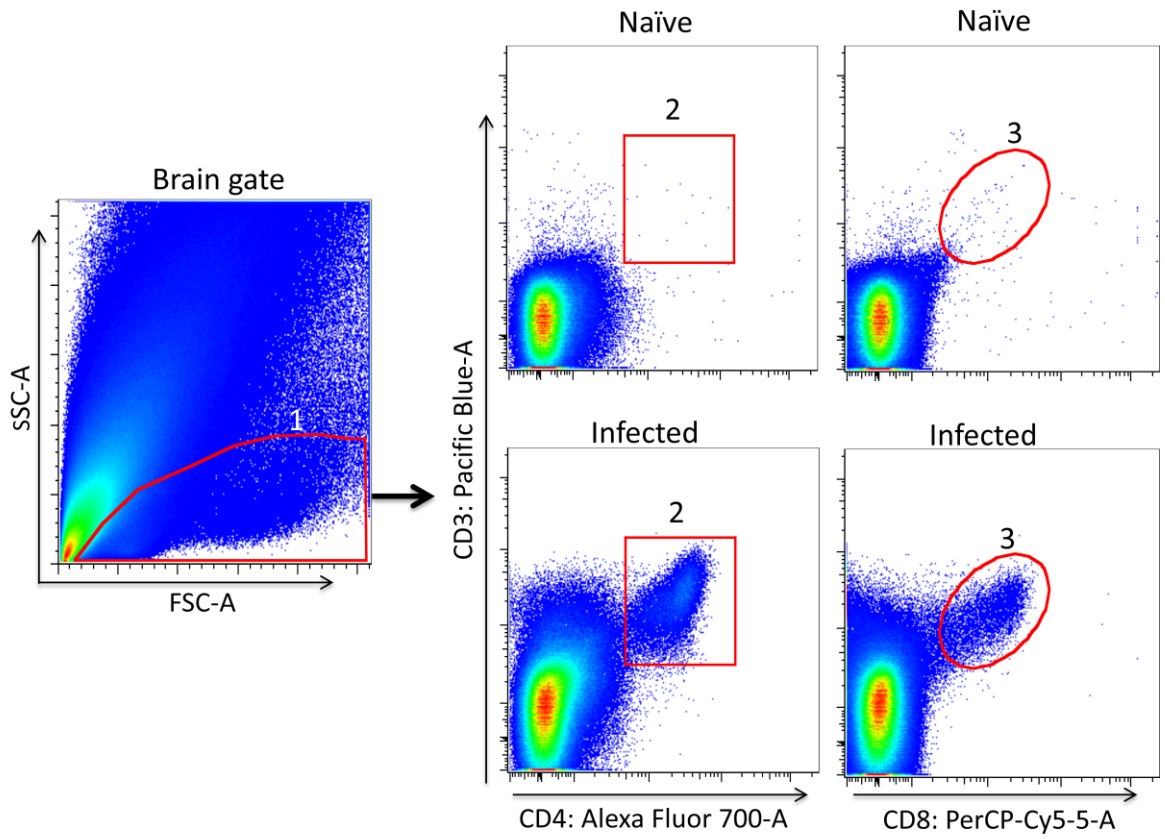

Figure 2.4: Gating strategy for effector T cells using naïve and infected mice. Brains were collected and directly harvested at week 0 (naïve), 1, 2 and 3 post-infection, and cells were isolated from naïve and intracerebrally infected $TNF^{f/f}$, $NsTNF^{-/-}$ and $TNF^{-/-}$ mice with *M. tuberculosis* at a dose of $1x10^5$ cfu/brain. Following the previously described gating strategy, $CD4^+$ and $CD8^+$ cells were analysed by multi-channel BD LSRFortessa flow cytometer analyser using T cell and activation markers (CD3e: Pacific Blue, CD4:Alexa 700, CD8:PerCP-Cy5.5 and CD44:PE). The leftmost panel shows, brain cells were gated with forward scatter versus side scatter to map live cells (1). The $CD4^+$ T cells were gated based on $CD3^+CD4^+$ (2), while the $CD8^+$ T cells were gated based on $CD3^+CD8^+$ T cells (3). Flow cytometry data of controls (wild type and $TNF^{-/-}$) used in result section 1 were the same data used as control in result section 2.

Table 2.9: Antibodies used for flow cytometry analysis of antigen presenting cells

Antibodies	Stock Concentration	Clone	Source
Rat-anti-mouse CD11b:PerCP-Cy5.5	0.1 mg/ml	M1/70	BD Pharmingen™
Rat-anti-mouse CD11c:Alexa 700	0.5 mg/ml	HL3	BD Pharmingen™
Hamster -anti-mouse CD45:APC	0.2 mg/ml	30- F11	BD Pharmingen™
Rat-anti-mouse CD80:FITC	0.2 mg/ml	16–10A1	BD Pharmingen™
Rat-anti-mouse CD86:V450	0.2 mg/ml	GL1	BD Horizon™
Rat-anti-mouse MHCII (I-A/I-E):PE	0.2 mg/ml	M5/114.15.2	BD Pharmingen™

Table 2.10: Antibodies used for flow cytometry analysis of B cells

Antibodies	Stock Concentration	Clone	Source
Rat-anti-mouse CD1d:PE	0.2 mg/ml	1B1	BD Pharmingen™
Rat -anti-mouse CD45R/B220:V500	0.2 mg/ml	RA3-6B2	BD Horizon™
Rat -anti-mouse CD86:V450	0.2 mg/ml	GL1	BD Horizon™
Rat-anti-mouse CD93 (AA4.1): PerCP-Cy5.5	0.2 mg/ml	AA4.1	BD Pharmingen™
Rat -anti-mouse CD138:APC	0.2 mg/ml	281-2	BD Pharmingen™
Rat -anti-mouse IgM:PE-Cy7	0.2 mg/ml	R6-60.2	BD Pharmingen™
anti-mouse MHCII:Alexa 700	0.2 mg/ml	M5/114.15.2	eBioscience

Table 2.11: Antibodies used for flow cytometry analysis of T cells subsets

Antibodies	Stock Concentration	Clone	Source
Rat -anti-mouse CD3e:Pacific Blue	0.5 mg/ml	145-2C 11	BD Pharmingen™
Rat -anti-mouse CD4:Alexa 700	0.2 mg/ml	RM4-5	BD Pharmingen™
Rat -anti-mouse CD8:PerCP-Cy5.5	0.2 mg/ml	53-6.7	BD Pharmingen™
Rat -anti-mouse CD44:PE	0.2 mg/ml	IM7	BD Pharmingen™

2.9 Organs homogenate preparations

Brain, lung and spleen were collected aseptically in 10 ml tubes. Whole organs were removed from infected mice at specific time points, weighed and homogenised in 1 ml 0.04% Tween 80 saline containing protease inhibitor (Lasec, South Africa). Samples were centrifuged at 2000 rpm for 4 minutes at 4°C and supernatants were collected. Samples were aliquoted and frozen at -80°C until assayed. Reagent preparation is further detailed in appendix F.

2.9.1 Cytokines and chemokines measurement

Supernatants from organ homogenates (Brain) were used to measure cytokines and chemokines concentrations by sandwich enzyme-linked immunosorbent assay (ELISA). The following cytokines and chemokines were measured using the commercially available ELISA reagents for cytokines IL-1β, IL-2, IL-6, IL-12p70, TNF and IFN-γ; and chemokines MCP-1, MIP-1α and RANTES (R&D Systems, Germany) according to the manufacturer's instructions, using a commercially (R&D) available antibodies kits and protocol, in ELISA multiplate reader with integrated SoftMax Pro 4.3.1 LS software (Table 2.12 and Table 2.13). Briefly, Nunc-Maxisorp 96-well microtiter plate (Nalge, Nunc International, Naperville, USA) were coated with 50 µl/well of either a cytokine or chemokine capture antibody diluted (0.4 – 4 µg/ml) in coating buffer

containing 0.02% NaN_3 in 1xPBS (pH 7.4) and incubated overnight at room temperature. All wells were washed for a total of three times with wash buffer containing 0.05% Tween 20 and 0.01% NaN_3 in 1xPBS. Non-specific binding was blocked with blocking buffer containing 4% BSA (bovine serum albumin fraction 5) (Roche, Roche Diagnostics GmbH, Mannheim, Germany), 10% of NaN_3 in PBS and incubated for a minimum of 1 hour at room temperature. In a different 96-well microtiter plate, the appropriate standards were diluted in Two-fold dilution series with an initial starting concentration of 250ρg/ml - 4000ρg/ml in dilution buffer (1% BSA in 1xPBS, pH7.4) (see Tables 2.12 and 2.13 for initial concentrations and sensitivity). Thereafter, a volume of 50µl/well of standards and samples were added to the coated 96-well microtiter plates respectively and incubated for 2 hours at room temperature. Thereafter, all wells were washed as described above, and then 50µl/well of the biotinylated (detection) antibody (0.2-50µg/ml) dissolved in dilution buffer was added and incubated for 2 hours at room temperature. 50µl/well of alkaline phosphatase labelled streptavidin diluted (1 in 1000) with dilution buffer were added to each well, and incubated for 20 minutes at room temperature. Wells were washed again as described above, and 50µl/well of P-Nitrophenol-Phosphate (PNPP) (1mg/ml) dissolved in substrate buffer (containing 0.3g NaN_3, 97 ml Diethanolamine and 0.8g $MgCl_2.6H_2O$) were added to each well. The optimal density of each well was determined within 30 minutes at 405nm (reference 492nm) using microplate spectrophotometer (Molecular Devices, Spectra MAXGemini, California, USA) with SoftMax Pro 4.3.1LS software. Reagent preparation is further described in appendix G.

Table 2.12: Cytokine antibodies used

Cytokines	Capture antibody	Standard	Detection antibody
IL-1β	4 µg/ml	2000 ρg/ml	400 ng/ml
IL-2	2 µg/ml	2000 ρg/ml	400 ng/ml
IL-6	2 µg/ml	1000 ρg/ml	400 ng/ml
IL-10	2 µg/ml	4000 ρg/ml	200 ng/ml
IL-12p70	4 µg/ml	2500 ρg/ml	400 ng/ml
IFN-γ	2 µg/ml	2000 ρg/ml	400 ng/ml
TNF	0.4 µg/ml	1000 ρg/ml	200 ng/ml

Table 2.13: Chemokine antibodies used

Chemokines	Capture antibody	Standard	Detection antibody
CCL2/MCP-1	500 µg/ml	250 ρg/ml	18 µg/µml
CCL3 /MIP-1α	250 µg/ml	500 ρg/ml	50 µg/ml
CCL5/RANTES	500 µg/ml	2000 ρg/ml	50 µg/ml

2.10 Statistical analysis

Data were analysed by comparing of $TNF^{f/f}$ wild type and gene-deficient mice (cell-type specific TNF: $NsTNF^{-/-}$, $M\text{-}TNF^{-/-}$ and $MT\text{-}TNF^{-/-}$ or global $TNF^{-/-}$ mice) at specific time points, and expressed as mean ± SD. All data were analysed using Prism 4 software (GraphPad), where the statistical analysis was performed by student *t*-Test and one-way or two-way analysis of variance (ANOVA), followed by Turkey's test for correction of multiple comparisons for all body weights, organ weights, clinical scores, CFU, all absolute cell numbers and activation data. One way ANOVA was used to compare three or more groups (time points), while the two way ANOVA was used to compares the differences among the mouse strains as function of time. For survival studies, statistical analysis was performed using the log-rank test. Data with a value of $p < 0.05$ was considered statistically significant. Each experiment was performed at least twice to ensure reproducibility.

CHAPTER III

RESULTS

Neuronal derived tumour necrosis factor is redundant for protective immunity against neurotuberculosis

R1.1 Generation of NsTNF$^{-/-}$ mice by cross breeding

To generate mice with specific deletion of TNF gene in neurons, we utilised the Cre/loxP recombination system and a knockin/transgenic approach. The genotypes of the original Syn1-Cre mice (lanes 1-4, from the left hand) were confirmed by PCR analysis using IMR1084, IMR1085, IMR7338 and IMR7339 which yielded an amplification product of 100bp, to confirm the presence of the Cre gene and a 324bp amplification product which represented Syn1-Cre$^{wt/wt}$ wild type allele (Figure 3.1.1A). Neuronal cell type-specific TNF deficient mice were generated by mating the Syn1-Cre$^{Cre/wt}$ mice with the knockin TNF$^{f/f}$ mice. Prior to mating, the genotype of TNF$^{f/f}$ mice was confirmed using PCR specific primers, KO41 and KO42 to yield an amplification product of 400bp, to confirm the presence of TNF floxed gene (Figure 3.1.1B). The wild type C57BL/6J mouse strain is represented by a 350bp amplification product (Figure 3.1.1B). The mating of Syn1-Cre$^{Cre/wt}$ mice and TNF$^{f/f}$ mice resulted in a Syn1-Cre$^{Cre/wt}$ TNF$^{f/wt}$ heterozygote mouse strain after verifying by PCR analysis using both TNF flox primers and Syn1-Cre primers. We named this strain as NsTNF$^{+/-}$ mice (Figure 3.1.2A). The NsTNF$^{+/-}$ mice (lanes 3-5, from the left hand) showed that both WT and flox bands are present when using TNF flox primers (Figure 3.1.2A). The results indicate the presence of the WT 350bp band in C57BL/6 mice and flox 400bp band in floxed TNF$^{f/f}$ mice. However, genotyping using Syn1-Cre primers showed the presence of 324bp band indicative of WT mice and 100bp (Cre gene) band in NsTNF$^{+/-}$ mice (lanes 3-5) thus confirming the genotypes of mutant and Cre expression mice (Figure 3.1.2B).

In order to generate the homozygote neuronal cell type-specific TNF mice, we mated the above generated NsTNF$^{+/-}$ mice with TNF$^{f/f}$ mice and analysed offspring by tail biopsy analysis (Figure 3.1.3). The PCR amplification product in NsTNF$^{-/-}$ mice (lanes 4-6, from the left hand) showed that only 400bp flox bands are present when using TNF flox primers (Figure 3.1.3A). The results indicate the presence of the WT 350bp band in C57BL/6 mice, and flox 400bp band in TNF$^{f/f}$ mice and in NsTNF$^{+/-}$ (Figure 3.1.3A). However, genotyping using Syn1-Cre primers showed the presence of 324bp band indicative of WT mice and 100bp (Cre gene) band in the control NsTNF$^{+/-}$ and NsTNF$^{-/-}$ mice. Thus, confirming the genotypes of mutant and Cre expression in mice (Figure 3.1.3B). Therefore, confirmed the correct genotype of Syn1-Cre$^{Cre/wt}$

TNF$^{f/f}$ mice on homozygous background, which we named NsTNF$^{-/-}$.

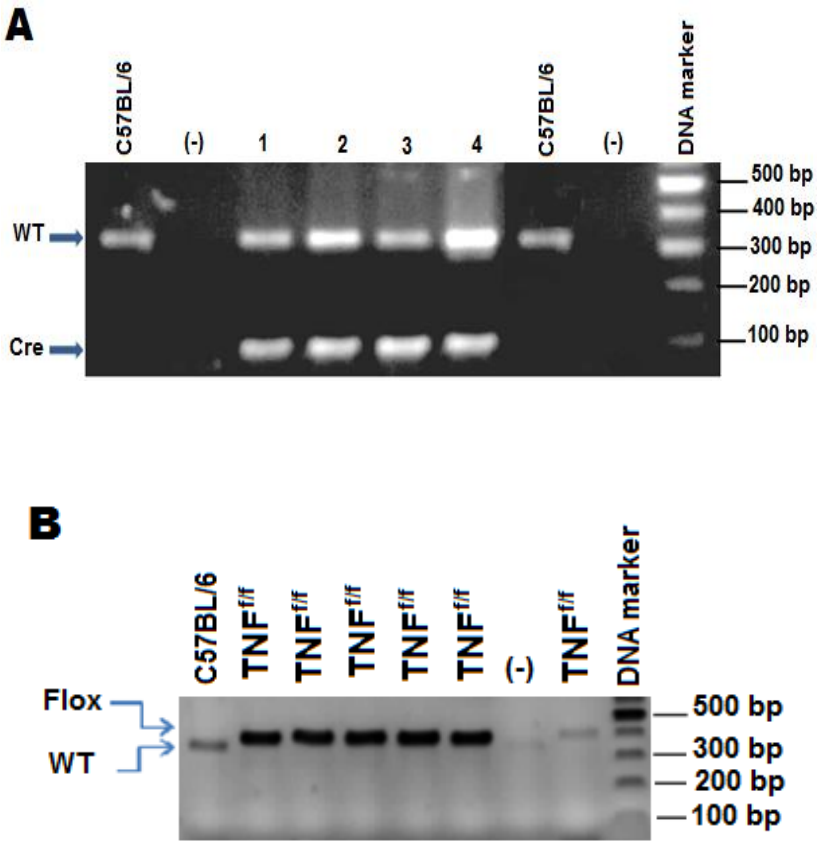

Figure 3.1.1: Genotyping of Syn1-Cre$^{cre/wt}$ mice and TNF$^{f/f}$ mice. PCR analysis was performed using genomic DNA extracted from tail biopsies using Syn 1-Cre specific primers IMR1084, IMR1085, IMR7338 and IMR7339. WT (C57BL/6J) and TNF$^{f/f}$ mice were used as positive controls and water (-) as a negative control. An amplification product of 324bp confirmed the presence of the WT gene in C57BL/6J (control mice). The presence of the Cre gene in mice (lanes 1 - 4, from the left hand are the original Syn1-Cre$^{cre/wt}$ mice) yielded an amplification product of 100bp (A). The PCR analysis of DNA extracted from tail biopsies of TNF$^{f/f}$ mice using KO41 and KO42 primers yielded an amplification product of 400bp to confirm the presence of the TNF floxed gene in TNF$^{f/f}$ mice. The unfloxed gene in C57BL/6J yielded an amplification product of 350bp (B).

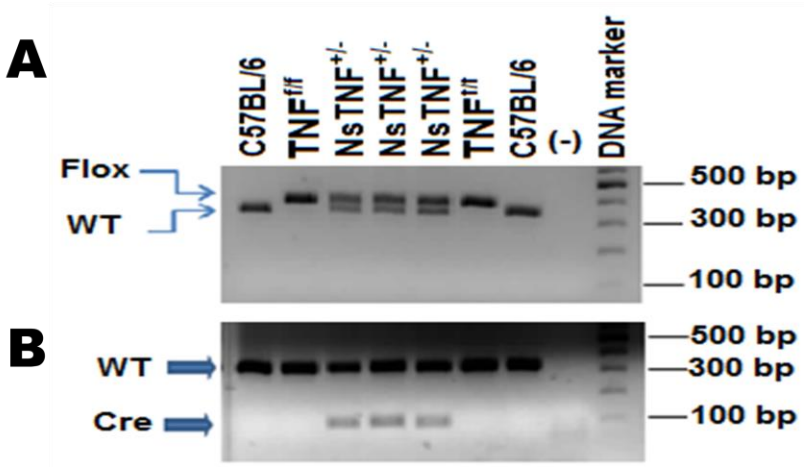

Figure 3.1.2: Genotyping of NsTNF$^{+/-}$ mice. Genotyping of NsTNF$^{+/-}$ mice strain was carried out by PCR analysis. WT (C57BL/6J) and TNF$^{f/f}$ mice were used as positive controls and water as a negative control (-). The results indicate the presence of the WT 350bp band in C57BL/6J mice and flox 400bp band in floxed TNF$^{f/f}$ mice. However, in NsTNF$^{+/-}$, both WT and flox bands are present when using flox TNF primers (Figure 3.1.2A). Genotyping using Syn1-Cre primers showed the 324bp amplification product indicative of WT mice and a 100bp (Cre gene) amplification product in heterozygous NsTNF$^{+/-}$ mice, thus confirming the genotypes of mutant and Cre expression mice (Figure 3.1.2B).

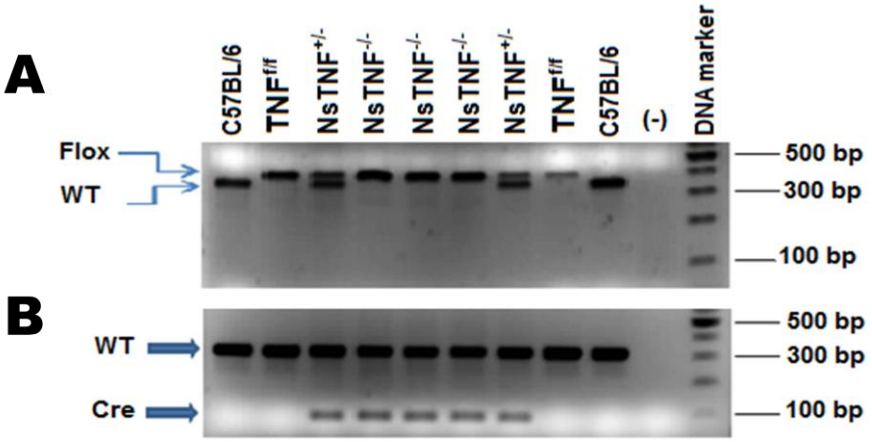

Figure 3.1.3: Genotyping of NsTNF$^{-/-}$ mice. PCR analysis of DNA from tail biopsies was performed using a WT (C57BL/6J), TNF$^{f/f}$ and NsTN$^{+/-}$ mice as controls, and water as a negative control (-). The results indicate the presence of the WT 350bp amplification product in C57BL/6 mice or NsTNF$^{+/-}$ mice (lanes 1, 3, 7 and 9, from the left hand) while TNF$^{f/f}$ or NsTNF$^{-/-}$ mice only expressed the 400bp amplification product when using flox primers (Figure 3.1.3A). Genotyping using Syn1-Cre primers showed the 324bp amplification product indicative of WT mice, and 100bp amplification product (Cre gene) in NsTNF$^{+/-}$ and NsTNF$^{-/-}$, mice thus confirming the genotypes of mutant mice and Cre expression (Figure 3.1.3B).

R1.1.1 Genotype confirmation of complete TNF$^{-/-}$ mice

Complete TNF deficient mice used in this study were generated by Cre/loxP recombination system (Kuprash *et al.,* 2005). Mice were genotyped for the confirmation of complete TNF gene ablation using KO41 and KO49 as primers to yield an amplification product of 450bp. However, primers MTNFRTP81 and MTNFRTP82 were used for the amplification of DNA in order to identify a WT allele corresponding to an amplification product of 350bp (Figure 3.1.4).

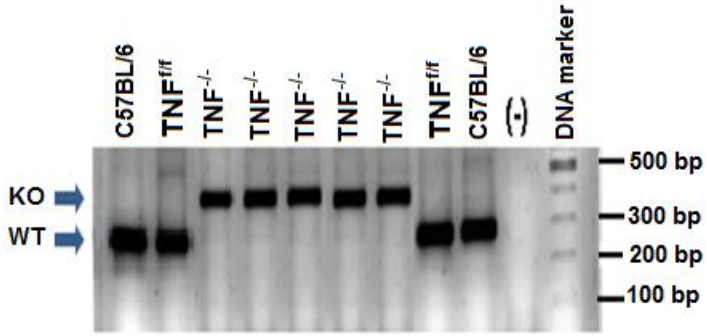

Figure 3.1.4: Genotyping of mutant mouse strains was carried out by PCR analysis of DNA from tail biopsies using WT (C57BL/6J) and TNF$^{f/f}$ as positive control samples and water as a negative control (- lane). The primers KO41, KO49, MTNFRTP81 and MTNFRTP82 were used to confirm the absence of the TNF gene in the global TNF$^{-/-}$ mice (450bp amplification product) and the presence of the TNF gene (350bp amplification product) in the TNF$^{f/f}$ mice. The unfloxed TNF gene is present in the normal C57BL/6J mice.

R1.2 Neuronal cells in NsTNF$^{-/-}$ mice do not synthesise TNF

NsTNF$^{-/-}$ mice were characterised by confirmation of neuronal specific TNF ablation using flow cytometry. TNF$^{f/f}$, NsTNF$^{-/-}$ and TNF$^{-/-}$ mice were stimulated by intracerebral injection with 5µg/ml of LPS for 90 minutes. Brain cells were harvested and single cells labelled using neurons-specific Beta III Tubulin, PE-conjugated secondary IgG and TNF-specific (TNF-Alexa Fluor 647) markers. Studies have reported the expression of TNF in neuron cells in different parts of the brain (Liu *et al.,* 1994 and Gahring *et al.,* 1994), however, no study have have shown the proportion of neuron expressing TNF in full brain. Our flow cytometric analysis shows the expression of TNF in naïve neurons of full brain to be ~8.03% (Appendix I). Flow cytometric analysis data demonstrated distinct synthesis of TNF by neurons in TNF$^{f/f}$ mice, in contrast to

expression in complete TNF$^{-/-}$ mice, which as expected showed complete abrogation of TNF expression (Figure 3.1.5A-B). Complete deletion from neurons was verified by the negative shift evident in the histogram overlay (Figure 3.1.5C).

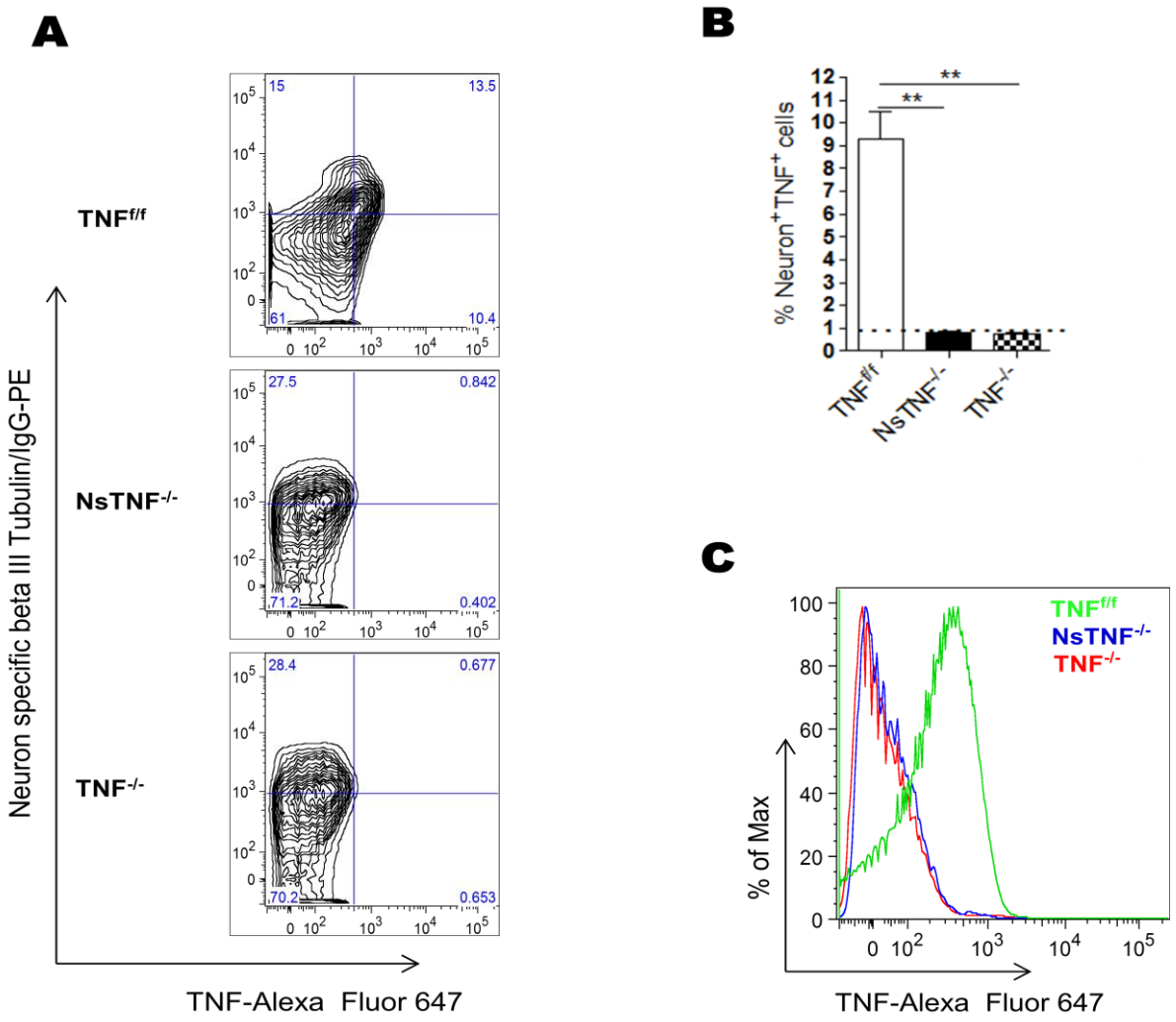

Figure 3.1.5: Efficiency of TNF ablation in NsTNF$^{-/-}$ mice following intracerebal stimulation with LPS. Representative FACS plots of Beta III Tubulin/IgG-PE versus TNF-Alexa Fluor 647; numbers represent the percentage of gated cells (A). Percentage of TNF$^+$ Neuron$^+$ cells are shown as mean ± SD of five mice per group, *p < 0.01 (B). A histogram overlay showing the TNF expression in TNF$^{f/f}$ (green), NsTNF$^{-/-}$ (blue) and TNF$^{-/-}$ mice (red) following the intracerebral stimulation with 5µg/ml of LPS for 90 minutes (C). Gates were drawn on unstimulated cells. The data represent one of at least three experiments with similar results (n= 5 mice/group).

R1.3 Protection of NsTNF$^{-/-}$ mice and clinical course during cerebral *M. tuberculosis* infection

Previous studies have demonstrated the role of TNF in pulmonary tuberculosis (Flynn *et al.,* 1995; Bean *et al.,* 1999; Kaneko *et al.,* 1999; Fremond *et al.,* 2005 and Allie *et al.,* 2008), neurotuberculosis (Tsenova *et al.,* 1999; Tobin *et al.,* 2010, Tobin *et al.,* 2012 and El-Kebir *et al.,* 2013) as well as in other cerebral infectious diseases (Wollebo *et al.,* 2011 and Kramer *et al.,* 2012). In order to define the role of neuronal derived TNF during neurotuberculosis, we intracerebrally infected TNF$^{f/f}$, NsTNF$^{-/-}$ and TNF$^{-/-}$ mice with 1x10^5 cfu/brain of *M. tuberculosis*. The survival rate of mice was monitored; mice body weights measured, clinical scores recorded and organs weights measured.

Our data showed that TNF$^{f/f}$ mice survived the cerebral *M. tuberculosis* infection and gained weight. The finding is in line with the previous studies in which long term survival in wild type mice after CNS *M. tuberculosis* infection was demonstrated (van Well *et al.,* 2007; Be *et al.,* 2008 and Lee *et al.,* 2009). Complete TNF$^{-/-}$ mice were highly susceptible to cerebral *M. tuberculosis* with an average body weight loss of > 20% and succumbed by day 21. In contrast, the newly generated NsTNF$^{-/-}$ mice showed high survival rates and exhibited increasing body weights similar to TNF$^{f/f}$ mice (Figure 3.1.6A-B). The postsurgery decreased body weight observed between day 1 and day 5 post *M. tuberculosis* infection is due to surgical intervention, as it has been reported (Weiergräber *et al.,* 2005 and Kirby *et al.,* 2012).

Clinical neurologic manifestations were not induced in the TNF$^{f/f}$ and NsTNF$^{-/-}$ mice, whereas, severe clinical neurologic manifestations were prominent ($p < 0.01$) within 16-21 day post-infection in TNF$^{-/-}$ mice. The maximum severity of disease was observed at day 21, where animals entered the moribund state (Figure 3.1.7A). Clinical neurologic outcomes correlated favourably with survival data.

In addition, we measured organ weight as a surrogate marker of inflammation. Brains, lungs and spleens were weighed during the course of the infection. The brain weights in NsTNF$^{-/-}$ mice were not significantly difference when compared to TNF$^{f/f}$ mice, both TNF$^{f/f}$ and NsTNF$^{-/-}$ mice showed significantly higher brain weight at week 3 post-infection when compared to earlier time points (Figure 3.1.7B). The brain weights of the TNF$^{-/-}$ mice were significantly lower ($p < 0.01$) at week 3 post-infection compared to TNF$^{f/f}$ and NsTNF$^{-/-}$ mice. No significant differences in brain weights were observed in TNF$^{-/-}$ mice when relative comparisons are made to earlier time points (Figure 3.1.7B).

The lung weights of the $TNF^{-/-}$ mice were significantly lower ($p < 0.05$) at week 3 post-infection compared to $TNF^{f/f}$ and $NsTNF^{-/-}$ mice. No significant differences in lung weights were observed in $TNF^{-/-}$ mice when relative comparisons are made to earlier time points (Figure 3.1.7C).

No significant difference in spleen weight was observed at $NsTNF^{-/-}$ mice at all time points post-infection compared with $TNF^{f/f}$ mice (Figure 3.1.7D). However, $TNF^{-/-}$ mice showed a significant increase ($p < 0.05$) in spleen weight at week 3 post-infection compared with $TNF^{f/f}$ and $NsTNF^{-/-}$ mice (Figure 3.1.7D).

Study has shown that TNF has four main actions during *M. tuberculosis* infection (Ray et *al.,* 2009). TNF plays a key role in (i) activation of macrophages, affecting their phagocytic and killing abilities (Hehlgans et al., 2005 and Saunders *et al.,* 2005); (ii) regulating the recruitment of many inflammatory cells (Algood *et al.,* 2004 and Roach *et al.,* 2002); (iii) regulating the induction of cytokine and chemokine production (Roach *et al.,* 2002 and Algood *et al.,* 2005); and (iv) induction of apoptosis of macrophages and T cells (Keane *et al.,* 1997). Its central role appears to be in the generation of a structurally effective granulomatous response. Thus, granuloma formation requires the activation of Ag-specific T cells, the accumulation of T cells and monocytes at the site of infection, and their local organisation into a mature granuloma that limits the infection (Bean *et al.,* 1999). We speculate that the increased brain weight observed in $TNF^{f/f}$ and $NsTNF^{-/-}$ mice may be associated with the pro-inflammatory response. However, we suggest that the clinical manifestations observed in the $TNF^{-/-}$ mice at week 3 post-infection could be associated with neuronal death, which may be caused by the increased bacterial overgrowth, leading to microglia or macrophages lysis and exudates formation occupying the subarachnoid spaces or the ventricular pathways. The thick gelatinous exudates block the subarachnoid spaces in the base of the brain (notably the interpeduncular and ambient cisterns) resulting in hydrocephalus (Dastur *et al.,* 1995). Recently, the underlying mechanism of neurotuberculosis susceptibility in both zebrafish and humans were studied (Tobin *et al.,* 2010, 2012). In the above mentioned studies, individuals with a specific mutation on both alleles of the gene LTA4H develop an anti-inflammatory response with little TNF production, whereas individuals having two wild-type alleles have a pro-inflammatory phenotype with abundant TNF levels. Both phenomena are detrimental to the host leading to bacterial overgrowth and hyper-inflammation, respectively. Therefore, the unchanged brain weight observed in $TNF^{-/-}$ mice indicate the anti-inflammatory response, despite the high phagocytes and T cells influx into the brain. The mechanism by which TNF can exert its paradoxical effects in the brain is via

crosstalk with signaling pathways of growth factors or other chemokines and cytokines (Perry *et al.,* 2002).

The no effect seen in lung weight of $TNF^{-/-}$ mice could be associated with the delay recruitment of immune cells into the lung. Thus, the increase spleen weight observed in $TNF^{-/-}$ mice could be attributed to the uncontrolled inflammation, where the increase in leukocytes produced in the spleen engulf bacteria, dead tissue, and foreign matter, trying to remove them from the blood as blood passes through it; leading to splenomegaly. From these findings, we report the critical importance of the cytokine TNF of the host immune response during neurotuberculosis, but concluded that neurons derived TNF does not confer any protection against experimental *M. tuberculosis* infection of the CNS. The data also indicate that neuro-inflammation in response to *M. tuberculosis* infection is TNF dependent.

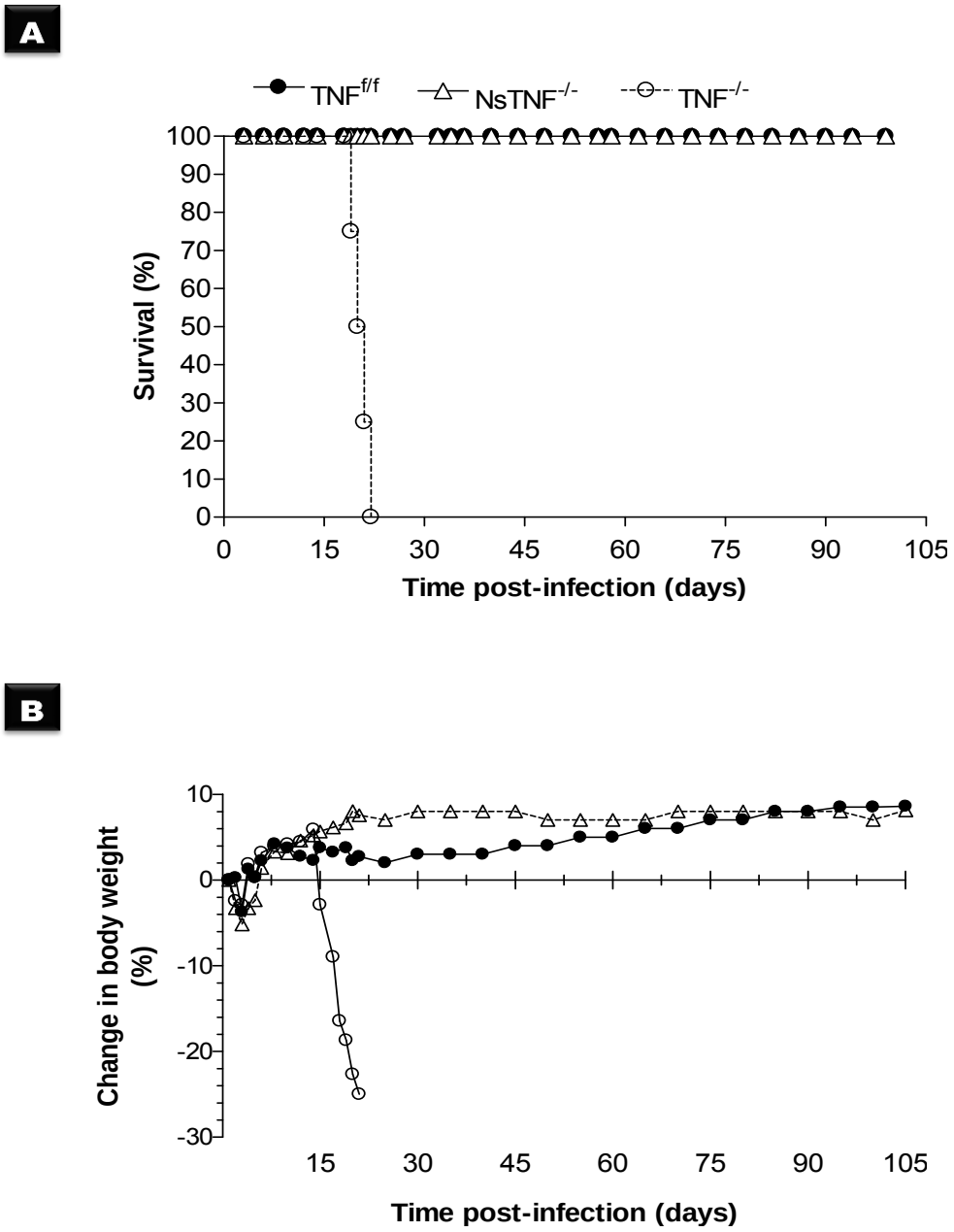

Figure 3.1.6: NsTNF$^{-/-}$ mice do not succumb to CNS *M. tuberculosis* infection. TNF$^{f/f}$, NsTNF$^{-/-}$ and TNF$^{-/-}$ mice were intracerebraly infected with 1x10^5 cfu/brain of *M. tuberculosis*. Percentage survival (*n*= 10 mice/group) (A), and changes in body weight (B) were monitored subsequent to infection. Change in body weight values are expressed as the mean of 10 mice/group. Data shown are representative of one of three independent experiments.

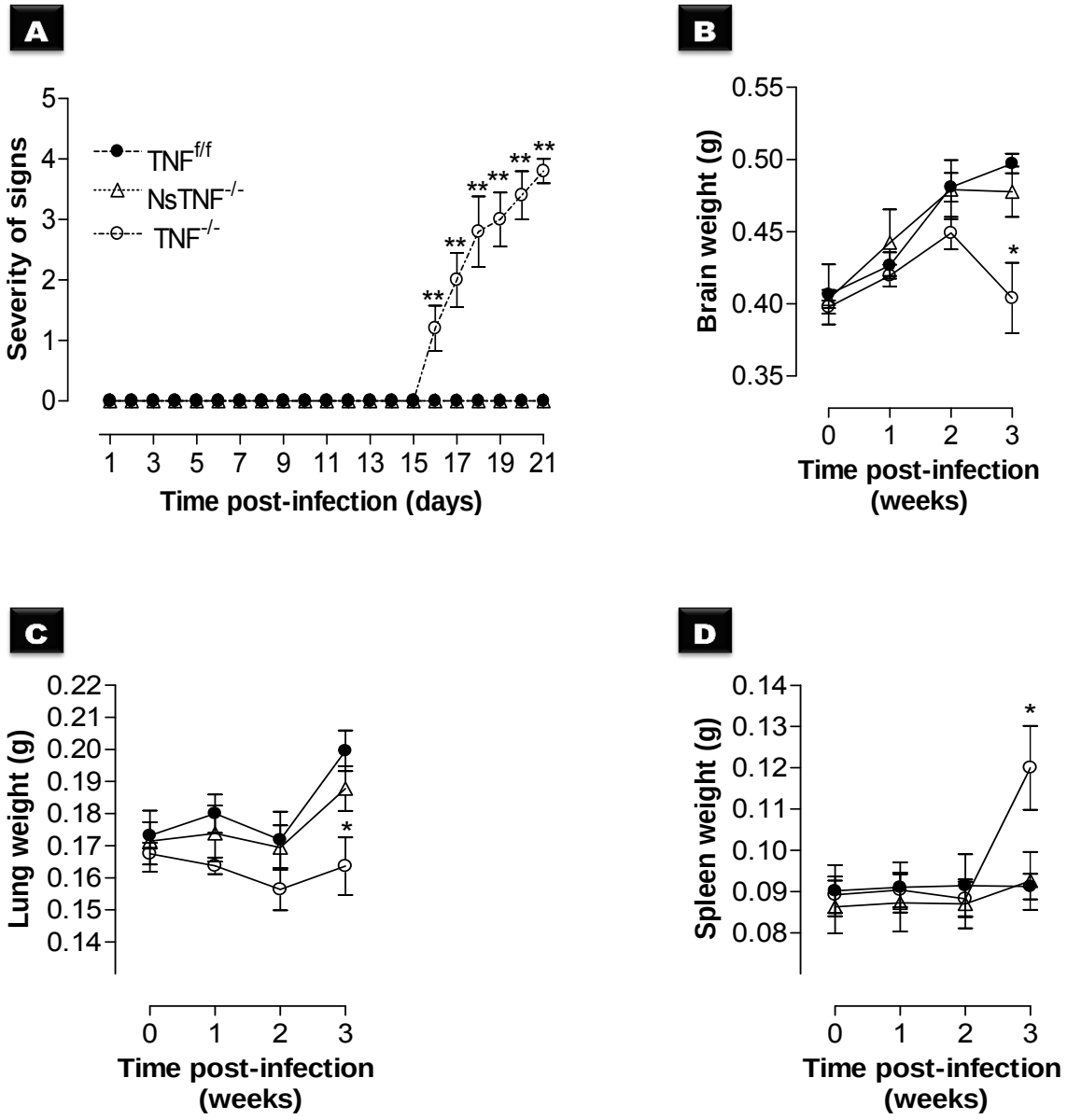

Figure 3.1.7: Clinical course and controlled inflammation in NsTNF$^{-/-}$ mice during acute CNS *M. tuberculosis* infection. TNF$^{f/f}$, NsTNF$^{-/-}$ and TNF$^{-/-}$ mice were intracerebrally infected with *M. tuberculosis* at a dose of 1x10^5 cfu/brain. For clinical signs, the scoring was recorded after intracerebrally infecting TNF$^{f/f}$, NsTNF$^{-/-}$ and TNF$^{-/-}$ mice with *M. tuberculosis* for 21 days (A). TNF$^{f/f}$ and NsTNF$^{-/-}$ mice did not exhibit overt clinical manifestations, while TNF$^{-/-}$ mice induced more clinical manifestations after day 14 post-infection. **p < 0.01 for TNF$^{-/-}$ vs TNF$^{f/f}$ and NsTNF$^{-/-}$. Each data point represents the mean ± SD of 10 animals per group. Organ weights of mice euthanised at week 0 (naïve), 1, 2 and 3 post-infection (B-D): brain weights (B), lung weights (C), and spleen weights (D) were assessed. The data represent the mean ± SD of 5 mice/group of one of three independent experiments. *=p < 0.05 and **=p < 0.01.

R1.4 Bacillary replication and dissemination in NsTNF$^{-/-}$ mice during neurotuberculosis

The importance of TNF for the control of bacillary replication was assessed by comparing pathogen burden in the brains, lungs and spleens of *M. tuberculosis* infected TNF$^{f/f}$, NsTNF$^{-/-}$ and TNF$^{-/-}$ mice during acute (3 weeks post-infection) and chronic (15 weeks post-infection) infection (Figure 3.1.8A-F). An overall increase in bacterial burden was observed in TNF$^{f/f}$ mice over the 3 weeks infection period. The *M. tuberculosis* bacterial burden in the brain was increased in TNF$^{f/f}$ mice at day 21 post-infection compared to the earlier time points post-infection ($p < 0.001$) (Figure 3.1.8A). NsTNF$^{-/-}$ mice had a similar bacterial burden trend to TNF$^{f/f}$ mice (Figure 3.1.8A) and no significant differences were observed in bacilli burdens of NsTNF$^{-/-}$ mice during either acute (Figure 3.1.8A) or chronic infection (Figure 3.1.8B) compared to TNF$^{f/f}$ mice. Similarly TNF$^{-/-}$ mice displayed an increasing bacilli burden over 3 weeks; however, TNF$^{-/-}$ mice exhibited a significant increased bacilli burden compared to the TNF$^{f/f}$ mice at week 2 ($p < 0.01$), and week 3 ($p < 0.001$) post-infection (Figure 3.1.8A).

We next assessed the extent of dissemination of bacilli from the brain by measuring the levels of bacilli burden in the lung and spleen. Bacilli dissemination occurred in the TNF$^{f/f}$ mice over 15 weeks post *M. tuberculosis* infection and was in agreement with the previously published studies using wild type (C57BL/6) mice (van Well *et al.,* 2007 and Lee *et al.,* 2009). The complete TNF$^{-/-}$ mice exhibited a significant increase (2-fold) in mycobacterial burden compared to TNF$^{f/f}$ mice at week 1 ($p < 0.05$), week 2 ($p < 0.01$), and week 3 ($p < 0.01$) post-infection in the lung, and in the spleen at week 1 ($p < 0.05$), week 2 and week 3 ($p < 0.01$) (Figure 3.1.8C and E). We observed control of bacilli replication in both lung and spleen of TNF$^{f/f}$ mice during chronic infection (Figure 3.1.8D and F). However, NsTNF$^{-/-}$ mice showed bacterial burden dissemination similar to the TNF$^{f/f}$ mice in both lung and spleen during acute and chronic (Figure 3.1.8C-F) infection.

Differences in bacterial growth in the brain were confirmed histologically by Ziehl-Neelsen staining with mycobacteria in NsTNF$^{-/-}$ mice largely localised intracellularly as in TNF$^{f/f}$ mice (Figure 3.1.9). The control bacterial growth in NsTNF$^{-/-}$ was therefore controlled at all time points post-infection. The significant increase of bacilli burdens seen in the brain of TNF$^{-/-}$ mice correlated, visual data obtained for acid fast bacilli, most being located extracellular at week 2 and 3 post-infection (Figure 3.1.9).

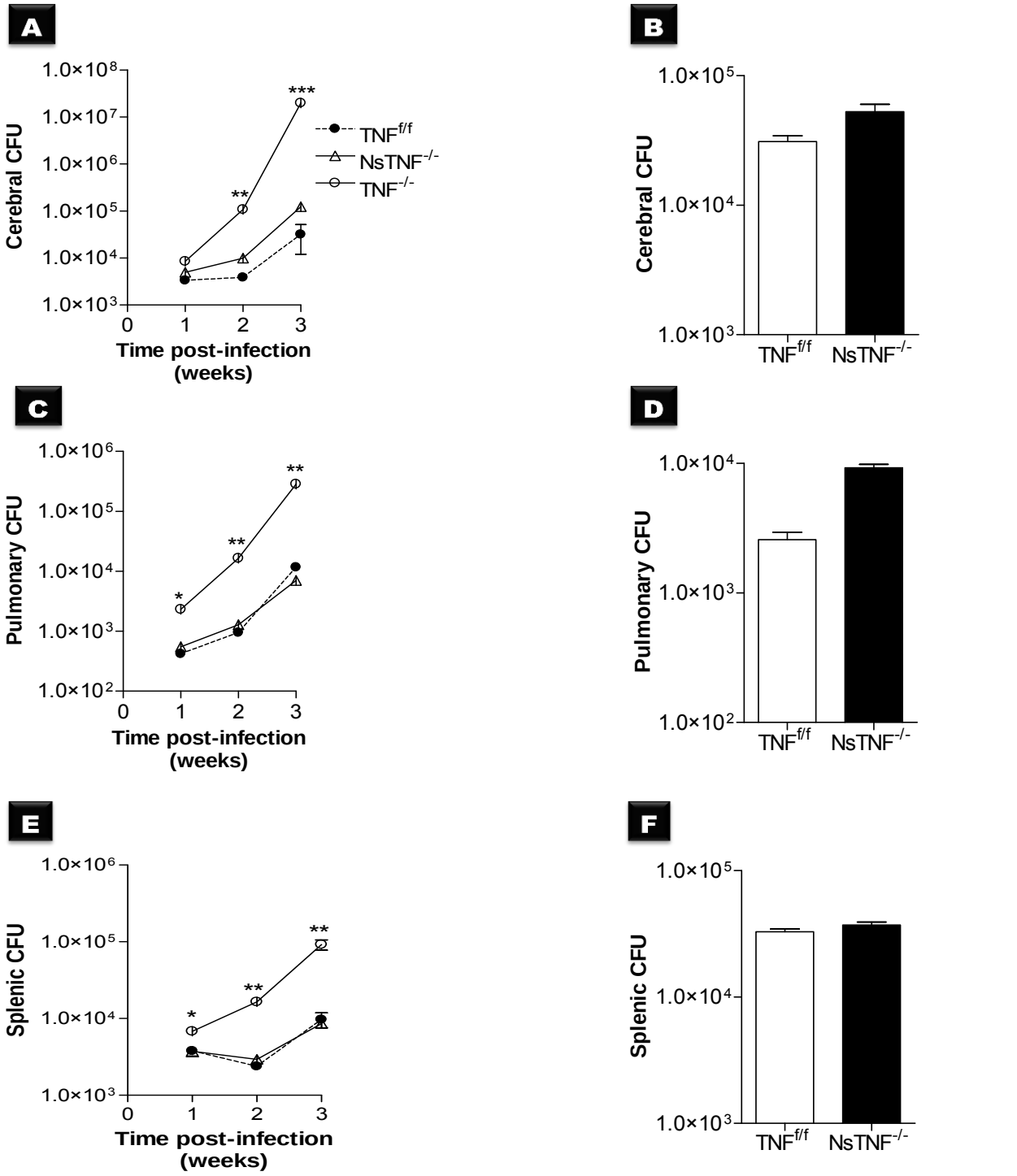

Figure 3.1.8: NsTNF$^{-/-}$ mice are resistant to CNS *M. tuberculosis* infection. TNF$^{f/f}$, NsTNF$^{-/-}$ and TNF$^{-/-}$ mice were intracerebrally infected with *M. tuberculosis* at a dose of 1x10^5 cfu/brain. The number of viable bacteria present in the brains (A), lungs (C) and spleens (E) were assessed at week 1, 2, 3 (acute) and 15 (chronic) post-infection in brains (B), lungs (D) and spleens (F). The results are expressed as the mean ± SD of 5 mice/group. Data is representative of one of three independent experiments. *=p < 0.05, **=p < 0.01 and ***=p < 0.001 are significant between TNF$^{-/-}$ vs TNF$^{f/f}$ and NsTNF$^{-/-}$.

Thus, the data demonstrate that complete loss of TNF renders mice susceptible to *M. tuberculosis* infection, and that neuronal derived TNF is not required for control of experimental cerebral bacterial growth, and the single neuronal derived TNF ablation resulted in a phenotype similar to wild type mice.

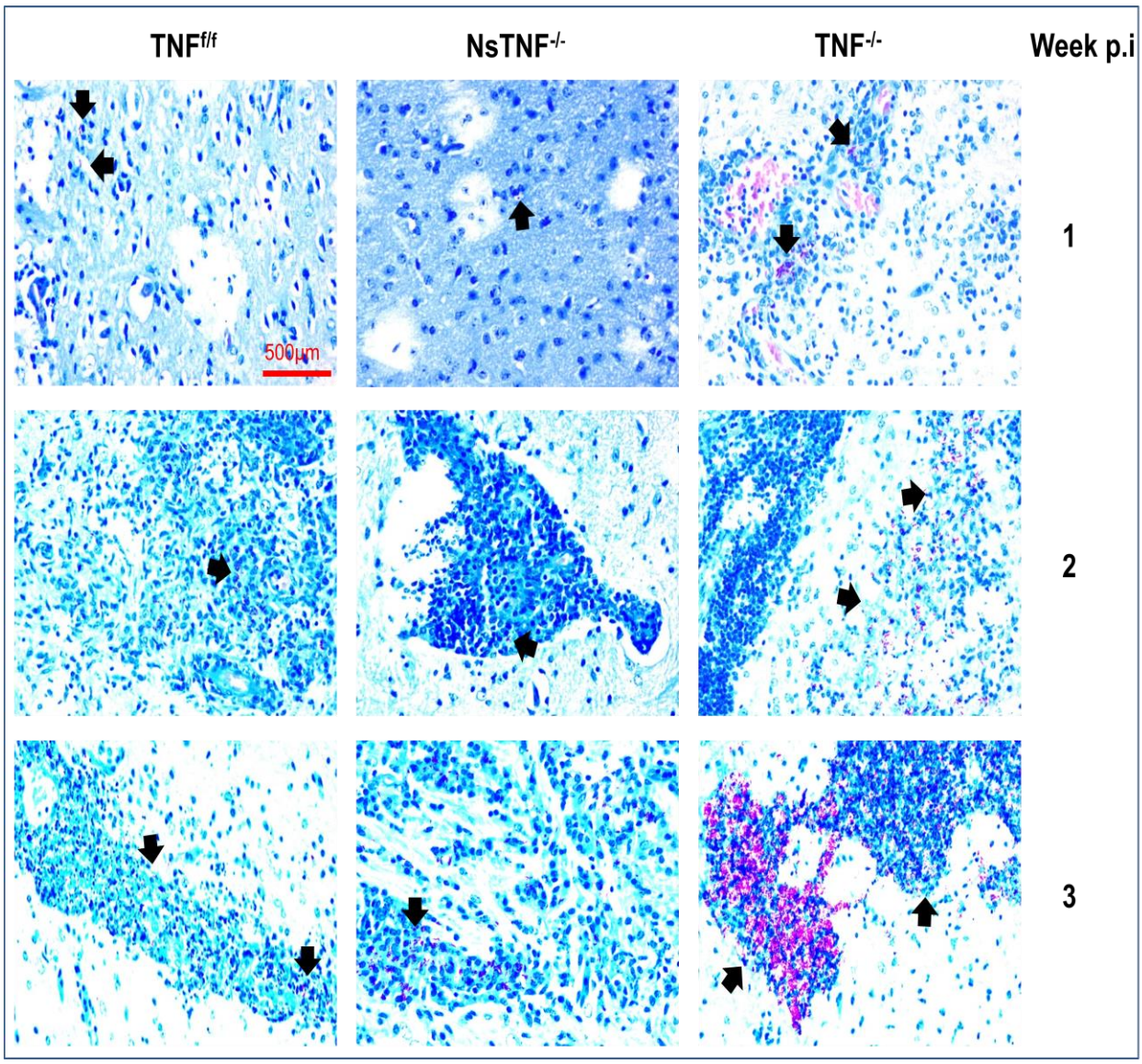

Figure 3.1.9: Control of *M. tuberculosis* growth in NsTNF$^{-/-}$ mice. TNF$^{f/f}$, NsTNF$^{-/-}$ and TNF$^{-/-}$ mice were intracerebrally infected with *M. tuberculosis* at a dose of 1x10^5 cfu/brain. The cerebral bacilli burden was confirmed by Ziehl-Neelsen staining tissue sections at week 1, 2 and 3 post-infection. The results represent one of three similar experiments. Arrows indicate the presence of acid fast bacilli (AFB) (*n*= 5 mice/group and magnification = 100x).

R1.5 Lymphocyte-Rich foci formation is controlled in NsTNF$^{-/-}$ mice during neurotuberculosis

Establishment of tuberculous granulomas is required to control mycobacterial growth during pulmonary TB (Saunders *et al.,* 1999). These organised structures are one of the main features of the immune response against *M. tuberculosis* (Miranda *et al.,* 2012). Rich foci are considered as tuberculous granulomas in the brain, mainly contain foamy macrophages, surrounded by epithelioid histiocytes, infiltrated lymphoid cells, new blood vessels, and variable fibrosis of adjacent parenchyma (Zucchi *et al.,* 2012). The aim of this study was to therefore investigate whether neurons derived TNF signalling induced lymphocyte-rich foci formation. NsTNF$^{-/-}$ mice were compared with TNF$^{f/f}$ and TNF$^{-/-}$ mice after intracerebral infection with *M. tuberculosis* at a dose of 1x10^{5} cfu/brain at week 1, 2 and 3 post-infection. NsTNF$^{-/-}$ mice controlled the perivascular lymphocytic infiltration like TNF$^{f/f}$ mice at week 2 and 3 post-infection (Figure 3.1.10b-f). In NsTNF$^{-/-}$ and TNF$^{f/f}$ mice, perivascular lymphocytic foci were limited to one site and there was no widespread inflammatory process (Figure 3.1.10c and f), however the TNF$^{-/-}$ mice exhibited exuberant perivascular lymphocytic infiltration at week 3 post-infection (Figure 3.1.10i).

All mice strains presented with meningeal lymphocytic infiltration at week 3 post-infection (Figure 3.1.11c, f and i), however meningeal lymphocytic infiltration in TNF$^{-/-}$ mice was excessive (Figure 3.1.11i).

Therefore, these findings suggested that neurons derived TNF has a limited role in regulating cellular recruitment to rich foci, in contrast the uncontrolled lymphocytic infiltration observed in TNF$^{-/-}$ mice at week 3 post-infection may be attributed to the lack of TNF in immune derived cells.

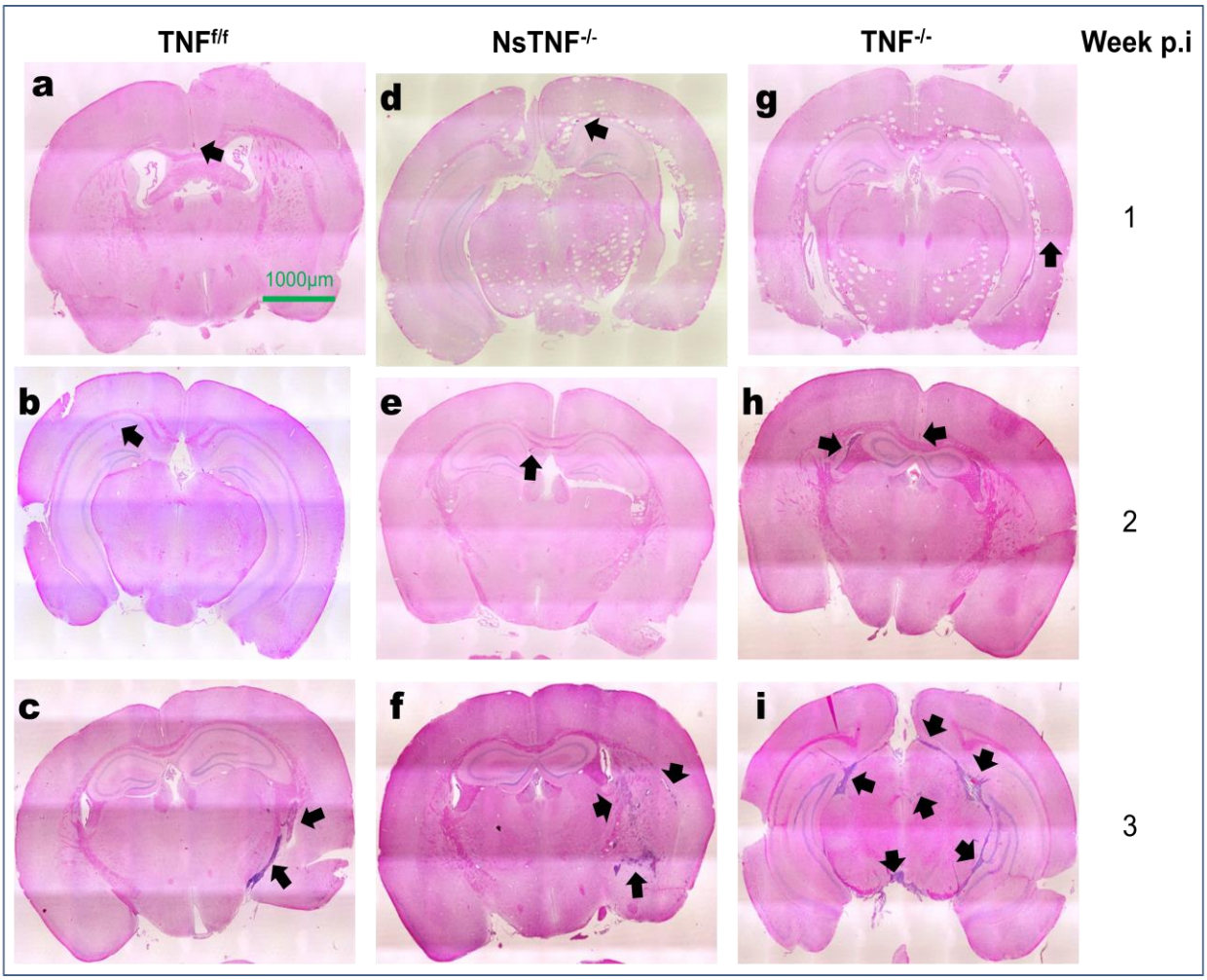

Figure 3.1.10: NsTNF$^{-/-}$ mice present with low perivascular lymphocytic infiltration foci. Low magnification (40x) of cerebral perivascular lymphocytic infiltration foci in TNF$^{f/f}$, NsTNF$^{-/-}$ and TNF$^{-/-}$ mice intracerebrally infected with *M. tuberculosis* at a dose of 1x10^5 cfu/brain. Morphology of 2µm brain sections was assessed at week 2 and 3 post-infection after haemotoxylin and eosin staining. Arrows indicate lymphocytic infiltration foci structure. The results represent one of three similar experiments (*n*= 5 mice/group).

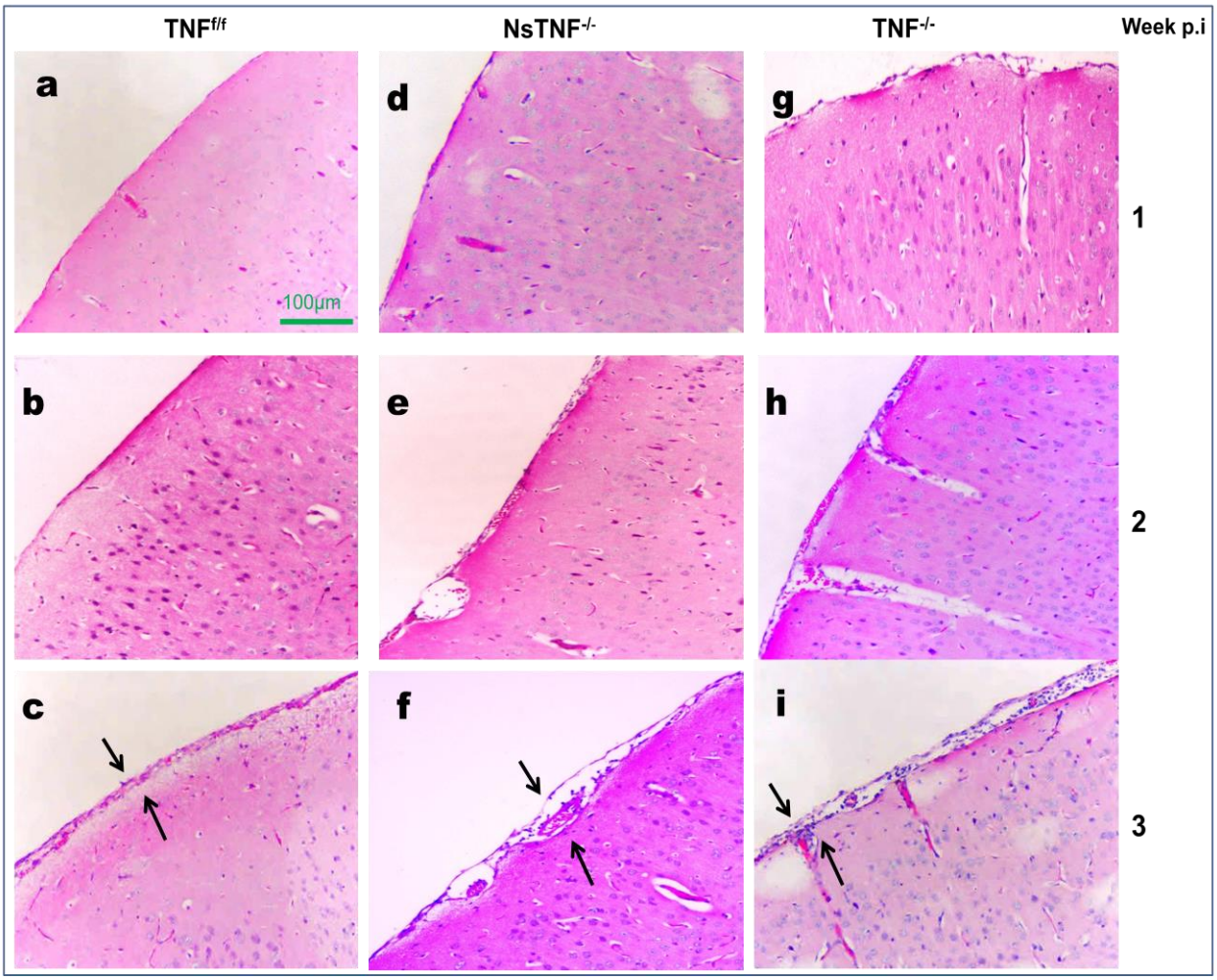

Figure 3.1.11: Presence of meningeal lymphocytic infiltration in NsTNF$^{-/-}$. Hematoxylin-eosin–stained sections of murine brain of TNF$^{f/f}$, NsTNF$^{-/-}$ and TNF$^{-/-}$ mice intracerebrally infected with *M. tuberculosis* at a dose of 1x10^{5} cfu/brain. Hematoxylin-eosin–stained sections were assessed at week 1, 2 and 3 post-infection. Presence of meningeal leukocyte infiltration was evident in TNF$^{f/f}$, NsTNF$^{-/-}$ and TNF$^{-/-}$ mice at week 3 post-infection. The results represent one of three similar experiments. Arrows indicate meningeal lymphocytic infiltration. (*n*= 5 mice/group and magnification= 100x).

R1.6 iNOS expression in NsTNF$^{-/-}$ mice after intracerebral infection with *M. tuberculosis*

MacMicking *et al.,* (1997) have convincingly identified iNOS (iNOS or NOS2) as a protective immune mediator during *M. tuberculosis* infection. We therefore investigated the expression of iNOS in the brain tissue of TNF$^{f/f}$, NsTNF$^{-/-}$ and TNF$^{-/-}$ mice intracerebrally infected with *M. tuberculosis* at a dose of 1x10^5 cfu/brain (Figure 3.1.12). NsTNF$^{-/-}$ mice displayed a similar increase in the expression of iNOS protein in the brain compared to TNF$^{f/f}$ mice at day 21 post-infection. In contrast, TNF$^{-/-}$ mice failed to produce significant levels of iNOS protein.

The data therefore showed that, neuronal derived TNF is not required for the regulation of iNOS expression.

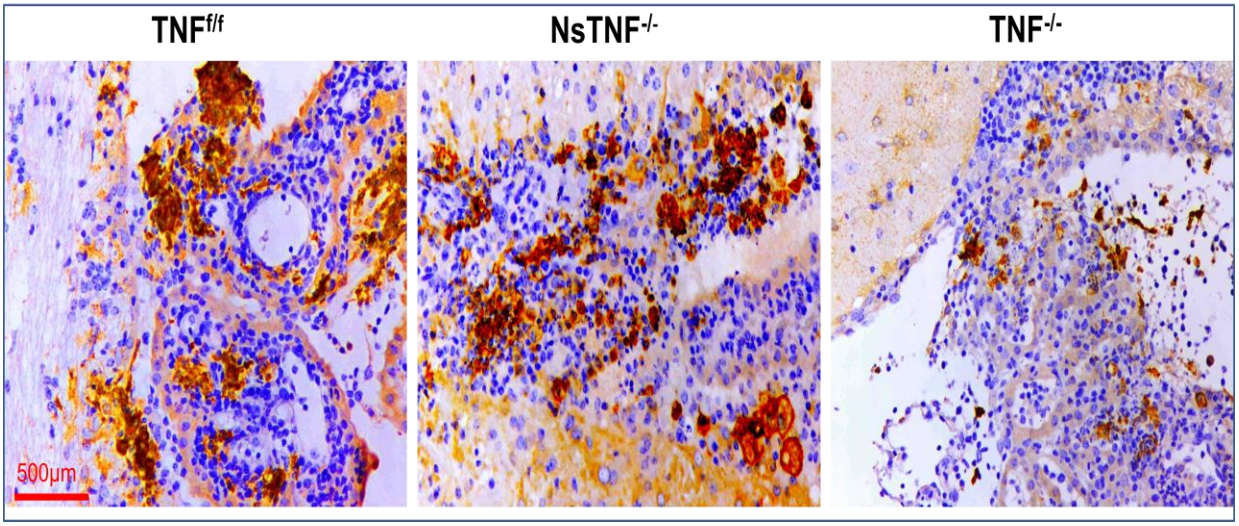

Figure 3.1.12: Normal iNOS expression in brains of NsTNF$^{-/-}$ mice infected with *M. tuberculosis*. Brains of TNF$^{f/f}$, NsTNF$^{-/-}$ and TNF$^{-/-}$ mice intracerebrally infected with *M. tuberculosis* at a dose of 1x10^5 cfu/brain were sectioned at 2µm, and iNOS expression detected by immunohistochemistry at week 3 post-infection. The results represent one out of three similar experiments. (*n*= 5 mice/group and magnification= 200x).

R1.7 TNF dependent recruitment of macrophages and dendritic cells, and microglia proliferation in the CNS in response to cerebral *M. tuberculosis* infection

To address whether neurons derived TNF regulates the influx and proliferation of myeloid cell subsets in response to *M. tuberculosis*, we analysed recruitment of macrophages, dendritic cells and resident microglia over a 3 week period. $TNF^{f/f}$, $NsTNF^{-/-}$ and $TNF^{-/-}$ mice were intracerebrally infected with *M. tuberculosis* at a dose of $1x10^5$ cfu/brain.

The $CD11b^+CD45^{low}$ (microglia) population in $TNF^{f/f}$ mice increased 2-fold at week 3 compared to week 1 post-infection (Figure 3.1.13). Similarly, $NsTNF^{-/-}$ mice showed a significant (1.48% vs 0.063%; $p < 0.05$) increase in the proliferation of the microglia population at week 3 post-infection compared to week 1 post-infection. However, there were no significant differences in the percentages of microglia in $NsTNF^{-/-}$ compared to $TNF^{f/f}$ mice at any time point. In $TNF^{-/-}$ mice, the microglial proliferation was higher compared to that of either $TNF^{f/f}$ or $NsTNF^{-/-}$ mice at 2 and 3 weeks points post-infection. We further investigated the cerebral infiltrating $CD11b^+CD45^{high}$ (macrophages) population and found that macrophages infiltration occurred subsequent to neurotuberculosis infection. The infiltration profile which peaked at week 2 was similar in $TNF^{f/f}$ and $NsTNF^{-/-}$ mice, while in the $TNF^{-/-}$ mice, the level was approximately 2-fold higher compared to $TNF^{f/f}$ mice or $NsTNF^{-/-}$ mice at all time points post-infection (Figure 3.1.13). Finally we examined the cerebral infiltrating $CD11b^{low}CD45^{high}$ (dendritic cells) population, where we found that DCs recruitment into the CNS occurred almost equally when comparing $NsTNF^{-/-}$ with $TNF^{f/f}$ mice at week 1, 2 and 3 post-infection. However, significantly higher DCs infiltration was observed in $TNF^{-/-}$ mice compared either to $NsTNF^{-/-}$ or $TNF^{f/f}$ mice (Figure 3.1.13).

Further, we investigated the kinetic response of $CD11b^+CD45^{low}$, $CD11b^+CD45^{high}$ and $CD11c^+CD45^{high}$ populations in the CNS after *M. tuberculosis* infection challenge. Initial assessment of all three mouse strains showed that naïve mice had an average of $3.4x10^6$ resident-microglia, while the number of macrophages were $1x10^3$, and DCs $0.8x10^3$ in all adult naïve mouse strains. This was in agreement with the previously published data in which the number of $CD11b^+CD45^{low}$ cells in adult naïve mice was reported to be $3.5x10^6$ (Lawson *et al.,* 1990), the number of $CD11b^+CD45^{high}$ was reported to be $1.1x10^3$ (Foley *et al.,* 2009), and the number of $CD11c^+CD45^{high}$ cells was reported to be ~$1x10^3$ (Karman *et al.,* 2004). All three strains demonstrated an equivalent increase in microglial proliferation at 1 week post-infection (Figure 3.1.14A). Whereas peak values were reached at 2 weeks post-infection for both $TNF^{f/f}$ and $NsTNF^{-/-}$ mice, $TNF^{-/-}$ mice exhibited uncontrolled microglial expansion, which was significantly higher ($1.3x10^7$ vs $8.7x10^6$; $p < 0.05$) at week 2 post-infection compared to $TNF^{f/f}$

mice, and at week 3 ($3.8x10^7$ vs $1x10^7$ and $9x10^6$; $p < 0.05$) post-infection compared to both $TNF^{f/f}$ and $NsTNF^{-/-}$ mice (Figure 3.1.14A). We next evaluated the absolute numbers of recruited macrophages and found a 5 and 3-fold increase in $TNF^{f/f}$ mice at week 2 and 3 post-infection, respectively compared with earlier week 1 post-infection. Similar increases were observed in $NsTNF^{-/-}$ mice at week 2 and 3 post-infection. Interestingly, we found that deletion of TNF in neurons resulted in a transient but significant ($5x10^6$ vs $3x10^6$; $p < 0.05$) increase in macrophage recruitment at week 2 post-infection (Figure 3.1.14B). However, complete deletion of TNF resulted in uncontrolled macrophage recruitment, represented by a significant increase in $TNF^{-/-}$ mice compared to $TNF^{f/f}$ mice at week 2 ($6x10^6$ vs $3x10^6$; $p < 0.05$) and 3 ($1.5x10^7$ vs $3x10^6$; $p < 0.01$) post-infection (Figure 3.1.14B). We thereafter assessed the absolute number of recruited DCs, and observed equivalent levels of infiltrating $CD11c^+CD45^{high}$ cells in the brain at 2 and 3 weeks in both $TNF^{f/f}$ and $NsTNF^{-/-}$ mice in response to *M. tuberculosis* infection (Figure 3.1.15C). $TNF^{-/-}$ mice, however, had a greater absolute number of recruiting DCs at week 2 ($1.7x10^6$ vs $1x10^4$ and $1.5x10^4$; $p < 0.05$) and 3 ($7.5x10^7$ vs $1x10^5$ and $1.6x10^4$; $p < 0.01$) post-infection compared to either $TNF^{f/f}$ or $NsTNF^{-/-}$ mice (Figure 3.1.14C).

Our results clearly demonstrate that, TNF is required to regulate the influx of infiltrating macrophages- and DCs as well as the proliferation of resident microglia population. However, TNF derived from neurons are redundant for this process".

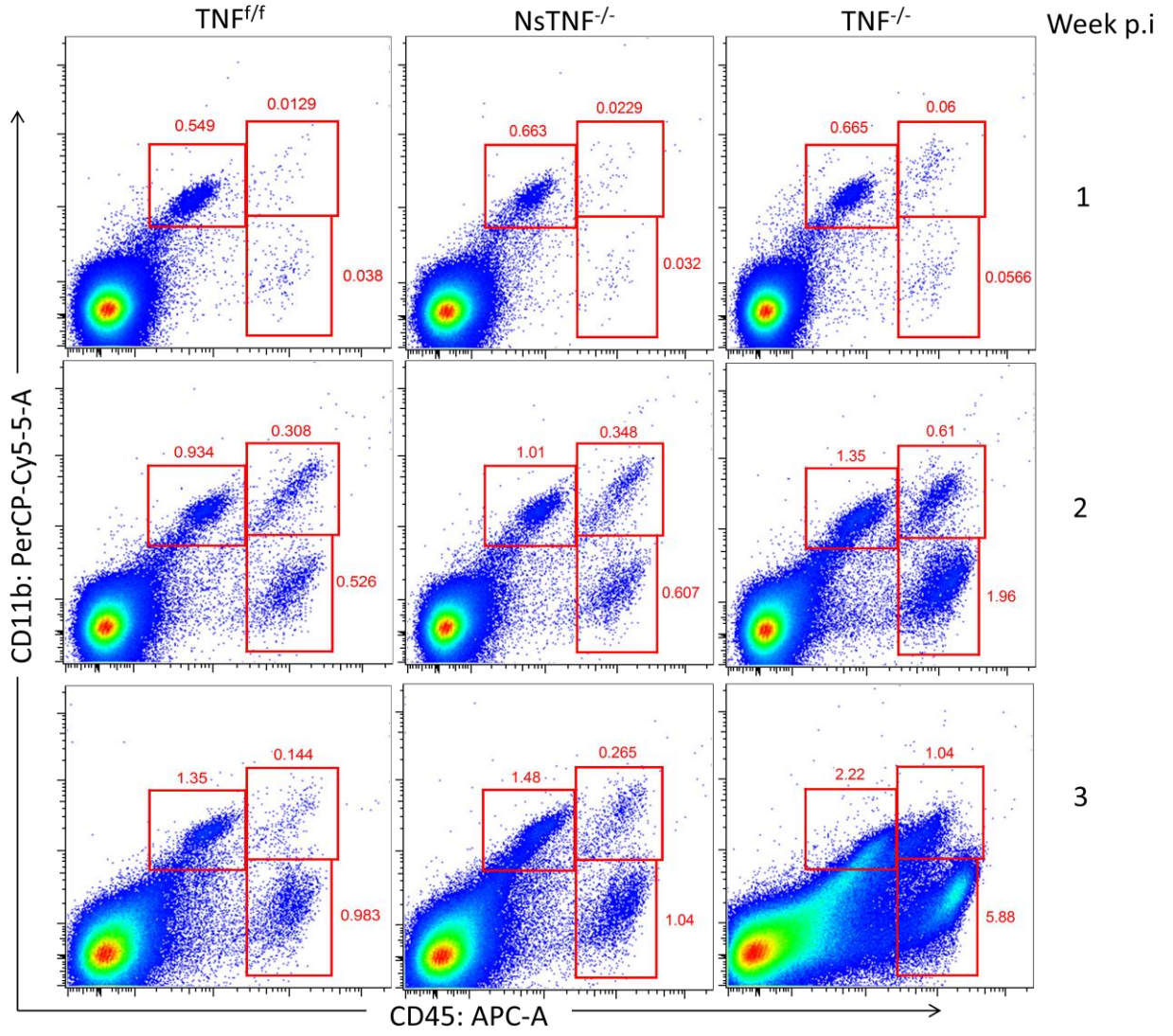

Figure 3.1.13: Frequency of antigen presenting cells infiltration during neurotuberculosis. Phenotypic analyses of myeloid derived APC isolated from $TNF^{f/f}$, $NsTNF^{-/-}$ and $TNF^{-/-}$ mice intracerebrally infected with *M. tuberculosis* at a dose of $1x10^5$ cfu/brain. Isolated brain cells were labelled and analysed at week 1, 2 and 3 post-infection for the expression of CD11b and CD45 by flow cytometry. Dot plots are representative of one of two experiments and show labelling of $CD11b^+CD45^{low}$, $CD11b^+CD45^{high}$, and $CD11b^{low}CD45^{high}$ cells. The frequency increase cell infiltration was evident as from week 2 post-infection in all populations. The values seen in the dot plot are the percentages of the parent gate which are positive. Data are representative of three independent experiments of 5 mice/group.

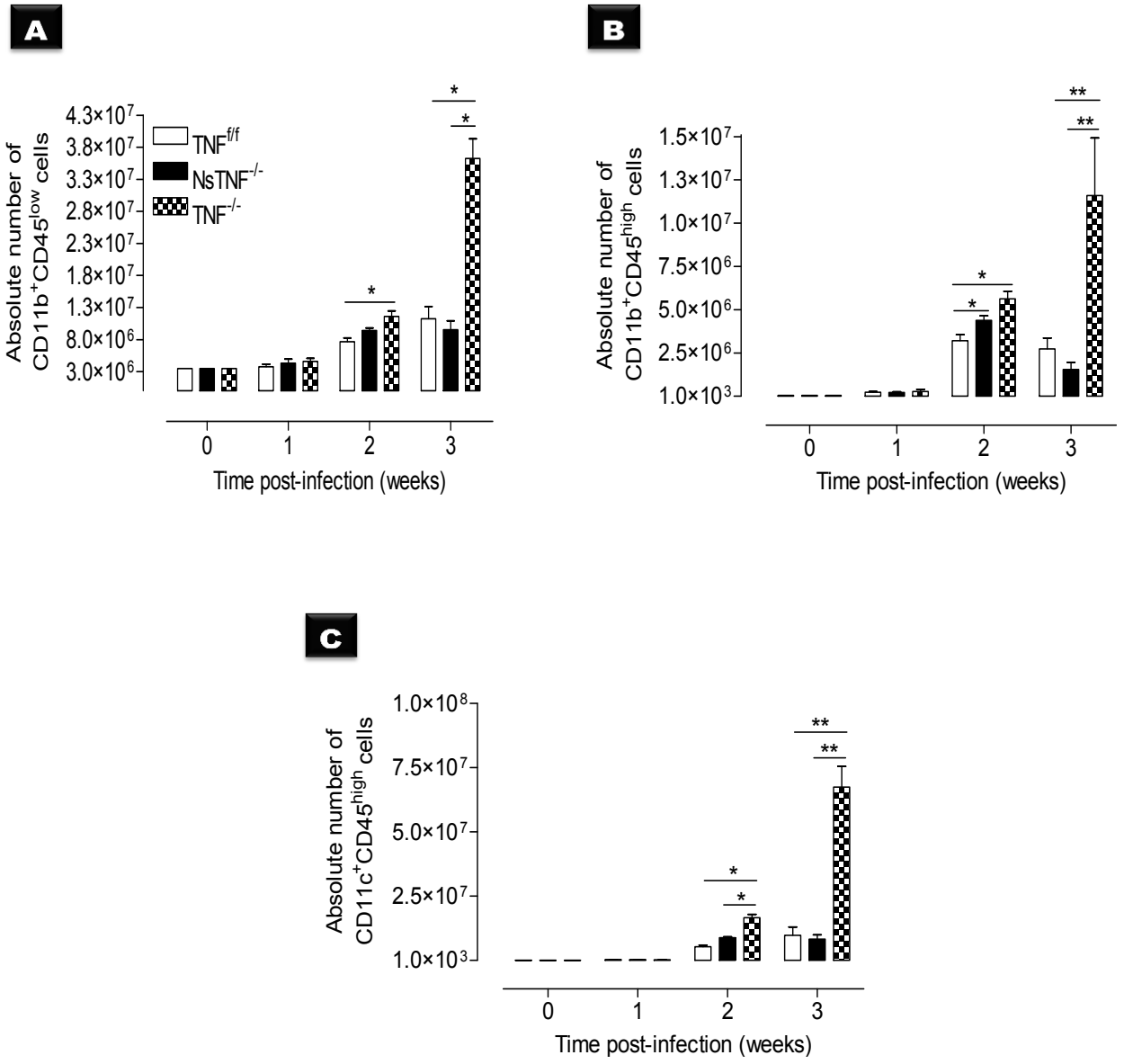

Figure 3.1.14: Kinetic profile of APCs during CNS *M. tuberculosis* infection: $TNF^{f/f}$, $NsTNF^{-/-}$ and $TNF^{-/-}$ mice were intracerebrally infected with *M. tuberculosis* at a dose of $1x10^5$ cfu/brain. Brains were harvested at 0 (naïve), 1, 2 and 3 weeks post-infection, and single cells were labelled for APC and activation markers. Shown are absolute numbers of $CD11b^+CD45^{low}$ cells (A), $CD11b^+CD45^{high}$ cells (B), and $CD11c^+CD45^{high}$ cells (C). Data are one representative of three independent experiments. The results represent the mean ± SD of 5 mice/group. *=$p < 0.05$ and **=$p < 0.01$.

R1.7.1 TNF dependent activation of microglia during neurotuberculosis

Different population of APCs are involved during the cerebral immune response, including microglia. Previously it was reported that glial activity can potentially be influenced by the neuronal response (Hansson & Rönnbäck, 2003). In this study, we investigated the role of TNF in general and the specific contribution of neuron derived TNF in the proliferation and activation microglia. $TNF^{f/f}$, $NsTNF^{-/-}$ and $TNF^{-/-}$ mice were challenged with *M. tuberculosis* intracerebral infection at a dose of $1x10^5$ cfu/brain. Whole brain's tissues were harvested at week 0 (naïve), 1, 2 and 3 post-infection, and single cells were labelled using lineage (CD11b:PerCP-Cy5-5 and CD45:APC), co-stimulatory (CD80:FITC and CD86:V450) and cell surface (MHCII (I-A/I-E): PE) marker (Figure 3.1.15).

We investigated the expression of co-stimulation markers (CD80 or B7-1) and (CD86 or B7-2) at week 0 (naïve), 1, 2 and 3 post-infection on microglia. We found that in all mouse strains, the CD80 expression on microglia were similar (~10%) at week 1 and 2 post-infection (Figure 3.1.15A). $CD80^+$ expressing microglia was significantly ($p < 0.01$) increased in both $TNF^{f/f}$ and $NsTNF^{-/-}$ mice at week 3 post-infection when compared to the earlier time point. In contrast, the percentage of $CD80^+$ expressing microglia cells remained altered in $TNF^{-/-}$ mice (Figure 3.1.15A) and was significantly ($p < 0.01$) lower compared to either $TNF^{f/f}$ and $NsTNF^{-/-}$ mice. Interestingly, microglia expression of CD86 peaked 1 week after infection, and remained constant thereafter being equivalent in all three strains over the experimental period (Figure 3.1.15C). Microglial $MHCII^+$ expression increased significantly in all three mouse strains at 2 weeks post-infection and was equivalent, however the percentage of $MHCII^+$ expressing microglial cells in $TNF^{f/f}$ and $NsTNF^{-/-}$ mice was maintained at 3 weeks post-infection, but decreased in $TNF^{-/-}$ mice and was significant ($p < 0.05$) lower (Figure 3.1.15E). In addition, we measured the MFI of CD80, CD86, and MHCII expression on microglia over 3 weeks. We found an escalation in $CD80^+$ MFI in $TNF^{f/f}$ and $NsTNF^{-/-}$ mice with maximum values obtained at 3 weeks post-infection. Although $CD80^+$ MFI values were equivalent in all three strains over the first two weeks, it decreased in $TNF^{-/-}$ mice after 3 weeks post-infection and was significantly ($p < 0.05$) lower when comparing to $TNF^{f/f}$ and $NsTNF^{-/-}$ mice (Figure 3.1.15B). Interestingly $CD86^+$ MFI expression remained equivalent for all three mouse strains over the 3 week experimental period (Figure 3.1.15D). However, a similar MFI profile was observed for $MHCII^+$ expression, however peak values were observed in all mouse strains at 2 weeks post-infection and sustained for the 3 week period in both $TNF^{f/f}$ and $NsTNF^{-/-}$ mice (Figure 3.1.15F). In contrast, MFI of $MHCII^+$ expressing microglia cells was altered in $TNF^{-/-}$ mice and was significantly ($p <$

0.05) lower compared to either $TNF^{f/f}$ and $NsTNF^{-/-}$ mice.

These data suggest that TNF is required for the control of microglial activation; however the neuronal TNF is not required.

R1.7.2 Defective response to antigen by macrophages in $TNF^{-/-}$ but not $NsTNF^{-/-}$ mice during experimental neurotuberculosis

To investigate the overall effect of TNF and in particular neuronal derived TNF on macrophage activation during neurotuberculosis, we intracerebrally infected $TNF^{f/f}$, $NsTNF^{-/-}$ and $TNF^{-/-}$ mice with *M. tuberculosis* at a dose of $1x10^5$ cfu/brain. At week 0 (naïve), 1, 2 and 3 post-infection, brains were harvested and isolated single cells were labelled for expression of lineage (CD11b:PerCP-Cy5-5 and CD45:APC), co-stimulatory (CD80:FITC and CD86:V450) and cell surface (MHCII (I-A/I-E):PE) markers (Figure 3.1.16).

We noted an equivalent kinetic increase in $CD80^+$ expression in macrophages over the first 2 weeks in $TNF^{f/f}$, $NsTNF^{-/-}$ and $TNF^{-/-}$ mice. The number of $CD80^+$ macrophages was sustained at 3 weeks post-infection in $NsTNF^{-/-}$ and $TNF^{f/f}$ mice, the percentage of macrophage cells expressing $CD80^+$ were significantly ($p < 0.05$) reduced in $TNF^{-/-}$ mice at week 3 post-infection when compared with $TNF^{f/f}$ and $NsTNF^{-/-}$ mice (Figure 3.1.16A). All mouse strains exhibited similar levels of macrophage cells expressing the $CD86^+$ marker at week 1, 2 and 3 post-infection with no difference among strains, although a decreasing trend was observed in $TNF^{-/-}$ at week 3 post-infection compared to $TNF^{f/f}$ and $NsTNF^{-/-}$ mice (Figure 3.1.16C). The kinetic profile of $MHCII^+$ expressing macrophages generally approximated that observed for $CD80^+$ expressing macrophages. $TNF^{f/f}$, $NsTNF^{-/-}$ and $TNF^{-/-}$ mice displayed an escalation in $MHCII^+$ macrophages over the first 2 weeks, which was maintained at 3 weeks post-infection in $TNF^{f/f}$ and $NsTNF^{-/-}$ mice. In contrast, the number of $MHCII^+$ expressing macrophages in $TNF^{-/-}$ mice was significant ($p < 0.05$) decreased when compared to either $TNF^{f/f}$ or $NsTNF^{-/-}$ mice (Figure 3.1.16E). In addition, we measured the MFI of $CD80^+$, $CD86^+$ and $MHCII^+$ expression on macrophages over 3 weeks. We found an equivalent kinetic increase in MFI of $CD80^+$ expressing macrophages in all mouse strains over the first two weeks, it decreased in $TNF^{-/-}$ mice after 3 weeks post-infection and was significantly lower compared to $TNF^{f/f}$ and $NsTNF^{-/-}$ mice where MFI levels were sustained (Figure 3.1.16B). Interestingly, the MFI of $CD86^+$ expressing macrophages remained increased and equivalent for $TNF^{f/f}$, $NsTNF^{-/-}$ and $TNF^{-/-}$ mice over the 3 week experimental period (Figure 3.1.16D). We observed a similar MFI profile for

$MHCII^+$ expression in macrophages at week 1 post-infection, however peak values were observed in all mouse strains at 2 weeks post-infection and sustained for the 3 week experimental period in both $TNF^{f/f}$ and $NsTNF^{-/-}$ mice. In contrast, the MFI of $MHCII^+$ expressing macrophages in $TNF^{-/-}$ mice was significantly ($p < 0.05$) lower compared to either turn-$off^{f/f}$ and $NsTNF^{-/-}$ mice (Figure 3.1.16F).

Our findings indicate that TNF is required to maintain activation of $CD80^+$ and $MHCII^+$ expressing macrophages during CNS *M. tuberculosis* infection. However, neurons derived TNF do not play a pivotal role in either macrophages activation or recruitment.

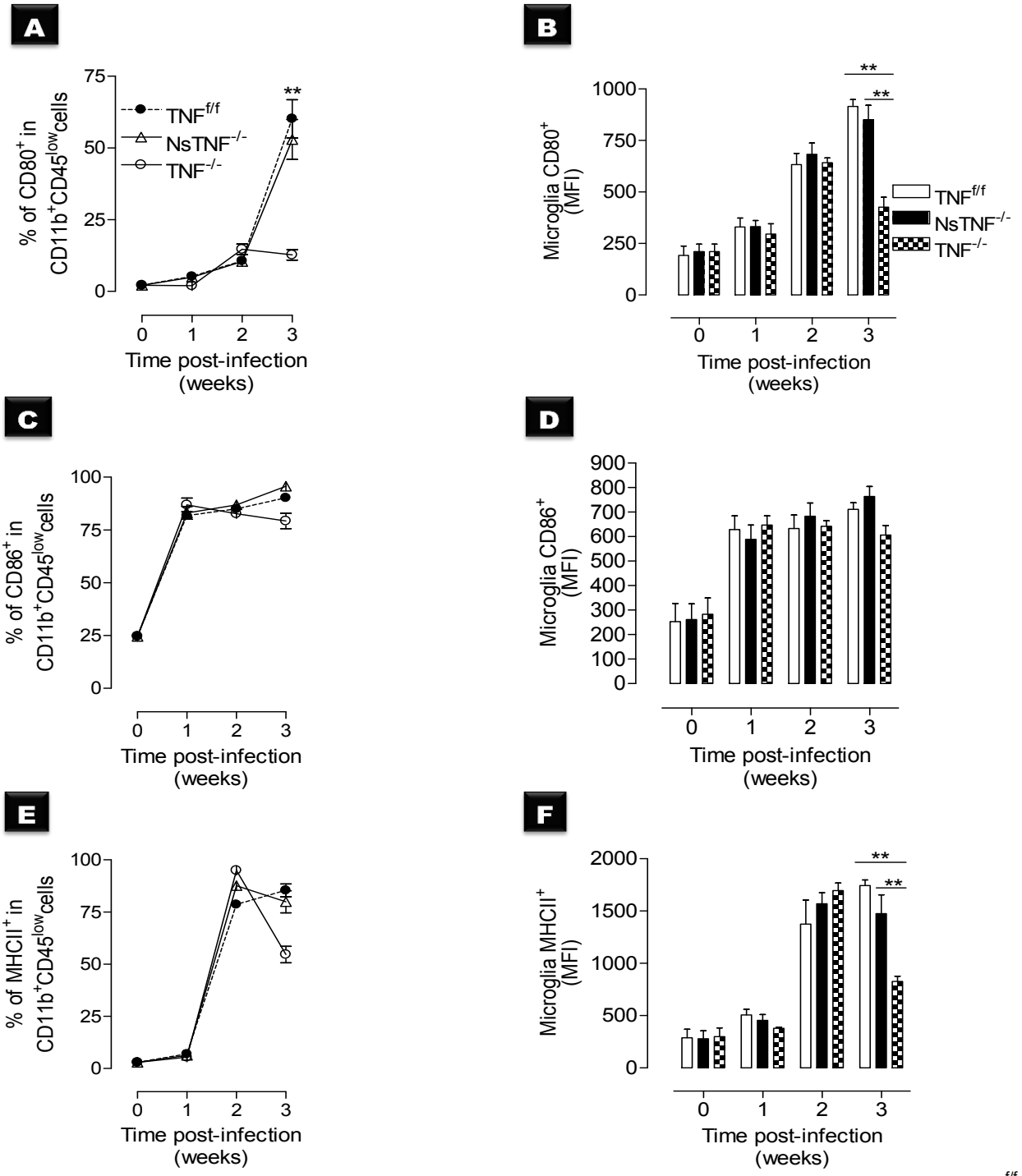

Figure 3.1.15: TNF dependent microglial activation during CNS *M. tuberculosis* infection. $TNF^{f/f}$, $NsTNF^{-/-}$ and $TNF^{-/-}$ mice were intracerebrally infected with *M. tuberculosis* at a dose of $1x10^5$ cfu/brain. Whole brain tissues were harvested at week 0 (naïve), 1, 2 and 3 post-infection, and single cells were labelled for specific APC surface markers. From the $CD11b^+CD45^{low}$ population were gated for percentage of cells expressing $CD11b^+CD45^{low}CD80^+$ (A), $CD11b^+CD45^{low}CD86^+$ (C) and $CD11b^+CD45^{low}MHCII^+$ (E) surface markers. Changes in MFIs values of $CD80^+$, $CD86^+$ and $MHCII^+$ expressing microglia are shown in B, D and F, respectively. *=$p < 0.05$ and **=$p < 0.01$. Data are one representative of three independent experiments. The results represent the mean ± SD of 5 mice/group.

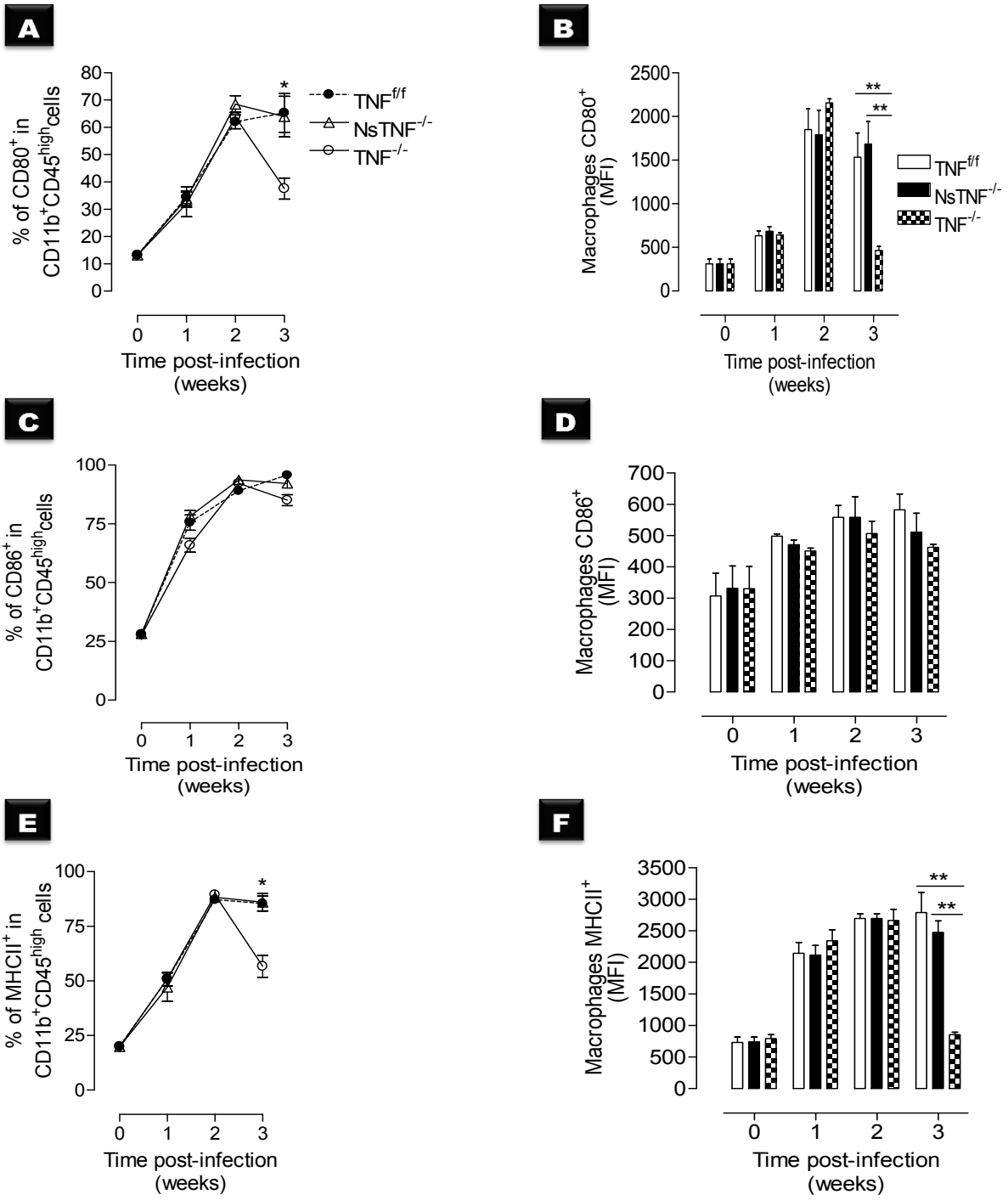

Figure 3.1.16: Defective response to antigen by macrophages in TNF$^{-/-}$ but not NsTNF$^{-/-}$ mice. TNF$^{f/f}$, NsTNF$^{-/-}$ and TNF$^{-/-}$ mice were intracerebrally infected with *M. tuberculosis* at a dose of 1x10^5 cfu/brain. Brains were harvested at week 0 (naïve), 1, 2 and 3 post-infection, and single cells were labelled for APC and activation. CD11b$^+$CD45^{high}CD80$^+$ (A), CD11b$^+$CD45^{high}CD86$^+$ (C), and CD11b$^+$CD45^{high}MHCII$^+$ (E) population were determined. MFI values of CD80$^+$, CD86$^+$ and MHCII$^+$ expressing macrophages are shown in B, D and F, respectively. *=p < 0.05. Data are one representative of three independent experiments. The results represent the mean ± SD of 5 mice/group.

R1.7.3 TNF mediates response to antigen in dendritic cells during neurotuberculosis

We then investigated whether TNF in general and in particular neuronal derived TNF play a critical role in the activation of the DCs population. $TNF^{f/f}$, $NsTNF^{-/-}$ and $TNF^{-/-}$ mice were intracerebrally infected with *M. tuberculosis* at a dose of $1x10^5$ cfu/brain. Brains were harvested at week 0 (naïve), 1, 2 and 3 post-infection, and single cells were labelled for expression of lineage (CD11b:PerCP-Cy5-5, CD11c:Alexa 700 and CD45:APC), co-stimulatory (CD80:FITC and CD86:V450) and cell surface (MHCII (I-A/I-E):PE) markers (Figure 3.1.17).

We found 10% of the DC population in all mouse strains expressed the $CD80^+$ marker at week 1 post-infection but decreased to 5% at week 2 post-infection and were equivalent in all mouse strains (Figure 3.1.18A). The $CD80^+$ expression in $NsTNF^{-/-}$ mice, then significantly increased from 5% to 8% in the DCs comparable to $TNF^{f/f}$ mice at week 3 post-infection. In contrast, a continuous significant decrease (3±0.1 vs 8±05 and 8±0.4; $p < 0.05$) in $CD80^+$ expression was observed in the $TNF^{-/-}$ mice compared to $TNF^{f/f}$ and $NsTNF^{-/-}$ mice (Figure 3.1.18A). Interestingly, DCs expression of $CD86^+$ peaked over the 2 week period after *M. tuberculosis* infection in all mouse strains, and the equivalent continuous increase was found in $TNF^{f/f}$ and $NsTNF^{-/-}$ mice at week 3 post-infection. In contrast, the percentage of $CD86^+$ in $TNF^{-/-}$ mice was significantly decreased (68±0.2 vs 80±01 and 80±0.2; $p < 0.05$) at week 3 post-infection (Figure 3.1.18C). DCs $MHCII^+$ expression increased significantly in all three mouse strains over 2 weeks post-infection period and was equivalent. However, where the percentage of $MHCII^+$ expressing DCs was continuously increased at 3 weeks post-infection in both $NsTNF^{-/-}$ and $TNF^{f/f}$ mice, it decreased in $TNF^{-/-}$ mice and was significantly lower (10±00 vs 32±07 and 30±08; $p < 0.05$) (Figure 3.1.18E).

Further, we measured the MFI of $CD80^+$, $CD86^+$ and $MHCII^+$ expressing DCs over 3 weeks. We observed that the MFI of $CD80^+$ expressing DCs peaked at week 1, and similarly decreased at week 2 post *M. tuberculosis* infection in all three mouse strains; however a continuous decrease was found in $TNF^{-/-}$ mice which were significantly lower (250±20 vs 400±30 and 450±45; $p < 0.05$) compared to $TNF^{f/f}$ and $NsTNF^{-/-}$ mice at week 3 post-infection (Figure 3.1.18B). Interestingly the MFI of $CD86^+$ expressing DCs remained increased and equivalent to $TNF^{f/f}$, $NsTNF^{-/-}$ and $TNF^{-/-}$ mice over the 3 week experimental period. A similar DCs MFI profile was observed for $MHCII^+$ expression at week 1, however peak values were observed at 2 weeks post-infection in all mouse strains and continuously increased for the 3 week period in both $NsTNF^{-/-}$ and $TNF^{f/f}$ mice (Figure 3.1.18F). In contrast, the MFI of $MHCII^+$

expressing DCs was significantly lower (230±20 vs 550±25 and 575±30 $p < 0.05$) in $TNF^{-/-}$ mice compared to both $TNF^{f/f}$ and $NsTNF^{-/-}$ mice (Figure 3.1.18F).

Our results indicate that TNF is required for the recruitment of $CD80^{+}$, $CD86^{+}$ and $MHCII^{+}$ DCs and regulates surface expression of co-stimulatory and antigen presentation markers during neurotuberculosis. However, neuronal derived TNF do not play a critical role in either DCs activation or recruitment.

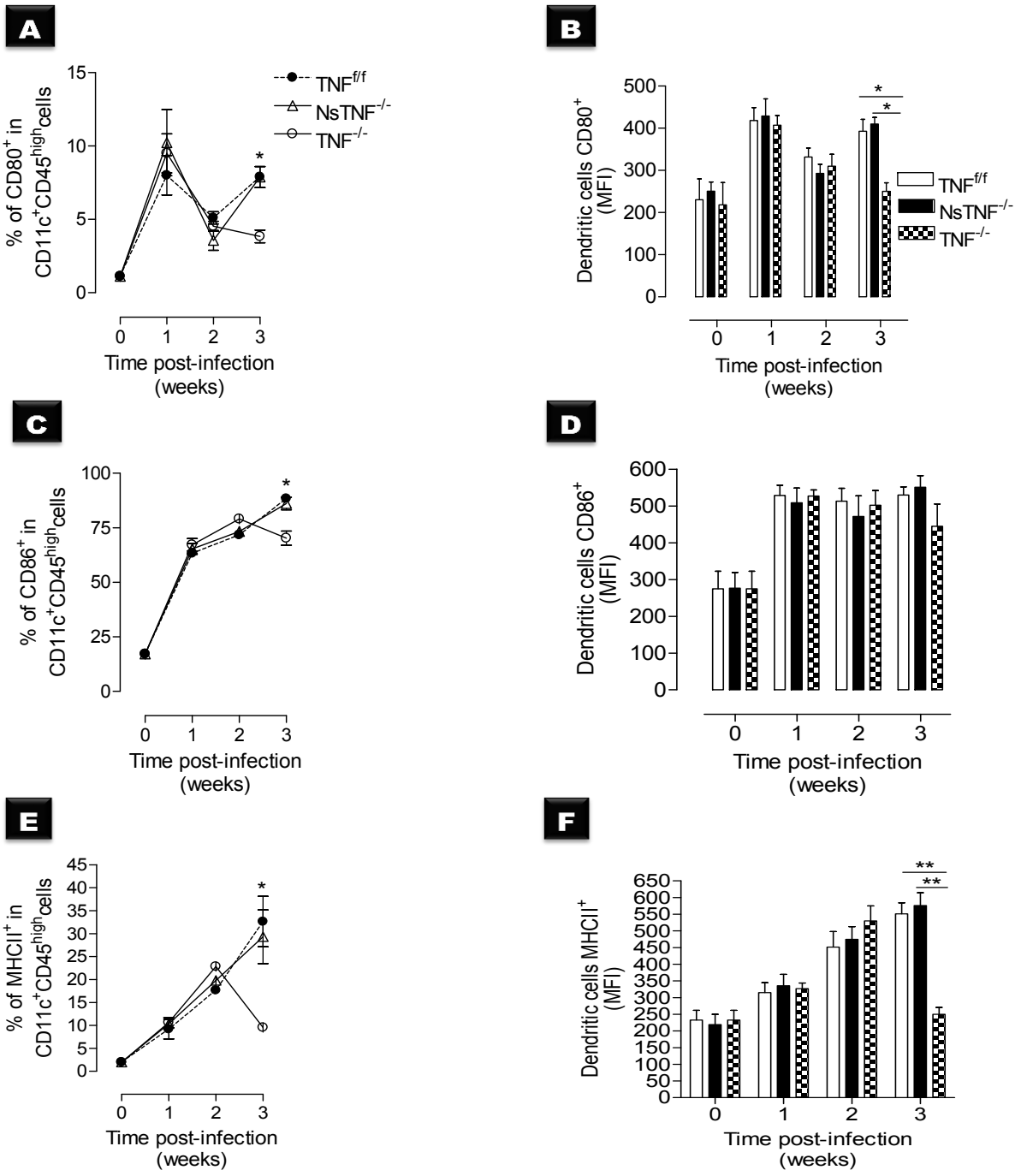

Figure 3.1.17: TNF mediates surface markers expression in DC population. $TNF^{f/f}$, $NsTNF^{-/-}$ and $TNF^{-/-}$ mice were intracerebrally infected with *M. tuberculosis* at a dose of $1x10^5$ cfu/brain. Brains were harvested at week 0 (naïve), 1, 2 and 3 post-infection, and isolated single cells were labelled for APC and surface markers. From the $CD11c^+CD45^{high}$ population were gated for percentage of cells expressing $CD11c^+CD45^{high}CD80^+$ (A), $CD11c^+CD45^{high}CD86^+$ (C), and $CD11c^+CD45^{high}MHCII^+$ (E) surface markers at week 0 (naïve), 1, 2 and 3 post-infection. Changes in MFIs values of $CD80^+$, $CD86^+$ and $MHCII^+$ expressing DCs are shown in B, D and F, respectively. Data are one representative of three independent experiments. The results represent the mean ± SD of 5 mice/group. *=$p < 0.05$.

R1.8 Infiltrating B-cell mediated immunity during neurotuberculosis

R1.8.1 TNF dependent recruitment of follicular B cells during neurotuberculosis

B cells enter the CNS as part of normal immune surveillance and also in the pathologic state (Alter *et al.,* 2003). B cells capture antigens via cell-surface receptors, thereafter activation is initiated. B cells aggregate into lymphoid follicle-like structures in the target organ (Franciotta *et al.,* 2008). Previous studies have reported the presence of follicle-like B cells aggregates in the lungs of TB patients (Ulrichs *et al.,* 2004; Tsai *et al.,* 2006 and Maglione & Chan, 2009), and of ectopic B-cell follicles in the meninges of patients with multiple sclerosis (Serafi *et al.,* 2004). The presence of pulmonary follicle-like B cells aggregates in TB patients suggests that B cells mediate immunity. B cells were also shown to contribute to host protection against pulmonary TB infection, and are believed to shape anti-tuberculous immune responses through various mechanisms such as antibody secretion and cytokine production (Maglione *et al.,* 2007 and Maglione & Chan, 2009). These include direct effects of antibody upon the pathogen, antigen-presentation, cytokine production, and influencing intracellular killing mechanisms of leukocytes (Maglione & Chan, 2009). The role of the follicular B cells (Fo B cells) subset in host immune response against CNS *M. tuberculosis* infection has not yet been well defined, although a few studies have documented its role during pulmonary tuberculosis (Sousa *et al.,* 2000; Ulrichs *et al.,* 2004; Tsai *et al.,* 2006 and Maglione & Chan, 2009). Activated Fo B cells responding to T cell-dependent antigens can also respond rapidly, forming short-lived IgM-secreting B cells (Owens *et al.,* 2006). We asked whether, complete ablation of TNF in general and particularly in neurons influences the infiltration of Fo B cells into the CNS during neurotuberculosis. Mice were intracerebrally infected with *M. tuberculosis* at a dose of $1x10^5$ cfu/brain. Brains were harvested at week 0 (naïve), 1, 2 and 3 post-infection from $TNF^{f/f}$, $NsTNF^{-/-}$ and $TNF^{-/-}$ mice and single cells were labelled with specific B-cell markers (CD1d:PE, CD93(AA4.1):PerCP-Cy5-5 and B200:Horizon V500). We observed no significant difference in the absolute number of infiltrating Fo B cells population in $NsTNF^{-/-}$ mice compared to $TNF^{f/f}$ mice at all time points post *M. tuberculosis* infection. However, the absolute number of infiltrating Fo B cells in $TNF^{-/-}$ mice were significantly ($p < 0.05$) higher at week 1, 2 and 3 points post-infection compared to the $TNF^{f/f}$ or $NsTNF^{-/-}$ mice (Figure 3.1.18).

These findings suggest that the ablation of TNF in neurons does not affect the influx of Fo B cells into the CNS. The increased infiltrating level of Fo B cells found in $TNF^{-/-}$ mice correlated with the onset of the disease in this mouse strain, and therefore indicates that TNF is

required to control follicular B-cell infiltration into the CNS during neurotuberculosis.

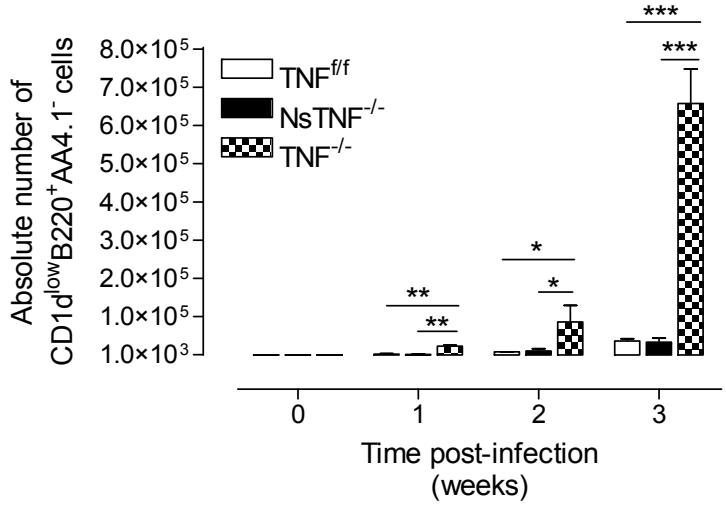

Figure 3.1.18: Fo B cells infiltrating cell number during neurotuberculosis. TNF$^{f/f}$, NsTNF$^{-/-}$ and TNF$^{-/-}$ mice were intracerebrally infected with *M. tuberculosis* at a dose of 1x10^5 cfu/brain. Brains were harvested at week 0 (naïve), 1, 2 and 3 post-infection, and single cells labelled and analysed using the BD LSRFortessa flow cytometer analyzer. In order to identify Fo B cells population, isolated single brain cells were labelled with CD1d:PE-A, CD93(AA4.1):PerCP-Cy5-5-A and B220:V500-A markers. *=p <0.05, **=p < 0.01 and ***=p < 0.001.

R1.8.1.1 TNF is essential for follicular B cell immunity during neurotuberculosis

TNF$^{f/f}$, NsTNF$^{-/-}$ and TNF$^{-/-}$ mice were intracerebrally infected with *M. tuberculosis* at a dose of 1x10^5 cfu/brain. Brains were harvested at week 0 (naïve), 1, 2 and 3 post-infection, and single cells were labelled with specific B cells (CD1d:PE, AA4.1:PerCP-Cy5-5 and B200:HorizonV500), co-stimulatory (CD86:V450) and surface (IgM:PE-Cy7, and MHCII:Alexa 700) markers. Preliminary studies have shown variability in CD86 but not CD80 surface expression, and therefore CD86 was included in the analysis. Little is known about the involvement of plasmablast during neurotuberculosis, we then hypothesis that if plasmablast play a role during neurotuberculosis, the antibody IgM may be altered in TNF deficient mice.

We investigated whether the ablation of TNF in the neurons affected the regulation of co-stimulatory markers. We found that the Fo B cells population in NsTNF$^{-/-}$ mice had similar percentage and MFI of CD86^{+} expressing Fo B-cell at all time points post-infection compared to TNF$^{f/f}$ mice (Figure 3.1.19A). In contrast, the percentage and MFI of cells expressing the CD86^{+}

marker in the Fo B-cell population in $TNF^{-/-}$ mice were significantly higher week 1 ($p < 0.05$), and lower ($p < 0.05$) at week 3 post-infection when compared either to $TNF^{f/f}$ or $NsTNF^{-/-}$ mice (Figure 3.1.19A and B). We further evaluated the role of neuronal derived TNF in the secretion of IgM. We observed a significant (25±0.3 and 20±0.5 vs 10±0.3; $p < 0.05$) escalating IgM secretion in $TNF^{f/f}$ and $NsTNF^{-/-}$ mice over the 3 weeks post-infection period. Although $TNF^{-/-}$ mice displayed lower IgM synthesis over the first 2 weeks post-infection, antibody product was not sustained and IgM concentration was significantly lower at week 3 post-infection compared to $TNF^{f/f}$ and $NsTNF^{-/-}$ mice (Figure 3.1.19C). The IgM percentage expression pattern correlated with IgM MFI values (Figure 3.1.19D). To examine the pattern expression of $MHCII^{+}$ in the Fo B cells population, comparative analysis between $TNF^{f/f}$ mice, $NsTNF^{-/-}$ and $TNF^{-/-}$ mice was performed. We found that the percentage and MFI of $MHCII^{+}$ expressing Fo B cells in $TNF^{f/f}$ and $NsTNF^{-/-}$ mice were similar, and peaked at week 1 post-infection. On the contrary, the increase in the percentage and MFI of $TNF^{-/-}$ mice cells expressing $MHCII^{+}$ were delayed at week 1 post-infection, and only peaked at week 2 post-infection, and subsequently decreased at week 3 post-infection as opposed to being maintained as was evident in $TNF^{f/f}$ and $NsTNF^{-/-}$ mice (Figure 3.1.19E and F).

Although TNF is essential for Fo B-cell immunity during experiment neurotuberculosis, our findings once again demonstrate that ablation of TNF in neurons does not affect the pattern of Fo B-cell functionality during neurotuberculosis.

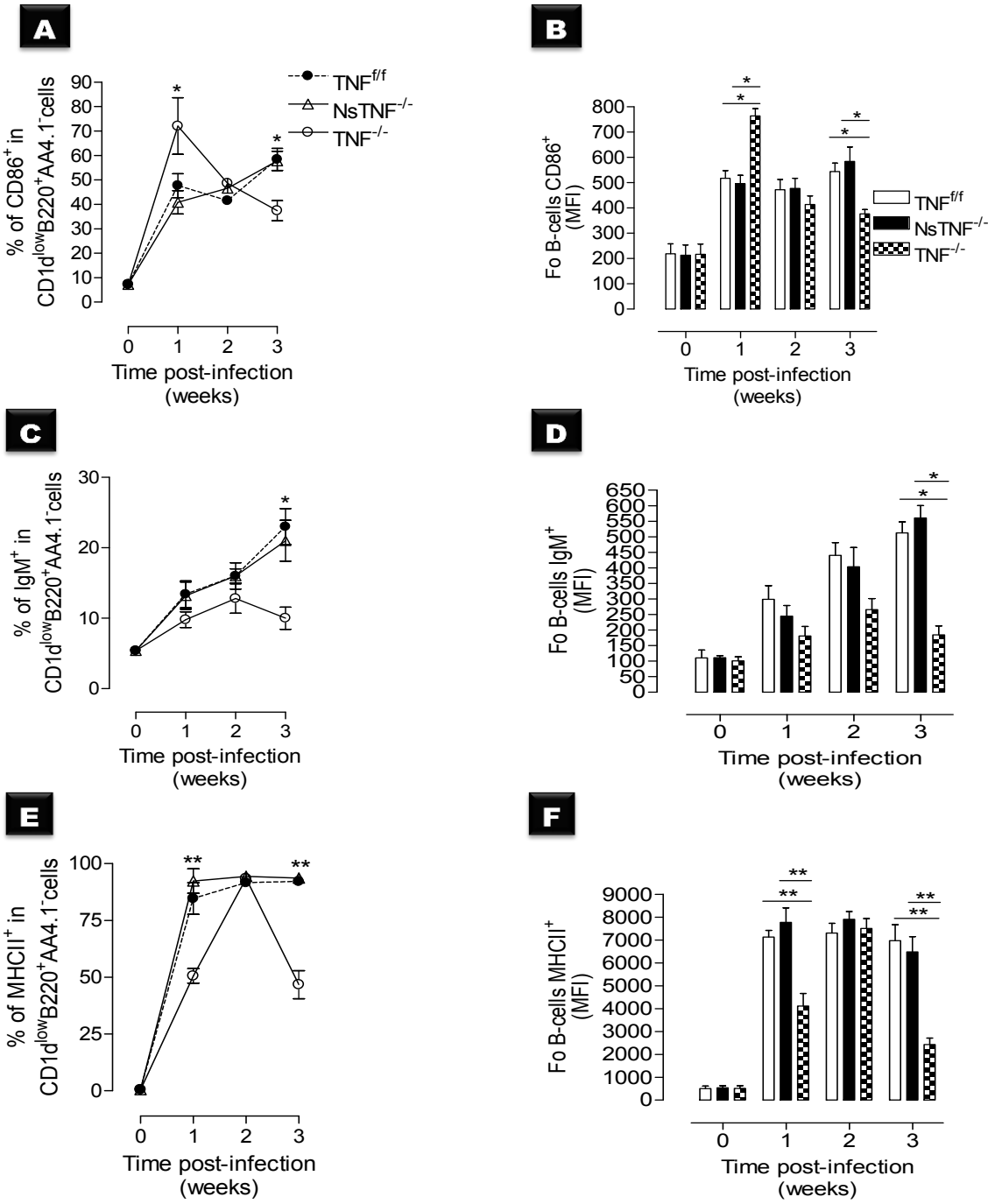

Figure 3.1.19: TNF mediates Fo B cells surface marker expression. $TNF^{f/f}$, $NsTNF^{-/-}$, and $TNF^{-/-}$ mice strains were intracerebrally infected with *M. tuberculosis* at a dose of $1x10^5$ cfu/brain. Brains were harvested at week 0 (naïve), 1, 2 and 3 post-infection, and isolated single cells were labelled for CD1d:PE-A, CD93(AA4.1):PerCP-Cy5-5-A and B220:V500-A with surface markers CD86, IgM and MHCII. The $CD1d^{low}B220^{+}AA4.1^{-}$ population were gated for percentage of cells expressing $CD1d^{low}B220^{+}AA4.1^{-}CD86^{+}$ (A), $CD1d^{low}B220^{+}AA4.1^{-}IgM^{+}$ (C) and for the $CD1d^{low}B220^{+}AA4.1^{-}MHCII^{+}$ (E). MFI values of $CD86^{+}$, IgM^{+} and $MHCII^{+}$ are shown in B, D and F, respectively. *=p <0.05 and **=p < 0.01. Data are one representative of three independent experiments. Results are represented as mean ± SD of 5 mice/group.

R1.8.2 Plasmablast and plasma cell infiltration during neurotuberculosis

Extrafollicular plasmablasts growth imparts the first antibodies to be secreted after exposure to antigen; B cells differentiate into plasmablasts approximately a day after cognate interaction with T cells (Toellner *et al.,* 1996 and Luther *et al.,* 1997) or activation by a T cell-independent antigen (García de Vinuesa *et al.,* 1999). Plasmablasts in extrafollicular responses divide rapidly for around 3 days before differentiating further into antibody producing plasma cells (Sze *et al*, 2000). To analyse the infiltrating $CD1d^{high}B220^{high}D138^{-}$ (plasmablast cells) and $B220^{low}D138^{+}$ (plasma cells) populations into the CNS during neurotuberculosis, we infected $TNF^{f/f}$, $NsTNF^{-/-}$ and $TNF^{-/-}$ mice with *M. tuberculosis* at a dose of $1x10^5$ cfu/brain. Brains were harvested at week 0 (naïve), 1, 2 and 3 post-infection and single cells were labelled with specific B-cell (CD1d:PE, CD93(AA4.1):PerCP-Cy5-5-A, CD138:APC and B200:Horizon V500) markers. Figure 3.1.20A shows the gating strategy used to identify the plasmablast and plasma cell populations.

There was no significant difference in the absolute numbers of the infiltrating plasmablast cells in $NsTNF^{-/-}$ mice compared with the $TNF^{f/f}$ mice at all time points post-infection. The absolute number of the infiltrating plasmablast cells in $TNF^{-/-}$ mice showed no significant difference at week 1 post-infection compared to $TNF^{f/f}$ and $NsTNF^{-/-}$ mice. However, a significant ($p < 0.05$) increase was observed in $TNF^{-/-}$ mice at week 2 post-infection compared to $TNF^{f/f}$ and $NsTNF^{-/-}$ mice, but was significantly reduced ($p < 0.001$) at week 3 post-infection compared to either $TNF^{f/f}$ or $NsTNF^{-/-}$ mice (Figure 3.1.20A). We next examined the absolute the number of plasma cell at week 1, 2 and 3 post-infection. The absolute number of the plasma cell in $TNF^{f/f}$ mice was 2-log higher at week 3 post-infection compared to week 1 post-infection. A similar trend was observed in $NsTNF^{-/-}$ mice. In this population, we found no significant difference in the absolute numbers of infiltrating plasma cells in $NsTNF^{-/-}$ mice compared with the $TNF^{f/f}$ mice at all time points post-infection. In contrast, at week 1 and 2 post-infection, the absolute number of the infiltrating plasma cells in $TNF^{-/-}$ mice were significantly ($p < 0.001$) increased compared to $TNF^{f/f}$ or $NsTNF^{-/-}$ mice. However, a significant ($p < 0.001$) decrease was seen at week 3 post-infection when comparing to $TNF^{f/f}$ or $NsTNF^{-/-}$ mice (Figure 3.1.20B).

These data demonstrate that ablation of TNF in neurons was not critical for the influx of plasmablast and plasma cell populations into the CNS.

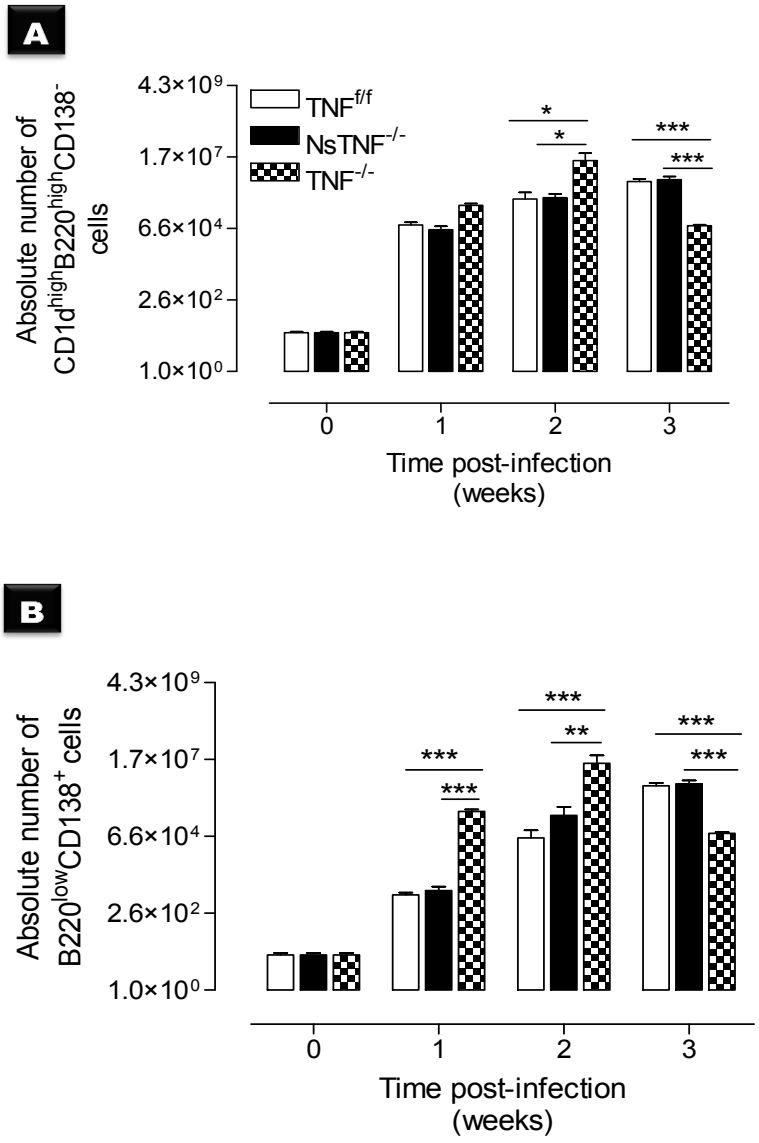

Figure 3.1.20: Plasmablast and plasma cell and their absolute numbers. Brains were harvested at week 0 (naïve), 1, 2 and 3 post-infection, and cells isolated from naïve and the intracerebrally infected $TNF^{f/f}$, $NsTNF^{-/-}$ and $TNF^{-/-}$ mice with *M. tuberculosis* at a dose of $1x10^5$ cfu/brain. Isolated single cells were labelled with CD1d:PE-A, AA4.1:PerCP-Cy5-5-A, CD138:APC-A and CD45R/B220:V500-A. Data shows the absolute numbers of $CD1d^{high}B220^{high}CD138^-$ cells (A) and $B220^{low}CD138^+$ cells (B). *=p < 0.05, **=p < 0.01 and ***=p < 0.001. Data are one representative of three independent experiments. Results in (B) and (C) are represented as mean ± SD of 5 mice/group.

R1.8.2.1 TNF influences plasmablast cellular activation patterns during neurotuberculosis

We evaluated the surface expression of co-stimulatory (CD86:V450) molecules, antibody (IgM:PE-Cy7I) secretion and antigen presenting (MHCII:Alexa 700) markers by multi-colour flow cytometric analysis of an infiltrating plasmablast population. $TNF^{f/f}$, $NsTNF^{-/-}$ and $TNF^{-/-}$ mice were intracerebrally infected with *M. tuberculosis* at a dose of $1x10^5$ cfu/brain. Brains were harvested at week 0 (naïve), 1, 2 and 3 post-infection, and single cells were labelled and analysed for $CD86^+$, IgM^+ and $MHCII^+$ expression. Preliminary studies have shown variability in CD86 but not CD80 surface expression, and therefore CD86 was included in the analysis. Little is known about the involvement of plasmablasts during neurotuberculosis. However, IgM antibody to heparin-binding hemagglutinin was shown to play a role in protection against extrapulmonary TB dissemination (Shin *et al.,* 2006). We hypothesised that if plasmablasts play a role during neurotuberculosis, the antibody IgM may be altered in TNF deficient mice.

When examining the percentage expression and MFI of co-stimulatory molecules, we found that the percentage of infiltrating plasmablast cells expressing $CD86^+$ was significantly increased in all mouse strains at week 1 and 2 post-infection. However, the percentage and MFI of plasmablast cells expressing $CD86^+$ in $TNF^{f/f}$ and $NsTNF^{-/-}$ mice were maintained to the same level at week 3 post-infection. In contrast, the percentage and MFI of $CD86^+$ expressing plasmablast cells was drastic reduced ($p < 0.001$) at week 3 post-infection in $TNF^{-/-}$ mice compared to $TNF^{f/f}$ and $NsTNF^{-/-}$ mice (Figure 3.1.21A and B).

We then examined the percentage and MFI of the infiltrating plasmablast population, which secreted the IgM antibody. Equivalent recruitment of plasmablast cells expressing IgM^+ was observed at week 1 and 2 post-infection in all mouse strains. However, the percentage of IgM^+ secreting plasmablast population was significant ($p < 0.01$) increased in $TNF^{f/f}$ and $NsTNF^{-/-}$ mice at week 3 post-infection. In contrast, IgM production level was significant ($p < 0.01$) decreased at week 3 post-infection in $TNF^{-/-}$ mice compared to $TNF^{f/f}$ or $NsTNF^{-/-}$ mice (Figure 3.1.21C and D). Next, we examined whether the ablation of TNF in general or in neurons in particular affected the ability to present antigen in the plasmablast population. We found no significant difference, in the percentage, or MFI of $MHCII^+$ expressing plasmablast cells at week 1 post-infection in all mouse strains. However, a significant ($p < 0.05$) increase was observed in $MHCII^+$ expressing plasmablast cells of the $TNF^{-/-}$ mice compared to $TNF^{f/f}$ and $NsTNF^{-/-}$ mice at week 2 post-infection. At week 3 post-infection, the percentage and MFI of $MHCII^+$ expressing plasmablast population in $NsTNF^{-/-}$ mice was similar to that of the $TNF^{f/f}$ mice. However, the percentage and MFI of $MHCII^+$ expressing plasmablast population in $TNF^{-/-}$ mice was

significantly ($p < 0.01$) decreased when comparing either to $TNF^{f/f}$ or $NsTNF^{-/-}$ mice (Figure 3.1.21E and F).

These data demonstrate that complete ablation of TNF is critical, but the ablation of TNF in the neurons was not critical for the activation of the plasmablast population.

R1.8.2.2 TNF mediates plasma cell antibody secretion during neurotuberculosis

Plasma cells can develop from naïve marginal zone B-cell, follicular B- cell and memory B cells. After encountering foreign antigen, marginal zone B cells are the first to differentiate, forming short-lived plasma cells that provide a rapid IgM response skewed towards T cell-independent antigens (Owens et al., 2006). Antibody secreting cells comprise of both terminally differentiated plasma cells as well as their plasmablasts precursors, and are integral to both the primary and secondary humoral immune response against pathogens (Marques *et al.,* 2011).

To evaluate the surface expression of co-stimulatory molecules, antibody secretion and antigen presenting cell markers in the plasma cells, $TNF^{f/f}$, $NsTNF^{-/-}$ and $TNF^{-/-}$ mice were intracerebrally infected with *M. tuberculosis* at a dose of $1x10^5$ cfu/brain. Brains were harvested at 0 (naïve), 1, 2 and 3 weeks post-infection, and isolated single cells were labelled and analysed. We found that the percentage of plasma cells expressing $CD86^+$ were increased in all mouse strains at week 1 and 3 post-infection. At week 2, the percentage of plasma cells expressing CD86 in $TNF^{-/-}$ mice showed a significant ($p < 0.05$) decrease compared to $TNF^{f/f}$ or $NsTNF^{-/-}$ mice (Figure 3.1.22A). No significant differences were seen in all mice strains and time point when analysing the MFI of CD86 (Figure 3.1.22B). We next asked whether the complete ablation of TNF in general and in neurons in particular influenced the antibody secretion. There was an increase in the percentage and MFI of plasma cells expressing IgM^+ in all mouse strains at week 1 and 2 post-infection. However, while the percentage and MFI in this population was maintained in $TNF^{f/f}$ and $NsTNF^{-/-}$ mice at week 3 post-infection, there was a significant ($p < 0.05$) decrease in this cell population in $TNF^{-/-}$ mice at this time point (Figure 3.1.22C and D). We examined whether the ablation of TNF in general or in neurons in particular affected the ability to present antigen in the plasma cell population. We found no significant difference, in $MHCII^+$ expressing plasma cells in all mice strains at all time points post *M. tuberculosis* infection (Figure 3.1.22E).

The data suggested that ablation of TNF in the neurons does not alter the plasma cell surface marker activation.

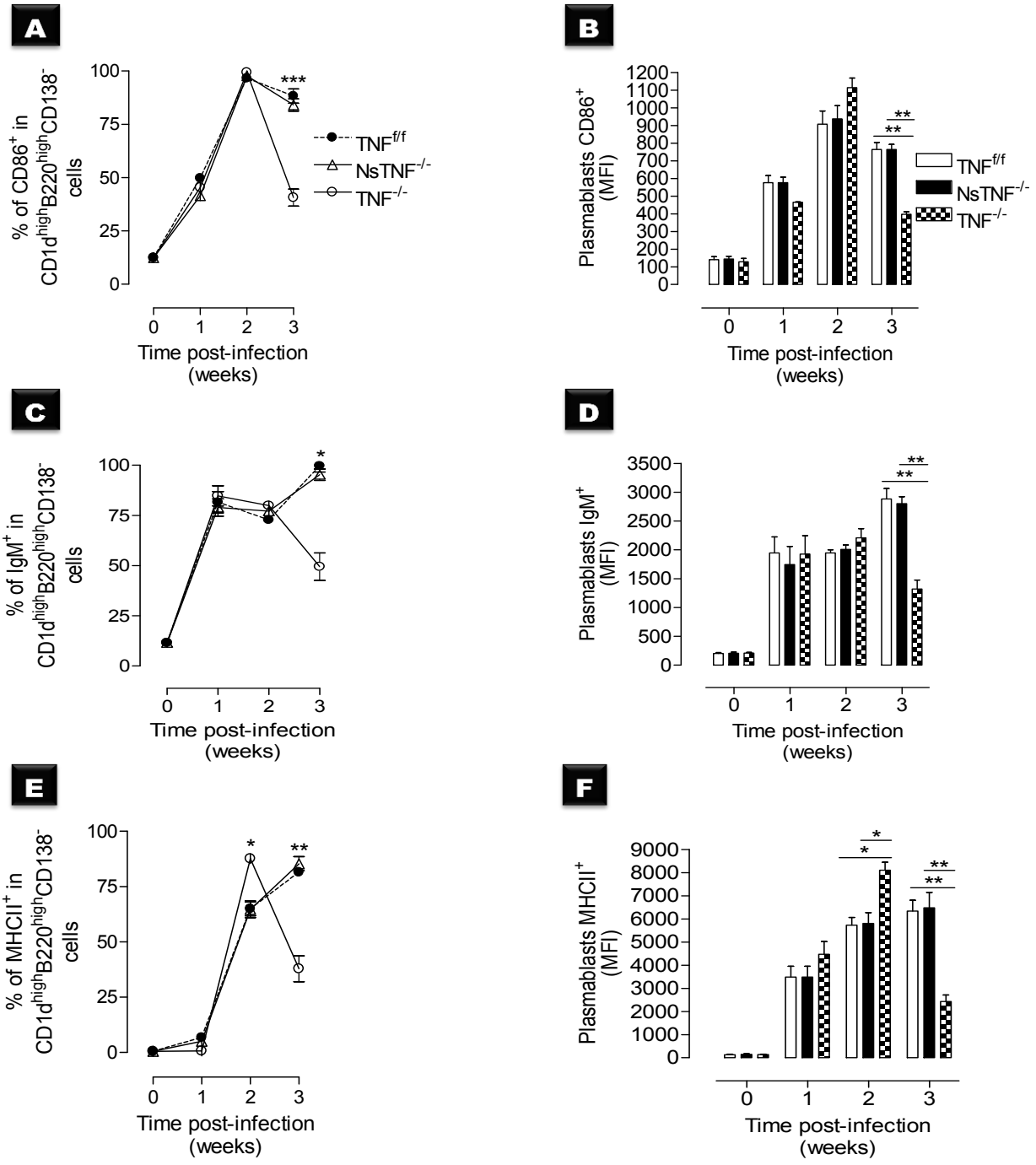

Figure 3.1.21: TNF mediates plasmablasts surface marker activation pattern during neurotuberculosis. $TNF^{f/f}$, $NsTNF^{-/-}$ and $TNF^{-/-}$ mice were intracerebrally infected at with *M. tuberculosis* at a dose of $1x10^5$ cfu/brain. Brains were harvested at week 0 (naïve), 1, 2 and 3 post-infection, and single cells were labelled for CD1d, AA4.1, CD138 and B220 with surface markers CD86, IgM and MHCII. The $CD1d^{high}B220^{high}D138^-$ population was gated for cells expressing $CD1d^{high}B220^{high}CD138^-CD86^+$ (A), $CD1d^{high}B220^{high}CD138^-IgM^+$ (C) and $CD1d^{high}B220^{high}CD138^-MHCII^+$ (D). The bar graphs show the MFI values for $CD86^+$ (B), IgM^+ (D) and $MHCII^+$ (F). *=$p < 0.05$, **=$p < 0.01$ and ***=$p < 0.001$. Data are one representative of three independent experiments. Results presented as mean ± SD of 5 mice/group.

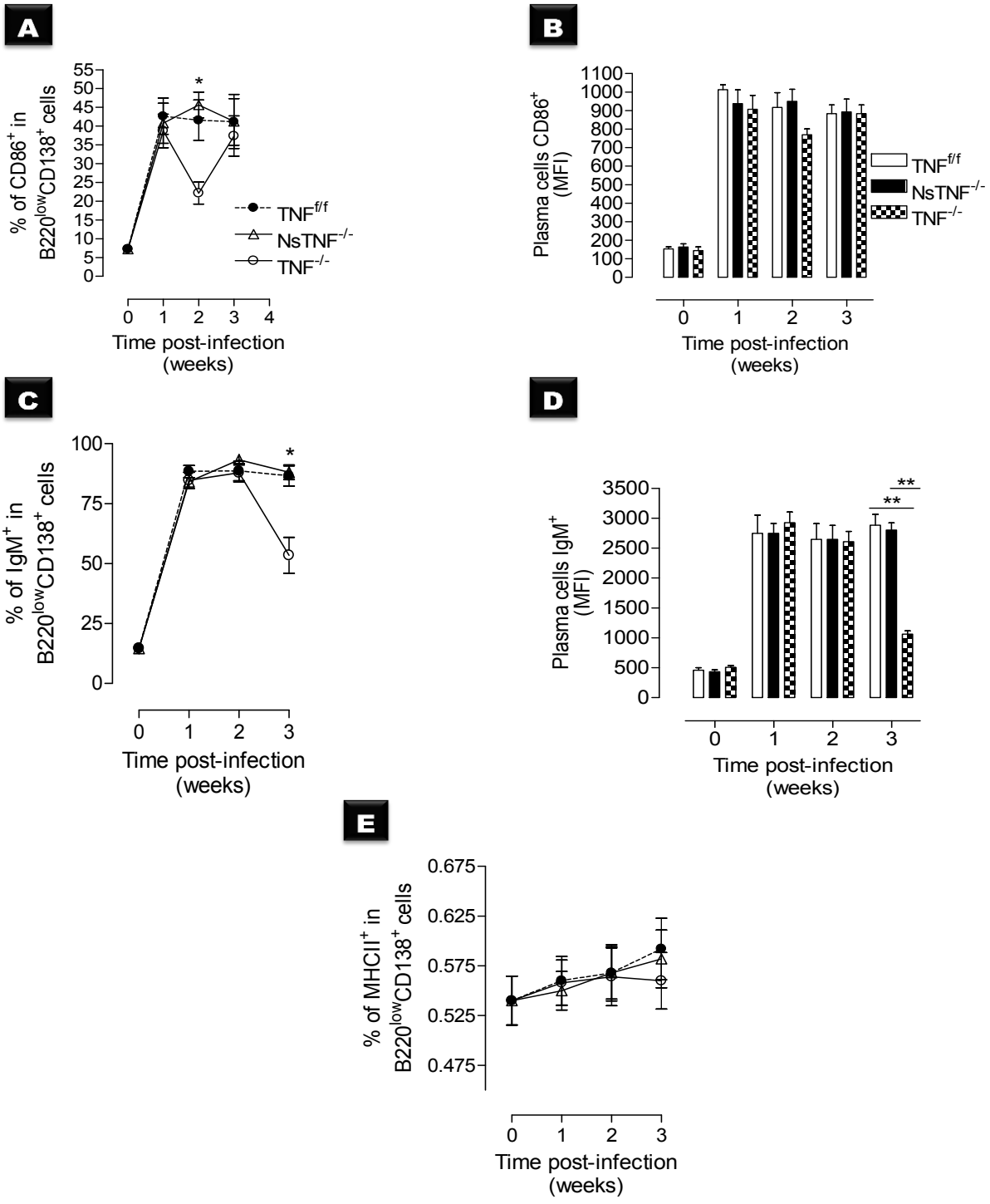

Figure 3.1.22: TNF mediates plasma cell antibody production. $TNF^{f/f}$, $NsTNF^{-/-}$ and $TNF^{-/-}$ mice were intracerebrally infected with *M. tuberculosis* at a dose of $1x10^5$ cfu/brain. Brains were harvested at week 0 (naïve), 1, 2 and 3 post-infection, and single cells were labelled for CD1d, AA4.1, CD138 and B220, with surface markers CD86, IgM and MHCII. The $B220^{low}D138^{-}$ population was gated for plasma cells expressing $CD86^+$ (A), IgM^+ (B) and $MHCII^+$ (C). *=$p < 0.05$ for $TNF^{f/f}$ and $NsTNF^{-/-}$ vs $TNF^{-/-}$. The bar graphs show the MFI values for $CD86^+$ (B) and IgM^+ (D). Data are one representative of three independent experiments. The results represent mean ± SD of 5 mice/group.

R1.9 TNF mediates infiltration of effectors CD4$^+$ and CD8$^+$ T cells into the CNS

Several reports have demonstrated the interaction between neurons and T cells, and the direct immune-regulatory role of neurons on T cells (Liu *et al.,* 2006; Kioussis & Pachnis, 2009 and Meuth *et al.,* 2009). We therefore asked whether complete ablation TNF in general and in neurons in particular would have an effect on CD4$^+$- and CD8$^+$ T cells. We intracerebrally infected TNF$^{f/f}$, NsTNF$^{-/-}$ and TNF$^{-/-}$ mice with *M. tuberculosis* at a dose of 1x10^5 cfu/brain. Brain tissues at week 0 (naïve), 1, 2 and 3 post-infection were harvested, and single cells were labelled for analysis of CD4$^+$- and CD8$^+$ T cell populations by flow cytometry.

We observed that the frequency of effector CD4$^+$ T cell in TNF$^{f/f}$ mice was 10-fold higher at week 2, and 30-fold higher at week 3 post-infection compared to week 1 post-infection. Similar trends were also observed in TNF$^{-/-}$ and NsTNF$^{-/-}$ mice (Figure 3.1.23). Recruited CD4$^+$ T cells in NsTNF$^{-/-}$ mice were similar to TNF$^{f/f}$ mice at week 1 post-infection, in contrast to TNF$^{-/-}$ mice, which already displayed 2-fold increase compared to TNF$^{f/f}$ or NsTNF$^{-/-}$ mice. We observed an equivalent increase in the frequency of inflammatory CD4$^+$ T cells in both TNF$^{f/f}$ or NsTNF$^{-/-}$ mice over the next weeks. However, uncontrolled CD4$^+$ lymphocytic inflammation was observed in TNF$^{-/-}$ mice, eventually being 3-fold higher compared to TNF$^{f/f}$ or NsTNF$^{-/-}$ mice (Figure 3.1.23). We next examined the frequency of CD8$^+$ T cells in the CNS during neurotuberculosis. CD8$^+$ T cells increased 2-fold at week 2 and 3 post-infection in all mouse strains compared to week 1. Similar to CD4$^+$ T cells, recruitment of CD8$^+$ T cells to the CNS was controlled in the absence of neuron specific TNF, but displayed an exacerbated influx of CD8$^+$ T cells in the absence of complete TNF (Figure 3.1.24). We next evaluated the absolute number of recruiting lymphocyte T cells to the CNS subsequent to infection. There was no significant differences in the absolute number of CD3$^+$CD4$^+$ cells or in CD3$^+$CD8$^+$ cells in NsTNF$^{-/-}$ mice at all time points post-infection compared to TNF$^{f/f}$ mice. However, significant ($p < 0.05$) increase was seen at week 1, 2 and 3 post-infection in CD4 T cell subset population as well as at week 1, 2 and 3 post-infection in CD8 T cell subset population were noted in TNF$^{-/-}$ mice compared to TNF$^{f/f}$ or NsTNF$^{-/-}$ mice (Figure 3.1.25A and B).

Overall the data demonstrated that the TNF derived from neurons is not required for controlling the T cell influx into the CNS, however, TNF in general regulates recruitment of CD4$^+$ and CD8$^+$ T cell populations to the CNS subsequent to *M. tuberculosis* infection.

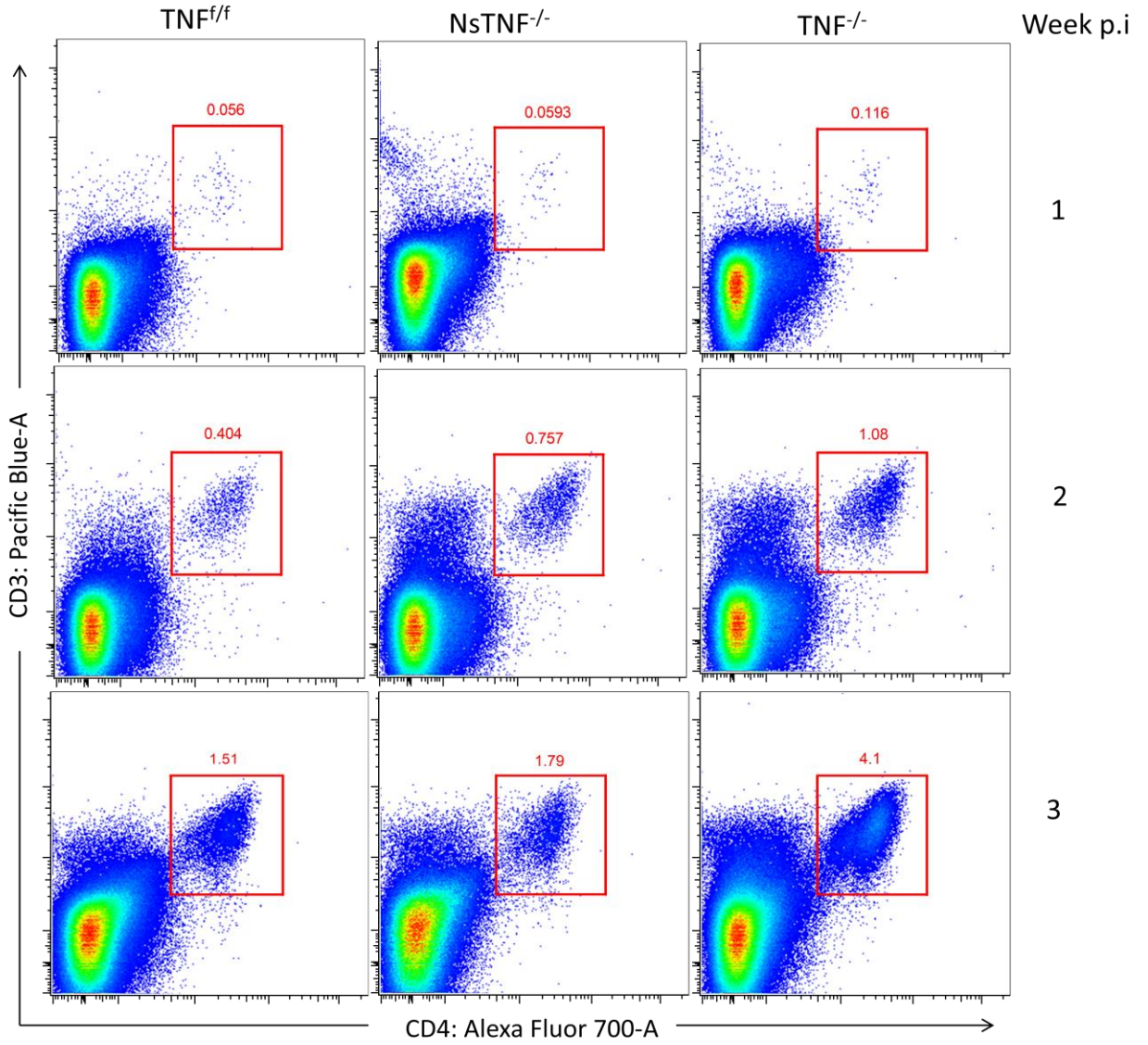

Figure 3.1.23: Frequency of effector CD4$^+$ T cells influx into the CNS during neurotuberculosis. TNF$^{f/f}$, NsTNF$^{-/-}$ and TNF$^{-/-}$ mice were intracerebrally infected with *M tuberculosis* at a dose of 1x10^5 cfu/brain. CD4$^+$ T cells analysis was performed at 1, 2 and 3 weeks post-infection where brain tissues were harvested, and isolated single cells were labelled for expression CD3 and CD4. The values seen in the dot plot are the percentages of the parent gate which are positive. Representative data from one of the three independent experiments (*n*= 5 mice/group) is shown.

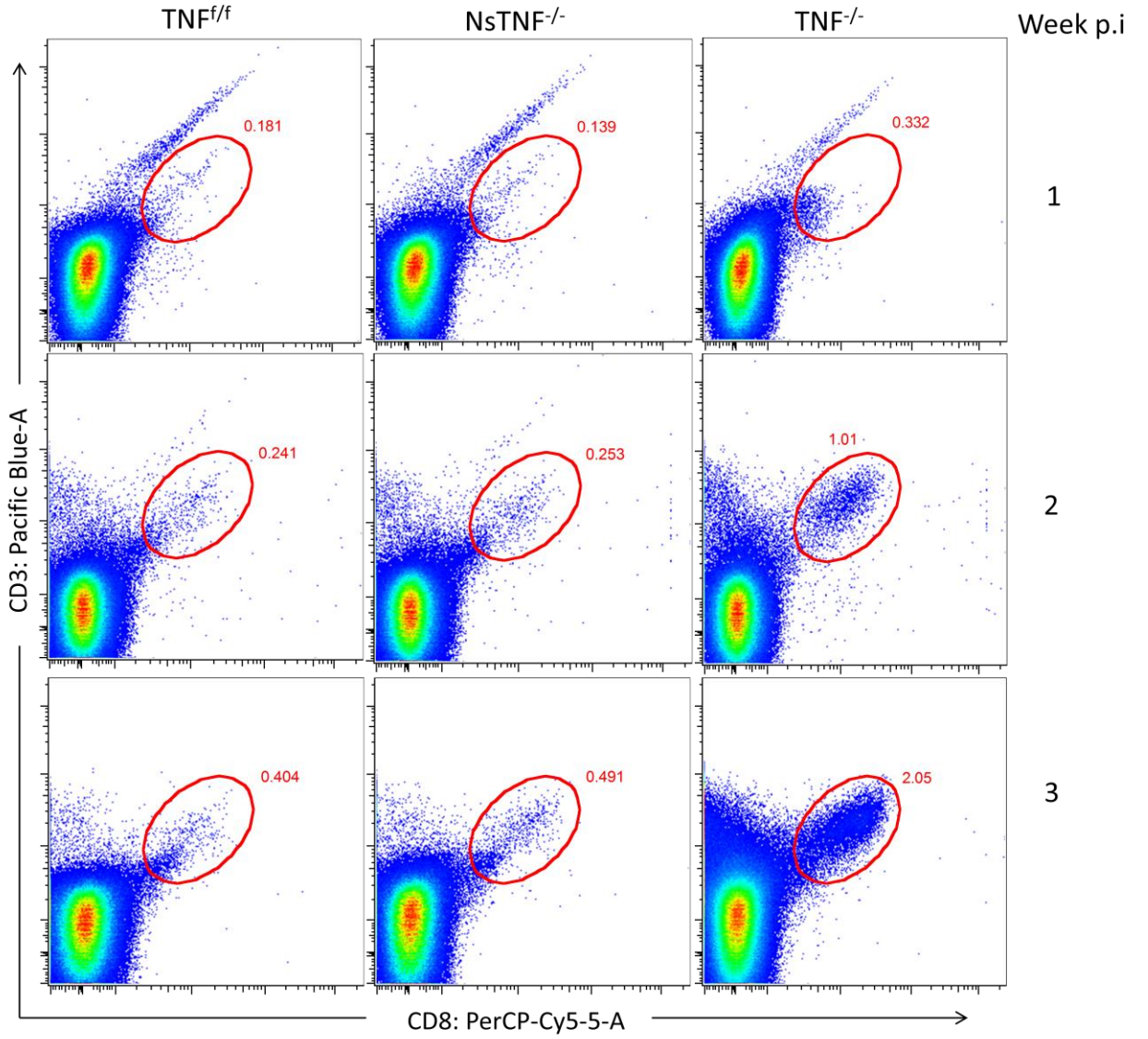

Figure 3.1.24: Frequency of CD8$^+$ T cells influx into the CNS during neurotuberculosis. TNF$^{f/f}$, NsTNF$^{-/-}$ and TNF$^{-/-}$ mice were intracerebrally infected with *M. tuberculosis* at a dose of 1x10^5 cfu/brain. CD8$^+$ T cells analysis was done at 1, 2 and 3 weeks post-infection where brain tissues were harvested, and isolated single cells were labelled for CD3 and CD8 expression. The values seen in the dot plot are the percentages of the parent gate which are positive. Representative data from one of the three independent experiments (*n*= 5 mice/group) is shown.

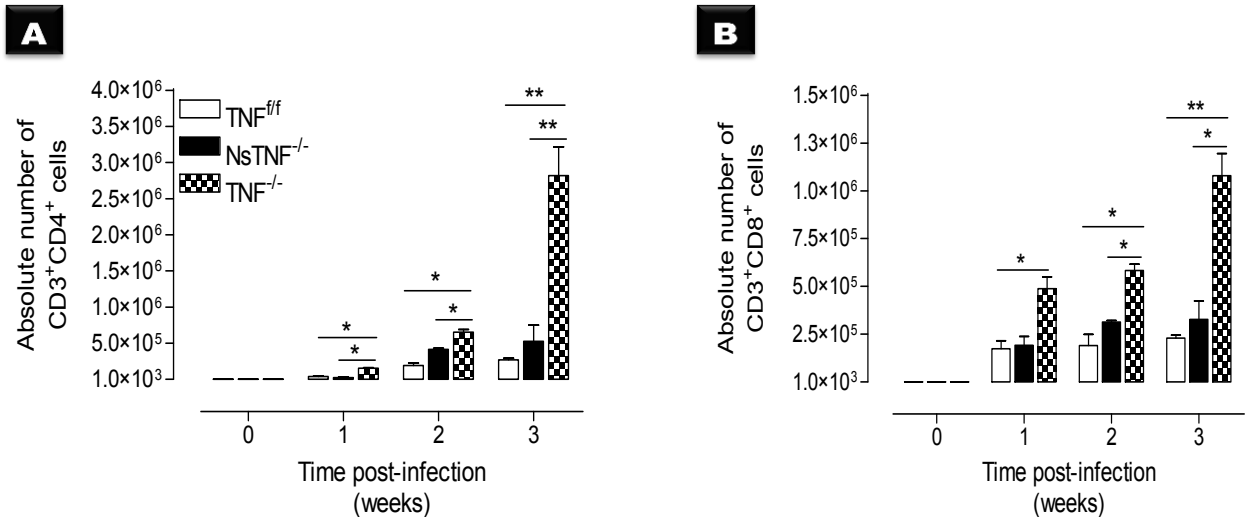

Figure 3.1.25: TNF dependent $CD4^+$ and $CD8^+$ T cells recruitment during CNS *M. tuberculosis* infection. $TNF^{f/f}$, $NsTNF^{-/-}$ and $TNF^{-/-}$ mice strains were intracerebrally infected with *M. tuberculosis* at a dose of $1x10^5$ cfu/brain. Brains were harvested at week 0 (naïve), 1, 2 and 3 post-infection, and single cells were labelled for CD3 and CD4 or CD8, with activation markers CD44. Shown are $CD4^+$ T cells ($CD3^+CD4^+$) absolute numbers (A), and also shown are $CD8^+$ T cells ($CD3^+CD8^+$) absolute numbers (B). *=p < 0.05 and **=p < 0.01. Data (mean ± SD) are representative of at least three independent experiments that yielded similar results (n= 5 mice/group).

R1.9.1 Activation of cerebral infiltrating effectors $CD4^+$ and $CD8^+$ T cells during neurotuberculosis

We further examined the effect of TNF and particularly neuronal derived TNF on the level of CD44 expression in $CD4^+$ and $CD8^+$ T cells. We observed no significant differences in $NsTNF^{-/-}$ mice effectors $CD4^+CD44^+$ cells at all time point post-infection compared to $TNF^{f/f}$ mice. Similarly, $CD44^+$ expressing $CD8^+$ cells of $NsTNF^{-/-}$ mice were not significantly different compared to $TNF^{f/f}$ mice at any of the time points post-infection (Figure 3.1.26A and B). In contrast, the percentage of $CD4^+$ T cells expressing $CD44^+$ were signed (5.5±0.5 vs 1.5±0.5 and 1.6±00; p < 0.05) higher in $TNF^{-/-}$ mice at week 3 post-infection (Figure 3.1.26A). While $CD8^+$ T cells expressing $CD44^+$ were significant increased (1.5±00 vs 0.2±00 and 0.5±00 at week 2, and 2.2±0.4 vs 0.2±00 and 0.4±01 at week 3; p < 0.05) at both week 2 and week 3 post-infection compared to $TNF^{f/f}$ or $NsTNF^{-/-}$ mice (Figure 3.1.26B).

Therefore, while TNF plays an important role in the activation of T cells recruited to the CNS, TNF derived from the neurons is not critical for T cell activation during experimental neurotuberculosis.

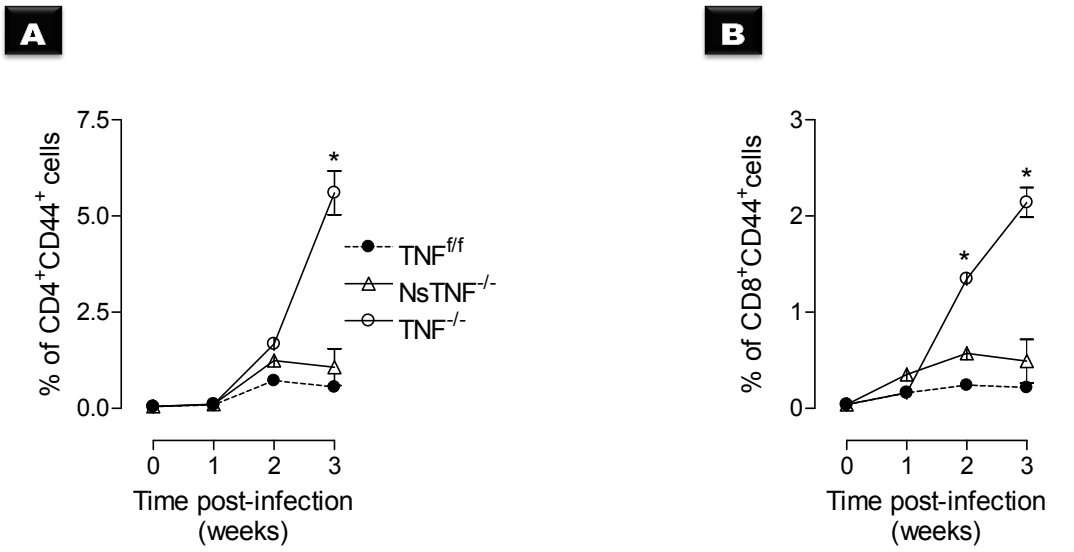

Figure 3.1.26: Percentage of effectors CD4$^+$ and CD8$^+$ T cells during CNS *M. tuberculosis* infection. TNF$^{f/f}$, NsTNF$^{-/-}$ and TNF$^{-/-}$ mice strains were intracerebrally infected with *M. tuberculosis* at a dose of 1x10^5 cfu/brain. Brains were harvested at week 0 (naïve), 1, 2 and 3 post-infection and, single cells were labelled for CD3 and CD4 or CD8, together with the activation markers CD44. The CD3$^+$CD4$^+$ population was gated to determine the percentage of cells expressing CD4$^+$CD44$^+$ (A), the CD3$^+$CD8$^+$ population were then gated to determine the percentage of cells expressing CD8$^+$CD44$^+$ (B). Data (mean ± SD) are representative of at least three independent experiments that yielded similar results (*n*= 5 mice/group). *=$p < 0.05$.

R1.10 Cytokine secretions in NsTNF$^{-/-}$ mice are not compromised following cerebral *M. tuberculosis* infection

The role of cytokines during pulmonary tuberculosis infection has been documented (Flesch & Kaufmann, 1993; Sharma & Bose, 2001 and Cooper & Khader, 2008). However, there is insufficient information on gene expression and regulation during neurotuberculosis. Thus, we selected genes expressed preferentially by neurons, microglia/macrophages or T cells. Several studies have demonstrated the secretion of TNF, IFN-γ, IL-1β, IL-2, IL-6 and IL-12p70 by infiltrating leukocytes and resident cells of the CNS, including neurons (Saliba & Henrot, 2001; Taoufik *et al.,* 2001; Sredni-Kenigsbuch, 2002; Kadhim *et al.,* 2003; Kawanokuchi *et al.,* 2006; Miyatake *et al.,* 2006; Jiao *et al.,* 2008 and Xin *et al.,* 2011). We therefore assessed whether complete ablation of TNF in general and in neurons, in particular, influences cerebral expression of TNF, IFN-γ, IL-1β, IL-2, IL-6 and IL-12p70 during CNS *M. tuberculosis* infection.

Cytokine concentrations were measured in the supernatants of whole brain homogenates at week 0 (naïve), 1, 2 and 3 post *M. tuberculosis* infection by ELISA. All mouse strains displayed cytokine induction subsequent to *M. tuberculosis* challenge in all three mouse strains. Although there was a trend towards a decrease in TNF concentration in $NsTNF^{-/-}$ mice compared to the $TNF^{f/f}$ mice, this was not significant. As expected, no TNF production was detected in $TNF^{-/-}$ mice at any of post-infection time points (Figure 3.1.27A). We next examined total cerebral IFN-γ production in response to *M. tuberculosis* infection. Interestingly, we observed peak concentrations early during infection (1 week post-infection) in $TNF^{f/f}$ and $NsTNF^{-/-}$ mice, while it decreased progressively during the course of infection with no significant differences present between $TNF^{f/f}$ and $NsTNF^{-/-}$ mice. In contrast, escalating IFN-γ concentrations were measured over 3 weeks in $TNF^{-/-}$ mice, which was significantly higher at week 2 ($p < 0.05$) and week 3 ($p < 0.001$) post-infection compared to $TNF^{f/f}$ and $NsTNF^{-/-}$ mice (Figure 3.1.27B). Maximum and equivalent induction of IL-1β was observed in $TNF^{f/f}$ and $NsTNF^{-/-}$ mice during early infection (week 1) and decreased thereafter. Interestingly, although $TNF^{-/-}$ mice induced IL-1β in response to *M. tuberculosis* infection, cerebral concentrations similarly peaked at week 1 post-infection, but never attained equivalent levels and remained significantly ($p < 0.05$) lower at each of the time points investigated (Figure 3.1.27C).

Total cerebral IL-2 production was similar at week 1 post-infection when comparing $TNF^{f/f}$ with $NsTNF^{-/-}$ mice, and progressively increased at a similar rate during week 2 and 3 post-infection. The levels of total cerebral IL-2 production in $TNF^{-/-}$ mice were significantly ($p < 0.001$) lower and delayed at week 1, and also lower at week 3 post-infection respectively, when compared to $TNF^{f/f}$ or $NsTNF^{-/-}$ mice. And no significant difference was observed in all mice strains at week 2 post-infection (Figure 3.1.27D). Maximum induction of cerebral IL-6 was measured at week 1 post-infection in $TNF^{f/f}$ and $NsTNF^{-/-}$ mice and decreased 2-fold thereafter. Interestingly, neuronal TNF deficiency presented with significantly ($p < 0.05$) reduced IL-6 concentrations at week 1 post-infection. Synthesis of IL-6 was delayed in the complete absence of TNF with significant ($p < 0.01$) lower concentrations measured in $TNF^{-/-}$ mice compared to $TNF^{f/f}$ and $NsTNF^{-/-}$ mice. TNF dependent regulation of IL-6 synthesis was evident as mice completely deficient in TNF displayed uncontrolled escalating concentrations at weeks 2 and 3 post-infection, which was significantly ($p < 0.01$) higher at week 2 and 3 post-infection compared to immune competent and neuron TNF deficient mice (Figure 3.1.27E). Examination of the total cerebral IL-12p70 production, found no significant difference in $TNF^{f/f}$ and $NsTNF^{-/-}$ mice at week 1, 2 and 3 post-infection. In contrast, the total cerebral IL-12p70 production in the $TNF^{-/-}$ mice were significantly ($p < 0.05$) lower at week 1 and 3 post-infection (Figure 3.1.27F).

The data thus show that ablation of TNF derived from neuron cells did not affect the overall production of cerebral cytokines. However, TNF had a definitive regulatory effect on cytokine synthesis, where it displayed roles for both induction and inhibitory control.

R1.11 TNF mediates chemokines production during CNS *M. tuberculosis* infection

Multiple CC chemokines are involved in leukocyte recruitment (Lukacs *et al.,* 1997; Hesselgesse & Horuk, 1999; Babcock *et al.,* 2003 and Locati *et al.,* 2005). Trafficking of peripheral myeloids and lymphoid cells to the inflamed CNS has been attributed to specific chemokines (Ransohoff, 2009) which are highly expressed by CNS resident neuronal and glial cells (Glabinski *et al.,* 1995; Godiska *et al.,* 1995; Berman *et al.,* 1996; McManus *et al.,* 1998; Simpson *et al.,* 1998; Xia *et al.,* 1998; Sorensen *et al.,* 1999; Van Der Voorn *et al.,* 1999; Simpson *et al.,* 2000; Che *et al.,* 2001; Flügel *et al.,* 2001; Sorensen *et al.,* 2002; Babcock & Owens, 2003 and de Haas *et al.,* 2007). To date, little is known about chemokines production during CNS *M. tuberculosis* infection. Here we investigated the major β-chemokines such as MCP-1 (CCL2), MIP-1α (CCL3) and RANTES (CCL5) produced in response to *M. tuberculosis* infection at week 1, 2 and 3 post-infection. MCP-1 is a potent β-chemokine mainly acting on monocytes and macrophages (Jiang *et al.,* 1992). Other important β-chemokines are MIP-1α and RANTES that induces the activation and proliferation of T cells (Taub *et al.,* 1996) and macrophages (Fahey *et al.,* 1992 and Lima *et al.,* 1997), and also MIP-1α is involved in the promotion of Th1 cell differentiation (Karpus & Kennedy, 1997 and Karpus *et al.,* 1997).

The level of MCP-1 in $TNF^{f/f}$ mice was 2-fold higher at week 3 post-infection compared to week 1. Similar trends were noticed in $NsTNF^{-/-}$ and $TNF^{-/-}$ mice at week 1 post-infection. No significant difference was observed in MCP-1 secretion in the brain of $NsTNF^{-/-}$ mice compared to $TNF^{f/f}$ mice at all time points post-infection. The level of MCP-1 in $TNF^{-/-}$ mice was significantly ($p < 0.001$) higher at week 1, 2 and 3 post-infection compared either with $TNF^{f/f}$ or $TNF^{-/-}$ mice (Figure 3.1.28A). Assessment of MIP-1α, found 2-fold higher levels at week 3 post-infection compared to week 1 in $TNF^{f/f}$ and $NsTNF^{-/-}$ mice. In contrast, a 5-fold increase was noted in MIP-1α levels of $TNF^{-/-}$ mice at week 3 post-infection compared to week 1 post-infection. In addition, no significant differences in MIP-1α levels were observed at any time points when comparing $NsTNF^{-/-}$ to $TNF^{f/f}$ mice (Figure 3.1.28B). However, the level expression of MIP-1α in $TNF^{-/-}$ mice were significantly ($p < 0.01$) higher at week 2 and 3 post-infection when compared either to $TNF^{f/f}$ or $NsTNF^{-/-}$ mice. No significant difference was seen in all mouse strains at week

1 post-infection (Figure 3.1.28B). The level of RANTES in $TNF^{f/f}$ and $NsTNF^{-/-}$ mice was 2-fold higher at week 3 post-infection compared to week 1. In contrast, 2- and 3-fold increases were noted in $TNF^{-/-}$ mice at week 2 and 3 post-infection respectively, when compared to week 1 post-infection. We found no significant difference at week 1 post-infection in all mouse groups, and no significant difference was observed at week 2 and 3 post-infection when comparing $NsTNF^{-/-}$ versus $TNF^{f/f}$ mice. The level of RANTES in $TNF^{-/-}$ mice was significantly ($p < 0.01$) increased at week 2 and 3 post-infection compared to $TNF^{f/f}$ or $NsTNF^{-/-}$ mice (Figure 3.1.28C).

The deletion of TNF in neuron cells has no effect on the control and immunoregulation of MCP-1, MIP-1α and RANTES after experimental CNS infection with *M. tuberculosis*. However, the data convincingly demonstrate TNF dependent control of each of chemokines in the host cerebral response during *M. tuberculosis* infection.

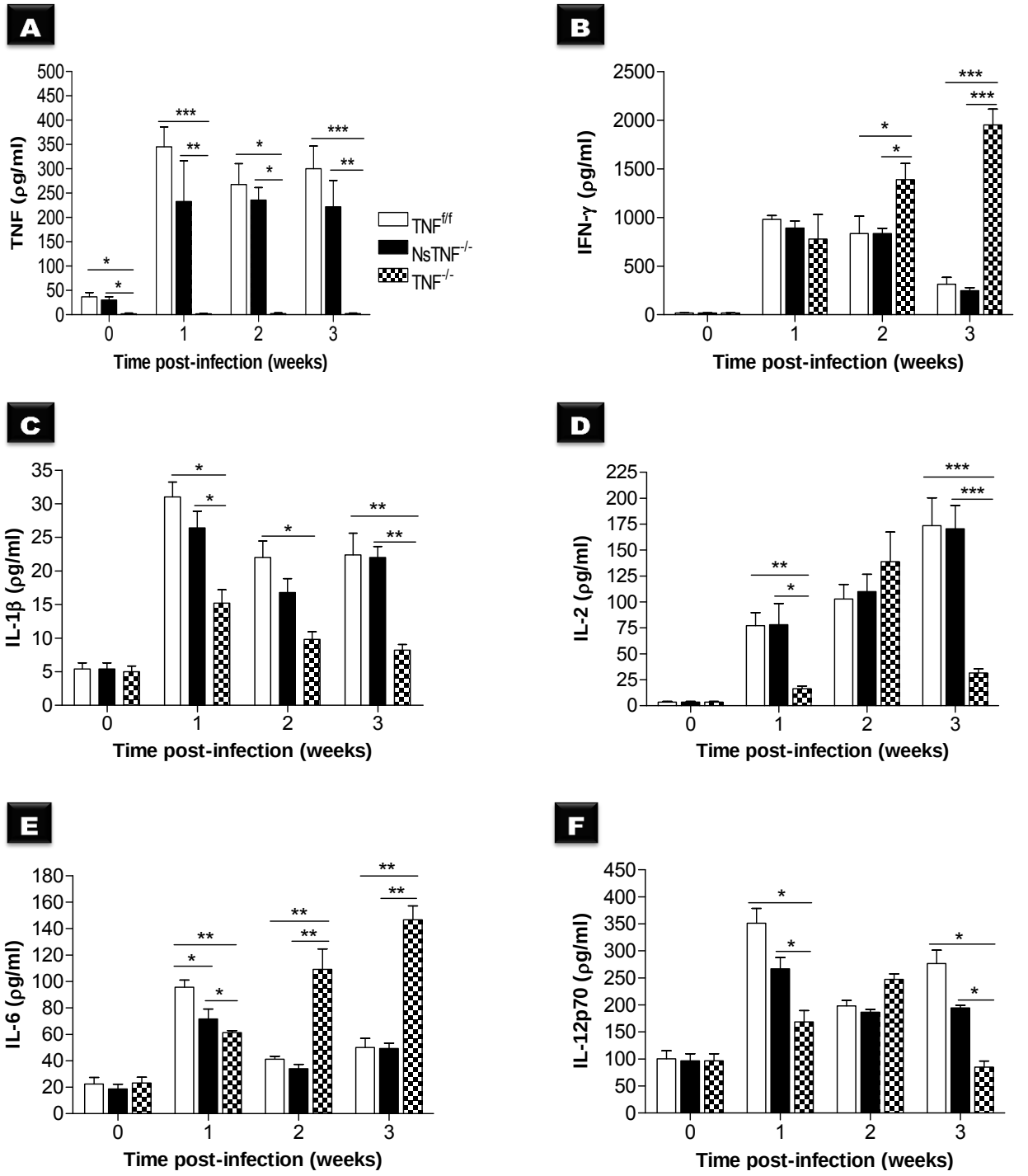

Figure 3.1.27: Relative expression of total cerebral cytokines during neurotuberculosis. $TNF^{f/f}$, $NsTNF^{-/-}$ and $TNF^{-/-}$ mice were intracerebrally infected with *M. tuberculosis* at a dose of $1x10^5$ cfu/brain at week 1, 2 and 3. Cytokine concentrations were measured at week 0 (naïve), 1, 2 and 3 weeks post-infection, where the brains of mice were homogenised and TNF (A), IFN-γ (B), IL-1β (C), IL-2 (D), IL-6 (E) and IL-12p70 (F) levels were measured in the supernatants by ELISA. Data are representative of at least three independent experiments that yielded similar results. Results are mean ± SD of 5 mice/group. *=p < 0.05, **=p < 0.01 and ***=p < 0.001.

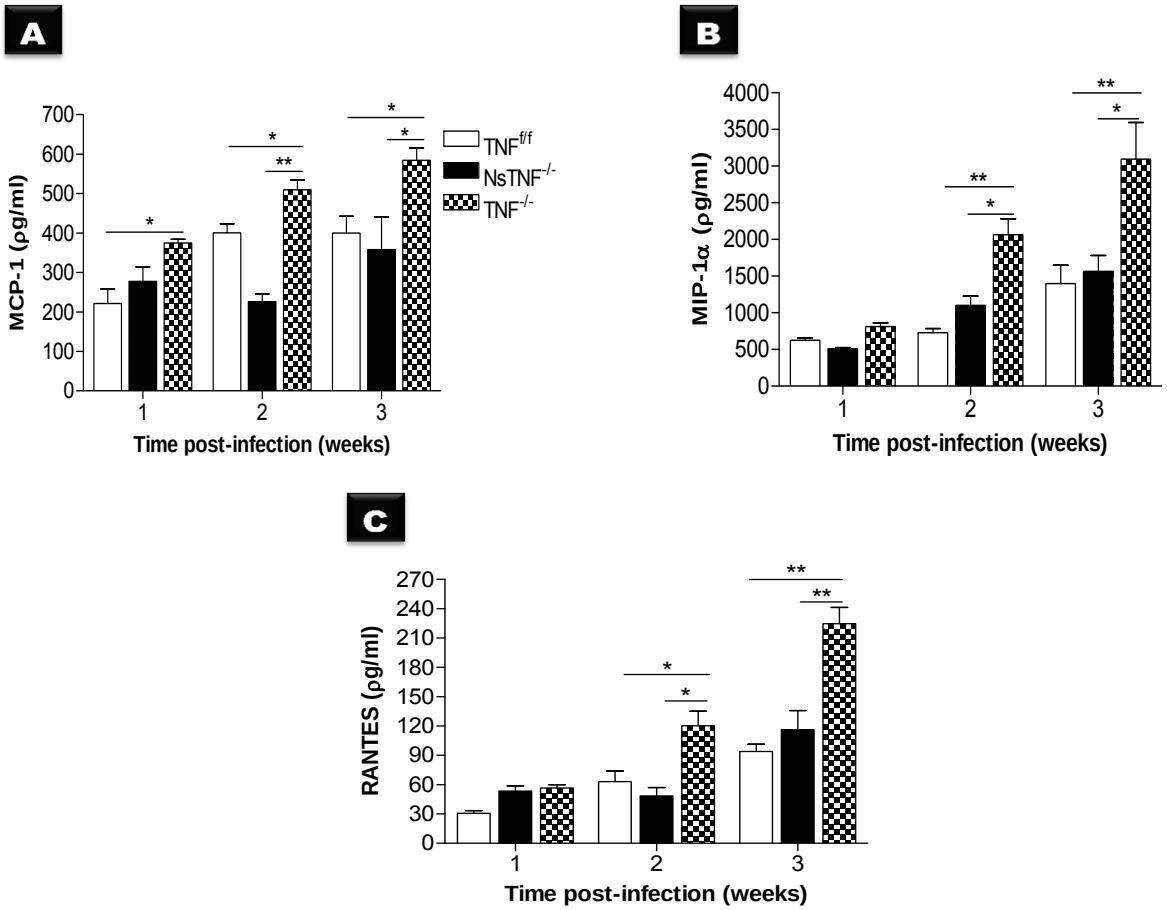

Figure 3.1.28: TNF regulates cerebral chemokines production during neurotuberculosis. $TNF^{f/f}$, $NsTNF^{-/-}$ and $TNF^{-/-}$ mice were intracerebrally infected with *M. tuberculosis* at a dose of $1x10^5$ cfu/brain. Chemokines concentration was measured at 1, 2 and 3 weeks post-infection, where the brains of infected mice were homogenised and MCP-1 (A), MIP-1α (B) and RANTES (C) levels were assessed in the supernatants by ELISA. Data are representative of at least three independent experiments that yielded similar results. Results are mean ± SD of 5 mice/group. *=$p < 0.05$ and **=$p < 0.01$.

R1.12 General summary

Taken together, our data suggest that neuronal derived TNF has very limited protection against cerebral *M. tuberculosis* infection. Thus, the resistance to cerebral *M. tuberculosis* infection observed in this mouse strain may be due to compensation from other TNF cellular sources such as myeloid TNF derived cell, or to the lack of redundancy of other cytokines such as lymphotoxin, which may signal through both TNFR1 and TNFR2 like TNF but cannot compensate for TNF. Data also show that complete ablation of TNF is detrimental to host immunity, leading to high susceptibility.

The role of microglia-macrophages, neutrophils and T cell subsets derived TNF in protective immunity against neurotuberculosis

R2.1 Confirmation of M-TNF$^{-/-}$ and MT-TNF$^{-/-}$ mice genotype by PCR analysis

To investigate the role of myeloid derived TNF during neurotuberculosis, we used cell-type specific microglia/macrophages and neutrophils TNF knockout (M-TNF$^{-/-}$), TNF floxed (TNF$^{f/f}$) and global TNF knockout (TNF$^{-/-}$) mice. The genotypes of TNF$^{f/f}$ and TNF$^{-/-}$ mice were confirmed as described in sections R1.1 and R1.1.1, respectively, (Figure 3.1.1B and Figure 3.1.4). M-TNF$^{-/-}$ mice were genotyped for the, presence of the Cre gene directed under the Mlys Cre promoter in the Mlys1 locus by using Mlys1, Mlys2 and Cre8 primers. The 700bp (primers Cre8 and Mlys1) amplification product confirmed the presence of the Cre transgene (lanes 3-6, from the left hand) as seen in Figure 3.2.1A. Mlys Cre transgene is constitutively expressed in cells of myeloid origin (Park *et al.,* 2002 and Greten *et al.,* 2004) including microglia (Perry *et al.,* 1985; Zucker-Franklin *et al.,* 1987; Hao *et al.,* 1991; Cho *et al.,* 2008; Solodova *et al.,* 2011 and Kallfass *et al.,* 2012). Amplification using primers Mlys1 and Mlys2 yielded the WT allele, represented by a 350bp amplification product (lanes 1-8) as shown in Figure 3.2.1A. To confirm the presence of the floxed TNF gene, specific flox primers (KO41 and KO42), yielded a 400bp amplification product (Figure 3.2.1B: lanes 2-7, from the left hand). The unfloxed TNF gene in C57BL/6J mice (lanes 1 and 8) is represented by a 350bp gene product. Thus, all M-TNF$^{-/-}$ mice used in this study were confirmed as being of the genotype TNF$^{f/f}$Mlys$^{Cre/wt}$.

Next, we confirmed the genotype of MT-TNF$^{-/-}$ mice. The Cre gene in the Mlys1 locus was identified using primers Mlys1, Mlys2 and Cre8 represented by a 700bp (primers Cre8 and Mlys1) amplification product (Figure 3.2.2A: lanes 2-6). The WT allele is represented by an amplification product of 350bp (Figure 3.2.2A: lanes 1-6, from the left hand). We also confirmed the presence of the Cre gene under control of the CD4 promoter using CD4Cre1, CD4Cre2 and CD4Cre3 primers. The Cre gene was confirmed by PCR analysis using primers CD4Cre1 and CD4Cre2 which resulted in a 242bp amplification product (Figure 3.2.2B: lanes 2-6), while amplification using primers CD4Cre1 and CD4Cre3 generated the 350bp WT allelic amplification product (Figure 3.2.2B: lanes 1-6, from the left hand). We further confirmed the presence of the TNF gene with two flanking loxP sequences using the flox specific primers (KO41 and KO42) represented by a 400bp amplification product (lanes 2-7, from the left hand), while the unfloxed allele in C57BL/6J mice (lanes 1-8, from the left hand) is represented by a

350 amplification product (Figure 3.2.2C).

MT-TNF$^{-/-}$ mice used in this study were confirmed as being of the genotype TNF$^{f/f}$Mlys$^{Cre/wt}$CD4$^{Cre/wt}$ as previously published (Allie *et al.,* 2013).

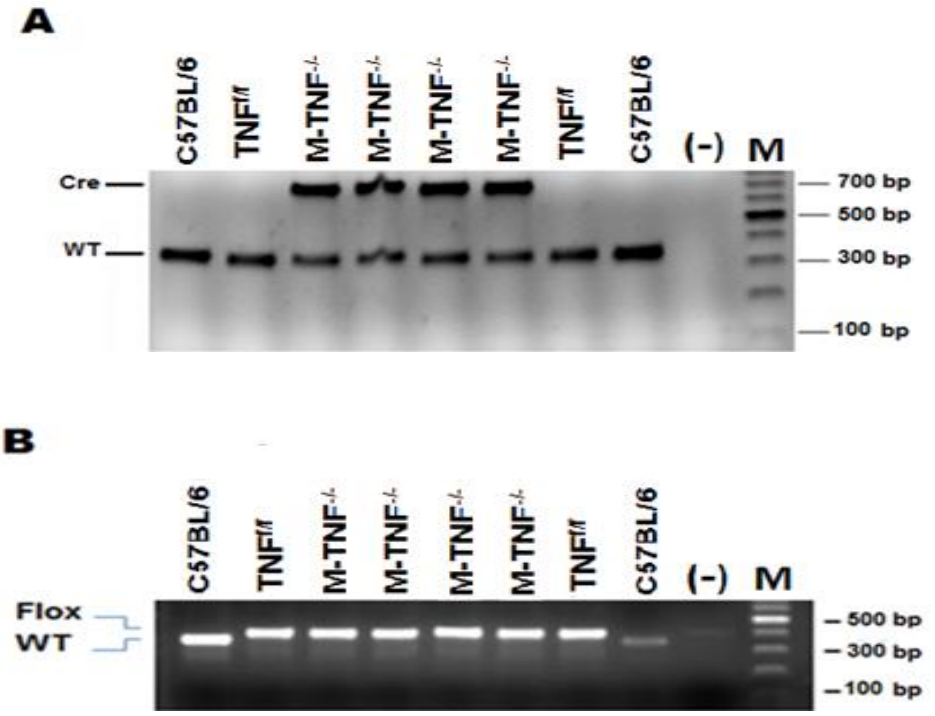

Figure 3.2.1: Genotyping of M-TNF$^{-/-}$ mice. PCR analysis was performed using genomic DNA extracted from tail biopsies using Mlys Cre specific primers Mlys 1, Mlys 2 and Cre8 (A). WT (C57BL/6J) and TNF$^{f/f}$ mice were used as positive controls and water as a negative control (-). The presence of the Cre gene in M-TNF$^{-/-}$ mice (lanes 3-6, from the left hand) yielded an amplification product of 700bp (primers Cre8 and Mlys 1) (A). An amplification product of 350bp (primers Mlys 1 and Mlys2) confirmed the presence of TNF gene in the WT mice indicative of C57BL/6J mice. We further used the flox specific primers (KO41 and KO42) to confirm the presence of the TNF gene with two flanking loxP sequences, confirming the TNF floxed gene (400bp). The unfloxed TNF gene in C57BL/6J mice is represented by a 350bp amplification product (B).

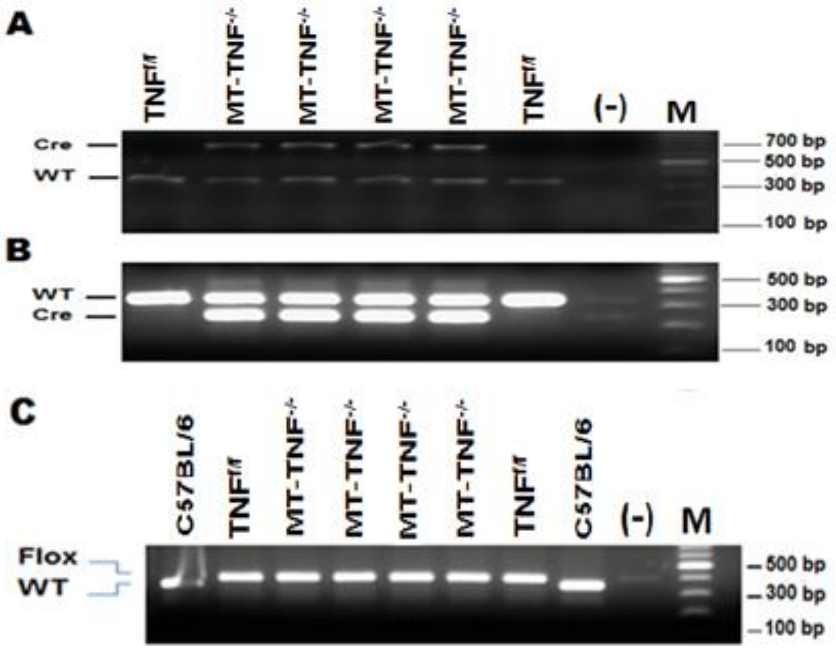

Figure 3.2.2: Genotyping of MT-TNF$^{-/-}$ mice. PCR analysis was performed using genomic DNA extracted from tail biopsies using Mlys Cre specific primers: Mlys1, Mlys 2 and Cre8. WT (C57BL/6J) and TNF$^{f/f}$ mice were used as positive controls and water as a negative control (-). Amplification product of 350bp (primers Mlys1 and Mlys2) confirmed the presence TNF gene in WT control C57BL/6J mice, however the presence of the Cre gene (lanes 2-5 from the lef hand) yielded an amplification product of 700bp (primers Cre8 and Mlys1) (A). The same DNA sample was subsequently analysed for the presence of CD4 Cre expression using CD4 Cre specific primers: CD4Cre1, CD4Cre2 and CD4Cre3. An amplification product of 350bp (primers CD4Cre1 and CD4Cre3) confirmed the presence TNF gene in the WT control mice indicative of C57BL/6J background. However, the presence of the Cre gene (lanes 2-5, from the left hand) yielded an amplification product of 242bp (primers CD4Cre1 and CD4Cre2) (B). When using the flox specific primers (KO41 and KO42), the presence of TNF gene with two flanking loxP sequences was confirmed, TNF floxed gene yielded 400bp (lanes 2-7, from the left hand), while the unfloxed TNF gene in C57BL/6J mice is represented by a 350bp amplification product as seen in lanes 1 and 8 (C).

R2.2 MT-TNF$^{-/-}$ mice but not M-TNF$^{-/-}$ are highly susceptible and induced clinical neurologic manifestations during experimental CNS *M. tuberculos*is infection

To investigate the cellular origin of protective TNF in experimental neurotuberculosis, we intracerebrally infected TNF$^{f/f}$, M-TNF$^{-/-}$, MT-TNF$^{-/-}$ and TNF$^{-/-}$ mice with 1x10^5 cfu/brain of *M. tuberculosis*. The survival rate of mice was monitored; body weights and organ weights measured, and clinical scores recorded.

Our data showed that M-TNF$^{-/-}$ mice survived experimental cerebral *M. tuberculosis* infection and subsequently gained weight together with the TNF$^{f/f}$ mice (Figure 3.2.3A-B). In contrast, we found that the MT-TNF$^{-/-}$ mice succumbed to experimental cerebral *M. tuberculosis* infection by 21 days post-infection similar to global TNF$^{-/-}$ mice. We also found that the MT-TNF$^{-/-}$ mice dramatically lost > 20% of their body weight by day 21 post-infection similar to TNF$^{-/-}$ mice (Figure 3.2.3A-B).

As previously reported, no clinical manifestations were induced in TNF$^{f/f}$ mice, and also no overt clinical neurologic manifestations were induced in the M-TNF$^{-/-}$ mice (Figure 3.2.4A). In contrast, the MT-TNF$^{-/-}$ mice induced severe clinical manifestations ($p < 0.01$) comparable to TNF$^{-/-}$ mice within 16-21 days post-infection (Figure 3.2.4A). The maximum severity of disease was observed at day 20, where animals entered moribund state. The severity of the clinical neurologic manifestations correlated with tuberculosis susceptibility.

In addition, we measured organ weights of brains, lungs and spleens during the course of the infection. The brain weights in M-TNF$^{-/-}$ mice showed no significant difference when compared to TNF$^{f/f}$ mice, both TNF$^{f/f}$ and M-TNF$^{-/-}$ mice showed significantly higher brain weight at week 3 post-infection when compared to earlier time points (Figure 3.2.4B). The brain weights of the MT-TNF$^{-/-}$ mice was similar to TNF$^{-/-}$ mice and significantly lower ($p < 0.01$) at week 3 post-infection compared to TNF$^{f/f}$ and M-TNF$^{-/-}$ mice. No significant differences in brain weights were observed in either MT-TNF$^{-/-}$ mice or TNF$^{-/-}$ mice when relative comparisons are made to earlier time points (Figure 3.2.4B).

Lung weights of all mouse strains showed no significant difference at week 1 and 2 post *M. tuberculosis* infection. Similarly, no significant difference was observed in M-TNF$^{-/-}$ mice at week 3 post-infection when compared to TNF$^{f/f}$ mice. The lung weights of the MT-TNF$^{-/-}$ mice was similar to TNF$^{-/-}$ mice and significantly lower ($p < 0.05$) at week 3 post-infection compared to TNF$^{f/f}$ and M-TNF$^{-/-}$ mice. No significant differences in lung weights were observed in either MT-TNF$^{-/-}$ mice or TNF$^{-/-}$ mice when relative comparisons are made to earlier time points (Figure 3.2.4C).

We found no significant difference in spleen weight of M-TNF$^{-/-}$ mice at all time points post-infection when compared with TNF$^{f/f}$ mice (Figure 3.2.4D). On the contrary, MT-TNF$^{-/-}$ mice showed significant ($p < 0.05$) increase in spleen weight similar to the TNF$^{-/-}$ mice at week 3 post-infection when compared with TNF$^{f/f}$ (Figure 3.2.4D). We have previously found that CD4/CD8-TNF$^{-/-}$ mice (T-TNF$^{-/-}$) are not susceptible to experimental cerebral *M. tuberculosis* infection (unpublished data).

The data from this study showed that myeloid derived TNF does not play a critical role in

the control of cerebral *M. tuberculosis* infection. Data also suggest strongly that T cell-derived TNF in the M-TNF$^{-/-}$ mice is responsible for controlling cerebral TB infection.

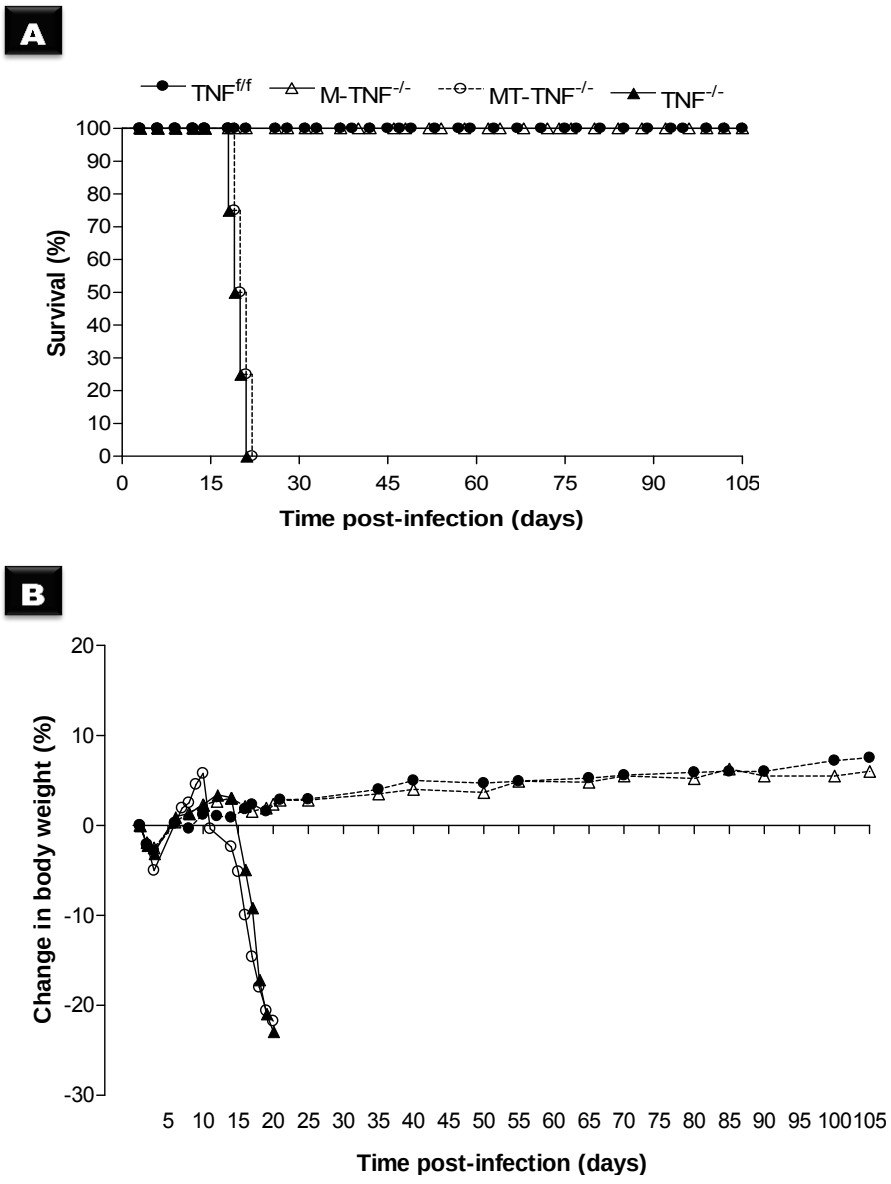

Figure 3.2.3: MT-TNF$^{-/-}$ mice succumbed to experimental CNS *M. tuberculosis* infection. TNF$^{f/f}$, M-TNF$^{-/-}$, MT-TNF$^{-/-}$ and TNF$^{-/-}$ mice were intracerebrally infected with 1x10^5 cfu/brain of *M. tuberculosis*. The percentage of survival (A) and changes in body weight (B) were monitored for 105 days subsequent to infection. Data shown are representative of one of three independent experiments. Results are expressed as the mean of 10 mice/group.

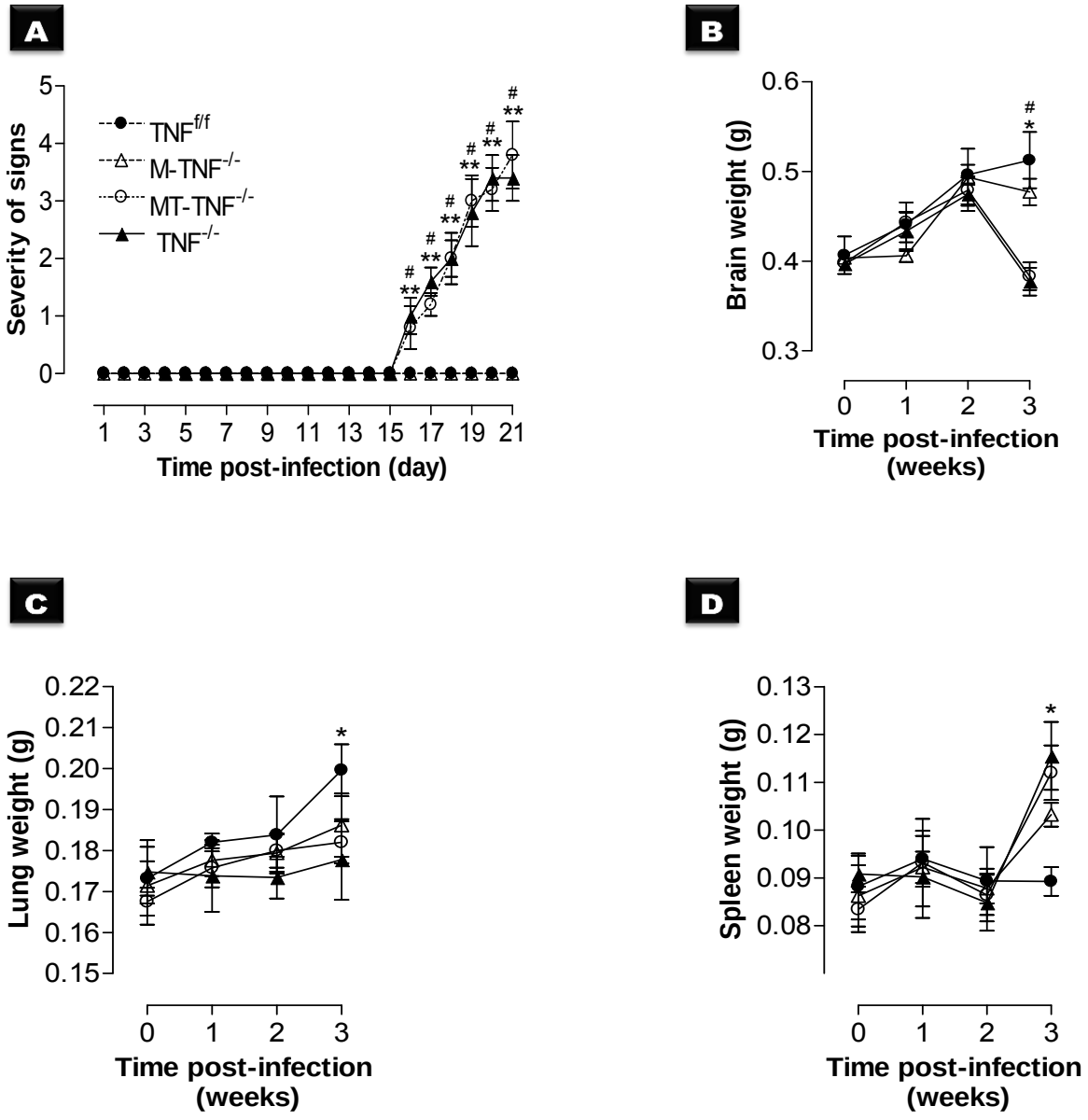

Figure 3.2.4: Clinical state deterioration and increase inflammation in MT-TNF$^{-/-}$ mice during acute CNS *M. tuberculosis* infection. TNF$^{f/f}$, M-TNF$^{-/-}$, MT-TNF$^{-/-}$ and TNF$^{-/-}$ mice were intracerebrally infected with *M. tuberculosis* at a dose of 1x10^5 cfu/brain. Clinical neurologic manifestations after intracerebral infection were scored and recorded during 21 days (A). $^{\#}$=p < 0.01 for MT-TNF$^{-/-}$ or TNF$^{-/-}$ vs M-TNF$^{-/-}$ mice. Each data point represents the mean ± SD of 10 animals per group. Organ weights (B-D): Mice were euthanised at week 0 (naïve), 1, 2 and 3 post-infection, brain weights (B), lung weights (C) and spleen weights (D) were measured. Data presented here are one of three independent experiments, and are means ± SD of 5 mice/group. *=p < 0.05 and **=p < 0.01.

R2.3 Uncontrolled *M. tuberculosis* replication in MT-TNF$^{-/-}$ but not in M-TNF$^{-/-}$ mice during neurotuberculosis

To assess the importance of TNF in the control of bacilli replication, we compared pathogen burden in the brains, lungs and spleens of *M. tuberculosis* infected TNF$^{f/f}$, M-TNF$^{-/-}$, MT-TNF$^{-/-}$ and TNF$^{-/-}$ mice (Figure 3.2.5A-F). Our data showed that the *M. tuberculosis* bacterial burden in the brain was increased in TNF$^{f/f}$ and M-TNF$^{-/-}$ mice over 3 weeks period compared to the earlier post-infection time point (Figure 3.2.5A). No significant differences were observed in cerebral bacilli burdens of M-TNF$^{-/-}$ mice during either acute or chronic infection compared to TNF$^{f/f}$ mice (Figure 3.2.5A and B). MT-TNF$^{-/-}$ and TNF$^{-/-}$ mice exhibited similar significant increases in bacilli burdens compared to TNF$^{f/f}$ and M-TNF$^{-/-}$ mice at week 2 ($p < 0.01$), and week 3 ($p < 0.001$) post-infection (Figure 3.2.5A). We next assessed the extent of dissemination of bacilli from the brain by measuring the levels of bacilli burden in the lung and spleen. M-TNF$^{-/-}$ mice showed mycobacterial dissemination similar to the TNF$^{f/f}$ mice in both lungs (Figure 3.2.5C) and spleen (Figure 3.2.5E) during acute infection. We observed a significant ($p < 0.05$) increase in the pulmonary bacilli burden in M-TNF$^{-/-}$ mice during chronic infection compared to TNF$^{f/f}$ mice (Figure 3.2.5D). No significant difference was seen between M-TNF$^{-/-}$ and TNF$^{f/f}$ splenic bacilli burden during chronic infection (Figure 3.2.5F). MT-TNF$^{-/-}$ and complete TNF$^{-/-}$ mice exhibited significant ($p < 0.01$) increases in mycobacterial dissemination at week 1, 2 and 3 post-infection in the lung, and at week 2 and 3 ($p < 0.01$) post-infection in the spleen when compared to TNF$^{f/f}$ and M-TNF$^{-/-}$ mice (Figure 3.2.5C and E).

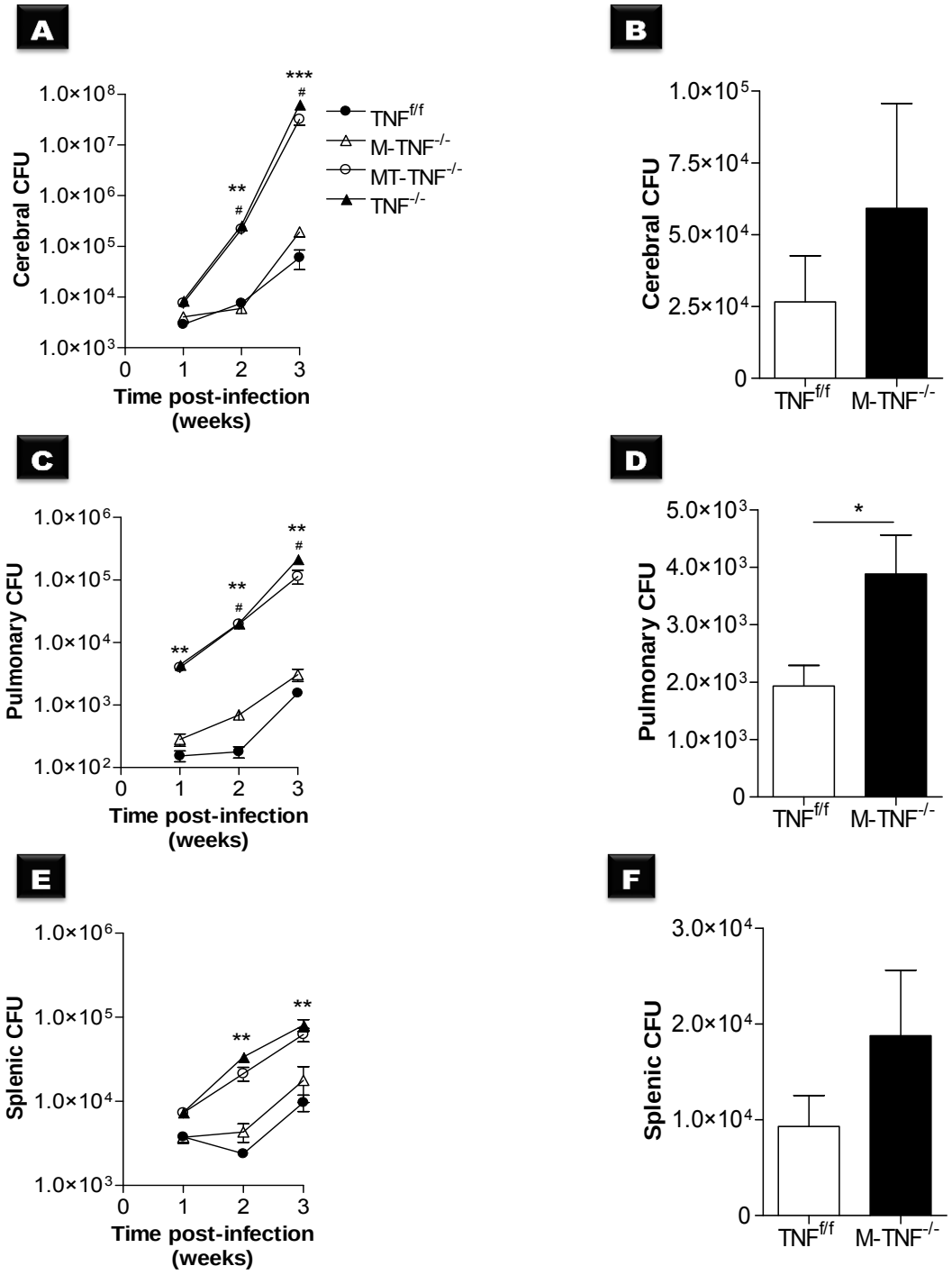

Figure 3.2.5: MT-TNF$^{-/-}$ mice are susceptible to CNS *M. tuberculosis* infection. TNF$^{f/f}$, M-TNF$^{-/-}$, MT-TNF$^{-/-}$ and TNF$^{-/-}$ mice were intracerebrally infected with *M. tuberculosis* at a dose of 1x10^5 cfu/brain. The number of viable bacteria present in the brains (A), lungs (B) and spleens (C) was assessed at week 1, 2, 3 (acute) and 15 (chronic) post-infection. Data is representative of one of three independent experiments. Results are expressed as the mean ± SD of 5 mice/group. *=p < 0.05, **=p < 0.01 and ***=p < 0.001. $^{\#}$=p < 0.01 for MT-TNF$^{-/-}$ or TNF$^{-/-}$ versus M-TNF$^{-/-}$ mice.

Differences in bacterial growth in the brain were confirmed histologically by Ziehl-Neelsen staining with mycobacteria in M-TNF$^{-/-}$ mice largely localized intracellularly as in TNF$^{f/f}$ mice (Figure 3.2.6). The bacterial growth in M-TNF$^{-/-}$ was therefore controlled at all time points post-infection. The significant increase of bacilli burdens seen in the brains of MT-TNF$^{-/-}$ mice and in TNF$^{-/-}$ mice correlated with the significantly higher presence of acid fast bacilli, being mostly extracellular, at week 2 and 3 post-infection (Figure 3.2.6).

Thus, these data demonstrate that deletion of T cells derived TNF in M-TNF$^{-/-}$ mice renders mice highly susceptible to the infection and that myeloid derived TNF alone is redundant for the control of experimental cerebral bacterial growth.

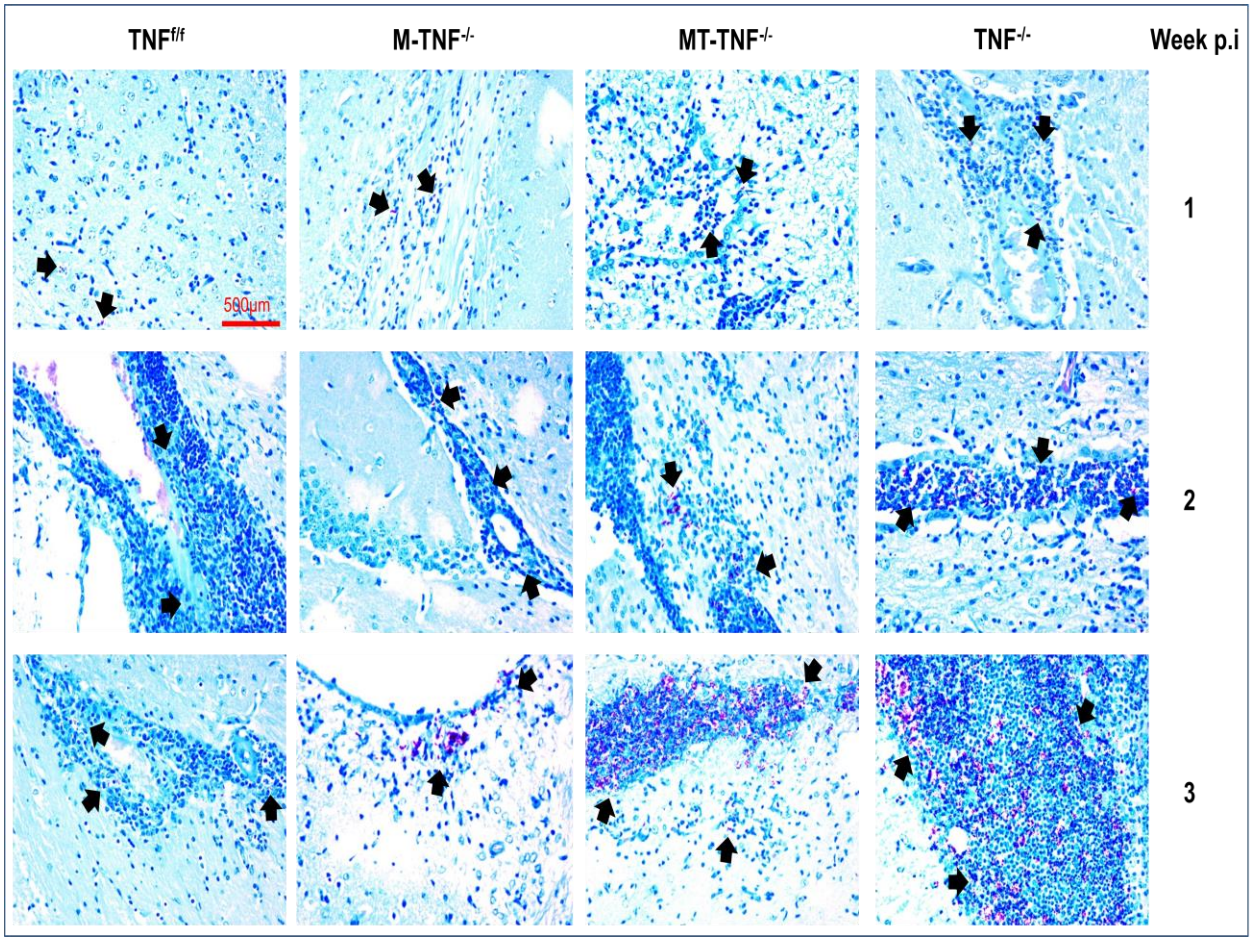

Figure 3.2.6: Uncontrolled *M. tuberculosis* growth in MT-TNF$^{-/-}$ mice. TNF$^{f/f}$, M-TNF$^{-/-}$, MT-TNF$^{-/-}$ and TNF$^{-/-}$ mice were intracerebrally infected with *M. tuberculosis* at a dose of 1x10^5 cfu/brain. The cerebral bacilli burden was confirmed by Ziehl-Neelsen staining at week 1, 2 and 3 post-infection. The results represent one of three similar experiments. Arrows indicate the presence of acid fast bacilli (AFB) (magnification= 100x).

R2.4 Increase of perivascular lymphocyte-rich foci formation in MT-TNF$^{-/-}$ mice during neurotuberculosis

Tuberculomas, also referred to as rich foci are the major characteristic of neurotuberculosis (Rich & Mc Cordock, 1933). Rich foci formation starts by the recruitment of infiltrating immune cells. Epithelioid cells, giant cells, macrophages, microglia, neutrophils, $CD4^+$- and $CD8^+$ T cells are the major constituents of the tuberculoma structure (Miranda *et al.,* 2012). We assessed whether microglia/macrophages, neutrophils and T cell subset-derived TNF signalling induced a lymphocyte-rich inflammatory foci formation (Figure 3.2.7). M-TNF$^{-/-}$ and the MT-TNF$^{-/-}$ mice were compared with TNF$^{f/f}$ and TNF$^{-/-}$ mice after intracerebral infection with *M. tuberculosis* at a dose of $1x10^5$ cfu per brain at week 1, 2 and 3 post-infection. Presence of perivascular lymphocytic infiltration in M-TNF$^{-/-}$ mice were evident, but controlled similar to that in TNF$^{f/f}$ mice at week 2 and 3 post-infection (Figure 3.2.7b-f). On the contrary, MT-TNF$^{-/-}$ mice exhibited exuberant perivascular lymphocytic infiltration similar to TNF$^{-/-}$ mice at week 3 post-infection (Figure 3.2.7i and l).

Furthermore, we examined the presence of meningeal lymphocytic infiltration in M-TNF$^{-/-}$ and MT-TNF$^{-/-}$ mice compared with TNF$^{f/f}$ and TNF$^{-/-}$ mice. All mice strains presented meningeal lymphocytic infiltration at week 3 post-infection (Figure 3.2.8c, f, i and l), however meningeal lymphocytic infiltration was more prominent in MT-TNF$^{-/-}$ than in TNF$^{f/f}$ mice, but in MT-TNF$^{-/-}$ and TNF$^{-/-}$ mice were excessive in (Figure 3.2.8i and l).

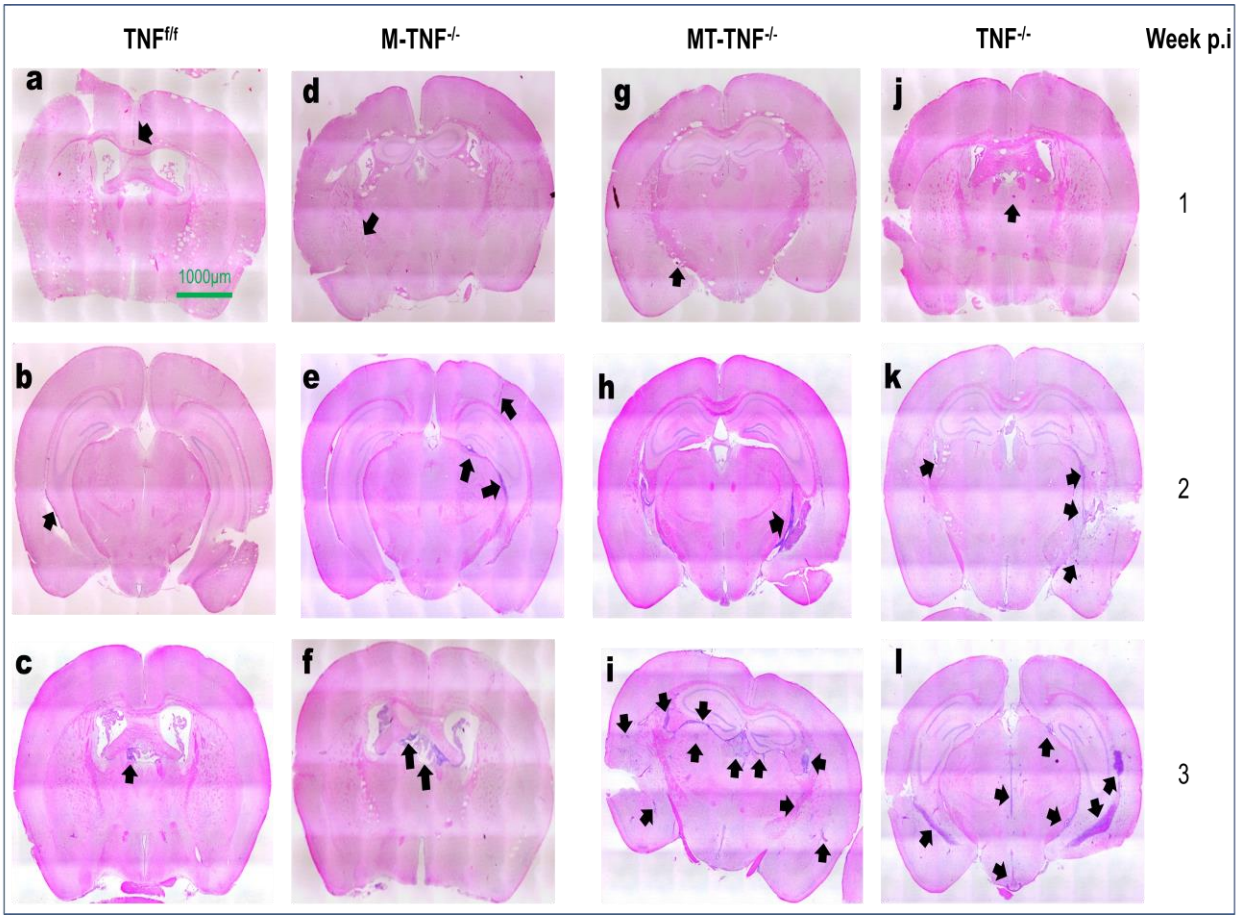

Figure 3.2.7: Increase of perivascular lymphocytic infiltration rich foci in MT-TNF$^{-/-}$ mice. Cerebral lymphocytic infiltration rich foci in TNF$^{f/f}$, M-TNF$^{-/-}$, MT-TNF$^{-/-}$ and TNF$^{-/-}$ mice intracerebrally infected with *M. tuberculosis* at a dose of 1x10^5 cfu/brain. Morphology of 2µm brain sections was assessed at week 2 and 3 post-infection after haemotoxylin and eosin staining. Arrows indicate lymphocytic infiltration foci structures. The results (*n*= 5 mice/group) represent one of three similar experiments. Magnification= 40x.

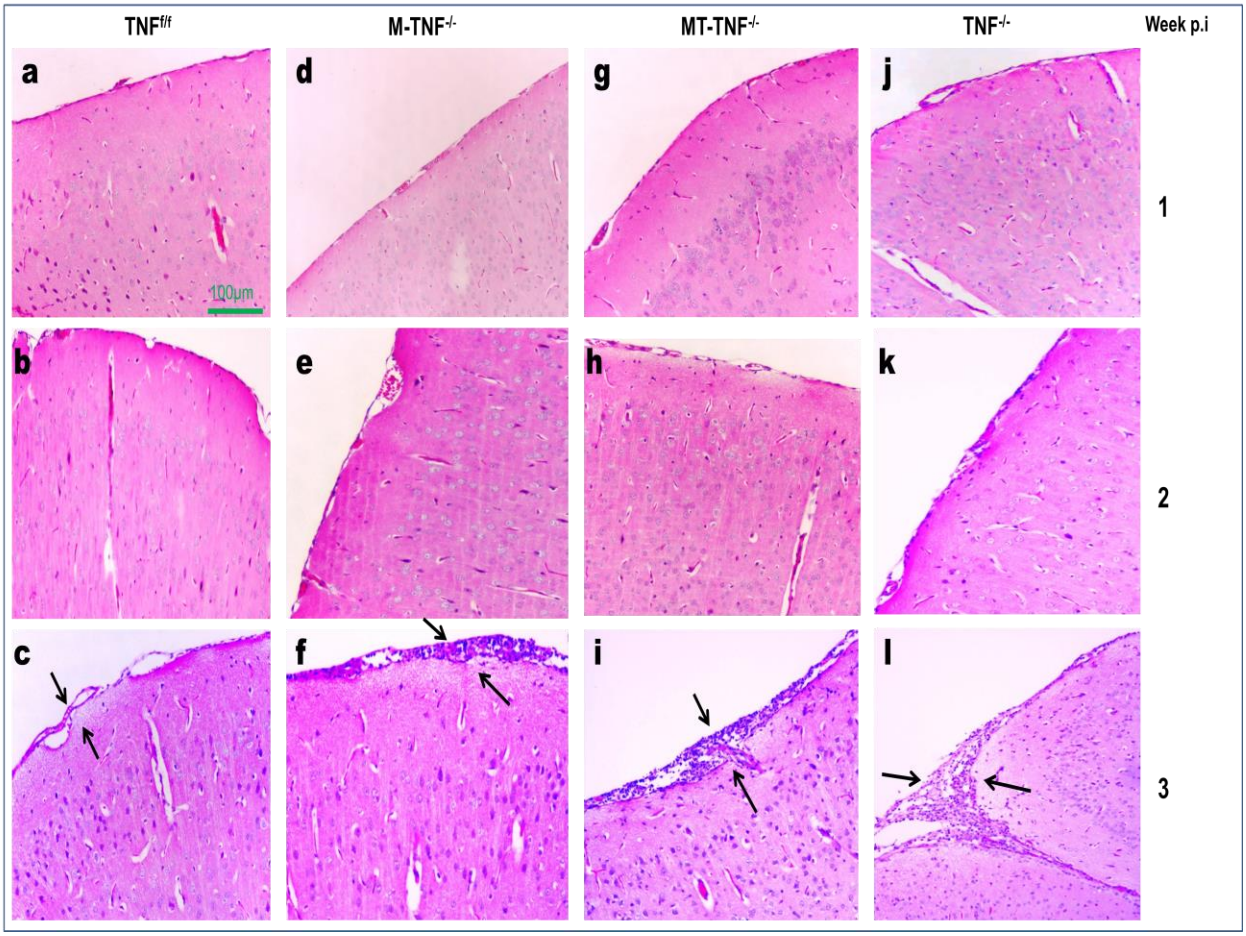

Figure 3.2.8: Exuberant meningeal lymphocytic infiltration in MT-TNF$^{-/-}$. Hematoxylin-eosin-stained section of murine brain of TNF$^{f/f}$, M-TNF$^{-/-}$, MT-TNF$^{-/-}$ and TNF$^{-/-}$ mice intracerebrally infected with *M. tuberculosis* at a dose of 1x10^5 cfu/brain and analysed at week 1, 2 and 3 post-infection. The results (*n*= 5 mice/group) represent one of three similar experiments. Arrows indicate meningeal lymphocytic infiltration. Magnification= 100x.

R2.5 Decreased expression of iNOS in MT-TNF$^{-/-}$ mice after CNS *M. tuberculosis* infection

We asked whether microglia/macrophages, neutrophils, CD4^{+}- and CD8^{+} T cells-derived TNF regulate the expression of iNOS in the brain of TNF$^{f/f}$, M-TNF$^{-/-}$, MT-TNF$^{-/-}$ and TNF$^{-/-}$ mice intracerebrally infected with *M. tuberculosis*, at a dose of 1x10^{5} cfu/brain (Figure 3.2.9). The iNOS expression pattern in M-TNF$^{-/-}$ mice were similar to TNF$^{f/f}$ mice, and largely distributed within the confinement of leukocytes infiltrating rich foci at week 3 post-infection. In contrast, both MT-TNF$^{-/-}$ and TNF$^{-/-}$ mice had a lower iNOS expression pattern, dispersed and associated with the diffused leukocytes infiltrating rich foci when compared either to TNF$^{f/f}$ or M-TNF$^{-/-}$ mice (Figure 3.2.9).

Our data show microglia/macrophages and neutrophils derived TNF is not required in the regulation of iNOS expression. This could be the result of compensation from T cell-derived TNF. Data also demonstrate that the ablation of T cells derived TNF in M-TNF$^{-/-}$ mice alter the iNOS induction during cerebral *M. tuberculosis* infection and present a phenotype similarly to complete TNF deficient mice. Therefore, the results obtained confirm a critical role of T cell-derived TNF in cerebral *M. tuberculosis* infection.

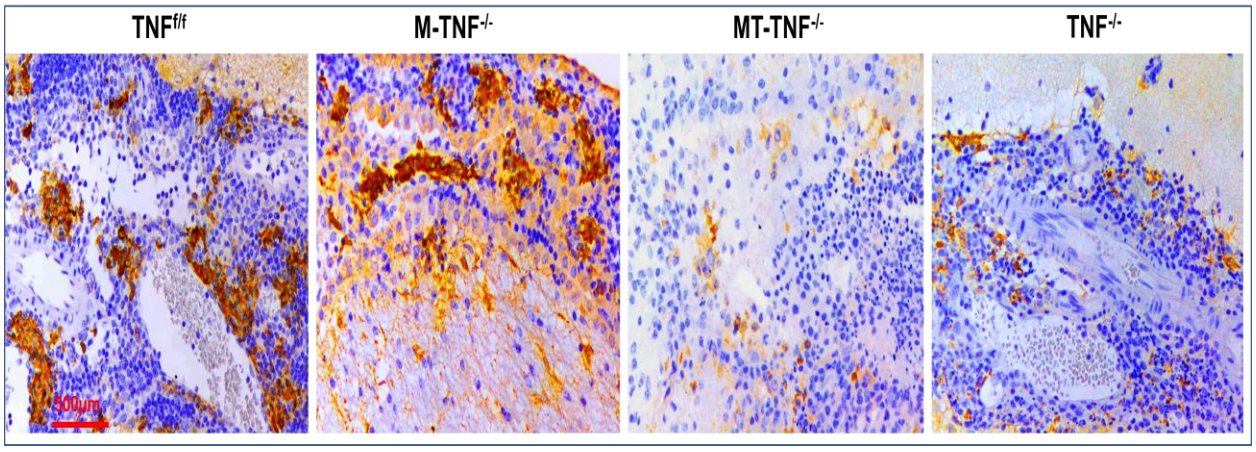

Figure 3.2.9: Decreased expression of iNOS in the brain of MT-TNF$^{-/-}$ mice. TNF$^{f/f}$, M-TNF$^{-/-}$, MT-TNF$^{-/-}$ and TNF$^{-/-}$ mice were intracerebrally infected with *M. tuberculosis* at a dose of 1x10^{5} cfu/brain and brain tissue sectioned at 2µm; for analysis of iNOS expression at week 3 post-infection. Data (*n*= 5 mice/group) represent one out of three similar experiments (magnification= 200x).

R2.6 Increased recruitment of myeloid derived cells in MT-TNF$^{-/-}$ mice but not M-TNF$^{-/-}$ mice during CNS *M. tuberculosis* infection

To address whether microglia/macrophages and neutrophils, CD4^{+}- and CD8^{+} T cells-derived TNF regulates cellular influx and proliferation in response to cerebral *M. tuberculosis* infection, we analysed macrophages, dendritic cells and resident microglia over a 3 week period. TNF$^{f/f}$, M-TNF$^{-/-}$, MT-TNF$^{-/-}$ and TNF$^{-/-}$ mice were intracerebrally infected with *M. tuberculosis* at a dose of 1x10^{5} cfu/brain. Whole brain tissues were harvested at week 0 (naïve) 1, 2 and 3 post-infection, and single cells were generated. Single cells were labelled with specific markers (CD11b:PerCP-Cy5-5, CD11c:Alexa 700 and CD45:APC) and flow cytometric analysis was used to identify the different cell populations.

The CD11b^{+}CD45^{low} (microglia) population in TNF$^{f/f}$ mice increased to 2-fold at week 3 compared to week 1 post-infection (Figure 3.2.10). Similarly, M-TNF$^{-/-}$ mice showed a significant (p < 0.05) increase in the proliferation of the microglia population at week 3 post-infection compared to week 1 post-infection. However, the microglia population in the M-TNF$^{-/-}$ mice increased to 2-fold at week 1 post-infection compared to TNF$^{f/f}$, MT-TNF$^{-/-}$ or TNF$^{-/-}$ mice. In MT-TNF$^{-/-}$ mice, the microglia population was significantly (p < 0.05) increased similar to TNF$^{-/-}$ mice at week 3 compared to week 1 post-infection. We also found a 2-fold increase in the microglia population of MT-TNF$^{-/-}$ mice at week 2 and 3 post-infection compared either to TNF$^{f/f}$ or M-TNF$^{-/-}$ mice. No significant difference was observed between MT-TNF$^{-/-}$ and TNF$^{-/-}$ mice at all time points (Figure 3.2.10). We further investigated the cerebral infiltrating CD11b^{+}CD45^{high} (macrophages) population, and we found that macrophage population infiltration occurred subsequent to neurotuberculosis infection. In M-TNF$^{-/-}$ mice, we found approximately 2-fold increase at week 3 post-infection compared to week 1 post-infection. In addition, a 2-fold increase was observed in M-TNF$^{-/-}$ mice at week 3 post-infection compared to TNF$^{f/f}$ mice, and no significant difference was observed at earlier time points (Figure 3.2.10). We next assessed the macrophage population in MT-TNF$^{-/-}$ mice and found that the percentage influx of infiltrating macrophage population was increased in both MT-TNF$^{-/-}$ and TNF$^{-/-}$ mice to 4-fold at week 1, 6-fold at week 2, and 10-fold at week 3 post-infection compared to TNF$^{f/f}$ mice (Figure 3.2.10). In addition, a 2-fold increase was also noticed in both MT-TNF$^{-/-}$ and TNF$^{-/-}$ mice at week 2 and 3 post-infection when comparing with M-TNF$^{-/-}$ mice (Figure 3.2.10). We last examined the cerebral infiltrating CD11b^{low}CD45^{high} (dendritic cells) population. In the dendritic cells population kinetic, we found a 30-fold increase in TNF$^{f/f}$ mice and 60-fold increase in M-TNF$^{-/-}$ mice at week 3 post-infection when comparing with week 1 post-infection. In addition, the dendritic cell

population infiltrated almost equally into the CNS when comparing M-TNF$^{-/-}$ with TNF$^{f/f}$ mice at week 1 post-infection. However, a 3-fold increase was observed in M-TNF$^{-/-}$ at week 2 and 3 post-infection compared to TNF$^{f/f}$ mice (Figure 3.2.10). In contrast, the DCs population in MT-TNF$^{-/-}$ mice showed 100-fold higher numbers at week 3 post-infection compared to week 1 post-infection. A similar trend was also seen in TNF$^{-/-}$ mice. We also observed an increase infiltrating DCs population in both MT-TNF$^{-/-}$ and TNF$^{-/-}$ mice to 2-fold at week 1, 4-fold at week 2, and almost 6-fold at week 3 post-infection when comparing with TNF$^{f/f}$ mice (Figure 3.2.10).

We thereafter investigated the absolute numbers of microglia, macrophages and dendritic cell population. Assessing the microglia absolute number, we found similar levels of absolute cell numbers in all the naïve mouse strains as in previous result section. No significant differences in absolute numbers were observed in all mouse strains at week 1 and 2 post-infection (Figure 3.2.11A). However, the microglia cells in both MT-TNF$^{-/-}$ and TNF$^{-/-}$ mice were significantly ($p < 0.05$) increased at week 3 post-infection when compared to TNF$^{f/f}$ mice (Figure 3.2.11A). No significant difference was observed between M-TNF$^{-/-}$ and MT-TNF$^{-/-}$ or TNF$^{-/-}$ mice.

We found 5- and 6-fold increases in the infiltrating macrophage population in TNF$^{f/f}$ mice at week 2 and 3 post-infection, respectively when compared to week 1 post-infection. Similar increases were observed in M-TNF$^{-/-}$, MT-TNF$^{-/-}$ and TNF$^{-/-}$ mice at week 2 and 3 post-infection. We also found that deletion of TNF in the microglia/macrophages and neutrophils resulted in a significant ($p < 0.05$) increase in the macrophage population of M-TNF$^{-/-}$ mice only at week 3 post-infection when compared with TNF$^{f/f}$ mice (Figure 3.2.11B). Also, a significant ($p < 0.01$) increasein the macrophage population was observed in the MT-TNF$^{-/-}$ and TNF$^{-/-}$ mice compared to TNF$^{f/f}$ mice at week 2 and 3 post-infection (Figure 3.2.11B). No significant difference was observed between M-TNF$^{-/-}$ and MT-TNF$^{-/-}$ mice or TNF$^{-/-}$ mice.

Approximately 3- to 4-fold increase of DCs population into the brain was observed at week 2 and 3 post-infection in all mouse strains compared to week 1 post-infection (Figure 3.2.12C). No significant differences in the absolute numbers of the DC population of M-TNF$^{-/-}$ mice were observed at all time points post-infection compared to TNF$^{f/f}$ mice. TNF$^{-/-}$ mice had a greater ($p < 0.05$) absolute number of the DC population at week 2 post-infection compared to TNF$^{f/f}$ mice. Remarkably, both MT-TNF$^{-/-}$ and TNF$^{-/-}$ mice had significant ($p < 0.01$) increase in absolute numbers at week 3 post-infection compared to TNF$^{f/f}$ mice (Figure 3.2.11C). We did not find any significant difference when comparing M-TNF$^{-/-}$ with either MT-TNF$^{-/-}$ or TNF$^{-/-}$ mice.

Our results clearly demonstrate that TNF derived from microglia/macrophages and neutrophils is not required to control the influx of infiltration macrophages and DC as well as the

proliferation of the microglia population. We speculated here that the protection observed in M-TNF$^{-/-}$ mice may result from the compensation of T cell or other non-imunne cell-type derived TNF. Also, data revealed that the deletion of TNF from T cells in the M-TNF$^{-/-}$ mice increases the influx infiltration of myeloid cell subsets during cerebral *M. tuberculosis* infection and argues for an important contribution of T cell-derived TNF in regulating inflammation in response to CNS-TB.

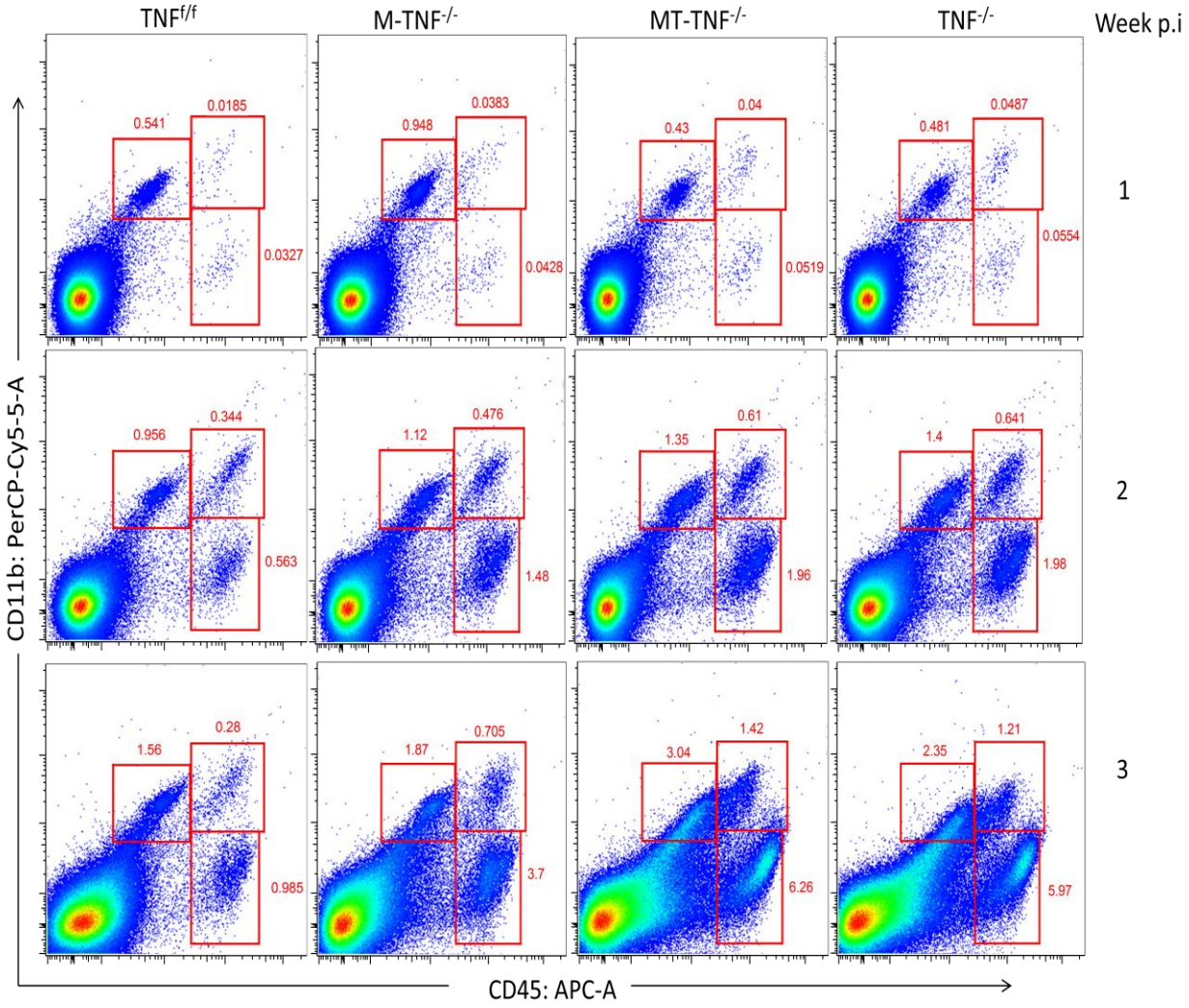

Figure 3.2.10: Increased myeloid APCs infiltration and proliferation in cell-type specific mice during neurotuberculosis. Phenotypic analyses of myeloid derived APC isolated from $TNF^{f/f}$, M-$TNF^{-/-}$, MT-$TNF^{-/-}$ and $TNF^{-/-}$ mice intracerebrally infected with *M. tuberculosis* at a dose of $1x10^5$ cfu/brain. Brains were harvested at week 1, 2 and 3 post-infection, and isolated brain cells were labelled and analysed for the expression of CD11b and CD45 by flow cytometry. The values seen in the dot plot are the percentages of the parent gate which are positive. Dot plots are representative of one of two experiments and show staining of respective $CD11b^+CD45^{low}$, $CD11b^+CD45^{high}$ and $CD11b^{low}CD45^{high}$ cells. Data are representative of three independent experiments of 5 mice/group.

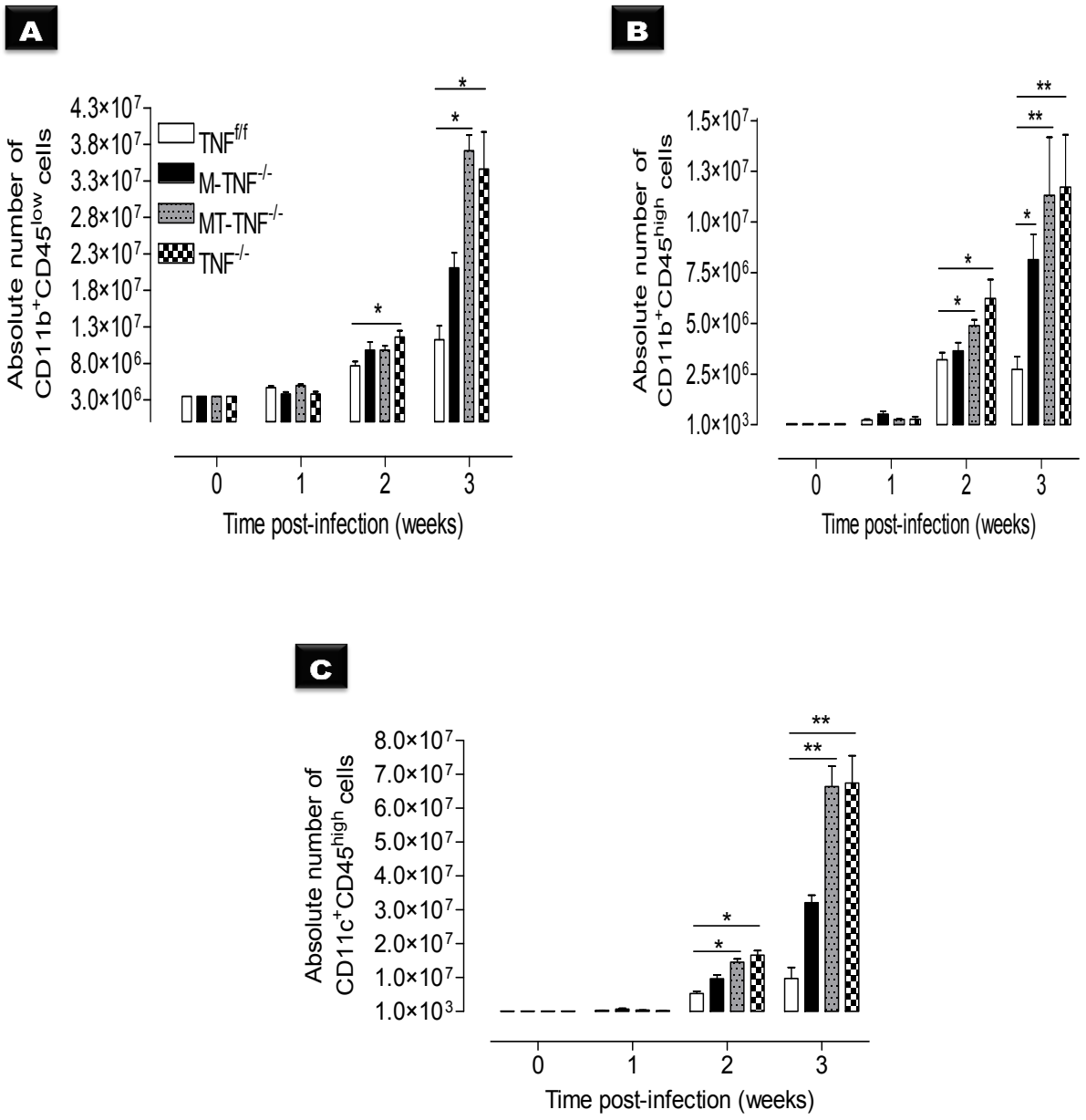

Figure 3.2.11: Increased cerebral absolute cell numbers in MT-TNF$^{-/-}$ mice. TNF$^{f/f}$, M-TNF$^{-/-}$, MT-TNF$^{-/-}$ and TNF$^{-/-}$ mice were intracerebrally infected at a different time points with *M. tuberculosis* at a dose of 1x10^5 cfu/brain. Whole brain tissues were harvested at week 0 (naïve) 1, 2 and 3 post-infection, and isolated single cells were labelled for APC and activation markers. Shown are absolute numbers of CD11b$^+$CD45^{low} cells (A), CD11b$^+$CD45^{high} cells (B) and CD11c$^+$CD45^{high} cells (C). Data (*n*= 5 mice/group) are one representative of three independent experiments. The results represent the mean ± SD and *=p < 0.05.

R2.6.1 Decreased antigen presentation by microglia of MT-TNF$^{-/-}$ mice during CNS *M. tuberculosis* infection

We investigated the role of TNF derived from microglia/macrophages, neutrophils, and CD4^{+} and CD8^{+} cells by activating microglia after intracerebrally infecting TNF$^{f/f}$, M-TNF$^{-/-}$, MT-TNF$^{-/-}$ and TNF$^{-/-}$ mice with *M. tuberculosis* at a dose of 1x10^{5} cfu/brain. Whole brain tissues were harvested at week 0 naïve, 1, 2 and 3 post-infection, and generated single cells were labelled using lineage (CD11b:PerCP-Cy5-5 and CD45:APC), co-stimulatory (CD80: FITC and CD86: V450) and antigen presenting cell marker (MHCII (I-A/I-E): PE) as seen in Figure 3.2.12.

We found that in all mouse strains, the microglia population expressed a similar percentage (~10%) of the CD80 marker at week 1 and 2 post-infection. However, in M-TNF$^{-/-}$ mice, a significant ($p < 0.01$) increase was equivalent to TNF$^{f/f}$ mice, which was observed at week 3 post-infection when compared to MT-TNF$^{-/-}$ and TNF$^{-/-}$ mice, whereby the MT-TNF$^{-/-}$ and TNF$^{-/-}$ mice maintained their percentage of CD80^{+} expressing microglia cells (Figure 3.2.12A). MFI activation of CD80^{+} was comparable to the percentage expression of CD80 marker (Figure 3.2.12B).

Similar up-regulation of CD86^{+} expressing microglia cells were found in all mouse strains at week 1, 2 and 3 post *M. tuberculosis* infection (Figure 3.2.12C). However, trend decrease was seen in MT-TNF$^{-/-}$ and TNF$^{-/-}$ mice at week 3 post-infection compared to TNF$^{f/f}$ and M-TNF$^{-/-}$ mice. Also, we found that MFI activation of CD80^{+} expressing microglia cells was comparable to the percentage expression of CD80 marker (Figure 3.2.12D).

Examining the MHCII expression, we found similar percentage and MFI expression in all mouse strains at week 1 and 2 post-infection. The percentage of MHCII^{+} expressing microglia cells was maintained the same in TNF$^{f/f}$ and M-TNF$^{-/-}$ mice at week 3 post-infection. Interestingly, the percentage of microglia cells expressing MHCII^{+} were significant ($p < 0.05$) lower in MT-TNF$^{-/-}$ mice comparable to TNF$^{-/-}$ mice at week 3 post-infection compared to TNF$^{f/f}$ and M-TNF$^{-/-}$ mice (Figure 3.2.12E and F).

The data suggest that although TNF is required for the control of microglia cell activation, the acclaimed microglia/macrophages and neutrophils TNF component is not critical for this control. In contrast, the ablation of T cells-derived TNF in the M-TNF$^{-/-}$ mice decreased the response to antigens in microglia.

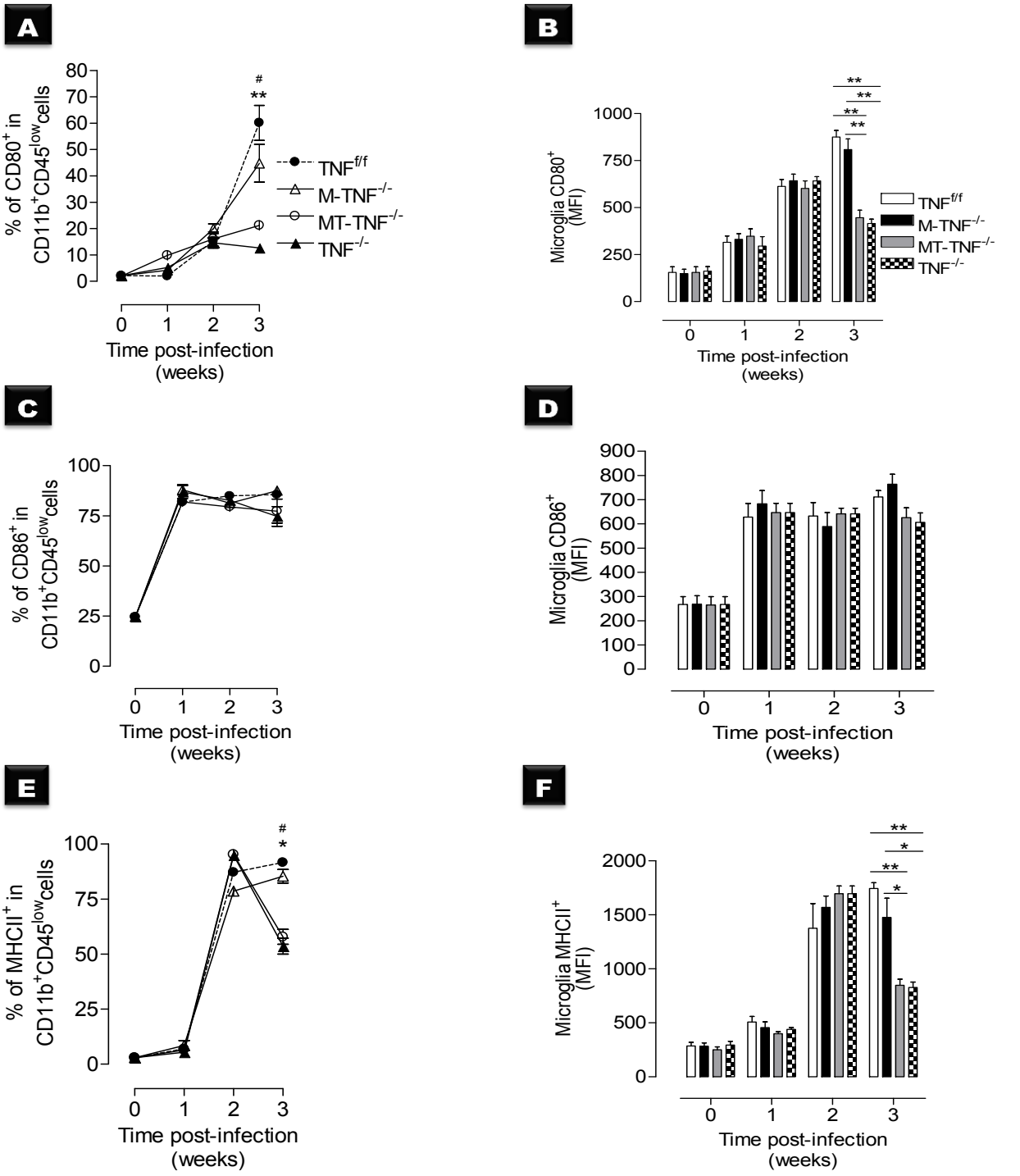

Figure 3.2.12: Decreased CD80$^+$ and MHCII$^+$ expressing microglia in MT-TNF$^{-/-}$ mice. TNF$^{f/f}$, M-TNF$^{-/-}$, MT-TNF$^{-/-}$ and TNF$^{-/-}$ mice were intracerebrally infected with *M. tuberculosis* at a dose of 1x10^5 cfu/brain. Whole brain tissues were harvested at week 0 (naïve) 1, 2 and 3 post-infection, and single cells labelled for APC and surface markers. From the CD11b$^+$CD45^{low} population were gated for percentage of cells expressing CD11b$^+$CD45^{low}CD80$^+$ (A), CD11b$^+$CD45^{low}CD86$^+$ (C) and CD11b$^+$CD45^{low}MHCII$^+$ (E) surface markers. MFI values of CD80$^+$ (B), CD86$^+$ (D) and MHCII$^+$ (F) are shown. *=p < 0.05, **=p < 0.01, and $^{\#}$=p < 0.05 for M-TNF$^{-/-}$ versus MT-TNF$^{-/-}$ and TNF$^{-/-}$ in (A). Data are one representative of three independent experiments. The results represent the mean ± SD of 5 mice/group.

R2.6.2 Defective response to antigen by macrophages of MT-TNF$^{-/-}$ but not M-TNF$^{-/-}$ mice during cerebral *M. tuberculosis* infection

To investigate whether microglia/macrophages, neutrophils, and CD4^{+}- and CD8^{+} T cells-derived TNF affects activation of CD11b^{+}CD45^{high} cells, we intracerebrally infected TNF$^{f/f}$, M-TNF$^{-/-}$, MT-TNF$^{-/-}$ and TNF$^{-/-}$ mice with *M. tuberculosis* at a dose of 1x10^{5} cfu/brain. Whole brain tissues were harvested at week 0 (naïve), 1, 2 and 3 post-infection, and single cells were labelled using lineage (CD11b:PerCP-Cy5-5 and CD45:APC), co-stimulatory (CD80: FITC and CD86: V450) and cell surface (MHCII (I-A/I-E): PE) markers as seen in Figure 3.2.13.

We assessed the co-stimulation (CD80 and CD86) and the cell surface markers (MHCII) expression in this population. Here we found that more than 60% of the macrophage population in TNF$^{f/f}$, M-TNF$^{-/-}$, MT-TNF$^{-/-}$ and TNF$^{-/-}$ mice highly expressed the CD80 marker by week 2 post-infection. However, by week 3 post-infection, the macrophages expressing CD80^{+} in M-TNF$^{-/-}$ mice had a 3-fold increase when compared to week 1 post-infection, and the increase was comparable to TNF$^{f/f}$ mice. In contrast, macrophages expressing CD80^{+} in MT-TNF$^{-/-}$ and TNF$^{-/-}$ mice significantly ($p < 0.05$) decreased to less than 50% compared to TNF$^{f/f}$ or M-TNF$^{-/-}$ mice (Figure 3.2.13A). The MFI activation of CD80^{+} expressing macrophages was comparable with the percentage expression (Figure 3.2.13B).

Although a delayed up-regulation was observed in MT-TNF$^{-/-}$ and TNF$^{-/-}$ mice at week 1 post-infection, all mouse strains exhibited high up-regulation (more than 50%) of the macrophage cells expressing the CD86^{+} marker at weeks 1, 2 and 3 post-infection with no difference among strains (Figure 3.2.13C and D). However, a trending decrease was observed in MT-TNF$^{-/-}$ and TNF$^{-/-}$ mice at week 3 post-infection compared to TNF$^{f/f}$ and M-TNF$^{-/-}$ mice.

Analysis of percentage and MFI of MHCII^{+} expression in the macrophage population of TNF$^{f/f}$, M-TNF$^{-/-}$, MT-TNF$^{-/-}$ and TNF$^{-/-}$ mice showed high expression of 40% by week 1, and 80% by week 2 post-infection. However, by week 3 post-infection, the level expression of MHCII^{+} in the macrophage population of both MT-TNF$^{-/-}$ and TNF$^{-/-}$ mice significantly decreased to 50% when comparing to TNF$^{f/f}$ or M-TNF$^{-/-}$ mice, while TNF$^{f/f}$ and M-TNF$^{-/-}$ mice maintained their MHCII^{+} expression (Figure 3.2.13E and F).

Our finding suggested that microglia/macrophages and neutrophils derived TNF do not play a pivotal role in the control of macrophage activation. The protective effect observed in M-TNF$^{-/-}$ mice could be the result of compensation from T cell-derived TNF. We speculate that during the first 2 weeks post-infection, the activation observed in macrophages could be driven by the early inflammatory response. The results also suggest that the regulation of CD80^{+} and MHCII^{+} expression in the macrophage population in the brain is TNF-dependent during late

inflammation after cerebral *M. tuberculosis* infection. Data also demonstrate that the ablation of T cell-derived TNF in M-TNF$^{-/-}$ mice alter the macrophage activation during cerebral *M. tuberculosis* infection to resemble a phenotype similar to complete TNF deficient mice.

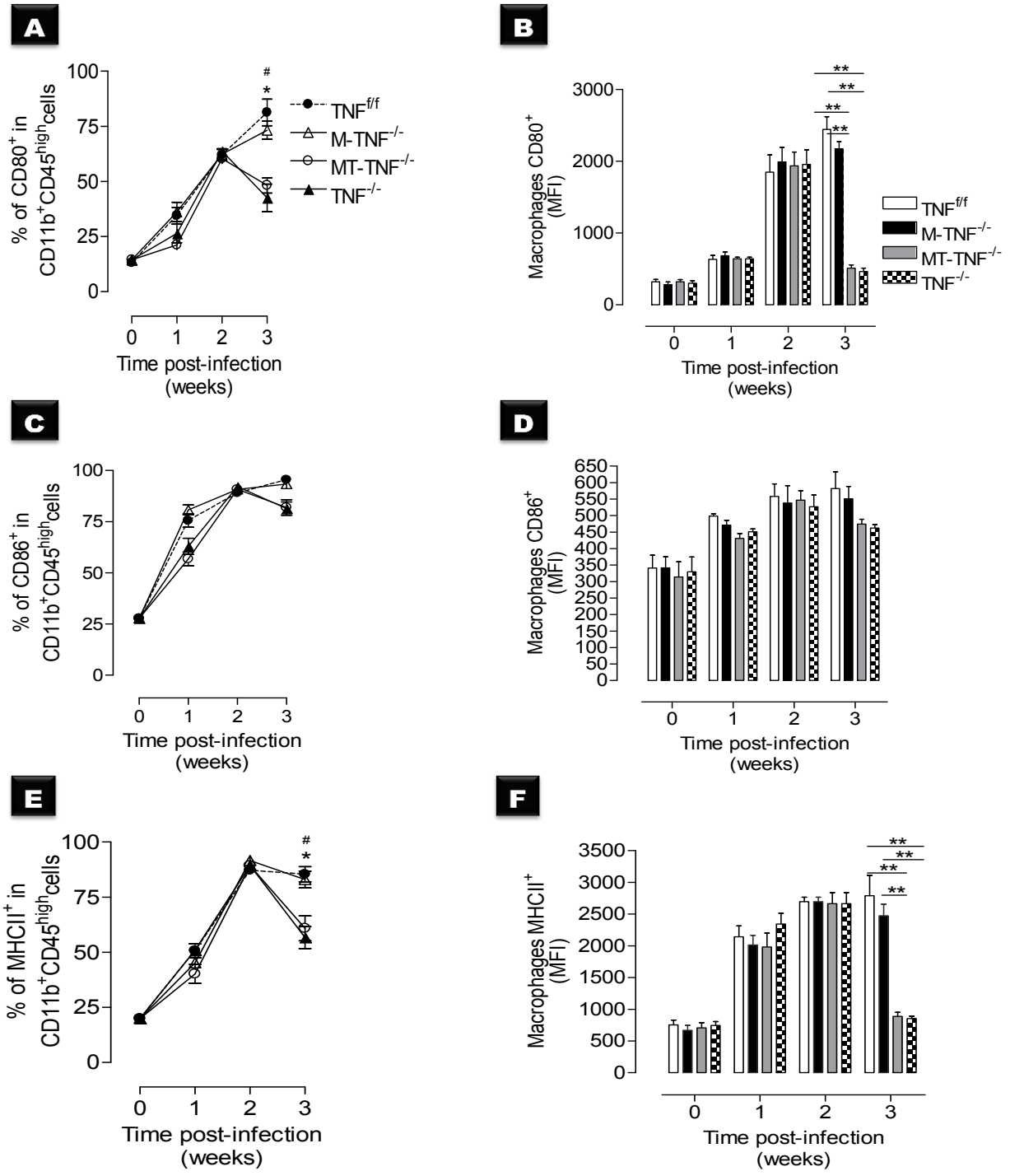

Figure 3.2.13: TNF dependent activation of macrophages during neurotuberculosis. $TNF^{f/f}$, $M\text{-}TNF^{-/-}$, $MT\text{-}TNF^{-/-}$ and $TNF^{-/-}$ mice were intracerebrally infected with *M. tuberculosis* at a dose of $1x10^5$ cfu/brain. Brains were harvested at week 0 (naïve) 1, 2 and 3 post-infection, and single cells were labelled for APC and surface markers. From the $CD11b^+CD45^{high}$ population was gated for cells expressing $CD11b^+CD45^{high}CD80^+$ (A), $CD11b^+CD45^{high}CD86^+$ (C) and $CD11b^+CD45^{high}MHCII^+$ (E) surface markers. MFIs of $CD80^+$ (B), $CD86^+$ (D) and $MHCII^+$ (F) are shown. *=$p < 0.05$, and #=$p < 0.05$ for $M\text{-}TNF^{-/-}$ versus $MT\text{-}TNF^{-/-}$ and $TNF^{-/-}$ in (A and E). Data (mean ± SD of 5 mice/group) are one representative of three independent experiments.

R2.6.3 Modulation of dendritic cells surface marker expression in MT-TNF$^{-/-}$ mice

We investigated whether myeloid and lymphoid T cell subset derived TNF plays a critical role in the activation of the CD11c^{+}CD45^{high} population. TNF$^{f/f}$, M-TNF$^{-/-}$, MT-TNF$^{-/-}$ and TNF$^{-/-}$ mice were intracerebrally infected with *M. tuberculosis* at a dose of 1x10^{5} cfu/brain. Brains were collected, harvested at week 0 (naïve), 1, 2 and 3 post-infection, and single cells were labelled using lineage (CD11b:PerCP-Cy5-5, CD11c:Alexa 700 and CD45:APC), co-stimulatory (CD80: FITC and CD86: V450) and cell surface marker (MHCII (I-A/I-E): PE) as is seen in Figure 3.2.14A-F and analysed using flow cytometry. We investigated the contribution of microglia/macrophages, neutrophils, and CD4^{+}- and CD8^{+} T cells-derived TNF to DCs activation by analysing the percentage expression and MFI of co-stimulatory (CD80^{+} and CD86^{+}) and antigen presenting cell (MHCII^{+}) markers. Interestingly, less than 10% of the DCs population in all mouse strains expressed the CD80^{+} marker at week 1 post-infection, and the expression level was decreased to 5% in all mouse strains at week 2 post-infection. The CD80^{+} expressing DCs in TNF$^{f/f}$ and M-TNF$^{-/-}$ mice significantly ($p < 0.05$) increased from 5% to 8% at week 3 post-infection compared to TNF$^{-/-}$ or MT-TNF$^{-/-}$ mice (Figure 3.2.14A). In contrast, a continuous decrease CD80^{+} expression was noticed in MT-TNF$^{-/-}$ and TNF$^{-/-}$ mice at week 3 post-infection (Figure 3.2.14A and B). Assessing the percentage and MFI of CD86^{+} expression on DCs, we found that ~75% of the DCs population in all mouse strains expressed CD86^{+} at week 1 and 2 post-infection, however a significant ($p < 0.05$) up-regulation was seen in M-TNF$^{-/-}$ mice compared to TNF$^{f/f}$ mice at week 3 post-infection when compared MT-TNF$^{-/-}$ and TNF$^{-/-}$ mice. The percentage and MFI of CD86^{+} expressing DCs was maintained at equivalent levels in both MT-TNF$^{-/-}$ and TNF$^{-/-}$ mice (Figure 3.2.14C and D). The expression of MHCII^{+} in the DCs population was significant ($p < 0.05$) increased in M-TNF$^{-/-}$ mice at week 2 post-infection compared to TNF$^{f/f}$, MT-TNF$^{-/-}$ and TNF$^{-/-}$ mice. The MHCII^{+} expressing DCs population in MT-TNF$^{-/-}$ had a significant ($p < 0.05$) reduction at week 3 post-infection compared to TNF$^{f/f}$ mice (Figure 3.2.14E and F). A Similar significant increase ($p < 0.05$) was found in TNF$^{-/-}$ mice at this time point.

Our finding suggested that microglia/macrophages and neutrophils derived TNF do not play a pivotal role in the control of dendritic cell activation, although TNF is required in the control of CD80^{+} and MHCII^{+} expression during CNS *M. tuberculosis* infection. The data also indicate that the ablation of T cell-derived TNF in M-TNF$^{-/-}$ mice has a critical effect on the presentation mechanism of the antigen during neurotuberculosis.

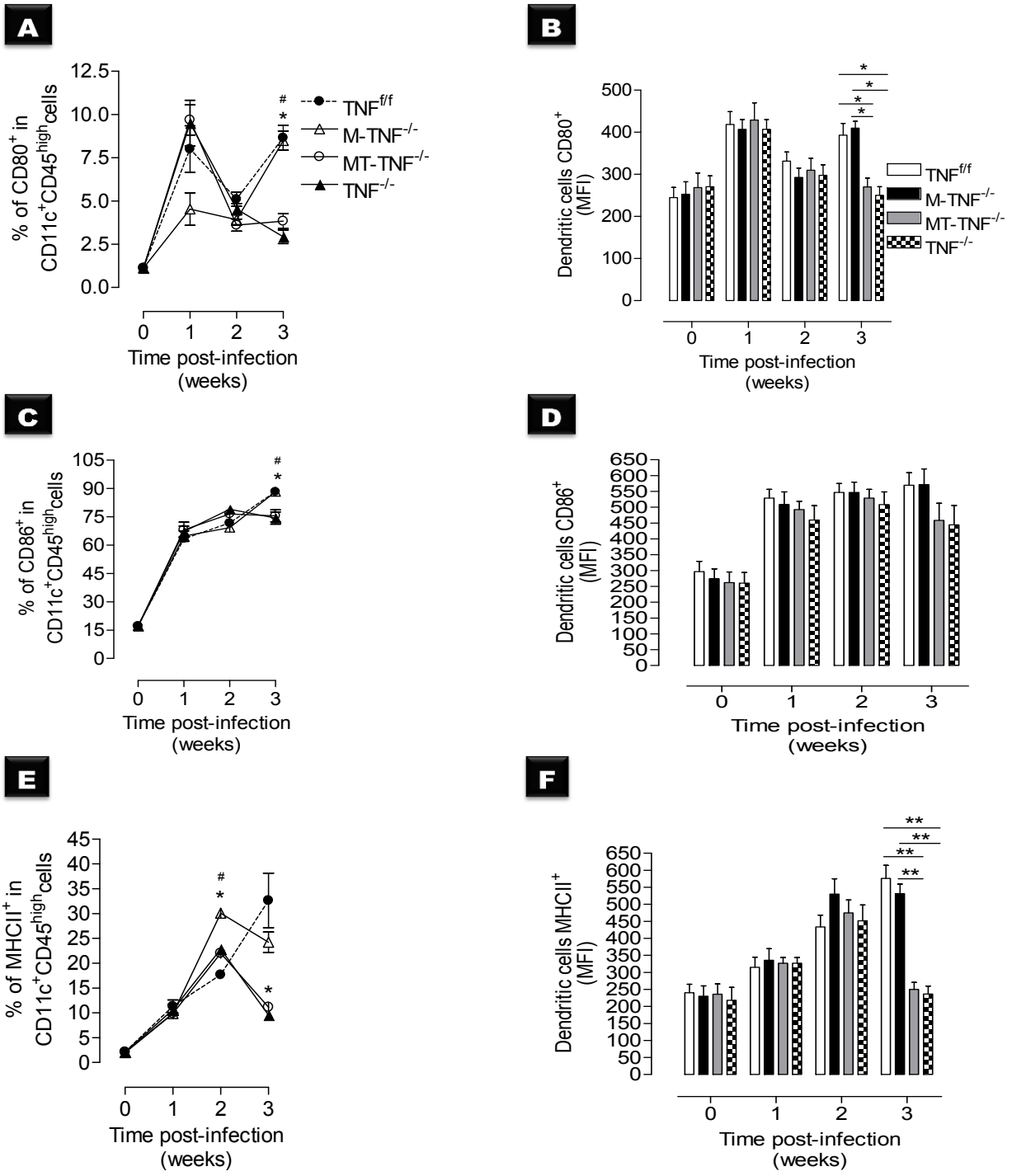

Figure 3.2.14: TNF mediated DCs surface marker expression. TNF$^{f/f}$, M-TNF$^{-/-}$, MT-TNF$^{-/-}$ and TNF$^{-/-}$ mice were intracerebrally infected at a different time points with *M. tuberculosis* at a dose of 1x10^5 cfu/brain. Brains were harvested at week 0 (naïve) 1, 2 and 3 post-infection, and single cells were labelled for APC and surface markers. From the CD11c$^+$CD45^{low} population was gated for percentage of cells expressing CD11c$^+$CD45^{high}CD80$^+$ (A), CD11c$^+$CD45^{high}CD86$^+$ (C) and CD11c$^+$CD45^{high}MHCII$^+$ (E) surface markers. MFI of CD80$^+$ (B), CD86$^+$ (D) and MHCII$^+$ (F) are shown *=$p < 0.05$, and $^{\#}$=$p < 0.05$ for M-TNF$^{-/-}$ versus MT-TNF$^{-/-}$ and TNF$^{-/-}$ in (A, C and E). Data are one representative of three independent experiments. The results represent the mean ± SD of 5 mice/group.

R2.7 TNF mediates cerebral B-cell subsets infiltration during neurotuberculosis

R2.7.1. Increase influx of follicular B cells in MT-TNF$^{-/-}$ but not M-TNF$^{-/-}$ mice

To address the question of whether the ablation of TNF in microglia/macrophages, neutrophils, and CD4^{+}- and CD8^{+} T cells impaired the CD1d^{low}B220^{+}AA4.1^{-} (Fo B cells) population during cerebral *M. tuberculosis* infection; TNF$^{f/f}$, M-TNF$^{-/-}$, MT-TNF$^{-/-}$ and TNF$^{-/-}$ mice were intracerebrally infected with *M. tuberculosis* at a dose of 1x10^{5} cfu/brain. Whole brain tissues were harvested at week 0 (naïve), 1, 2 and 3 post-infection, and single cells were labelled with specific B cells markers (CD1d:PE, CD93(AA4.1):PerCP-Cy5-5, and B200:HorizonV500), and the gating strategy used to identify the CD1d^{low}B220^{+}AA4.1^{-} population is shown again in Figure 3.2.15A.

We observed no significant difference in the absolute number of infiltrating Fo B cells in M-TNF$^{-/-}$ mice compared to TNF$^{f/f}$ mice at all time points post *M. tuberculosis* infection. However, the absolute number of infiltrating Fo B cells in MT-TNF$^{-/-}$ and TNF$^{-/-}$ were significantly ($p < 0.01$) higher at week 1, 2 and 3 post-infection compared to the TNF$^{f/f}$ mice at all time points post-infection. No significant difference was observed between M-TNF$^{-/-}$ and MT-TNF$^{-/-}$ mice (Figure 3.1.15).

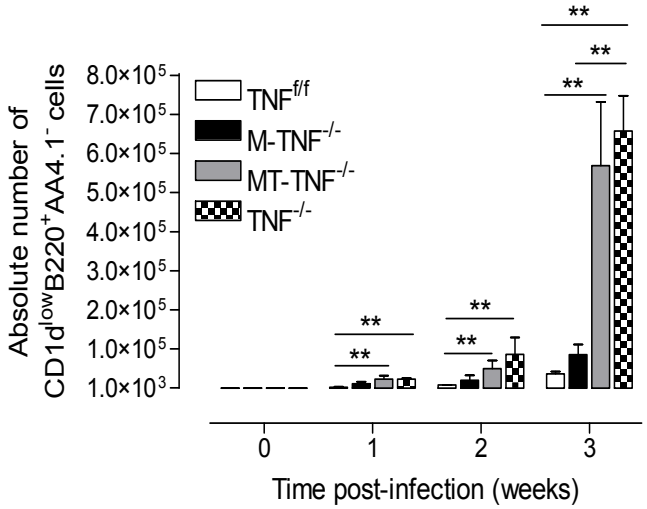

Figure 3.2.15: Absolute cell number during neurotuberculosis. $TNF^{f/f}$, $M\text{-}TNF^{-/-}$, $MT\text{-}TNF^{-/-}$ and $TNF^{-/-}$ mice were intracerebrally infected with *M. tuberculosis* at a dose of $1x10^5$ cfu/brain. In order to identify Fo B cells population, whole brain tissues were harvested at week 0 (naïve), 1, 2 and 3 post-infection, and single cells were labelled with CD1d:PE-A, CD93(AA4.1):PerCP-Cy5-5-A and CD45R/B220:V500-A. *=$p < 0.05$ and **=$p < 0.01$. (n= 5 mice/group).

R2.7.1.1 Down-regulation of follicular B-cell antibody production in $MT\text{-}TNF^{-/-}$ mice but not in $M\text{-}TNF^{-/-}$ mice during neurotuberculosis

We evaluated the activation of Fo B cells in $TNF^{f/f}$, $M\text{-}TNF^{-/-}$, $MT\text{-}TNF^{-/-}$ and $TNF^{-/-}$ mice. Mice were intracerebrally infected with *M. tuberculosis* at a dose of $1x10^5$ cfu/brain. Brains were harvested and single cells were labelled at week 0 (naïve), 1, 2 and 3 post-infection with specific B cells (CD1d:PE, CD93(AA4.1):PerCP-Cy5-5 and B200:Horizon V500), co-stimulatory (CD86:V450) and surface (IgM:PE-Cy7 and MHCII:Alexa 700) markers. We next investigated whether the ablation of TNF in microglia/macrophages, neutrophils, $CD4^+$- and $CD8^+$ T cells affected the regulation of co-stimulatory marker. We found no significant difference in the percentage and MFI of Fo B cells expressing CD86 in $M\text{-}TNF^{-/-}$ mice compared to $TNF^{f/f}$ mice (Figure 3.2.16A and B). In contrast, the percentage and MFI of cells expressing the $CD86^+$ marker in the Fo B cells population of $MT\text{-}TNF^{-/-}$ and $TNF^{-/-}$ mice were significantly ($p < 0.05$) higher at week 1 and lower at week 3 post-infection compared either to $TNF^{f/f}$ or $M\text{-}TNF^{-/-}$ mice (Figure 3.2.16A and B). We further assessed the role of microglia/macrophages, neutrophils, $CD4^+$- and $CD8^+$ T cells-derived TNF in the secretion of antibody (IgM). Figure 3.2.16C and D

show that the Fo B cells of $TNF^{f/f}$ and M-$TNF^{-/-}$ mice secreted similar levels at week 3 post-infection, which was significant ($p < 0.05$) higher compared to week 1 post-infection. In contrast, the MT-$TNF^{-/-}$ and $TNF^{-/-}$ mice secreted significant ($p < 0.05$) lower levels of IgM^{+} at week 3 post-infection compared either to $TNF^{f/f}$ or M-$TNF^{-/-}$ mice (Figure 3.2.6C and D). We examine the expression pattern of $MHCII^{+}$ in the Fo B-cell population, and found that the percentage expression and MFI values of $MHCII^{+}$ on Fo B cells in $TNF^{f/f}$ and M-$TNF^{-/-}$ mice were similar and peaked at week 1 post-infection. In contrast, the increase in the percentage and MFI of Fo B cells expressing $MHCII^{+}$ in both MT-$TNF^{-/-}$ and $TNF^{-/-}$ mice were significantly ($p < 0.05$) delayed at week 1 post-infection and only peaked at week 2 post-infection and subsequently dropped at week 3 post-infection as opposed to being maintained as was evident in $TNF^{f/f}$ and M-$TNF^{-/-}$ mice (Figure 3.2.16E and F).

Our findings demonstrate that ablation of TNF in microglia/macrophages and neutrophils cells does not affect the expression pattern of Fo B-cell surface marker and antibody secretion during neurotuberculosis. The immune effects observed in M-$TNF^{-/-}$ mice could be associated with the compensation of T cell-derived TNF or other cerebral TNF cellular sources. Our results also indicate that the ablation of TNF in T cells of M-$TNF^{-/-}$ mice results in the incapacity of Fo B cells to secrete antibody and express MHCII.

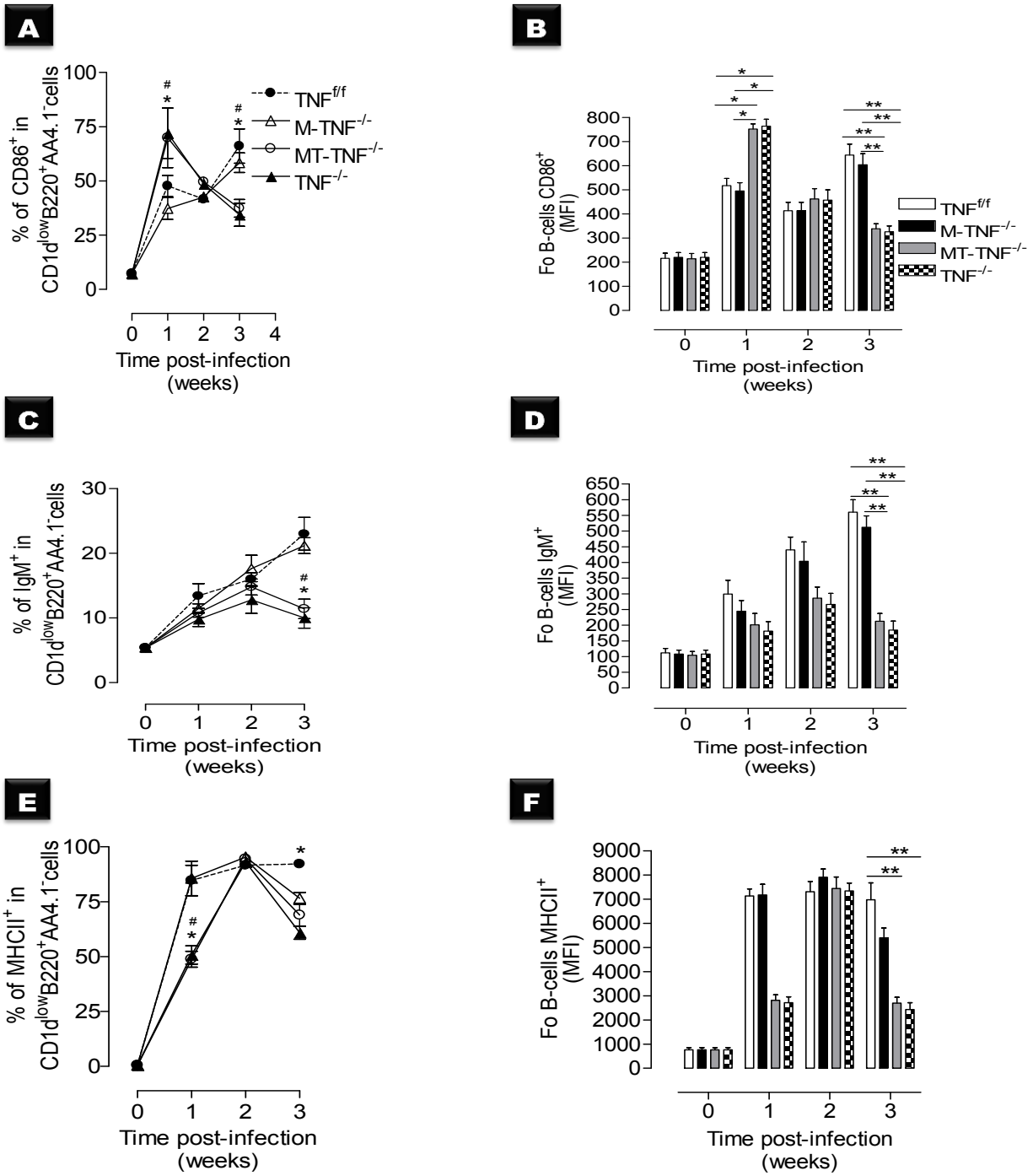

Figure 3.2.16: Impairment in antibody secretion and antigenic response by Fo B cells in MT-TNF$^{-/-}$ but not M-TNF mice: TNF$^{f/f}$, M-TNF$^{-/-}$, MT-TNF$^{-/-}$ and TNF$^{-/-}$ mice were intracerebrally infected with *M. tuberculosis* at a dose of 1x10^5 cfu/brain. Brains were harvested at week 0 (naïve), 1, 2 and 3 post-infection, and single cells were labelled for CD1d, AA4.1, and B220, with surface markers CD86, IgM and MHCII. The CD1d^{low}B220$^+$AA4.1$^-$ population were gated for percentage of cells expressing CD1d^{low}B220$^+$AA4.1$^-$CD86$^+$ (A), CD1d^{low}B220$^+$AA4.1$^-$IgM$^+$, (C) and CD1d^{low}B220$^+$AA4.1$^-$MHCII$^+$ (E). MFI values of CD86$^+$ (B), IgM$^+$ (D) and MHCII$^+$ (F) are shown. *=p < 0.05, and $^{\#}$=p < 0.05 for M-TNF$^{-/-}$ versus MT-TNF$^{-/-}$ and TNF$^{-/-}$ in (A), (C) and (E). Data are one representative of three independent experiments. Results are represented as mean ± SD of 5 mice/group.

R2.7.2 Modulation of plasmablast and plasma cells absolute numbers during experimental neurotuberculosis

To analyse the infiltrating $CD1d^{high}B220^{high}D138^{-}$ (plasmablasts) population into the CNS during neurotuberculosis, we intracerebrally infected $TNF^{f/f}$, M-$TNF^{-/-}$, MT-$TNF^{-/-}$ and $TNF^{-/-}$ mice with *M. tuberculosis* at a dose of $1x10^5$ cfu/brain. Whole brain tissues were harvested at week 0 (naïve), 1, 2 and 3 post-infection and single cells were labelled with specific B-cell (CD1d:PE, CD93(AA4.1):PerCP-Cy5-5, CD138:APCPerCP-Cy5-5 and B200:Horizon V500) markers.

No significant difference was found in the absolute cell numbers of the infiltrating plasmablast population in the M-$TNF^{-/-}$ mice compared with the $TNF^{f/f}$ mice, at all time points post-infection. However, the absolute cell numbers of the infiltrating plasmablast population in MT-$TNF^{-/-}$ and $TNF^{-/-}$ mice were increased (non-significant) at week 1 post-infection compared either to $TNF^{f/f}$ or M-$TNF^{-/-}$ mice. Significant ($p < 0.05$) increases were found in MT-$TNF^{-/-}$ and $TNF^{-/-}$ at week 2 post-infection, and also a significant ($p < 0.01$) decrease was observed at week 3 post-infection compared to either $TNF^{f/f}$ or M-$TNF^{-/-}$ mice (Figure 3.2.17A). Next, we examine the absolute numbers of plasma cells in $TNF^{f/f}$, M-$TNF^{-/-}$, MT-$TNF^{-/-}$ and $TNF^{-/-}$ mice, and found that the absolute number of the plasma cell population in $TNF^{f/f}$ mice was 2-log higher at week 3 post-infection compared to week 1 post-infection. A similar trend was observed in M-$TNF^{-/-}$ mice. In this population, we found no significant difference in plasma cell absolute numbers of M-$TNF^{-/-}$ mice compared with the $TNF^{f/f}$ mice at all time points post-infection. Interestingly, the absolute number of the plasma cells in both MT-$TNF^{-/-}$ and $TNF^{-/-}$ mice was significantly ($p < 0.001$) increased when compared to $TNF^{f/f}$ or M-$TNF^{-/-}$ mice at week 1 and 2 post-infection, and was followed by a significant ($p < 0.001$) decrease in both MT-$TNF^{-/-}$ and $TNF^{-/-}$ mice at week 3 post-infection when compared to $TNF^{f/f}$ or M-$TNF^{-/-}$ mice (Figure 3.2.17B).

These data demonstrate that ablation of TNF in the microglia/macrophages and neutrophils were not critical to the influx of the plasmablast and plasma cell populations, suggesting that there is is better control of the influx of plasmablasts and plasma cells into the CNS in the presence of T cell-derived TNF in M-$TNF^{-/-}$ mice.

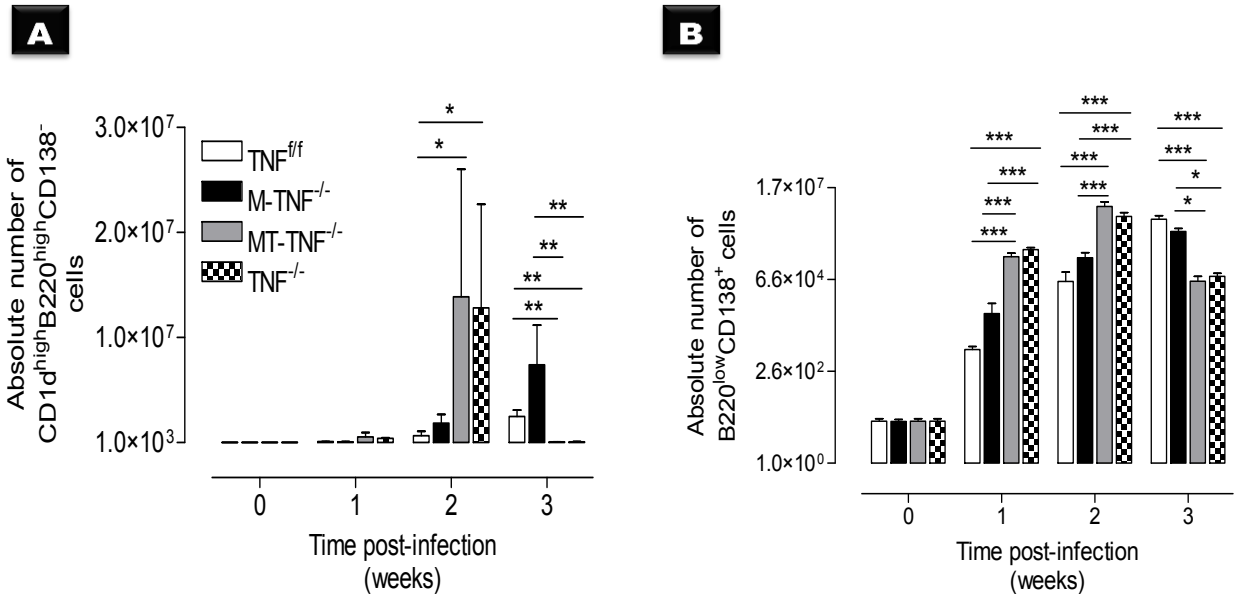

Figure 3.2.17: TNF modulates the plasmablasts and plasma cells absolute number during neurotuberculosis. TNF$^{f/f}$, M-TNF$^{-/-}$, MT-TNF$^{-/-}$ and TNF$^{-/-}$ mice were intracerebrally infected with *M. tuberculosis* at a dose of 1x10^5 cfu/brain. Whole brain tissues were harvested at week 0 (naïve), 1, 2 and 3 post-infection, and isolated single cells were labeled for CD1d, AA4.1, CD138 and B220. Shown are absolute numbers of CD1d^{high}B220^{high}D138$^-$ cells (A), also shown are absolute numbers of B220^{low}CD138$^+$ cells (B). *=p < 0.05, **=p < 0.01 and ***=p < 0.001. Data are one representative of three independent experiments. Results are represented as mean ± SD of 5 mice/group.

R2.7.2.1 Reduced humoral immunity and antigenic response by plasmablast cell in MT-TNF$^{-/-}$ but not M-TNF$^{-/-}$ mice

To examine the activation of the plasmablast population into the CNS during neurotuberculosis, we infected TNF$^{f/f}$, M-TNF$^{-/-}$, MT-TNF$^{-/-}$ and TNF$^{-/-}$ mice with *M. tuberculosis* at a dose of 1x10^5 cfu/brain. Whole brain tissues were harvested at week 0 (naïve), 1, 2 and 3 post-infection, and single cells were labelled with specific B cells (CD1d:PE, CD93(AA4.1):PerCP-Cy5-5, CD138:APC and B200:Horizon V500) and surface (CD86 and MHCII) and antibody (IgM) markers.

Analysing the surface expression of co-stimulatory molecules, we found that the percentage and MFI of infiltrating plasmablast cells expressing CD86$^+$ was increased in all mouse strains at week 1 and 2 post-infection. However, the percentage and MFI of plasmablast cells expressing CD86$^+$ in TNF$^{f/f}$ and M-TNF$^{-/-}$ mice were maintained the same level at week 3 post-infection (Figure 3.2.18A and B). Interestingly, at week 3 post-infection, the percentage and

MFI of plasmablast cells expressing $CD86^+$ in both MT-$TNF^{-/-}$ and $TNF^{-/-}$ mice were significantly ($p < 0.05$) lower compared to $TNF^{f/f}$ and M-$TNF^{-/-}$ mice (Figure 3.2.18A and B). We thereafter examined the percentage and MFI of the infiltrating plasmablasts which secreted the antibody IgM. A similar up-regulation of cells expressing IgM^+ was observed at week 1 and 2 post-infection in all mouse strains. However, the percentage of the IgM secreting plasmablast population was significant ($p < 0.05$) increased in $TNF^{f/f}$ and M-$TNF^{-/-}$ mice at week 3 post-infection. On the contrary, both MT-$TNF^{-/-}$ and $TNF^{-/-}$ mice had significantly ($p < 0.05$) decreased percentage and MFI of plasmablasts expressing IgM^+ at week 3 post-infection compared to $TNF^{f/f}$ or M-$TNF^{-/-}$ mice (Figure 3.2.18C and D). Next, we assessed whether the ablation of TNF in the microglia/macrophages, neutrophils, and $CD4^+$- and $CD8^+$ T cells affected the antigen presentation ability in the plasmablast population. We found no significant difference in percentage and MFI of $MHCII^+$ expressing plasmablast cells at week 1 post-infection in all mouse strains. However, a significant ($p < 0.05$) difference was observed in the $MHCII^+$ expressing plasmablasts of the MT-$TNF^{-/-}$ and $TNF^{-/-}$ mice at week 2 post-infection compared to $TNF^{f/f}$ mice. Following the kinetic at week 3 post-infection, no significant difference was observed in the percentage and MFI of the $MHCII^+$ expressing plasmablasts in M-$TNF^{-/-}$ mice compared to $TNF^{f/f}$ mice. Interestingly, the percentage of the $MHCII^+$ expressing plasmablasts in MT-$TNF^{-/-}$ and $TNF^{-/-}$ mice was significantly ($p < 0.05$) decreased when comparing to either turn-$off^{/f}$ or M-$TNF^{-/-}$ mice (Figure 3.2.18E and F).

These data demonstrate that ablation of TNF in the microglia/macrophages and neutrophils is not critical for the activation of the plasmablasts. The resistance observed in M-$TNF^{-/-}$ mice may derive from the compensation of T cell-derived TNF. In addition, the results clearly demonstrate that the ablation of T cell-derived TNF in M-$TNF^{-/-}$ mice leads to the deregulation of surface markers.

R2.7.3 Impaired humoral immunity by plasma cells in MT-$TNF^{-/-}$ but not M-$TNF^{-/-}$ mice

To evaluate the absolute number and examine the surface expression of co-stimulatory molecules, and antibody secretion of plasma cells, we intracerebrally infected $TNF^{f/f}$, M-$TNF^{-/-}$, MT-$TNF^{-/-}$ and $TNF^{-/-}$ mice with *M. tuberculosis* at a dose of $1x10^5$ cfu/brain. Whole brain tissues were harvested at week 0 (naïve), 1, 2 and 3 post-infection, and single cells were labelled with specific B cells (CD1d:PE, CD93(AA4.1):PerCP-Cy5-5, CD138:APC and B200:Horizon V500)

surface markers and analysed for CD86, IgM and MHCII expression.

Examining the percentage and MFI of $CD86^+$ expressed on the plasma cells, we found that the percentage and MFI of plasma cells expressing this co-stimulatory marker was increased in all mouse strains at week 1 and 3 post-infection. At week 2 post-infection, the percentage and MFI of plasma cells expressing $CD86^+$ in MT-$TNF^{-/-}$ and $TNF^{-/-}$ mice showed a significant ($p < 0.05$) decrease compared to $TNF^{f/f}$ and M-$TNF^{-/-}$ mice (Figure 3.2.19A and B). We next asked whether the microglia/macrophages, neutrophils, and $CD4^+$- and $CD8^+$ T cells-derived TNF influenced antibody secretion. There was an increase in the percentage and MFI of plasma cells expressing IgM^+ in all mouse strains at week 1 and 2 post-infection. However, this expression was maintained at week 3 post-infection in $TNF^{f/f}$ and M-$TNF^{-/-}$ mice. In contrast, there was a significant ($p < 0.05$) decrease in IgM of both MT-$TNF^{-/-}$ and $TNF^{-/-}$ mice at week 3 post-infection (Figure 3.2.19C and D). Assessing the expression of $MHCII^+$, we found very low and no significant difference in all mice strains and time points post-infection (Figure 3.2.19E).

The data show that ablation of TNF in the microglia/macrophages and neutrophils does not alter the plasma cell activation, suggesting that the no effect observed in M-$TNF^{-/-}$ mice may derived from the T cells-derived TNF. Also data show that T cells-derived TNF deletion in M-$TNF^{-/-}$ mice results in the failure to control the secretion of antibody at a later stage of the disease.

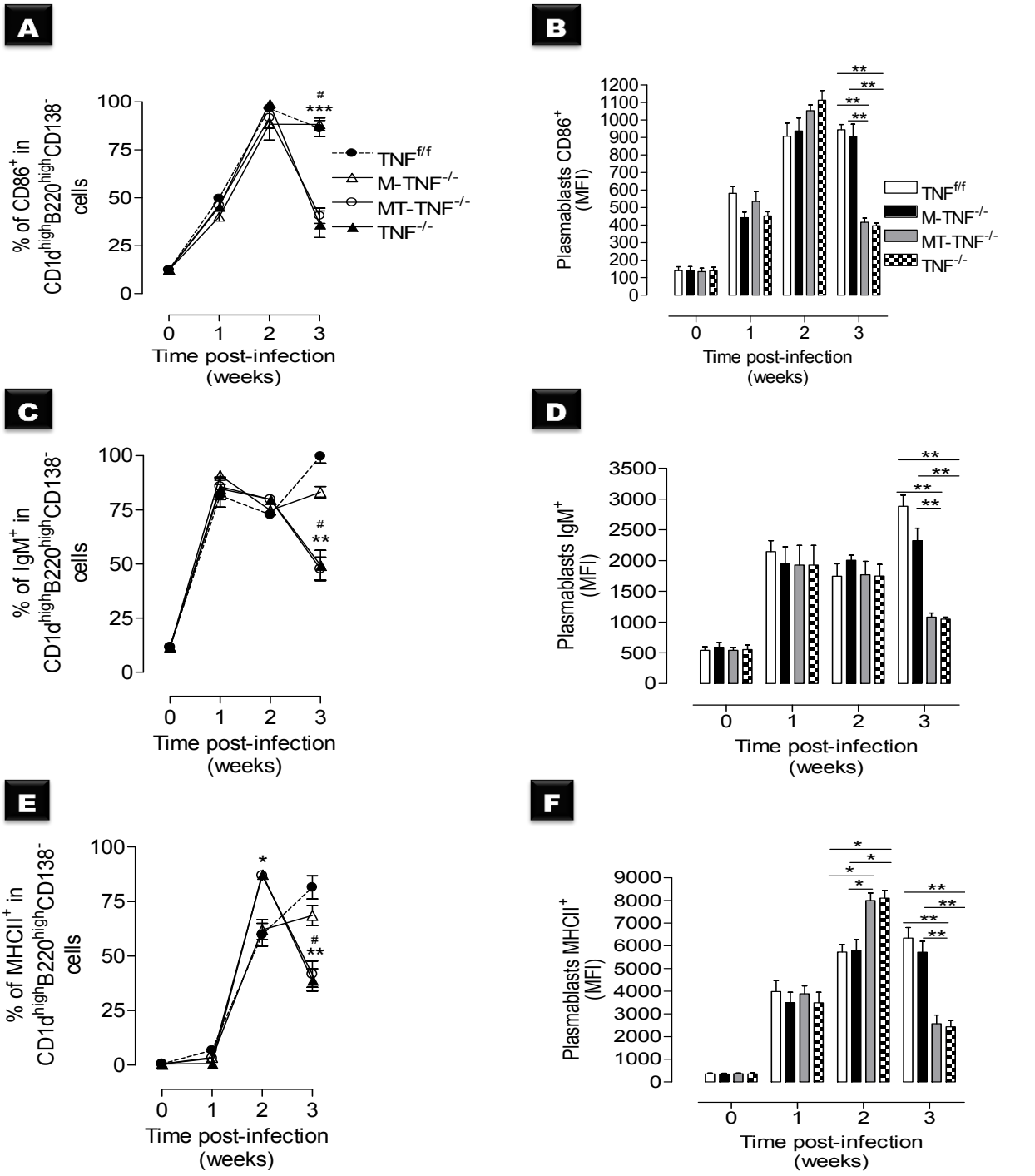

Figure 3.2.18: Defective humoral immunity and antigenic response by plasmablast cells in MT-TNF$^{-/-}$ but not M-TNF$^{-/-}$ mice. TNF$^{f/f}$, M-TNF$^{-/-}$, MT-TNF$^{-/-}$ and TNF$^{-/-}$ mice were intracerebrally infected with *M. tuberculosis* at a dose of 1x10^5 cfu/brain. Brains single cells were labelled at week 0 (naïve) 1, 2 and 3 post-infection for CD1d, AA4.1, CD138 and B220 with surface markers CD86, IgM and MHCII. The CD1d^{high}B220$^+$D138$^-$ population were gated for cells expressing CD1d^{high}B220$^+$D138$^-$CD86$^+$ (A), CD1d^{high}B220$^+$D138$^-$IgM$^+$ (C) and CD1d^{high}B220$^+$D138$^-$ MHCII$^+$ (E). Also shown are bar graphs of MFI values of CD86$^+$ (B), IgM$^+$ (D) and MHCII$^+$ (F). *=p < 0.05 and **=p < 0.01 and $^{\#}$=p < 0.01 for M-TNF$^{-/-}$ versus MT-TNF$^{-/-}$ and TNF$^{-/-}$ in A, C and E. Data are one representative of three independent experiments. Results are represented as mean ± SD of 5 mice/group.

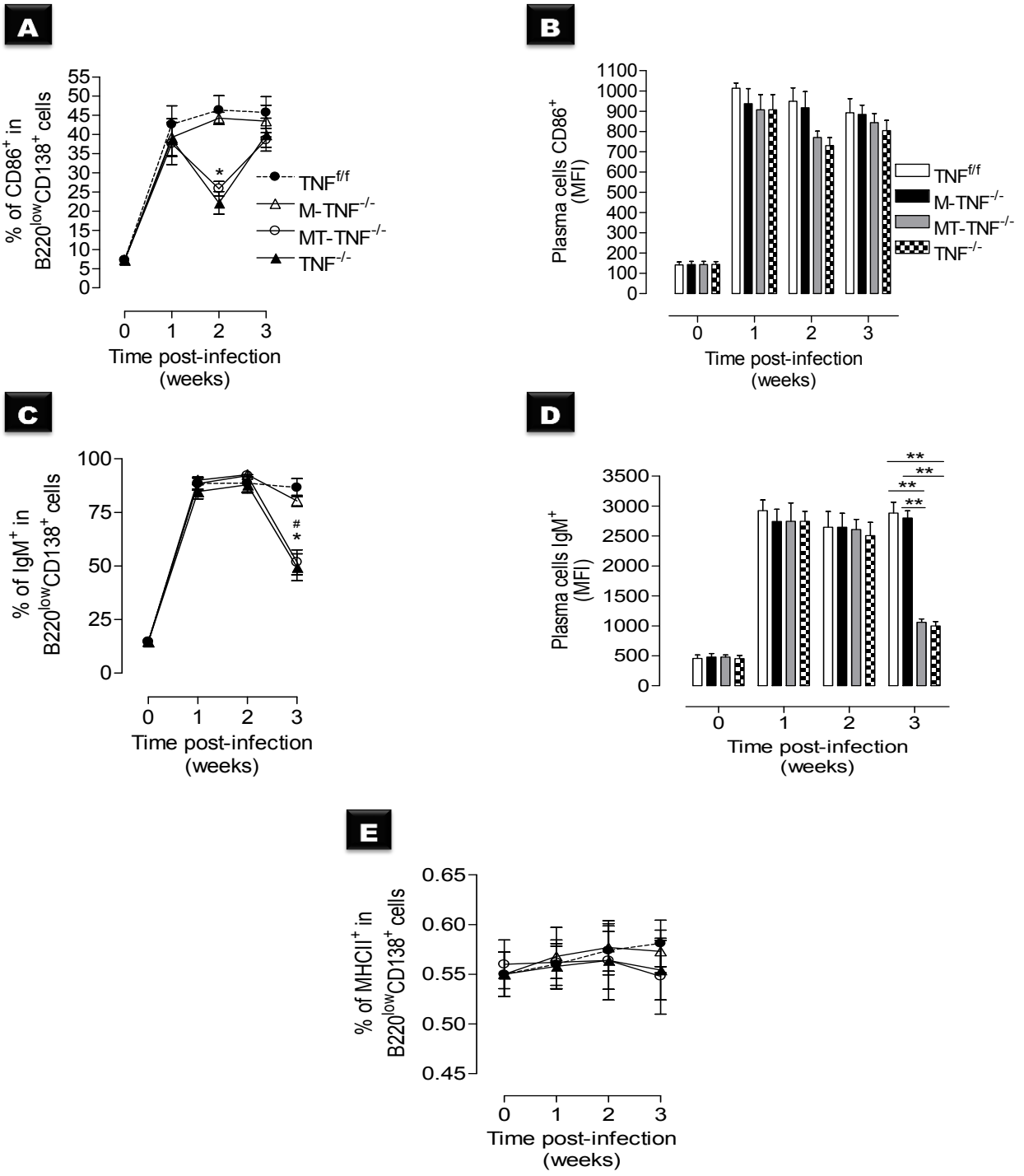

Figure 3.2.19: Reduced antibody production in MT-TNF$^{-/-}$ mice but not M-TNF$^{-/-}$ mice. TNF$^{f/f}$, M-TNF$^{-/-}$, MT-TNF$^{-/-}$ and TNF$^{-/-}$ mice were intracerebrally infected with *M. tuberculosis* at a dose of 1x10^5 cfu/brain. Brain single cells were labelled at week 0 (naïve) 1, 2 and 3 post-infection for CD1d, AA4.1, CD138 and B220, with surface markers CD86, IgM and MHCII. Shown are the B220^{low}D138$^+$ population was gated for cells expressing B220^{low}D138$^+$CD86$^+$ (A), B220^{low}D138$^+$IgM$^+$ (C) and B220^{low}D138$^+$MHCII$^+$ (E). *=p < 0.05, and $^{\#}$=p < 0.05 for M-TNF$^{-/-}$ versus MT-TNF$^{-/-}$ and TNF$^{-/-}$ in (C). MFI values of CD86$^+$ (B), IgM$^+$ (D) and MHCII$^+$ (F) are shown. Data (mean ± SD of 5 mice/group) are one representative of three independent experiments.

R2.8 Increased influx of infiltrating of $CD4^+$- and $CD8^+$ T cells in MT-$TNF^{-/-}$ mice during neurotuberculosis

To explore whether the microglia/macrophages, neutrophils, and $CD4^+$- and $CD8^+$ T cells-derived TNF alter the influx of infiltrating $CD4^+$- and $CD8^+$ T cells into the brain during experimental neurotuberculosis, $TNF^{f/f}$, M-$TNF^{-/-}$, MT-$TNF^{-/-}$ and $TNF^{-/-}$ mice were intracerebrally infected with *M. tuberculosis* at a dose of $1x10^5$ cfu/brain. Whole brain tissues were harvested at week 1, 2 and 3 post-infection, and single cells were analysed for expression of CD3, CD4, and CD8 using flow cytometry.

We observed an overall increase in the frequency of effector $CD4^+$ T cells in $TNF^{f/f}$ mice, which was almost ~8-fold higher at week 2 and ~35-fold higher at week 3 post-infection compared to week 1 post-infection. In M-$TNF^{-/-}$ the frequency of effector $CD4^+$ T cells was ~14-fold higher at week 2 and 35-fold higher at week 3 post-infection compared to week 1 post-infection, the effector $CD4^+$ T cells in MT-$TNF^{-/-}$ was ~10-fold higher at week 2 and ~33-fold higher at week 3 post-infection compared to week 1 post-infection and while overall in the frequency of effector $CD4^+$ T cells in $TNF^{-/-}$ mice was ~10-fold higher at week 2 and ~35-fold higher at week 3 post-infection compared to week 1 post-infection (Figure 3.2.20). The frequency of infiltrating $CD4^+$ T cells in the M-$TNF^{-/-}$ mice have approximated that of $TNF^{f/f}$ mice at week 1 post-infection. The frequency of MT-$TNF^{-/-}$ and $TNF^{-/-}$ mice had 2-fold higher at week 2 and 4-fold higher at week 3 post-infection compared to $TNF^{f/f}$ mice (Figure 3.2.20). We similarly examined the influx of $CD8^+$ T cells into the brain during experimental neurotuberculosis. The effectors $CD8^+$ T cell population increased 2-fold at week 2 and 3 post-infection in all mouse strains compared to week 1 post-infection. A significantly ($p < 0.05$) higher frequency of $CD8^+$ T cells was observed in M-$TNF^{-/-}$ mice at week 3 post-infection compared with $TNF^{f/f}$ mice, while the MT-$TNF^{-/-}$ and $TNF^{-/-}$ mice exhibited a higher influx of $CD8^+$ T cells at week 2 and 3 post-infection (Figure 3.2.21). When assessing the absolute cell numbers of infiltrating cells, we found equivalent numbers of $CD3^+CD4^+$ cells in the M-$TNF^{-/-}$ mice at week 1 and 2 post-infection compared to $TNF^{f/f}$ mice. In contrast, when assessing the $CD3^+CD4^+$ T cell influx in MT-$TNF^{-/-}$ and $TNF^{-/-}$ mice, we found a significant ($p < 0.05$) increase at week 1, 2 and 3 post-infection compared to $TNF^{f/f}$ mice (Figure 3.2.22A), suggesting that the absence T cell-derived TNF induced susceptibility in MT-$TNF^{-/-}$ mice. This phenotype was not evident in M-$TNF^{-/-}$ mice.

Further, we examined the absolute number of $CD3^+CD8^+$ cellular influx. We observed no significant differences between M-$TNF^{-/-}$ and $TNF^{f/f}$ mice or in any of the time points post-infection. However, significant difference was observed in MT-$TNF^{-/-}$ and $TNF^{-/-}$ mice at week 1

post-infection compared with $TNF^{f/f}$ mice. No significant difference was observed in absolute number of $CD3^+CD8^+$ T cells in all mouse strains at week 1 post-infection, and in $MT\text{-}TNF^{-/-}$ mice at week 2 post-infection compared with $TNF^{-/-}$ mice. In contrast, only $TNF^{-/-}$ mice had a significant ($p < 0.05$) increase at week 2 post-infection compared with $TNF^{f/f}$ mice (Figure 3.2.22B), while, both $MT\text{-}TNF^{-/-}$ and $TNF^{-/-}$ had a significant ($p < 0.05$) increase in absolute number of $CD3^+CD8^+$ T cells at week 3 post-infection compared to $TNF^{f/f}$ mice (Figure 3.2.22B).

Seeing that an intermediary increase in $CD4^+$ and $CD8^+$ T cells were observed in $M\text{-}TNF^{-/-}$ versus $TNF^{f/f}$ mice, data indicated that TNF derived from myeloid and T cells is required in controlling the $CD4^+$ and $CD8^+$ T cell influx into the CNS.

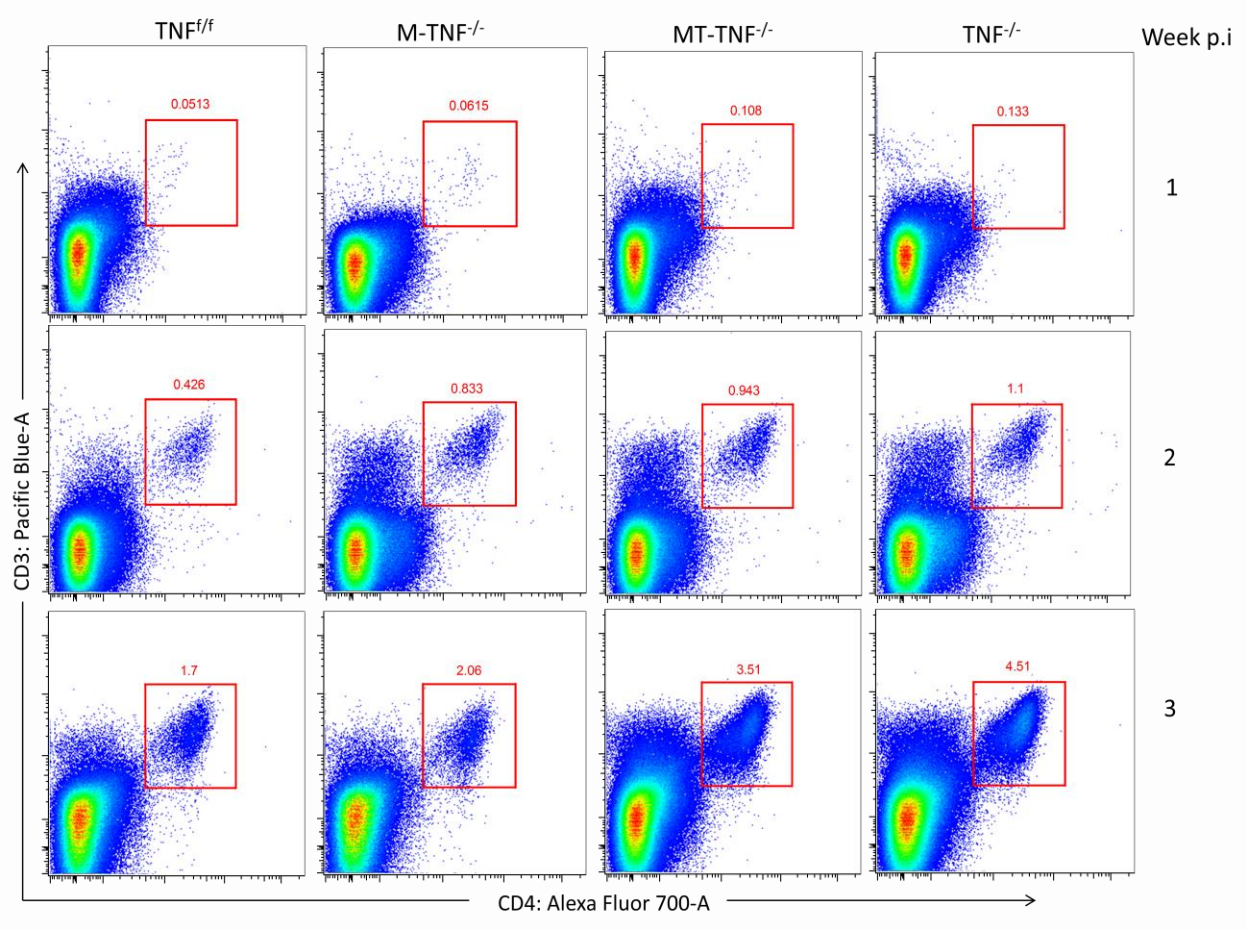

Figure 3.2.20: Increased infiltration of $CD4^+$ T cells in $MT\text{-}TNF^{-/-}$ but not $M\text{-}TNF^{-/-}$ mice. $TNF^{f/f}$, $M\text{-}TNF^{-/-}$, $MT\text{-}TNF^{-/-}$ and $TNF^{-/-}$ mice strains were intracerebrally infected with *M. tuberculosis* at a dose of $1x10^5$ cfu/brain. Whole brain tissues were harvested at week 1, 2 and 3 post-infection, and single cells were labelled for CD3 and CD4 expression. The flow cytometry dot plots show prominent infiltration of cerebral $CD4^+$ T cells. The values seen in the dot plot are the percentages of the parent gate which are positive. Data (n= 5 mice/group) are representative of one of the three independent experiments.

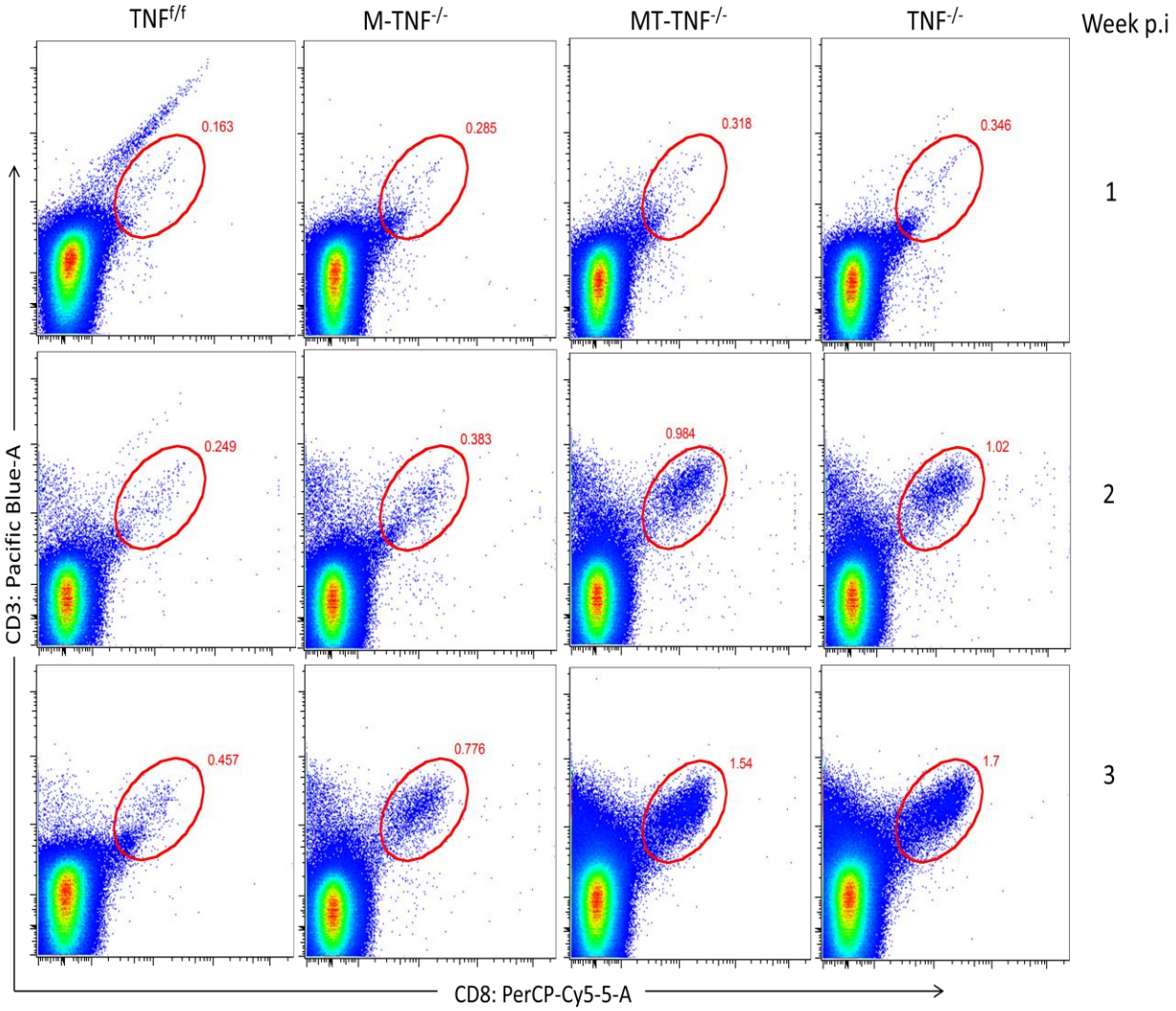

Figure 3.2.21: Increase influx of cerebral CD8$^+$ T cells in MT-TNF$^{-/-}$ but not M-TNF$^{-/-}$ mice. TNF$^{f/f}$, M-TNF$^{-/-}$, MT-TNF$^{-/-}$ and TNF$^{-/-}$ mice were intracerebrally infected with *M. tuberculosis* at a dose of 1x10^5 cfu/brain. Whole brain tissues were harvested at week 1, 2 and 3 post-infection, and single cells were labelled and data analysed for CD3 and CD8 expression. The flow cytometry dot plots show prominent infiltration of cerebral CD8$^+$ T cells. The values seen in the dot plot are the percentages of the parent gate which are positive. Data (*n*= 5 mice/group) represent one of the three independent experiments.

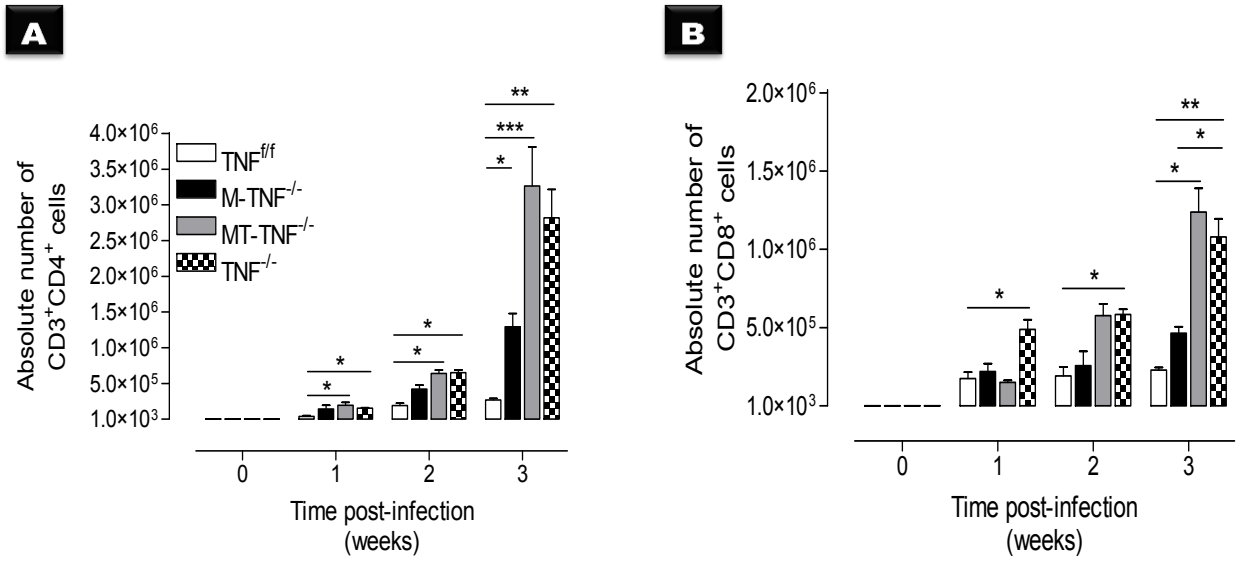

Figure 3.2.22: Uncontrolled increase of $CD3^+CD4^+$ and $CD3^+CD8^+$ T cells in cell-specific TNF mice. $TNF^{f/f}$, M-$TNF^{-/-}$, MT-$TNF^{-/-}$ and $TNF^{-/-}$ mice were intracerebrally infected with *M. tuberculosis* at a dose of $1x10^5$ cfu/brain. Whole brain tissues were harvested at week 0 (naïve), 1, 2 and 3 post-infection, and isolated single cells were labelled and data analysed for CD3, CD4 and CD8 markers. Shown are $CD4^+$ T cells ($CD3^+CD4^+$) absolute numbers (A), and also shown are $CD8^+$ T cells ($CD3^+CD8^+$) absolute numbers (B). *=$p < 0.05$, **=$p < 0.01$ and ***=$p < 0.001$. Data are one representative of three independent experiments. Results are represented as mean ± SD of 5 mice/group.

R2.8.1 TNF influences activation of effector $CD4^+$ and $CD8^+$ T cells during neurotuberculosis

We further evaluated the CD44 expression of cerebral infiltrating $CD4^+$ and $CD8^+$ T cells in $TNF^{f/f}$, M-$TNF^{-/-}$, MT-$TNF^{-/-}$ and $TNF^{-/-}$ mice by flow cytometer. The data showed no significant differences in $CD44^+$ expressing $CD4^+$ or $CD8^+$ T cells in M-$TNF^{-/-}$, MT-$TNF^{-/-}$ or $TNF^{-/-}$ mice at week 1 and 2 post-infection compared with $TNF^{f/f}$ mice (Figure 3.2.23A and B). However, a significant ($p < 0.05$) increase in the percentage of $CD4^+$ and $CD8^+$ T cells expressing $CD44^+$ was observed in M-$TNF^{-/-}$ mice at week 3 post-infection compared to $TNF^{f/f}$ mice. The percentage of $CD4^+$ and $CD8^+$ T cells expressing $CD44^+$ in both MT-$TNF^{-/-}$ and $TNF^{-/-}$ mice were significantly ($p < 0.05$) higher than in $TNF^{f/f}$ and M-$TNF^{-/-}$ mice at week 3 post-infection (Figure 3.2.23A and B).

These data suggest that TNF derived from myeloid or T cells play a critical role in the T cells activation.

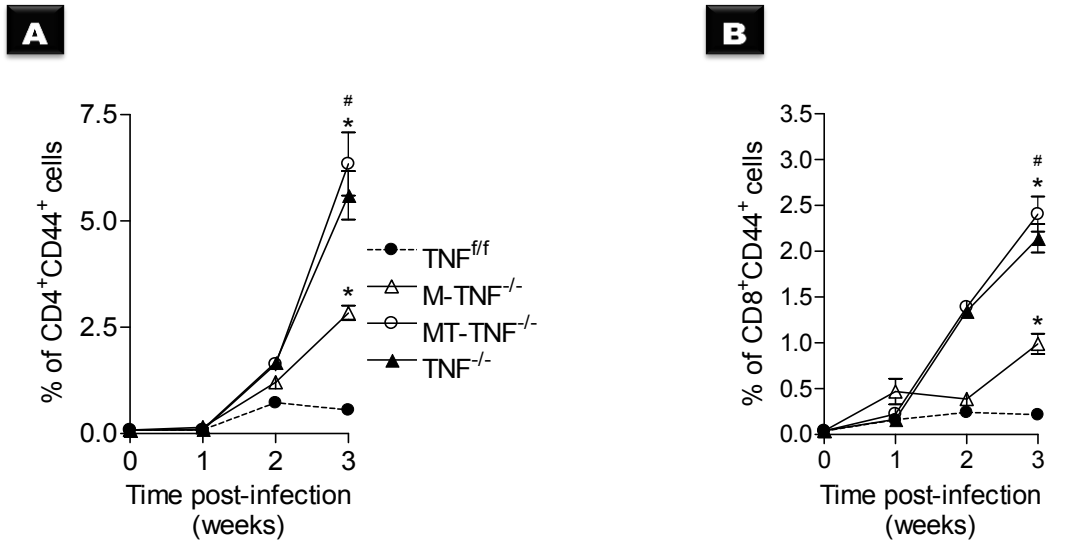

Figure 3.2.23: TNF increased effector CD4$^+$ and CD8$^+$ T cell percentage in cell-specific TNF mice. TNF$^{f/f}$, M-TNF$^{-/-}$, MT-TNF$^{-/-}$ and TNF$^{-/-}$ mice strains were intracerebrally infected with *M. tuberculosis* at a dose of 1x10^5 cfu/brain. Brains were harvested at week 0 (naïve), 1, 2 and 3 post-infection, and isolated brain single cells were labelled and analysed for CD3, CD4, CD8 and CD44 expression. Shown are the CD4$^+$ T cells expressing CD44$^+$ (A), and the CD8$^+$ population cells expressing CD44$^+$ (B). *=p < 0.05, and $^{\#}$=p < 0.05 for M-TNF$^{-/-}$ versus MT-TNF$^{-/-}$ and TNF$^{-/-}$. In this study, week 0 refers to naïve. Data are one representative of three independent experiments. Results are represented as mean ± SD of 5 mice/group.

R2.9 TNF mediates proinflammatory Th1-type cytokines production in MT-TNF$^{-/-}$ but not in M-TNF$^{-/-}$ mice.

We examined whether TNF derived from microglia/macrophages, neutrophils, CD4$^+$- and CD8$^+$ T cells modulate the production of proinflammatory Th1-type cytokines such as TNF, IFN-γ, IL-1β, IL-2, IL-6 and IL-12p70 during experimental cerebral *M. tuberculosis* infection. TNF$^{f/f}$, M-TNF$^{-/-}$, MT-TNF$^{-/-}$and TNF$^{-/-}$ mouse strains were intracerebrally infected with *M. tuberculosis* at a dose of 1x10^5 cfu/brain. Whole brain tissues were homogenised at week 0 (naïve), 1, 2 and 3 post-infection, and supernatants were collected and assayed for TNF, IFN-γ, IL-1β, IL-2, IL-6 and IL-12p70 by ELISA.

TNF production in TNF$^{f/f}$ mice remained relatively constant for the duration of the experiment within a narrow margin of between 300pg/m - 400pg/ml during acute *M. tuberculosis* infection (Figure 3.2.24A), suggesting that peak concentration were established early prior to week 1. Thus, similar concentrations were found in M-TNF$^{-/-}$ mice compared to TNF$^{f/f}$ mice and

although the data in M-TNF$^{-/-}$ mice showed an overall decreasing trend, this was not significant. The TNF level in MT-TNF$^{-/-}$ mice were significantly ($p < 0.01$) lower at all time points post-infection when compared either to TNF$^{f/f}$ or M-TNF$^{-/-}$ mice. As expected TNF levels in the complete TNF$^{-/-}$ mice were not detectable (Figure 3.2.24A).

We next measured the IFN-γ production levels, where we found that all mouse strains had a similar production level at week 1 post-infection, and it remained constant in TNF$^{f/f}$ and M-TNF$^{-/-}$ mice at week 2 post-infection. IFN-γ production levels were significantly ($p < 0.001$) lowered in TNF$^{f/f}$ and M-TNF$^{-/-}$ mice at week 3 post-infection compared to MT-TNF$^{-/-}$ and TNF$^{-/-}$ mice. In contrast, significantly ($p < 0.001$) higher concentrations were measured in MT-TNF$^{-/-}$ comparable to TNF$^{-/-}$ mice at week 2 and 3 post-infection compared either to TNF$^{f/f}$ and M-TNF$^{-/-}$ mice (Figure 3.2.24B).

The IL-1β concentration was significantly ($p < 0.05$) higher in TNF$^{f/f}$ at week 1 post-infection compared to MT-TNF$^{-/-}$ and TNF$^{-/-}$ mice, however, not significant difference was observed at this time point when compared with M-TNF$^{-/-}$ mice. The IL-1β concentration remained similar and relatively constant in both TNF$^{f/f}$ and M-TNF$^{-/-}$ mice at week 2 and week 3 post-infection. However, continuous significant ($p < 0.05$) reduction in IL-1β concentrations were observed in both MT-TNF$^{-/-}$ and TNF$^{-/-}$ mice at 2 and 3 week post-infection compared to TNF$^{f/f}$ and M-TNF$^{-/-}$ mice (Figure 3.2.24C).

IL-2 production levels in M-TNF$^{-/-}$, MT-TNF$^{-/-}$ and TNF$^{-/-}$ mice were significantly ($p < 0.01$) lower compared to TNF$^{f/f}$ mice at week 1 post-infection. IL-2 production levels in all mouse strains increased relatively constant at week 2 post-infection. Interestingly, IL-2 production levels in TNF$^{f/f}$ and M-TNF$^{-/-}$ mice continue to increase at week 3 post-infection. Moreover, a transient increase was noticed in IL-2 production at week 2 post-infection. Concentrations of IL-2 in MT-TNF$^{-/-}$ and TNF$^{-/-}$ mice were significantly ($p < 0.01$) lowered at week 3 post-infection compared either to TNF$^{f/f}$ or M-TNF$^{-/-}$ mice (Figure 3.2.24D).

We found similar production of IL-6 expression in TNF$^{f/f}$, M-TNF$^{-/-}$ and MT-TNF$^{-/-}$ mice at week 1 post-infection, while in TNF$^{-/-}$ mice, a significantly lower level was found at week 1 post-infection compared to TNF$^{f/f}$ mice. We found lower IL-6 production in TNF$^{f/f}$ and M-TNF$^{-/-}$ mice at week 2 and 3 post-infection compared to the earlier time point. IL-6 production was significantly ($p < 0.05$) higher in MT-TNF$^{-/-}$ and TNF$^{-/-}$ mice at week 2 post-infection compared to TNF$^{f/f}$ mice. Significantly ($p < 0.01$) higher IL-6 production was also observed in MT-TNF$^{-/-}$ and TNF$^{-/-}$ mice at week 3 when compared to TNF$^{f/f}$ and M-TNF$^{-/-}$ mice (Figure 3.2.24E).

No significant differences were detected in IL-12p70 production levels between M-TNF$^{-/-}$ and TNF$^{f/f}$ mice at all time points. In contrast, MT-TNF$^{-/-}$ and TNF$^{-/-}$ mice had significantly ($p <$

0.05) lower IL-12p70 production at week 1 post-infection compared to $TNF^{f/f}$ mice. The IL-12p70 levels in MT-$TNF^{-/-}$ and $TNF^{-/-}$ mice at week 2 post-infection were similar to $TNF^{f/f}$ and M-$TNF^{-/-}$ mice, but significantly ($p < 0.05$) lower production was found in MT-$TNF^{-/-}$ and $TNF^{-/-}$ mice at week 3 post-infection compared to $TNF^{f/f}$ mice (Figure 3.2.24F).

The overproduction observed at the site of disease in TNF, IL1β, IL-2 and IL-12p70 concentrations suggest that early regulation of immune responses was present in $TNF^{f/f}$ and M-$TNF^{-/-}$ mice but not in MT-$TNF^{-/-}$ or $TNF^{-/-}$ mice. Furthermore, the uncontrolled IL-6 and IFN-γ production observed in MT-$TNF^{-/-}$ or $TNF^{-/-}$ mice, but not in $TNF^{f/f}$ and M-$TNF^{-/-}$ mice point towards compensation of either source of TNF during inflammatory regulation.

Therefore, data showed that microglia/macrophages and neutrophils derived TNF have differential effects on proinflammatory Th1-type cytokines during CNS *M. tuberculosis* infection. These results also illustrated that the deletion of TNF from microglia/macrophages, neutrophils, and $CD4^+$- and $CD8^+$ T cells resulted in an uncontrolled increase of IL-6 and IFN-γ protein and reduced of IL1β, IL-2 and IL-12p70 production at the later stage of the disease.

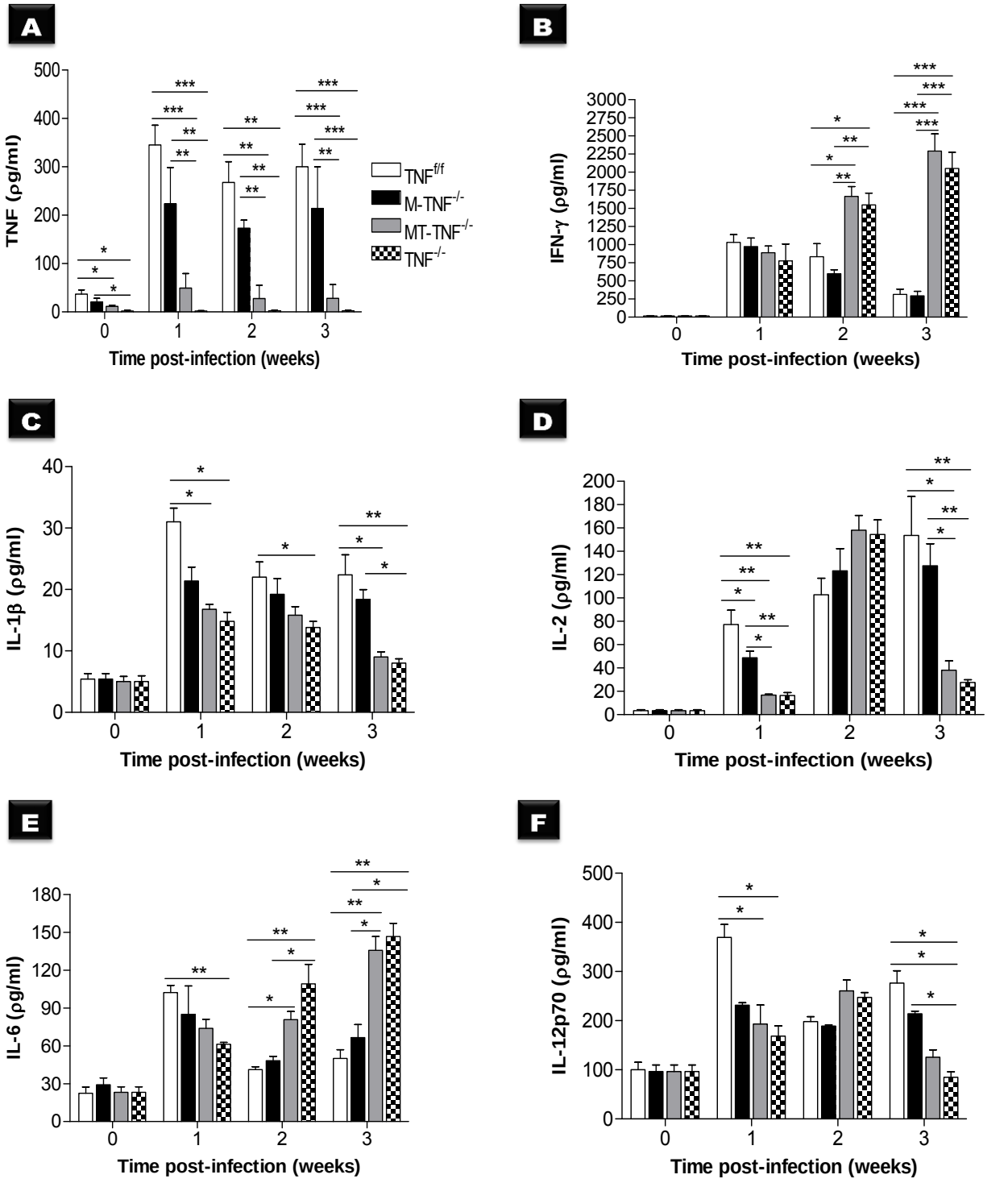

Figure 3.2.24: Modulation of proinflammatory Th1-type cerebral cytokines in cell-specific TNF mice. TNF$^{f/f}$, M-TNF$^{-/-}$, MT-TNF$^{-/-}$ and TNF$^{-/-}$ mice were intracerebrally infected with *M. tuberculosis* at a dose of 1x10^5 cfu/brain. The brains of mice were homogenised at week 0 (naïve), 1, 2 and 3 post-infection, and TNF (A), IFN-γ (B), IL-1β (C), IL-2 (D), IL-6 (E) and IL-12p70 (F) concentrations were measured in the supernatants by ELISA. Data are representative of at least three independent experiments that yielded similar results. Data are mean ± SD of 5 mice/group. *=$p < 0.05$, **=$p < 0.01$ and **=$p < 0.001$.

R2.10 Cerebral chemokine production following CNS *M. tuberculosis* infection

To further understand the factors associated with an increased leukocyte influx into the brain leading to susceptibility, we postulated that increased pathology was driven by an increased in leukocyte chemoattractants. We therefore measured cerebral MCP-1, MIP-1α and RANTES concentration in *M. tuberculosis* infected $TNF^{f/f}$, M-$TNF^{-/-}$, MT-$TNF^{-/-}$and $TNF^{-/-}$ mice at week 1, 2 and 3 post-infection. Several studies have supported the association of MCP-1 with TB (Flores-Villanueva *et al.,* 2005; Buijtels *et al.,* 2008; Hasan *et al.,* 2005; Thye *et al.,* 2009 and Ben-Selma *et al.,* 2011). Also MIP-1α has been found to be implicated in *M. tuberculosis* infection (Jussi *et al.,* 2002). The association has also been found between RANTES and *M. tuberculosis* infection (Chu *et al.,* 2007; Sanchez-Castanon *et al.,* 2009 and Ben-Selma *et al.,* 2011).

We found that the MCP-1 concentration in both $TNF^{f/f}$ and M-$TNF^{-/-}$ mice were equivalent at week 1, 2 and 3 post-infection. In contrast, MCP-1 production was significantly higher (400±55 and 390±280 vs $p < 0.05$) in MT-$TNF^{-/-}$ and complete $TNF^{-/-}$ mice at week 1 post-infection compared to $TNF^{f/f}$ (Figure 3.2.25A). No significant difference was found between MT-$TNF^{-/-}$ and $TNF^{f/f}$ mice at week 2 post-infection, however, MCP-1 production was significantly ($p < 0.05$) higher in $TNF^{-/-}$ mice at this time point post-infection. In addition, significant ($p < 0.05$) increases in the MCP-1 production levels were observed in both MT-$TNF^{-/-}$ and $TNF^{-/-}$ mice at week 3 post-infection when comparing with either $TNF^{f/f}$ or M-$TNF^{-/-}$ mice (Figure 3.2.25A). Equivalent MIP-1α production was measured in all mouse strains at week 1 post-infection. A significant difference was found in MIP-1α production of $TNF^{-/-}$ mice at week 2 post-infection when compared either with $TNF^{f/f}$ or M-$TNF^{-/-}$ mice (Figure 3.2.25B). No significant difference was detected in the MIP-1a production of MT-$TNF^{-/-}$ mice at week 2 post-infection compared either to $TNF^{f/f}$, M-$TNF^{-/-}$ or $TNF^{-/-}$ mice. Interestingly, MIP-1α production levels were significantly ($p < 0.01$) higher in MT-$TNF^{-/-}$ and $TNF^{-/-}$ mice at week 3 post-infection compared either with $TNF^{f/f}$ or M-$TNF^{-/-}$ mice (Figure 3.2.25B). Similar to MIP-1α production, no significant ($p < 0.01$) difference was detected in RANTES production in all mice at week 1 post-infection. A significant difference was found in RANTES production of $TNF^{-/-}$ mice at week 2 post-infection compared either with $TNF^{f/f}$ mice (Figure 3.2.25C). No significant difference was detected in RANTES production of MT-$TNF^{-/-}$ mice at week 2 post-infection compared either to $TNF^{f/f}$, M-$TNF^{-/-}$ or $TNF^{-/-}$ mice. RANTES production levels were significantly ($p < 0.01$) higher in MT-$TNF^{-/-}$ and $TNF^{-/-}$ mice at week 3 post-infection compared either with $TNF^{f/f}$ or M-$TNF^{-/-}$ mice (Figure 3.2.25C).

Our results clearly demonstrated that deficiency of TNF in microglia/macrophages and neutrophils does not impair the chemoattractant response during cerebral *M. tuberculosis* infection. In contrast, ablation of TNF in microglia/macrophages, neutrophils, and $CD4^+$- and $CD8^+$ T cells increases the expression of chemokines during cerebral *M. tuberculosis* infection, suggesting that TNF is required for chemokines regulation.

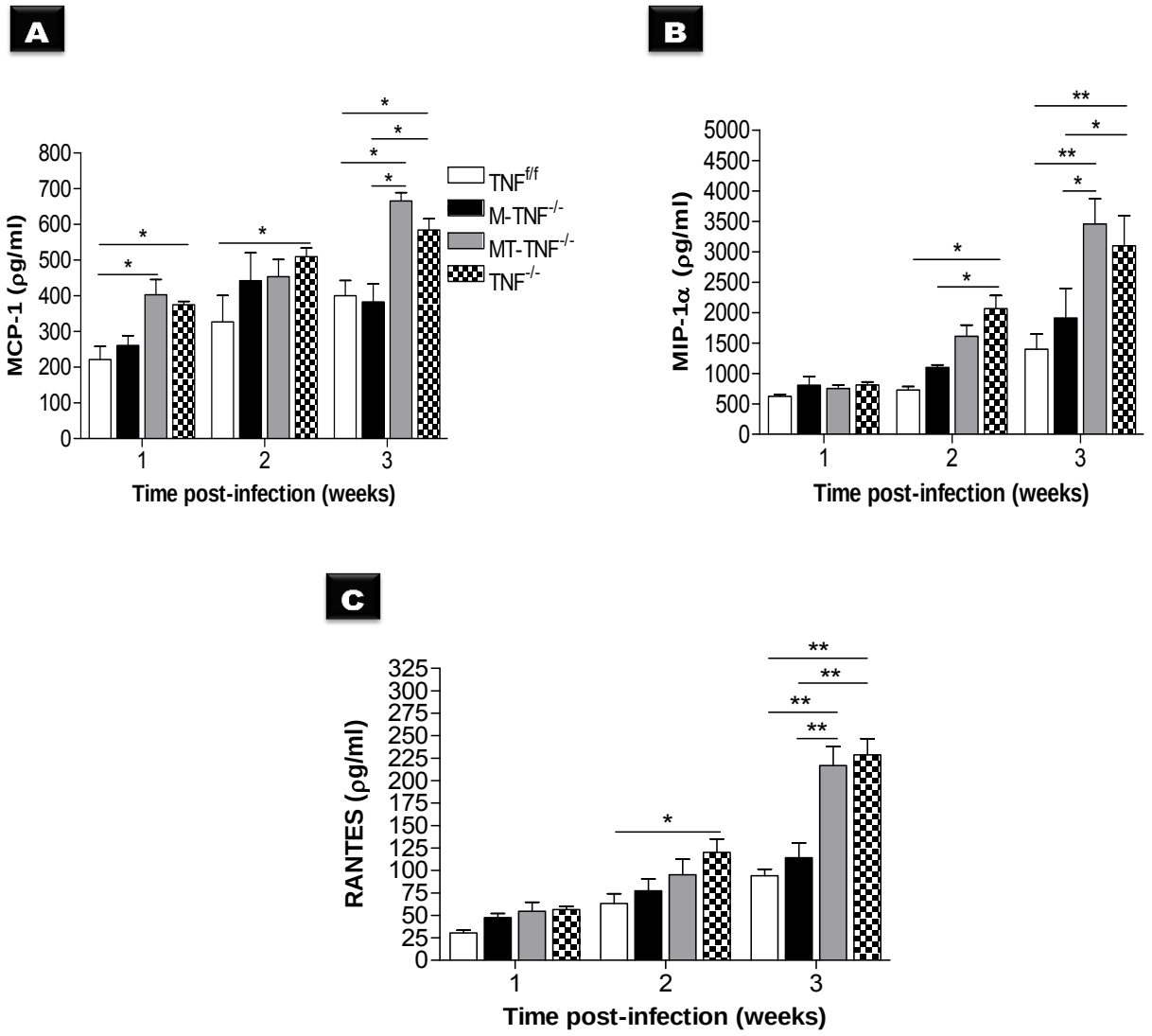

Figure 3.2.25: Total cerebral chemokines expressions during experimental neurotuberculosis. $TNF^{f/f}$, M-$TNF^{-/-}$, MT-$TNF^{-/-}$ and $TNF^{-/-}$ mice were intracerebrally infected with *M. tuberculosis* at a dose of $1x10^5$ cfu/brain. Brains of infected mice were homogenised at week 1, 2 and 3 post-infection, and MCP-1 (A), MIP-1α (B) and RANTES (C) levels in supernatants were assessed by ELISA. Data are representative of at least three independent experiments that yielded similar results. Results are mean ± SD of 5 mice/group, *=$p < 0.05$ and **=$p < 0.01$.

CHAPTER IV

DISCUSSION

Previous studies with both rabbits (Tsenova *et al.,* 2005) and mice (van Well *et al.,* 2007 and Zucchi *et al.,* 2012) demonstrated formation of meningitis after intracerebral *M. tuberculosis* injection. These models enabled investigation of therapeutic strategies and understanding of immune regulation during neurotuberculosis, despite the limitation in the route of pathogen entry to the CNS. In humans, neurotuberculosis occurs by lympho-hematogenous dissemination after primary lung infection, whereas in the experimental models, bacteria were directly inoculated into the cerebellum. To exclude that the intracerebral injection procedure induced substantial infiltration of peripheral immune cells by damaging the BBB; it was established that saline injected mice exhibited neither clinical manifestations nor pathology (appendix H). We investigated the role of cell specific TNF in mediating immune protection, focusing mainly on the contribution of neurons, microglia, macrophages, neutrophils, and CD4 and CD8 T cells-derived TNF in host immunity against *M. tuberculosis*. Importantly, *M. tuberculosis* infected animals showed characteristics of TB meningitis and tuberculomas similar to the studies described by Tsenova *et al.,* (2005); van Well *et al.,* (2007) and Zucchi *et al.,* (2012). Therefore, there is a need for neuro-immunopathology investigation, as susceptibility to TB infection has been historically ascribed, to an inadequate immune response that fails to control infected mycobacteria pathogen (Tobin *et al.,* 2012) with limited understanding of neuro-immunology. Genetic deficiencies of immune effectors such as TNF, IFN-γ and iNOS have confirmed its importance as critical for immune protection against tuberculosis (Fortin *et al.,* 2007). Also, non genetic immunosuppression, such as TNF-neutralisation and biological immunosuppressors such as HIV infection increase susceptibility of TB (Kwan & Ernst, 2011 and Lawn & Zumla, 2011). Studies using animals and humans have found that the mutation of the leukotriene A4 hydrolase (LTA4H) locus, which controls the balance of pro- and anti-inflammatory eicosanoids, showed two distinct molecular routes to mycobacterial susceptibility converging on dysregulated levels of TNF (Tobin *et al.,* 2010 and Tobin *et al.,* 2012). These studies demonstrated two different baseline response levels of TNF, one where insufficient levels lead to mycobacterial overgrowth, while high levels result in uncontrolled inflammation being detrimental to the host. These two baseline response levels of TNF indicate that individuals are susceptible to *M. tuberculosis* infection for two fundamentally different reasons.

In the brain, the BBB separates the CNS from the regular systemic blood circulation. Unlike other organs, the CNS lacks a draining lymph node system where immune cells, such as APC and T-cells may interact (El-Kebir *et al.,* 2013). For these reasons, the CNS was previously thought to be an immunologically privileged area. Research findings have demonstrated that this concept is incorrect. Both resident and infiltrating immune cells participate actively in

immune responses in the CNS (Rock *et al.,* 2004; Carson *et al.,* 2006 and Galea *et al.,* 2007), which upon activation may secrete cytokines including TNF.

Several immunomodulatory drugs have been used to downregulate the production of TNF such as etanercept, which is a fusion protein consisting of 2 soluble TNFR2 receptors linked to a human immunoglobulin Fc fragment. Etanercept therapy was implicated in TB reactivation (Mohan *et al.,* 2004). Dexamethasone is another drug that was found to cause latent TB reactivation in non-human primates (Lin *et al.,* 2010). Although this drug proved to be detrimental by influencing the matrix metalloproteinases, which play a role in collagen breakdown and cerebral tissue damage (Green *et al.,* 2009); in TBM patients, the co-administration of dexamethasone with tuberculostatic drugs has shown to be effective in early stages of TBM (Thwaites *et al.,* 2004; Prasad & Singh, 2009 and Török *et al.,* 2011). A study by Tsenova *et al.,* (1998) proved that combining the TNF targeting immunomodulatory drug such as thalidomide (Peterson *et al.,* 1995), with antibiotics results in a reduction of TNF levels and higher survival rate in rabbits. However, its clinical use showed less effect in children with TBM (Schoeman *et al.,* 2004). In addition, infliximab a monoclonal antibody that completely inhibits TNF is used for treatment of inflammatory diseases such as rheumatic and bowel disease. Previous studies have shown that patients on infliximab therapy reactivate with pulmonary tuberculosis (Fallahi-Sichani *et al.,* 2012), and may potentially have similar contributory effects in the development of TBM.

In humans, primates and mice, TNF has been shown to be essential for the maintenance of granuloma structures and for effective control of pulmonary mycobacterial infection (Kindler *et al.,* 1989; Tracey *et al.,* 1993; Flynn *et al.,* 1995; Rock *et al.,* 2004; Tsai *et al.,* 2006 and El-Kebir *et al.,* 2013). In the brain, TNF is synthesised by both immune (including infiltrating cells) and non-immune cells (including neurons). Therefore, identifying the cellular sources of TNF that contribute to the pathology is of significant interest. We have recently found that *M. tuberculosis* can infect neurons *in vitro* and *in vivo* (Randall & Hsu *et al.,* 2014). Many studies have suggested the existence of an extensive crosstalk between the CNS and immune system, whereby immune cells protect neurons from degeneration (Kerschensteiner *et al.,* 1999; Moalem *et al.,* 1999 and Medana *et al.,* 2001), and neurons can mediate the generation of T regulatory cells during inflammation (Liu *et al.,* 2006). With this understanding, we opted to investigate independently the role of neuronal derived TNF during neurotuberculosis. Because neurons are the basic functional unit of the CNS, we then thought to first generate mice that are deficient specifically for neuronal TNF synthesis and investigate its contribution to immune responses against *M. tuberculosis*. We and others have shown that neurons express TNF and

findings from $TNF^{f/f}$ mice confirmed the expression of TNF in neurons as previously reported (Liu *et al.,* 1994; Gahring *et al.,* 1996 and Tchelingerian *et al.,* 1996). TNF expression in neurons has also been reported against other pathogens (Cowan *et al.,* 1997 and Zhang *et al.,* 2010). We found that $NsTNF^{-/-}$ mice are not susceptible to *M. tuberculosis* infection compared to $TNF^{f/f}$ mice. An inflammatory response was observed in $TNF^{f/f}$ mice as was described in previous published studies in rabbits (Tsenova *et al.,* 2005) and mice (van Well *et al.,* 2007 and Zuchi *et al.,* 2012). As the disease progressed, $NsTNF^{-/-}$ mice showed lymphocytic rich foci, and extracerebral dissemination with no clinical manifestations similar to $TNF^{f/f}$ mice. In contrast, $TNF^{-/-}$ mice developed severe clinical manifestations which correlated with high bacterial burden, uncontrolled leukocyte infiltration, severe lymphocytic rich foci, high extracerebral dissemination and subsequently these mice succumbed to infection. The failure of $TNF^{-/-}$ mice to control infection verifies the absolute requirement of TNF for immune protection against neurotuberculosis.

Both $NsTNF^{-/-}$ and $TNF^{f/f}$ mice survived *M. tuberculosis* infection, indicating that neuronal derived TNF is not required for neuroimmune protection. Immune cells from the periphery migrate into the brain during inflammation response of CNS, where these cells may produce antimycobacterial molecules such as iNOS (Dogan *et al.,* 2008). Here we have shown that in the absence of TNF of neurons, the expression of iNOS was not altered and expression level was equivalent to $TNF^{f/f}$ mice, indicating that neuronal derived TNF is not involved in the overall synthesis of iNOS. Induction of iNOS mediates the production of nitric oxide, which is an effector molecule for bacterial inhibition (Barnes & Belvisi, 1993). In $TNF^{-/-}$ mice where uncontrolled bacterial growth was observed, the production level of iNOS was lower compared to $TNF^{f/f}$ mice. Although iNOS synthesis is regulated by several cytokines, we found that complete ablation of TNF leads to impaired production of iNOS in the brain, while others have shown iNOS detection in $TNF^{-/-}$ mice after pulmonary *M. tuberculosis* infection (Flynn *et al.,* 1995 and Bean *et al.,* 1999), and also in the brains of $TNF^{-/-}$ mice with experimental allergic encephalitis (Korner *et al.,* 1997 and Riminton *et al.,* 1998); we and other pulmonary tuberculosis studies (Jacobs *et al.,* 2000; Botha *et al.,* 2003 and Allie *et al.,* 2008) have shown opposite findings, suggesting that, the regulation of iNOS is TNF independent. Our findings support the Olin *et al.,* (2008) study where the authors elegantly illustrated that $iNOS^{-/-}$ mice infected with *M. tuberculosis* developed serious clinical manifestations and exuberant lymphocyte meningeal infiltration. Mice with ablation of TNF from the neurons had a moderate percentage of infiltrating myeloid and T cells equivalent to $TNF^{f/f}$ mice, whereas mice with complete TNF ablation had an exacerbated increase, with pronounced lymphocytes rich foci. A

pulmonary TB study has demonstrated that effector T cells are rapidly recruited to the existing granulomas and are retained within this structure with edged egress from the lesions (Egen *et al.,* 2008). Indeed, during neurotuberculosis infection, recruited myeloid and T cells were fully mature effector cells, expressing CD45 and activation marker CD44, respectively. Taken together, the data suggest that infiltration of leukocytes is regulated by TNF. We also found that the absence of TNF in the neurons had no regulatory effect on the expression of cell surface markers such as $CD80^{+}$, $CD86^{+}$ and $MHCII^{+}$ especially in microglia, macrophages and DCs, and was comparable to $TNF^{f/f}$ mice. The increased co-stimulation expression observed in CD86 may be explained by the fact that corresponding receptors for CD80 and CD86 are CD28 and CTLA-4, and their receptors are expressed on both T and B cells; with CD80 having a higher affinity for CTLA-4 whereas CD86 binds more effectively to CD28 (Collins *et al*., 2002). However, both CD80 and CD86 are able to initiate both costimulatory and coinhibitory signals upon binding to their receptors. The cells continuously interaction with stimuli led to high expression of CD86 which interact with CD28, and resulted in the initiation of a costimulatory signal. While, in other hand, these cells started also to express the CD80 which interacts with CTLA-4 to induce a coinhibitory signal that counteracts costimulatory signals (Collins *et al*., 2005). However, our data are in agreement with the studies using recombinant TNF and TNF neutralisation in which they have shown that the presence or absence of TNF does not affect the CD86 expression (Salgado *et al.,* 1999 and Miyazawa *et al.,* 2008).

The high MHCII expression observed in APCs of both $TNF^{f/f}$ and $NsTNF^{-/-}$ mice may contribute to a protective mechanism to regulate immune activation in the CNS during later stages of disease, while complete ablation of TNF resulted in low antigenic responses by APCs. Decreased expression of $MHCII^{+}$ observed in $TNF^{-/-}$ mice, which was associated with decreased co-stimulatory markers expression may suggest the impediment of antigen presentation processes and a failure to induce *M. tuberculosis* specific immunity leading to an increase in mycobacterial intra-macrophage growth and mycobacterial susceptibility. TNF has been implicated in the regulation of MHCII, CD80 and CD86 expression on APCs (Pessara *et al.,* 1990; Ranheim *et al.,* 1995; Pechhold *et al.,* 1997; Ishikawa *et al.,* 2002; Kim *et al.,* 2002; Iijima *et al.,* 2003; Baldwin *et al.,* 2010 and Keller *et al.,* 2011). We found that complete ablation of TNF led to decreased expression of $CD80^{+}$ and $MHCII^{+}$ observed in $TNF^{-/-}$ mice. Our data is consistent with previously published results where cells in the granulomas of TNF-LT-$\alpha^{-/-}$ mice expressed low levels of MHCII during pulmonary *Mycobacterium bovis* BCG infection (Jacobs *et al.,* 2000), also our data is consistent with the CD86 expression pattern reported in other infection studies using $TNF^{-/-}$ mice (Torres *et al.,* 2005).

Our data showed the presence of infiltrating B-cell subsets in the brain at the onset of disease. The presence of Fo B cells, plasmablast and plasma cells observed here suggest that B cells may contribute to the host immune response and intervene during CNS infection, as the role for B cells during early immune responses to pulmonary *M. tuberculosis* infection was reported to be associated with the delay of in dissemination, development of lung pathology and alteration of cellular infiltrate in the lungs in B-cell knockout mice (Bosio *et al.,* 2000). Studies using other types of infection have shown that B- and T cell responses function complementary to repel infection, and both cell-types are able to contribute to long-lived protection (Amanna *et al.,* 2006 and Doherty *et al.,* 2006). B cells as professional antigen presenting cells, express various cell surface markers to promote the maturation and activation of T cells (Sharpe *et al.,* 2002). Notably, B cells can modulate this maturation process through the production of antibodies and cytokines, by either enhancing or suppressing immune responses (Kalergis *et al.,* 2002; Rafiq *et al.,* 2002; Mauri *et al.,* 2003; Dhodapkar *et al.,* 2005; Mizoguchi *et al.,* 2007 and Sugimoto *et al.,* 2007). Also B cells have been reported to polarize T cell responses through the production of cytokines (Harris *et al.,* 2000). Furthermore, B cells mediate adaptive immunity that evolves both humoral and cellular component (Maglione & Chan, 2009), and most importantly, B cells produce antibodies that neutralize invasion and further target infectious agents for destruction (Moore *et al.,* 2001). Our data showed low level production of antibody in Fo B cells compared to plasmabast and plasma cells, but had the highest antigen-presenting cell marker expression. B-cell subsets in NsTNF$^{-/-}$ mice showed high percentage levels of co-stimulatory, antibody and antigen presenting cell markers resembling that of TNF$^{f/f}$ mice. On the contrary, B-cell populations in TNF$^{-/-}$ mice resulted in decreased co-stimulatory, antibody and antigen presenting cell marker expression. Furthermore, plasma cells expressing MHCII^{+} found in all mouse strains confirmed the phenotype of mature plasma cell (Arko-Mensah *et al.,* 2009). B cells interaction with naïve CD4^{+} helper T cells stimulates cytokine synthesis that reciprocally regulates the antibody responses of B cells (Vascotto *et al.,* 2007). Amongst the cytokines produced by T cells, TNF has been reported to play a major role in B-cell activation to produce immunoglobulin antibody (Higuchi *et al.,* 1997). Deficiency in B-cell responses in TNF$^{-/-}$ has been well-documented (Pasparakis *et al.,* 1996; Pasparakis *et al.,* 1997; Grivennikov *et al.,* 2005 and Kuprash *et al.,* 2005). Our data are consistent with the previously published studies where others have shown that B cells play a role in shaping the immune response against *M. tuberculosis* infection (Phuah *et al.,* 2012) and in other neurodegenerative disease (Serafini *et al.,* 2004). The decreased antigenic and humoral response observed in B cells of TNF$^{-/-}$ mice

may be attributed to the absence of stimulation of T cell-derived TNF, therefore suggesting that T cell TNF may be critical in mediating B cells immunity during neurotuberculosis.

Early Th1-type cytokine response was found where comparable up-regulation of the proinflammatory cytokines TNF, IL-1β, IL-6 and IL-12p70 was measured in $NsTNF^{-/-}$ and $TNF^{f/f}$ mice. Thereafter, $NsTNF^{-/-}$ mice had moderate cytokine and chemokines expression throughout the experimental period resembling $TNF^{f/f}$ mice, which coincided with control of mycobacterial burden. The expression levels of cytokines (IL-6, TNF, and IFN-γ) and chemokine expression observed in $TNF^{f/f}$ mice were in line with previously published data (van Well *et al.,* 2007). Our findings are in agreement with the previous report by Arko-Mensaha *et al.,* (2009) where they reported the protection in C57BL/6J and BALB/c mice was directly associated early increase in immunological events such as increases in IL-12 and TNF. On the contrary, $TNF^{-/-}$ mice had uncontrolled up-regulation of proinflammatory IL-6 and IFN-γ, and chemokines (MCP-1, MIP-1α and RANTES) compared to the $TNF^{f/f}$ and $NsTNF^{-/-}$ mice. The over expression of cerebral IL-6 and IFN-γ as well as chemokines observed in $TNF^{-/-}$ mice correlated with the higher influx of leukocytes, ultimately inducing an inflammatory signature which was probably sustained by the high infection burden. Proinflammatory Th1-type cytokines and chemokines are crucial to the brain's immune function serving to maintain immune surveillance, facilitate leukocyte traffic, and recruit other inflammatory factors (Takeshita & Ransohoff, 2012). However, uncontrolled proinflammatory cytokine and chemokine production may lead to excessive neurodegenerative pathology, microcirculatory dysfunction or uncontrolled host's tissue damage (Beutler *et al.,* 1985; Björkbacka *et al.,* 2004 and Ramesh *et al.,* 2013). IL-2 promotes selective expansion of effector T cells after antigen activation, was found to be induced in $NsTNF^{-/-}$ mice at concentration levels equivalent to $TNF^{f/f}$ mice. In contrast, significant lower IL-2 production was found in $TNF^{-/-}$ mice despite a higher percentage of infiltrating T cells compared to $TNF^{f/f}$ and $NsTNF^{-/-}$ mice suggesting that T cell proliferation is TNF independent. Our data are consistent with human pulmonary tuberculosis results with those of Toossi *et al.,* (1986) and Khanna *et al.,* (2003) where the authors reported significant lower IL-2 in patients compared to normal controls. However, impaired production and responses of IL-2 are critical factors in the defective cellular immune response during pulmonary *M. tuberculosis* infection (Toossi *et al.,* 1986); where TNF plays a critical role in the regulation of IL-2 synthesis.

Uncontrolled cellular influx and protein expression of cytokines and chemokines observed in $TNF^{-/-}$ mice are characteristic of TB meningitis in humans, and have been reported to cause perivascular inflammation and occlusion of small vessels, which leads to infarcts and cranial nerve palsies (Saez-Llorens *et al.,* 1990). In human TB meningitis and bacterial

meningitis other than TB meningitis, the levels of cytokines in CSF correlate with the clinical course of meningitis (Mustafa *et al.,* 1989; Saez-Llorens *et al.,* 1990 and Ceyhan *et al.,* 1997). Both, $TNF^{f/f}$ and $NsTNF^{-/-}$ mice exhibited similar phenotypes, and indicated that neuronal derived TNF is redundant and does not contribute to cytokine mediated immunity against CNS *M. tuberculosis* infection. TNF produced by other immune and non-immune cellular sources can partially compensate neuronal derived TNF to control of infection, and leading to some redundant functions. Research demonstrated that during inflammation, resident and infiltrating myeloid cells are found to be the main cellular sources of TNF in the CNS, following by the T cells and other non-immune cells. TNF produced by myeloid cells has been shown to accelerate the onset of disease by regulation of chemokine expression in the CNS, driving the recruitment of inflammatory cells into the CNS, while TNF produced by lymphoid T cells exacerbated the damage to the CNS inflammation, by regulating infiltration of inflammatory myeloid cells into the CNS (Kruglov *et al.,* 2011).

We hypothesised that TNF derived from myeloid phagocytic cells, including microglia and macrophages, could affect the resistance to mycobacteria infection. Relevant to this study is the widely accepted view that microglia and infiltrating macrophages are significant sources of TNF as contributory to host immune responses during bacterial infection (Hirsch *et al.,* 1994; Renno *et al.,* 1995; Britton *et al.,* 1998 and Welser-Alves *et al.,* 2013). We then investigated host immune function against CNS *M. tuberculosis* in $M\text{-}TNF^{-/-}$ mice, where microglia/macrophages and neutrophils were incapable of synthesising TNF (Grivennikov *et al.,* 2004). We speculated that the ablation of TNF from myeloid origin, especially from microglia and macrophages, could result in high susceptibility, defective activation and increase intra-microglia/macrophages bacterial growth. Interestingly, we found that $M\text{-}TNF^{-/-}$ mice did not succumb to CNS *M. tuberculosis* infection, did not exhibit overt clinical manifestations and had pathology resembling $TNF^{f/f}$ mice. The histopathological data demonstrated meningeal lymphocytic infiltration similar to $TNF^{f/f}$ mice. Furthermore, similar iNOS protein expression was observed in $M\text{-}TNF^{-/-}$ mice compared to $TNF^{f/f}$ mice, suggesting that myeloid derived TNF do not impair iNOS synthesis. This iNOS expression level observed in $M\text{-}TNF^{-/-}$ mice could be the result of compensation from T cell-derived TNF. Unlike human macrophages, murine macrophages induce expression of iNOS which generate nitric oxide that is capable of reacting with oxygen and reactive oxygen intermediates to form a nitrite anion (NO_2^-), nitrate anion (NO_3^-), dinitrogen trioxide N_2O_3, and the highly mycobactericidal peroxynitrite anion ($ONOO^-$) (McMicking *et al.,* 1997 and Schneemann & Schoeden, 2007). The influx of myeloid cells into the CNS was slightly increased in $M\text{-}TNF^{-/-}$ mice compared to $TNF^{f/f}$ mice. The resident and the

recruited myeloid cells were fully functional and mature effector cells, expressing CD45 markers. Immunity against *M. tuberculosis* is multifactorial, involving a network of innate and adaptive immune responses (Mihret, 2012). In CNS, microglia, and infiltrating macrophages, neutrophils and DCs are crucial cells in the immune response to *M. tuberculosis* by presenting antigens to T cells in the context of both MHC class I and II (Rock *et al.,* 2005 and Mihret, 2012). Also, microglia, and infiltrating macrophages and DCs plays an important role in recruitment of cells to the site of infection through secretion of proinflammatory cytokines (Giacomini *et al.,* 2001 and Saijo & Glass. 2011). We have found that, in general, infiltrating DCs in the brain had low expression levels of the co-stimulatory and MHCII markers compared with macrophages. DCs are not resident cells of the brain, therefore they are required to transport *M. tuberculosis* from the site of infection to the local lymph node, but because the brain lacks specific lymph nodes; the antigenic response may be impaired therefore resulting in lower expression of co-stimulatory and MHC markers as observed in the DCs population. This phenomenon has been previously reported in the lung during *M. tuberculosis* infection (Wolf *et al.,* 2007 and Wolf *et al.,* 2008).

Little evidence exists to indicate that macrophages interact with B cells during *M. tuberculosis* infection. However, exchange of antigen between B cells and other APC has been indirectly demonstrated by Townsend & Goodnow, (1998) based on their finding that HEL/ I-Ak-specific T cells were activated *in vivo* following adoptive transfer of in vitro Ag-pulsed IgHEL B cells. The interaction between macrophages and B cells has also been reported to be an important feature of B cells activation for the response to polysaccharide (Boswell *et al.,* 1980). The ablation of TNF from the myeloid cell subsets did not alter the influx or the activation of B cells. The influx and expression of B-cell subsets surface markers and antibody secretion in M-TNF$^{-/-}$ mice was similar to that of TNF$^{f/f}$ mice. B-cell humoral and antigenic responses observed in both M-TNF$^{-/-}$ and TNF$^{f/f}$ mice is subjective to protection against *M. tuberculosis* infection. Our data is consistent with the non-human primate pulmonary TB study, where Phuah *et al.,* (2012) have found that B cells are present and actively secrete antibodies specific for *M. tuberculosis* antigens. Thus, our data indicate that the ablation of TNF in myeloid cells does not impair B cells immunity against *M. tuberculosis* infection.

We showed in this study that deletion of TNF from microglia/macrophages and neutrophils had a transient and significant influence in the recruitment and activation of CD4^{+}- and CD8^{+} cells, which were also fully mature effector cells and expressing CD44 activation marker, suggesting that TNF derived from microglia/macrophages and neutrophils had a redundant role in humoral immunity but had a limited role in T cell activation. We have also

shown that the ablation of TNF from microglia/macrophages and neutrophils do not affect the inflammatory response. Levels of IL-1β, IL-2, IL-6, IL-12p70, TNF and IFN-γ in M-TNF$^{-/-}$ mice were comparable to TNF$^{f/f}$ mice. Cytokines and chemokines are potential modulators of immune responses during acute neurotuberculosis. Chemokines produced by local CNS cells mediate leukocytes trafficking into the CNS (Cardona *et al,* 2003 and Glass *et al.,* 2005), which thereafter produce cytokines including TNF. A higher inflammatory response was documented in respect to chemokine production, but do not appear to be significantly different compared to TNF$^{f/f}$ mice. The data correlate with the phenotype profile of M-TNF$^{-/-}$ mice, and are indicative of the limited role of myeloid derived TNF in proinflammatory response against CNS *M. tuberculosis* infection.

Although TNF plays a critical role in granuloma formation and containment of mycobacterial infection (Folgueira *et al.,* 1994 and Flynn *et al.,* 1995), studies have also found that local CNS production of TNF in experimental bacterial meningitis lead to, alteration of BBB permeability and increased leukocyte infiltration in cerebro-spinal fluid (Ramilo *et al.,* 1990; Saez-Llorens *et al.,* 1990 and Saukkonen *et al.,* 1990), and enhances of CNS-TB (Tsenova *et al.,* 1999). In contrast, decreased TNF level has been shown to increase intra-macrophages bacterial growth leading to necrotic cells (Flynn *et al.,* 1995; Bean *et al.,* 1999; Botha *et al.,* 2003; Allie *et al.,* 2008 and Tobin *et al.,* 2012). Although widely acclaimed as the main cellular sources of TNF, microglia/macrophages and neutrophils derived TNF have limited role in restricting mycobacterial replication through TNF dependent synthesis during CNS *M. tuberculosis* infection. Our finding is consistent with the Allie *et al.,* (2013) results where they found similar phenotypic outcomes in M-TNF$^{-/-}$ mice during pulmonary TB. We show here that resident and infiltrating macrophages as well as neutrophils derived TNF is redundant during host immunity against CNS *M. tuberculosis* infection. How can these observations be explained? Given the similarities between M-TNF$^{-/-}$ and TNF$^{f/f}$ mice in phenotype, it is conceivable that the protective immunity observed in M-TNF$^{-/-}$ mice may be due to compensatory effects of T cell or other non-immune cell-derived TNF, generating sufficient TNF concentration levels for containment of *M. tuberculosis* infection. However, since data of T-TNF$^{-/-}$ mice are not shown it is difficult to conclude with 100% of certainty that T cell-derived TNF is a compensatory source.

We have also found that mice lacking TNF in CD4 and CD8 T cells (T-TNF$^{-/-}$) are not susceptible to cerebral *M. tuberculosis* infection (Unpublished data). We speculate here that the protective immunity observed in T-TNF$^{-/-}$ mice may derive from the TNF compensated by the myeloid derived TNF, neuron derived TNF, or from other circulating TNF (soluble TNF)

produced by other non-immune cells. In a pulmonary model, Allie *et al.,* (2013) showed that T-TNF$^{-/-}$ mice had a similar phenotype as TNF$^{f/f}$ mice during acute *M. tuberculosis,* and is in line with the observation we found in CNS-TB.

To determine whether TNF derived from myeloid and lymphoid T cell origins have a synergistic requirement for protection against neurotuberculosis, we characterised the host immune responses in MT-TNF$^{-/-}$ mice. In this model, microglia/macrophages, neutrophils, and T cells (CD4^{+}- and CD8^{+}) in MT-TNF$^{-/-}$ mice were unable to synthesise TNF. Myeloid cells as APCs, present antigens in association with MHC II molecules to stimulate lymphoid CD4^{+} T cells, and this process is essential to contain *M. tuberculosis* infection (Harding & Boom, 2010). We hypothesised that deleting TNF from CD4^{+}- and CD8^{+} T cell subsets in M-TNF$^{-/-}$ mice would lead to CNS host *M. tuberculosis* susceptibility. The finding that MT-TNF$^{-/-}$ mice were highly susceptible to CNS infection provide important and new evidence that synergistic activity of TNF derived from myeloid cells and T cells is required for optimum protection; its absence resulting in high susceptibility with exacerbated disease progression comparable to TNF$^{-/-}$ mice. The phenotype displayed by MT-TNF$^{-/-}$ mice were characterised by pronounced clinical manifestations with uncontrolled cerebral bacterial growth mainly extracellular, severe lymphocytic rich foci and meningeal lymphocytic infiltration. The overall lymphocytic rich foci architecture was similar in MT-TNF$^{-/-}$ mice to that seen in complete TNF$^{-/-}$ mice. A spectrum of extra-cerebral dissemination was noted in MT-TNF$^{-/-}$ mice that resembled to TNF$^{-/-}$ mice, which was higher compared to TNF$^{f/f}$ and M-TNF$^{-/-}$ mice. Although the infection route applied in this study does not reflect the course of natural infection in humans, clinical and pathological findings observed in this study are consistent with neurotuberculosis in humans (Rich & McCordock, 1933 and Donald *et al.,* 2005). MT-TNF$^{-/-}$ and TNF$^{-/-}$ mice strains exhibited a low expression of iNOS compared to TNF$^{f/f}$ mice which have been associated with susceptibility to *M. tuberculosis* infection (McMicking *et al* 1997). Interestingly, ablation of TNF from microglia/macrophages, neutrophils, and T cells (CD4^{+}- and CD8^{+} cells) lead to high peripheral leukocyte subsets migration and infiltration into the parenchyma. In MT-TNF$^{-/-}$ mice, the overall APCs antigenic responsiveness with respect to *M. tuberculosis* infection was lower, while their effector T cell percentage was higher resembling to TNF$^{-/-}$ mice, suggesting that TNF is critical in mediating the adaptive immune response.

The overall B cells humoral and antigenic response in MT-TNF$^{-/-}$ mice resembled that of TNF$^{-/-}$ mice; where the ablation of TNF from myeloid and lymphoid cells decreased the activation of B-cell population. Humoral and antigenic responses in MT-TNF$^{-/-}$ mice were impaired in B-cell subsets studied, indicating that both myeloid and T cell-derived TNF are

required during humoral immunity. Our data are consistent with the previously published study, where authors demonstrated that TNF and LTα deficient mice habour B cells defect responsiveness during *L. monocytogenes* challenges and immunisation (Pasparakis *et al.,* 1996 and Alexopoulou *et al.,* 1998).

Like in TNF$^{-/-}$ mice, cytokine expression levels in MT-TNF$^{-/-}$ mice were characterised by increased production of IL-6 and IFN-γ comparable to TNF$^{-/-}$ mice. The kinetic profile for IL-6 production appears to be delayed in MT-TNF$^{-/-}$ mice and TNF$^{-/-}$ mice, indicating that TNF is required to induce an early response. IFN-γ is mainly produced by T cells (Abbas *et al.,* 1996, Romagnani, 1996 and Wenner *et al.,* 1996) and natural killer cells in response to dying bacterial-infected macrophages (Kubota, 2009); the uncontrolled increase IFN-γ concentrations observed in the respective mouse strains correlated with the increase infiltrating of effector CD4^{+} and CD8^{+} T cells. A study by Flynn *et al.,* (1993) using IFN-γ$^{-/-}$ mice clearly demonstrated the important role of IFN-γ in the protective immune response to *M. tuberculosis* infection, while other studies using transgenic mice have shown that IFN-γ overexpression in the CNS increases disease progression (Corbin *et al.,* 1996 and Renno *et al.,* 1998). Our studies which show a correlation between high IFN-γ expression and advanced TB disease support these findings. We speculate that the over production of IL-6 and IFN-γ observed in MT-TNF$^{-/-}$ mice could be due to the ablation of TNF in T cells as myeloid derived TNF alone resulted in controlled production of IL-6 and IFN-γ. Beside increase production levels of IL-6 and IFN-γ, cytokines IL-2 was found to be lower in MT-TNF$^{-/-}$ and once again in TNF$^{-/-}$ mice compared to TNF$^{f/f}$ and M-TNF$^{-/-}$ mice. As previously addressed, here we speculate that the dysregulation of IL-2 observed in MT-TNF$^{-/-}$ mice may be a direct result of TNF ablation in T cells of this mouse strain; because M-TNF$^{-/-}$ mice have not demonstrated any dysregulation in IL-2 production. Data once again suggest that TNF is pivotal in regulating IL-2 expression. The increase in chemokine production observed in MT-TNF$^{-/-}$ mice were comparable to TNF$^{-/-}$ mice, and correlated with increased recruitment of infiltrating leukocytes into the brain of these strains.

The fact that TNF is produced by microglia/macrophages and neutrophils, as well as by T-cells, raises the possibility of partial compensation to control infection, and may lead to some redundant functions which may be provided by either source of TNF. The similarity in phenotype between TNF$^{f/f}$ and M-TNF$^{-/-}$ mice, and with high disparate phenotypes between TNF$^{f/f}$ and MT-TNF$^{-/-}$ mice, and also with M-TNF$^{-/-}$ and MT-TNF$^{-/-}$ mice during CNS *M. tuberculosis* infection suggests that the absence of T cell-derived TNF exacerbate the susceptibility phenotype. From this outcome we conclude that T cell-derived TNF is required for downregulation of inflammation. Synergising TNF deficiency in myeloid and lymphoid T cells was characterised by

increase disease severity with overt clinical manifestations, severe pathology, uncontrolled mycobacterial growth in the brain, impaired antigenic response and mortality; clearly confirming the essential function of TNF from these distinct and important cellular sources of TNF.

Although, there are differences in organ-specific make-up between the brain and lungs, the overall results in neurotuberculosis are consistent with those seen in pulmonary TB (Allie *et al.,* 2013), indicating that the underlying immune protection mechanisms in both pulmonary and CNS-TB model are similar. Since the protective immunity to tuberculosis depends on $CD4^+$ T cells in mice and humans (Perlman *et al.,* 1997 and Mogues *et al.,* 2001), we speculate here that the ablation of TNF in myeloid and lymphoid lineage may impede the adaptive immune response, which is required for effective control of *M. tuberculosis* infection. TNF plays a major role in the initial and long-term control of tuberculosis (Lin *et al.,* 2007). TNF is important in myeloid cells activation as well as cell recruitment to the site of infection. It is the primary important signal in granuloma formation, as neutralisation leads to lack of control of initial or chronic infection, and loss of granuloma structure. The overall protective immunity observed in M-$TNF^{-/-}$ mice is suggestive that TNF from myeloid cells is not required to control acute infection although TNF plays a major role in the initial and long-term control of tuberculosis (Lin *et al.,* 2007).

Our data showed that the expression level of TNF in this mouse strain was comparable to that of $TNF^{f/f}$ mice, suggesting that TNF from non-myeloid cells in M-$TNF^{-/-}$ mice may be responsible in driving the innate and adaptive immune response. In the CNS, TNF is produced by immune and non-immune cells, however the mechanisms by which TNF acts to control neurotuberculosis, as well as recruitment of cells to the site of infection leading to latency are not clearly defined. Reactivation of latent infection can be triggered by several factors which can lead to the development of active disease (Ahmad, 2011). From a clinical point of view, HIV infection is the most single risk factor for progression to active disease, since HIV infection causes depletion of $CD4^+$ T cells and functional abnormalities of lymphoid T cells, and which play an important role in providing protection against active TB disease (Wells *et al.,* 2007 and WHO, 2009). The hallmark of *M. tuberculosis* infection in humans is the inability of an effective immune response to completely repel the pathogen (Ahmad, 2011). Host responses which are important in controlling the latent infection may include macrophage activation, maintenance of granuloma structure, T cells, IFN-γ and TNF (Flynn & Chan, 2001). Studies in mice have shown that without TNF, effective granuloma formation is diminished and mycobacterial numbers rapidly increase, resulting in susceptibility (Bean *et al.,* 1995 and Bean *et al.,* 1999). Understanding latent and reactivation tuberculosis, at the level of both the host and the bacillus,

is crucial to worldwide control of this disease. In approximately, 5 to 10% of latently infected persons reactivation will occur and cause active tuberculosis (Flynn & Ernst, 2000). Cytokine TNF has been shown to play a major role in the initial and long-term control of tuberculosis (Lin *et al.,* 2007). Tuberculous granuloma is typically composed of macrophages, multinucleated giant cells, lymphocytes (both $CD4^+$- and $CD8^+$ T cells, and B cells), neutrophils, and sometimes fibroblasts (Lin *et al.,* 2007). However, the granuloma formation and also its maintenance require TNF. In this study we convincingly demonstrated that MT-$TNF^{-/-}$ and $TNF^{-/-}$ mice are highly susceptible to cerebral *M. tuberculosis* infection. Our data are in agreement with the previously reported data where mice with complete deficient in TNF are completely unable to control pulmonary *M. tuberculosis* infection (Flynn *et al.*, 1995 and Bean *et al.*, 1999). Studies in both human and mice have also demonstrated the critical role that TNF produced by macrophages, dendritic cells, and T cells play in protective role against pulmonary *M. tuberculosis* infection (Bean *et al.,* 1999 and Keane, 2005). A study by Algood *et al.,* (2003) has reported that TNF produced by the infected macrophages induces the expression of chemokines, such as IL-8, MCP-1, and RANTES which provide signals for migration of immune cells to the sites of *M. tuberculosis* infection. It has also been demonstrated that both macrophage and T cell-derived TNF are required for sufficient and long-term protection against *M. tuberculosis* infection (Saunders *et al.,* 2005).

It has been demonstrated that high levels of TNF are associated with TB meningitis. More recently data from human and zebrafish obtained with a persistent CNS *M. tuberculosis* infection indicate that a relative deficiency of TNF results in destructive immunopathology (Tobin *et al.,* 2012). Our study has shown that TNF is absolutely required for protective host immune responses during neurotuberculosis and is in agreement with the previous mentioned study. Further, we established that TNF derived from both myeloid and lymphoid T cellular origins are required to generate complete protection during CNS *M. tuberculosis* infection. Based on the susceptibility observed in MT-$TNF^{-/-}$ mice and the resistance of M-$TNF^{-/-}$ mice we propose that T cells in particular forms a critical source of TNF to generate protective immunity. $CD4^+$ T cells perform several functions that are important to control infection in the granuloma. These include production of cytokines (such as TNF), apoptosis of infected macrophages through Fas/Fas ligand interaction, induction of other immune cells (macrophages or dendritic cells) to produce immunoregulatory cytokines, such as IL-10, IL-12, and IL-15, and activation of macrophages through direct contact via CD40 ligand (Cella *et al.,* 1996; Oddo *et al.,* 1998; Chan & Flynn, 2004 and Cooper, 2009). In addition, $CD4^+$ T cells can control the intracellular growth of *M. tuberculosis* by a nitric oxide-dependent mechanism that is independent of IFN-γ production

(Cowley & Elkins, 2003 and Cooper, 2009); as previously shown, the mycobacteriocidal effect of TNF is associated with iNOS-mediated production of NO (Bekker *et al.,* 2001). TNF is involved in both immune and immunomodulatory responses and acts in synergy with T cell-derived IFN-γ to enhance the macrophages antimycobactericidal activity of nitric oxide and other RNI by iNOS (Scanga *et al.,* 2001 and Chan *et al.,* 2004).

We have recently shown that neurons are the host cells for *M. tuberculosis,* and that neuron cells upon infection by *M. tuberculosis* can express cytokines including TNF (Randall & Hsu *et al.,* 2014). Our evidence presented in this study shows that neuronal derived TNF has a very limited protective response during cerebral *M. tuberculosis* infection, with a phenotype resembling to wild type mice. However, the phenotype observed in NsTNF$^{-/-}$ mice which resembles wild type control mice could be due to the compensatory mechanisms from other TNF cellular sources. In contrast, mice with complete ablation of TNF were highly susceptible to cerebral *M. tuberculosis* infection. M-TNF$^{-/-}$ mice exhibited a protective response during cerebral *M. tuberculosis* infection. We speculated that during cerebral *M. tuberculosis* infection, NsTNF$^{-/-}$ and M-TNF$^{-/-}$ mice may acquire protective responses by the compensatory mechanism of other cellular sources including T cells derived TNF, as it has been previously shown that T cells play an important role in the defence against *M. tuberculosis* (Caruso *et al.,* 1999). Deletion of TNF in T cells of M-TNF$^{-/-}$ mice lead to high susceptibility during cerebral *M. tuberculosis* infection with a phenotype comparable to complete TNF deficient mice, confirming that T cells derived TNF is crucial for host immunity. Moreover, T cells derived TNF has recently been shown to be non-redundant in pulmonary TB (Allie *et al.,* 2013).

Taken together, our data demonstrate that mice with ablation in a single cell-type or lineage derived TNF, produce an optimal baseline response level of TNF similar to wild type, and confer protection to immune response against neurotuberculosis. The protection observed in these mice may be related to the compensation of TNF from other cellular sources. However, dual ablation of TNF in myeloid and lymphoid T cells, produces low baseline response levels of TNF comparable to complete TNF$^{-/-}$ mice, and is detrimental, leading to host death. Myeloid and T cells participate in TB adaptive immune response (Wolf *et al.,* 2008). During this process, TNF is required in the recruitment of cells that participate in adaptive immune response, and also, TNF is capable of enhancing the activation of these cells (Brighenti & Lerm, 2012 and Allie *et al.,* 2013). However, we have here demonstrated that neuronal and microglia/macrophages and neutrophil derived TNF is not required during acute *M. tuberculosis* infection. We also demonstrated that ablation of TNF in neurons as well as in microglia/macrophages and neutrophil did not compromise myeloid and lymphoid (T or B) cells infiltration and activation, the

control of bacterial growth, and the functional integrity of the lymphocytic rich foci response. In contrast, deletion of $CD4^+$- and $CD8^+$ T cell-derived TNF in M-$TNF^{-/-}$ mice resulted in exacerbated disease progression with uncontrolled bacterial growth and severe cerebral pathology and mortality. Therefore, the deletion of TNF in both lineages is crucial as it renders the adaptive immunity ineffective, leading to increase susceptibility.

CHAPTER V

CONCLUSION

Several studies have investigated neurotuberculosis using animal models that employed different *mycobacterium species* (Peterson *et al.,* 1995; Mazzolla *et al.,* 2002; Tsenova *et al.,* 2005; Be *et al.,* 2008 and Lee *et al.,* 2009). The significance of murine TB models has been demonstrated by its similarity with human models, characterised by both its genetics and the severity of its effects on the CNS (Apt, 2011). We were able to develop a reproducible *in vivo* model to study the inflammatory response of cell type-specific TNF in neurotuberculosis. However, we acknowledge the limitations of the model, specifically the infection route which does not approximate the natural way neurotuberculosis is acquired in humans. Nonetheless, the model reflects many of the clinical, pathological and immune responses observed in humans.

The neurotuberculosis experimental murine model used herein highlights the important cellular sources of TNF, and its modulation of host immune response. This study, using the cell type-specific TNF and complete deficient TNF mice has produced a novel and significant outcomes, with respect to the cellular requirement, organ pathology, cytokine and chemokine induction during host immunity against CNS *M. tuberculosis* infection. Overall, the role of neurons derived TNF appeared to be redundant for protective host immunity against neurotuberculosis. The widely acclaimed view that myeloid cells act as a primary source for TNF induced protection are contradicted and had a limited role in the control of CNS *M. tuberculosis* infection. The comparable wild type phenotype observed in NsTNF$^{-/-}$ and M-TNF$^{-/-}$ mice could be due to the compensation from T cell-derived TNF or from other TNF cellular sources. We found that the ablation of TNF in T cells of M-TNF$^{-/-}$ mice and mice with complete TNF ablation showed clinical manifestations of disease and pathology resembling that in humans. Data indicate that TNF mediated protective immunity against CNS *M. tuberculosis* infection requires T cell-derived TNF. However, future studies involving synergistic ablation of other cell-type combinations such as deletion of TNF in neurons and T cells or in neurons and myeloid cells are needed to substantiate our claim that T-cells derived TNF, is a key cellular source in driving neurotuberculosis susceptibility. Characterising cellular TNF sources during CNS *M. tuberculosis* infection has contributed substantially to understanding host-mycobacterial interaction, and may be useful in the development of clinical therapeutic applications against neurotuberculosis.

REFERENCES

Abbas, A.K., Murphy, K.M. and Sher, A. **1996**. Functional diversity of helper T lymphocytes. *Nature,* **383:** 787-793.

Abdallah, A.M., Gey van Pittius, N.C., DiGiuseppe Champion, P. A., Cox, J., Luirink, J., Vandenbroucke-Grauls, C. M.J.E., Appelmelk, B.J. and Bitter, W. **2007.** Type VII secretion - mycobacteria show the way. *Nature Reviews Microbiology,* **5:** 883-891.

Abebe, F. and Bjune, G. **2009.** The protective role of antibody responses during Mycobacterium tuberculosis infection. *Clinical and Experimental Immunology,* **157:** 235-243.

Ahmad, S. **2011.** Pathogenesis, Immunology, and Diagnosis of Latent *Mycobacterium tuberculosis* Infection. *Clinical and Developmental Immunology,* 1-17.

Akassoglou, K., Bauer, J., Kassiotis, G., Pasparakis, M., Lassmann, H., Kollias, G. and Probert, L. **1998.** Oligodendrocyte apoptosis and primary demyelination induced by local TNF/p55TNF receptor signaling in the central nervous system of transgenic mice: models for multiple sclerosis with primary oligodendrogliopathy. *The American Journal of Pathology,* **153:**801-813.

Akiyama, H. and McGeer, P.L. **1990.** Brain microglia constitutively express β-2 integrins. *Journal of Neuroimmunology,* **30**:81-93.

Akiyama, H., Barger, S., Barnum, S., Bradt, B., Bauer, J., Cole, G.M., Cooper, N.R., Eikelenboom, P., Emmerling, M., Fiebich, B.L., Finch, C.E., Frautschy, S., Griffin, W.S., Hampel, H., Hull, M., Landreth, G., Lue, L., Mrak, R., Mackenzie, I.R., McGeer, P.L., O'Banion, M.K., Pachter, J., Pasinetti, G., Plata-Salaman, C., Rogers, J., Rydel, R., Shen, Y., Streit, W., Strohmeyer, R., Tooyoma, I., Van Muiswinkel, F.L., Veerhuis, R., Walker, D., Webster, S., Wegrzyniak, B., Wenk, G. and Wyss-Coray, T. **2000.** Inflammation and Alzheimer's disease. *Neurobiology Aging,* **21(3):** 383-421.

Alexopoulou, L., Pasparakis, M. and Kollias, G. 1998. Complementation of Lymphotoxin-α Knockout Mice with Tumor Necrosis Factor-expressing Transgenes Rectifies Defective Splenic Structure and Function. *Journal of Experimental Medicine*, **188(4):** 745-754.

Algood, H.M.S., Chan, J. and Flynn, J.L. **2003.** Chemokines and tuberculosis. *Cytokine and Growth Factor Reviews,* **14(6):** 467-477.

Algood, H.M., Lin, P.L. and Flynn, J.L. **2005.** Tumor necrosis factor and chemokine interactions in the formation and maintenance of granulomas in tuberculosis. *Clinical Infection Diseases*, **41(Suppl. 3):** S189-S193.

Algood, H.M., Lin, P.L., Yankura, D., Jones, A., Chan, J. and Flynn, J.L. **2004.** TNF influences chemokine expression of macrophages in vitro and that of $CD11b^{+}$ cells in vivo during *Mycobacterium tuberculosis* infection. *The Journal of Immunology,* **172(11):** 6846-6857.

Allie, N., Alexopoulou, L., Quesniaux, V.J.F., Fick, L., Kranidioti, K., Kollias, G., Ryffel, B. and Jacobs, M. **2008.** Protective role of membrane tumour necrosis factor in the host's resistance to mycobacterial infection. *The Journal of Immunology,* **125(4):** 522-534.

Allie, N., Grivennikov, S.I., Keeton, R., Hsu, N-J., Bourigault, M-L., Court, N., Fremond, C., Yeremeev, V., Shebzukhov, Y., Ryffel, B., Nedospasov, S.A., Quesniaux, V.F.J. and Jacobs, M. **2013.** Prominent role for T cell-derived Tumour Necrosis Factor for sustained control of *Mycobacterium tuberculosis* infection. *Scientific Reports,* **3(1809):** 1-14.

Allie, N., Keeton, R., Court, N., Abel, B., Fick, L., Vasseur, V., Vacher, R., Olleros, M.L., Drutskaya, M.S., Guler, R., Nedospasov, S.A., Garcia, I., Ryffel, B., Quesniaux, V.F.J. and Jacobs, M. **2010.** Limited Role for Lymphotoxin α in the Host Immune Response to *Mycobacterium tuberculosis*. *The Journal of Immunology,* **185(7):** 4292-301.

Aloisi, F., Penna, G., Cerase, J., Menendez Iglesias, B. and Adorini, L. **1997.** IL-12 production by central nervous system microglia is inhibited by astrocytes. *The Journal of Immunology,* **159:**1604-1612.

Alter, A., Duddy, M.., Hebert, S., Biernacki, K., Prat, A., Antel, J.P., Yong, V.W., Nuttall, R.K., Pennington, C.J., Edwards, D.R. and Bar-Or, A. **2003.** Determinants of Human B Cell Migration Across Brain Endothelial Cells. *The Journal of Immunology,* **170:** 4497-4505.

Amanna, I.J., Slifka, M.K. and Crotty, S. **2006.** Immunity and immunological memory following smallpox vaccination. *Immunologcal Reviews,* **211:** 320-337.

Andersona, N.E., Somaratnea, J., Masona, D.F., Hollandb, D. and Thomas, M.G. **2010.** Neurological and systemic complications of tuberculous meningitis and its treatment at Auckland City Hospital. New Zealand. *Journal of Clinical Neuroscience,* **17:** 1114-1118.

Andersson, J., Samarina, A., Fink, J., Rahman, S. and Grundström, S. **2007.** Impaired expression of perforin and granulysin in CD8+ T cells at the site of infection in human chronic pulmonary tuberculosis. *Infection and Immunity,* **75(11):** 5210-5222.

Apt, A.S. **2011.** Are mouse models of human mycobacterial diseases relevant? Genetics says: 'yes!'. *Immunology,* **134(2):** 109-115.

Arko-Mensaha, J., Rahmana, M.J., Déganoa, I.R., Chuquimiaa, O.D., Fotiob, A.L., Garciab, I. and Fernándeza, C. **2009.** Resistance to mycobacterial infection: A pattern of early immune responses leads to a better control of pulmonary infection in C57BL/6 compared with BALB/c mice. *Vaccine,* **27:** 7418-7427.

Aversa, G., Punnonen, J., and De Vries, J.E. **1993.** The 26-kD trans- membrane form of tumor necrosis factor (x on activated $CD4^+$ T cell clones provides a costimulatory signal for human B cell activation. *Journal of Experimental Medicine,* **177:** 1575-1585.

Babcock, A. and Owensm, T. **2003.** Chemokines in experimental autoimmune encephalomyelitis and multiple sclerosis. *Advances in Experimental Medicine and Biology,* **520:** 120-132.

Babcock, A.A., Kuziel, W.A., Rivest, S. and Owens, T. **2003.** Chemokine Expression by Glial Cells Directs Leukocytes to Sites of Axonal Injury in the CNS. *The Journal of Neuroscience,* **23(21):** 7922-7930.

Bailey, S.L. Carpentier, P.A., McMahon, E.J., Begolka, W.S., Miller, S.D. **2006.** Innate and adaptive immune Innate and adaptive immune responses of the central nervous system. *Critical Review Immunology,* **26(2):** 149-88.

Baker, M., Das, D., Venugopal, K. and Howden-Chapman, P. **2008.** Tuberculosis associated with household crowding in a developed country. *Journal of Epidemiology and Community Health,* **62(8):** 715-721.

Balabanova, Y., Drobniewski, F., Nikolayevskyy, V., Kruuner, A., Malomanova, N., Simak, T., Ilyina, N., Zakharova, S., Lebedeva, N., Alexander, H. L., O'Brien, R., Sohn, H., Shakhmistova, A. and Fedorin, I. **2009.** An integrated approach to rapid diagnosis of tuberculosis and multidrug resistance using liquid culture and molecular methods in Russia. *PLoS ONE,* **4(9):** 1-9.

Baldwin, H.M., Ito-Ihara, T., Isaacs, J.D., Hilkens, C.M.U. **2010.** Tumour necrosis factor alpha blockade impairs dendritic cell survival and function in rheumatoid arthritis. *Annals of the Rheumatic Diseases,* **69:** 1200-1207.

Bamford, C. **2008.** Update on the laboratory diagnosis of tuberculosis. *Continuing Medical Education Journal,* **26(11):** 524-527.

Banchereau, J. and Steinman, R. M. **1998.** Dendritic cells and the control of immunity. *Nature,* **392:** 245-252.

Banchereau, J., Briere, F., Caux, C., Davoust, J., Lebecque, S., Liu, Y. J., Pulendran, B. and Palucka, K. **2000.** Immunobiology of dendritic cells. *Annual Review of Immunology,* 1**8:** 767-811.

Bano, S., Chaudhary, V. and Yadav, S. **2012.** Central Nervous System Tuberculosis, Neuroimaging - Clinical Applications, Prof. Peter Bright (Ed.), ISBN: 978-953-51-0200-7, InTech, Available from: http://www.intechopen.com/books/neuroimaging-clinical-applications/central-nervous-systemtuberculosis.

Barclay, L. **2009.** CDC Updates Guidelines for Nucleic Acid Amplification Tests to Diagnose Tuberculosis. *Morbidity and Mortality Weekly Report,* **58:** 7-10.

Barnes, P.J. and Belvisi, M.G. **1993.** Nitric oxide and lung disease. *Thorax,* **48:** 1034-1043.

Baud, V. and Karin, M. **2001.** Signal transduction by tumor necrosis factor and its relatives. *Trends in Cell Biology,* **11:** 372-377.

Be, N.A., Lamichhane, G., Grosset, J., Tyagi, S., Cheng, Q.J., Kim, K.S., Bishai, W.R. and Jain, S.K. **2008.** Murine model to study the invasion and survival of Mycobacterium tuberculosis in the central nervous system. *Journal of Infectious Disease,* **198(10):** 1520-1528.

Bean, A.G., Roach, D.R., Briscoe, H., France, M.P., Korner, H., Sedgwick, J.D. and Britton, W.J. **1999.** Structural deficiencies in granuloma formation in TNF gene-targeted mice underlie the heightened susceptibility to aerosol Mycobacterium tuberculosis infection, which is not compensated for by lymphotoxin. *The Journal of Immunology,* **162(6):** 3504-3511.

Becher, B., Dodelet, V., Fedorowicz, V. and Antel, J. **1996.** Soluble tumor necrosis factor receptor inhibits interleukin 12 production by stimulated human adult microglial cells in vitro. *Journal of Clinical Investigation,* **98:**1539-1543.

Beckman, J.S., Beckman, T.W., Chen, J., Marshall, P.A., Freeman, B.A. **1990.** Apparent hydroxyl radical production by peroxynitrite: implications for endothelial injury from nitric oxide and superoxide. *Proceedings of the National Academy of Sciences,* **87:** 1620-1624.

Bekker, L-G., Freeman, S., Murray, P.J., Ryffel, B. and Kaplan, G. **2001.** TNF-a Controls Intracellular Mycobacterial Growth by Both Inducible Nitric Oxide Synthase-Dependent and Inducible Nitric Oxide Synthase-Independent Pathways. *The Journal of Immunology,* **166:** 6728-6734.

Beltinger, C.P., White, P.S., Maris, J.M., Sulman, E.P., Jensen, S.J., LePaslier D., Stallard, B.J., Goeddel, D.V., de Sauvage, F.J., Brodeur, G.M. **1996.** Physical mapping and genomic structure of the human TNFR2 gene. *Genomics,* **35(1):** 94-100.

Ben-Selma, W., Harizi, H. and Boukadida, J. **2011.** MCP-1-2518 A/G functional polymorphism is associated with increased susceptibility to active pulmonary tuberculosis in Tunisian patients. *Molecular Biology Reports.* **38:** 5413-5419.

Ben-Selma, W., Harizi, H., Bougmiza, I., Ben Kahla, I., Letaief, M. and Boukadida, J. **2011.** Polymorphisms in the RANTES gene increase susceptibility to active tuberculosis in Tunisia. *DNA Cell Biology,* **30:** 789-800.

Berger, C., Braegger, C.P., Albisetti, M., Landau, K. and Nadal, D. **1996.** Cerebral tuberculosis presenting as complex febrile convulsions. *Neuropediatrics,* **27(3):** 161-63.

Bergqvist, I., Eriksson, B., Eriksson, M. and Holmberg, D. **1998.** Transgenic Cre recombinase expression in germ cells and early embryogenesis directs homogeneous and ubiquitous deletion of loxP-flanked gene segments. *FEBS letters,* **438:** 76-80.

Berman, J.W., Guida, M.P., Warren, J., Amat, J. and Brosnan, C.F. **1996.** Localization of monocyte chemoattractant peptide-1 expression in the central nervous system in experimental autoimmune encephalomyelitis and trauma in the rat. *The Journal of Immunology,* **156:** 3017-3023.

Betts, J.C., Dodson, P., Quan, S., Lewis, A.P., Thomas, P.J., Duncan, K. and McAdam, R.A. **2000.** Comparison of the proteome of Mycobacterium tuberculosis strain H37Rv with clinical isolate CDC 1551. *Microbiology,* **146:** 3205-3216.

Beutler, B., Milsark, I.W. and Cerami, A.C. 1985. Passive immunization against cachectin/tumor necrosis factor protects mice from lethal effect of endotoxin. Science, **229:** 869-871.

Bezzi, P., Domercq, M., Brambilla, L., Galli, R., Schols, D., De Clercq, E., Vescovi, A., Bagetta, G., Kollias, G. and Meldolesi J, Volterra A. **2001.** CXCR4-activated astrocyte glutamate release via TNFalpha: amplification by microglia triggers neurotoxicity. *Nature Neuroscience,* **4:** 702-710.

Birland, T.P. Sypek, P.P. and Wyler, D.J. **1992.** Soluble TNF and membrane TNF expressed on $CD4^+$ T lymphocytes differ in their ability to activate macrophage antileishmanial defense. *Journal of Leukocyte Biology,* **51:** 296-299.

Bissonnette, E.Y., Chin, B. and Befus, A.D. **1995.** Interferons differentially regulate histamine and TNF-alpha in rat intestinal mucosal mast cells. *Immunology,* **86:** 12-17.

Björkbacka, H., Kunjathoor, V.V., Moore, K.J., Koehn, S., Ordija, C.M., Lee, M.A., Means, T. Halmen, K., Luster, A.D., Golenbock, D.T. and Freeman, M.W. **2004.** Reduced atherosclerosis in MyD88-null mice links elevated serum cholesterol levels to activation of innate immunity signaling pathways. *Nature Medicine,* **10:** 416-421.

Blackwell, K., Zhang, L., Thomas, G.S., Sun, S., Nakano, H. and Habelhah, H. **2009.** TRAF2 Phosphorylation Modulates Tumor Necrosis Factor Alpha-Induced Gene Expression and Cell Resistance to Apoptosis. *Journal of Molecular Cell Biology,* **29(2):** 303-314.

Boccia, D., Hargreaves, J., Ayles, H., Fielding, K., Simwinga, M. and Godfrey-Faussett, P. **2009.** Tuberculosis infection in Zambia: the association with relative wealth. *American Journal of Tropical Medicine and Hygiene,* **80(6):** 1004-1011.

Boissel, J.P., Schwarz, P.M. and Forstermann, U. **1998.** Neuronal-type NO synthase: transcript diversity and expressional regulation. *Nitric Oxide,* **2(5):** 337-49.

Bosio,C.M., Gardner, D. and Elkins, K.L. **2000.** Infection of B Cell-Deficient Mice with CDC 1551, a Clinical Isolate of *Mycobacterium tuberculosis*: Delay in Dissemination and Development of Lung Pathology1. *The Journal of Immunolology,* **164:** 6417-6425.

Boswell, H.S., Sharrow, S.O. and Singer, A. **1980.** Role of Accessory cells in B Cell activation I. Macrophage Presentation of TNP-Ficoll: Evidence for Macrophage - B Cell Interaction. 1980. *Journal of Experimental Medicine*, **124:** 989-996.

Botha, T. and Ryffel. B. **2003.** Reactivation of latent Tuberculosis infection in TNF-Deficient Mice. *The Journal of Immunology,* **171(6):** 3110-3118.

Brambilla, R., Ashbaugh, J.A., Magliozzi, R., Dellarole, A., Karmally, S., David E. Szymkowski, D.E. and Bethea, J.R. **2011.** Inhibition of soluble tumour necrosis factor is therapeutic in experimental autoimmune encephalomyelitis and promotes axon preservation and remyelination. *Brain,* **134:** 2736-2754.

Brighenti, S. and Andersson, J. **2010.** Induction and regulation of $CD8^+$ cytolytic T cells in human tuberculosis and HIV infection. *Biochemical and Biophysical Research Communications,* **396:** 50-57.

Brighenti, S. and Lerm, M. **2012.** *How Mycobacterium tuberculosis Manipulates Innate and Adaptive Immunity: New Views of an Old Topic, in Understanding Tuberculosis: Analyzing the Origin of Mycobacterium Tuberculosis Pathogenicity*. ed. Pere-Joan Cardona, 207-234.

Britton, W.J., Meadows, N., Rathjen, D.A., Roach, D.R. and Briscoe, H.A. **1998.** Tumor necrosis factor mimetic peptide activates a murine macrophage cell line to inhibit mycobacterial growth in a nitric oxide-dependent fashion. *Infection and immunity,* **66**: 2122-2127.

Bronte, V. and Gabrilovich, D. **2010.** Myeloid-derived suppressor cells. *Nature Reviews Immunology,* 1-2.

Brooks-Pollock,E., Conlan, A.J.K., Mitchell, A.P., Blackwell, R., McKinley, T.J. and Wood, J.L.N. **2013.** Age-dependent patterns of bovine tuberculosis in cattle. *Veterinary Research,* **44:** 97.

Buijtels, P.C., van de Sande, W.W., Parkinson, S., Petit, P.L., van der Sande, M.A., van Soolingen, D., Verbrugh, H.A. and van Belkum, A. **2008.** Polymorphism in CC-chemokine ligand 2 associated with tuberculosis in Zambia. *International Journal of Tuberculosis, Lung Disease,* **12:** 1485-1488.

Buonsenso, D. Serranti, D. and Valentini, P. 2010. Management of central nervous system tuberculosis in children: light and shade. *European Review for Medical and Pharmacological Sciences,* **14(10):** 845-853.

Cambrea, S.C., Rugină, N.C., Urjan, C., Vasiliu, E. and Rugină, S. **2009.** Tuberculous meningoencephalitis in immunocompentent. Child. Th erapeutics, *Pharmacology and Clinical Toxicology,* **XIII(2):** 215-221.

Campanella, M., Sciorati, C., Tarozzo, G. and Beltramo, M. **2002.** Flow Cytometric Analysis of Inflammatory Cells in Ischemic Rat Brain. *Stroke,* **33:** 586-592.

Cardona, A.E., Gonzalez, P.A. and Teale, J.M. **2003.** CC chemokines mediate leukocyte trafficking into the central nervous system during murine neurocysticercosis: role of gamma delta T cells in amplification of the host immune response. *Infection and immunity,* **71(5):** 2634-42.

Carpentier, P.A. and Palmer, T.D. **2009.** Immune influence on adult neural stem cell regulation and function. *Neuron,* **64:** 79-92.

Carragher, D.M., Rangel-Moreno, J. and Randall, T.D. **2008.** Ectopic lymphoid tissues and local immunity. *Seminars in Immunology,* **20(1):** 26-42.

Carson, M.J., Doose, J.M., Melchior, B., Schmid, C.D. and Ploix, C.C. **2006.** CNS immune privilege: hiding in plain sight. *Immunology Review,* **213(1):** 48-65.

Carson, M.J., Reilly, C.R. Sutcliffe, J.G. and Lo, D. **1998.** Mature microglia resemble immature antigen-presenting cells. *Glia,* **22:** 72-85.

Caruso, A.M., Serbina, N., Klein, E., Triebold, K., Bloom, B.R. and Flynn, J.L. **1999.** Mice Deficient in CD4 T Cells Have Only Transiently Diminished Levels of IFN-g, Yet Succumb to Tuberculosis. *The Journal of Immunology,* **162:** 5407–5416.

Castillo-Méndez, S.I., Zago, C.A., Sardinha, L.R., Freitas do Rosário, A.P., Alvarez, J.M. and D'Império Lima, M.R. **2007.** Characterization of the spleen B-cell compartment at the early and late blood-stage Plasmodium chabaudi malaria. *Scandinavian Journal of Immunology,* **66(2-3):** 309-19.

Caws, M., Thwaites, G., Dunstan, S.,Thomas R. Hawn, T.R. *et al*. **2008.** The influence of Host and Bacterial Genotype on the Development of Disseminated Disease with Mycobacterium tuberculosis. *Plos Pathogens,* **4(3):** 1-9.

Cegielski, J.P. and McMurray, D.N. **2004.** The relationship between malnutrition and tuberculosis: evidence from studies in humans and experimental animals. *The International Jounal of Tuberculosis and Lung Disease,* **8**: 286-298.

Cella, M., Scheidegger, D., Palmer-Lehmann, K., Lane, P., Lanzavecchia, A. and Alber, G. **1996.** Ligation of CD40 on dendritic cells triggers production of high levels of interleukin-12 and enhances T cell stimulatory capacity: T-T help via APC activation. *Journal of Experimental Medicine*, **184(2):** 747-752.

Centers for Disease Control and Prevention. 2010. http://www.cdc. gov/tb/ publications /reports articles/ 2010.htm.

Centers for Disease Control and Prevention. Morbidity tables reporting areas. **2008.** Available from: http://www.cdc.gov/ tb/statistics/reports/2008/pdf/6_MorbRA08.pdf [updated 18 Sept 2009].

Ceyhan, M., Kanra, G., Ecevit, Z., Seçmeer, G., Erdem, G., Akan, O. and Müftüoğlu, O. **1997.** Tumor necrosis factor-alpha and interleukin-1 beta levels in children with bacterial, tuberculous and aseptic meningitis. *The Turkish Journal of Pediatrics,* **39(2):** 177-184.

Chambers, M.A., Williams, A., Gavier-widén, D., Whelan, A., Hall, G., Marsh, P.D., Bloom, B. R., Jacobs, W.R. and Hewinsion, G. **2000.** Identification of a Mycobacterium bovis BCG Auxotrophic Mutant That Protects Guinea Pigs against M. bovis andHematogenous Spread of Mycobacterium tuberculosis without Sensitization to Tuberculin. *Infection and immunity,* **68(12):** 7094-7099.

Chan, E.D., Morris, K.R., Belisle, J.T., Hill, P., Remigio, L.K., Brennan, P.J. and Riches, D.W.H. **2001.** Induction of Inducible Nitric Oxide Synthase-NOz By Lipoarabinomannan of Mycobacterium tuberculosis Is Mediated MEK1-ERK, MKK7-JNK, and NF-kB Signaling Pathways. *Infection and Immunity,* **69(4):** 2001-2010.

Chan, E.D., Winston, B.W., Uh, S.T., Wynes, M.W., Rose, D.M. and Riches, D.W. **1999.** Evaluation of the role of mitogen-activated protein kinases in the expression of inducible nitric oxide synthase by IFN-ϒ and TNF-α in mouse macrophages. *The Journal of Immunology,* **162(1):** 415-422.

Chan, J. and Flynn, J. **2004.** The immunological aspects of latency in tuberculosis. *Clinical Immunology*, **110(1):** 2-12.

Chan, J., Tanaka, K., Carroll, D., Flynn, J., Bloom, B.R. **1995.** Effects of nitric oxide synthase inhibitors on murine infection with Mycobacterium tuberculosis. *Infection & Immunity,* **63:** 736-740.

Chatzidakis, I. and Mamalaki, C.T. **2010.** Cells as sources and targets of TNF: Implications for immunity and autoimmunity. *Current Directions in Autoimmunity,* **11:** 105-118.

Che, X., Ye, W., Panga, L., Wu, D.C. and Yang, G.Y. **2001.** Monocyte chemoattractant protein-1 expressed in neurons and astrocytes during focal ischemia in mice. *Brain Research,* **902:** 171-177.

Cheng, M.H. **2009.** Ministerial meeting agrees plan for tuberculosis control. *Lancet,* **373:** 1328.

Cho, I-H., Hong, J., Suh, E.C., Kim, J.H., Lee, H., Lee, J.E., Lee, S., Kim, C-H., Kim, D.W., Jo, E-K., Lee, K.E., Karin, M. and Lee, S.J. **2008.** Role of microglial IKKb in kainic acid-induced hippocampal neuronal cell death. *Brain,* **131:** 3019-3033.

Chu, S.F., Tam, C.M., Wong, H.S., Kam, K.M., Lau, Y.L. and Chiang, A.K. **2007.** Association between RANTES functional polymorphisms and tuberculosis in Hong Kong Chinese. *Genes Immunology,* **8:** 475-479.

Coico, R. and Sunshine, G. **2009.** Immunology: a short course. 6th ed. Wiley Blackwell, New Jersy. 1-392.

Cole, S.T., Brosch, R., Parkhill, J., Garnier, T., Churcher, C., Harris, D., Gordon, S.V., Eiglmeier, K., Gas, S., Barry, C.E 3rd., Tekaia, F., Badcock, K., Basham, D., Brown, D., Chillingworth, T., Connor, R., Davies, R., Devlin, K., Feltwell, T., Gentles, S., Hamlin, N., Holroyd, S., Hornsby, T., Jagels, K., Krogh, A., McLean, J., Moule, S., Murphy, L., Oliver, K., Osborne, J., Quail, M.A., Rajandream, M.A., Rogers, J., Rutter, S., Seeger, K., Skelton, J., Squares, R., Squares, S., Sulston, J.E., Taylor, K., Whitehead, S. and Barrell, B.G. **1998.** Deciphering the biology of Mycobacterium tuberculosis from the complete genome sequence. *Nature,* **393:** 537-544.

Collins, A.V., Brodie, D.W. Gilbert, R.J.C., Laboni, A., Manso-Sancho, R., Walse, B. and Stuart, D.I. **2002.** The interaction properties of costimulatory molecules revisited. *Immunity,* **17:** 201-210.

Collins, M., Ling, V. and Carreno, B.M. **2005.** The B7 family of immune-regulatory ligands. *Genome biology,* **6:** 223.1-223.7.

Comstock, G.W. **1982.** Epidemiology of tuberculosis. *The American Review of Respiratory Diseases,* **125:** 8.

Cooper, A.M. and Khader, S.A. **2008.** The role of cytokines in the initiation, expansion, and control of cellular immunity to tuberculosis. *Immunological Reviews,* **226:** 191-204.

Cooper, A.M. **2009.** Cell-mediated immune responses in tuberculosis, *Annual Review of Immunology*, **27:** 393-422.

Cooper, A.M., Adams, L.B., Dalton, D.K., Appelberg, R. and Ehlers, S. **2002.** IFNgamma and NO in mycobacterial disease: new jobs for old hands. *Trends in Microbiology,* **10:** 221-226.

Cooper, A.M., Roberts, A.D, Rhoades, E.R., Callahan, J.E., Getzy, D.M., Orme, I.M: **1995.** The role of interleukin-12 in acquired immunity to Mycobacterium tuberculosis infection. *Immunology,* **84:** 423-432.

Corbett, E.L., Watt, C.J., Walker, N., Maher, D., Williams, B.G., Raviglione, M.C, and Dye, C. **2003.** The growing burden of tuberculosis: global trends and interactions with the HIV epidemic. *Archives of Internal Medicine,* **163(19):** 1009-1021.

Corbin, J.G., Kelly, D., Rath, E.M., Baerwald, K.D., Suzuki, K. and Popko, B. **1996.** Targeted CNS expression of interferon-gamma in transgenic mice leads to hypomyelination, reactive gliosis, and abnormal cerebellar development. *Molecular and Cellular Neuroscience*, **7(5):** 354-370.

Cowan, E.P., Alexander, R.K., Daniel, S., Kashanchi, F. and Brady, J.N. **1997.** Induction of tumor necrosis factor alpha in human neuronal cells by extracellular human T-cell lymphotropic virus type 1 Tax. *Journal of Virology,* **(71)9:** 6982-6989.

Cowley, S.C. and Elkins, K.L. **2003.** $Ca4^{+}$ T Cells Mediate IFN-*γ*- Independent Control of*Mycobacterium tuberculosis* Infection Both In Vitro and In Vivo. *The Journal of Immunology*, **171(9):** 4689-4699.

Cubillas, R., Kintner, K., Phillips, F., Karandikar, N.J., Thiele, D.L. and Brown. G.R. **2010.** Tumor necrosis factor receptor 1 expression is up-regulated in dendritic cells in patients with chronic HCV who respond to therapy. *Hepatitis Research and Treatment,* **2010:** 1-10.

Curto, M., Reali, C., Palmieri, G., Scintu, F., Schivo, M.L., Sogos, V., Marcialis, M.A., Ennas, M.G., Schwarz, H., Pozzi, G. and Gremo, F. **2004.** Inhibition of cytokines expression in human microglia infected by virulent and non-virulent mycobacteria. *Neurochemistry International,* **44:** 381-392.

Dannenberg, A.M. **2006.** *Pathogenesis of human pulmonary tuberculosis.insights from the rabbit model.* Washington, DC: ASM Press. xiv-453.

Dastur, D.K., Manghani, D.K. and Udani, P.M. **1995.** Pathology and pathogenetic mechanisms in neurotuberculosis. *Radiologic Clinics of North America,* **33:** 733-752.

Davies, P.D. **1995.** Tuberculosis and migration. The Mitchell Lecture, 1994. *The Journal of the Royal College of Physicians of London,* **29:** 113-118.

Davis, J.M. and Ramakrishnan, L. **2009.** The role of the granuloma in expansion and dissemination of early tuberculous infection. *Cell,* **136(1):** 37-49.

De Backer, A.I., Mortelé, K.J., De Keulenaer, B.L. and Parizel. P.M. **2006.** Tuberculosis: Epidemiology, manifestations and the value of medical imaging in diagnosis. *Journal Belge de Radiologie - Belgisch Tijdschrift voor Radiologi,* **89:** 243-250.

de Haas, A.H., van Weering, H.R.J., de Jong, E.K., Boddeke, H.W.G.M. and Biber. K.P.H. **2007.** Neuronal Chemokines: Versatile Messengers In Central Nervous System Cell Interaction. *Molecular Neurobiology,* **36(2):** 137-151.

De Vries, H.E., Kuiper, J., De Boer, A.G., Van Berkel, T.J.C. and Breimer, D.D. **1997.** The Blood-Brain Barrier in Neuroinflammatory Diseases. *Pharmacological Review,* **49(2):**143-156.

Delcher, A.L., Kasi, S., Fleischmann, R.D., Peterson, J., White, O. and Salzberg, S.L. **1999.** Alignment of whole genomes. *Nucleic Acids Research,* **27:** 2369-2376.

Demers, A-M., Mostowy, S., Coetzee, D., Warren, R. and van Helden, P., Behr, M.A. **2010.** Mycobacterium africanum is not a major cause of human tuberculosis in Cape Town, South Africa. *Tuberculosis,* **90:** 143-144.

Department: Health, Republic of South Africa: "National tuberculosis management guidelines 2009" and http://www.doh.gov.za/docs/stats/2011/ SouthAfrican Tuberculosis Profile 2011 WHO.pdf).

DesJardin, L.E., Kaufman, T.M.., Potts, B., Kutzbach, B., Yi, H. and Schlesinger, L.S. **2002.** Mycobacterium tuberculosis-infected human macrophages exhibit enhanced cellular adhesion with increased expression of LFA-1 and ICAM-1 and reduced expression and/or function of complement receptors, FccRII and the mannose receptor. *Microbiology,* **148:** 3161-3171.

Dheda, K., Schwander, S.K., Zhu, B., Van Zyl-Smit, R.N. and Zhang, Y. **2010.** The immunology of tuberculosis: From bench to bedside. *Respirology,* **15:** 433-450.

Dhillon, M.S. and Tuli, S.M. **2001.** Osteoarticular tuberculosis of the foot and ankle*. Foot and Ankle International,* **22(8):** 679-686.

Dhodapkar, K.M., Kaufman, J.L., Ehlers, M., Banerjee, D.K., Bonvini, E., Koenig, S., Steinman, R.M., Ravetch, J.V. and Dhodapkar, M.V. **2005.** Selective blockade of inhibitory Fcgamma receptor enables human dendritic cell maturation with IL-12p70 production and immunity to antibody-coated tumor cells. *Proceedings of the National Academy of Sciences,* **102:** 2910-2915.

Dimitrijevic, O.B., Stamatovic, S.M., Keep, R.F. and Andjelkovic, A.V. **2006.** Effects of the chemokine CCL2 on blood-brain barrier permeability during ischemia–reperfusion injury. *Journal of Cerebral Blood Flow & Metabolism*, **26:** 797-810.

Dogan, R-N.E., Elhofy, A. and Karpus, W.J. **2008.** Production of CCL2 by Central Nervous System Cells Regulates Development of Murine Experimental Autoimmune Encephalomyelitis through the Recruitment of TNF- and iNOS Expressing Macrophages and Myeloid Dendritic Cells1. *The Journal of Immunology,* **180:** 7376-7384.

Doherty, P.C., Turner, S.J., Webby, R.G. and Thomas, P.G. **2006.** Influenza and the challenge for immunology. *Nature Immunology,* **7:** 449-455.

Donald, P.R. **2010.** The chemotherapy of tuberculous meningitis in children and adults. *Tuberculosis (Edinb),* **90(6):** 375-392.

Donald, P.R., Schaaf, H.S. and Schoeman, J.F. **2005.** Tuberculous meningitis and military tuberculosis: the Rich focus revisited. *The Journal of Infection,* **50(3):** 193-195.

Dong, C. and Martinez, G.J. **2010.** T cells: the usual subsets. *Nature Reviews Immunology,* **10(9):** 1.

Dorhoi, A. and Kaufmann, S.H.E. **2009.** Fine-tuning of T cell responses during infection. *Current Opinion in Immunology,* **21:** 367-377.

Duraiswami, P.K. and Tuli, S.M. **1991.** Five thousand years of orthopaedics in India. *Clinical Orthopaedics and Related Research,* **75:** 269-280.

Dye, C. **2006.** Global epidemiology of tuberculosis. *Lancet,* **367:** 938-940.

Dye, C., Williams, B.G., Espinal, M.A., and Raviglione, M.C. **2002.** Erasing the world's slow stain: strategies to beat multidrug-resistant tuberculosis. *Science,* **295:** 2042-2046.

Egen, J.G., Rothfuchs, A.G., Feng, C.G., Winter, N.F., Sher, A.F. and Germain, R.N. **2008.** Macrophage and T cell dynamics during the development and disintegration of mycobacterial granulomas. *Immunity,* **28:** 271-284.

Ehlers, S. **2010.** DC-SIGN and mannosylated surface structures of Mycobacterium tuberculosis: a deceptiveliaison. *European Journal of Cell Biology,* **89:** 95-101.

Eissner, G., Kolch, W. and Scheurich, P. **2004.** Ligands working as receptors: reverse signaling by members of the TNF superfamily enhance the plasticity of the immune system. *Cytokine and Growth Factor Reviews,* **15:** 353-366.

EKirschner, D., Young, D. and JoAnneLFlynn, J. **2010.** Tuberculosis: global approaches to a global disease. *Current Opinion in Biotechnology*, **21:** 1-8.

El-Kebir, M., van der Kuipa, M., van Furtha, A.M. and Kirschner, D.E. **2013.** Computational modeling of tuberculous meningitis reveals an important role for tumor necrosis factor-α. *Journal of Theoretical Biology,* **328(2013):** 43-53.

Ellard, G.A., Humphries, M.J. and Allen, B.W. **1993.** Cerebrospinal fluid drug concentrations and the treatment of tuberculousmeningitis. *American Review of Respiratory Disease,* **148:** 650-655.

Ellard, G.A., Humphries, M.J., Gabriel, M., Teoh, R. **1987.** Penetration of pyrazinamide into the cerebrospinal fluid in tuberculous meningitis. *British Medical Journal*, **294:** 284-285.

Fahey, T., Tracey, K., Tekamp-Olson, P., Cousens, L., Jones, W., Shires, G., Cerami, A. and Sherry, B. **1992.** Macrophage inflammatory protein-1 modulates macrophage function. *The Journal of Immunology,* **148:** 2764-2769.

Fallahi-Sichani, M., Flynn, J.L., Linderman, J.J. and Kirschner, D.E. **2012.** Differential risk of tuberculosis reactivation among anti-tnf therapies is due to drug binding kinetics and permeability. *Journal Immunology,* **188(7):** 3169-3178.

Fiacco, T.A., Agulhon, C. and McCarthy, K.D. **2009.** Sorting out Astrocyte Physiology from Pharmacology. 2009. *Annual Reviews of Pharmacology and Toxicology,* **49:** 49:151-174.

Fischer, H-G. and Reichmann, G. **2001.** Brain Dendritic Cells and Macrophages/Microglia in Central Nervous System Inflammation. *The Journal of Immunology,* **166:** 2717-2726.

Flavell, R.A., Sanjabi, S., Wrzesinski, S.H. and Licona-Limón, P. **2010.** The polarization of immune cells in the tumour environment by TGFβ. *Nature Reviews Immunology,* **10:** 554-567.

Flesch, I.E.A and Kaufmann, S.H.E. **1993.** Role of Cytokines in Tuberculosis. *The Journal of Immunobiology,* **189(3-4):** 316-339.

Flores-Villanueva, P.O., Ruiz-Morales, J.A., Song, C.H., Flores, L.M., Jo, E.K., Montaño, M., Barnes, P.F., Selman, M. and Granados, J. **2005.** A functional promoter polymorphism in monocyte chemoattractant protein-1 is associated with increased susceptibility to pulmonary tuberculosis. *Journal of Experimental Medicine,* **202:** 1649-1658.

Flügel, A., Hager, G., Horvat, A., Spitzer, C., Singer, G.M., Graeber, M.B., Kreutzberg, G.W., Schwaiger, F.W. **2001.** Neuronal MCP-1 expression in response to remote nerve injury. *Journal of Cerebral Blood Flow & Metabolism,* **21:** 6976.

Flynn, J.L. and Chan, J. **2001.** Tuberculosis: Latency and Reactivation. *Infection and Immunity*, **69(7):** 4195-4201.

Flynn, J.L., Chan, J. and Lin, P.L. **2011.** Macrophages and control of granulomatous inflammation in tuberculosis. *Mucosal Immunology,* **4(3):** 271-278.

Flynn, J.L., Chan, J., Triebold, K.J, Dalton, D.K., Stewart, T.A., Bloom, B.R. **1993.** An essential role for interferon gamma in resistance to Mycobacterium tuberculosis infection. *Journal of Experimental Medicine,* **178:** 2249-2254.

Flynn, J. L. and Ernst, J.D. **2000.** Immune responses in tuberculosis. *Current Opinion in Immunology,* **12:** 432-436.

Flynn, J.L., Goldstein, M.M., Chan, J., Triebold, K.J., Pfeffer, K., Lowenstein, C.J., Schreiber, R., Mak, T.W. and Bloom, B.R. **1995.** Tumor necrosis factor-alpha is required in the protective immune response against Mycobacterium tuberculosis in mice. *Immunity,* **2:** 561-572.

Flynn, J.L., Capuano, S.V., Croix, D., Pawar, S., Myers, A., Zinovik, A. and Klein, E. **2003.** Non-human primates: a model for tuberculosis research. *Tuberculosis*, **83(1-3):** 116-118.

Foghsgaard, L., Wissing, D., Mauch, D., Lademann, U., Bastholm, L., Boes, M., Elling, F. and Jäättelä, M. **2001.** Cathepsin B Acts as a Dominant Execution Protease in Tumor Cell Apoptosis Induced by Tumor Necrosis Factor. *The Journal of Cell Biology,* **153(5):** 999-1009.

Foley, L.M., Hitchens, T.K., Ho,C., Janesko-Feldman,K.L., Melick, J.A. Bayır,H. and Kochanek, P.M. **2009.** Magnetic Resonance Imaging Assessment of Macrophage Accumulation in Mouse Brain after Experimental Traumatic Brain Injury. *Journal of Neurotrauma,* **26:** 1509-1519.

Folgueira, L., Delgado, R., Palenque, E. and Noriega, A.R. **1994.** Polymerase chain reaction for rapid diagnosis of tuberculous meningitis in AIDS patients. *Neurology*, **44:** 1336-1338.

Ford, A.L., Goodsall, A.L., Hickey, W.F. and Sedgwick, J.D. **1995.** Normal adult ramified microglia separated from other central nervous system macrophages by flow cytometric sorting. Phenotypic differencesdefined and direct ex vivo antigen presentation to myelin basic proteinreactive CD4-T cells compared. *The Journal of Immunology,* **154:** 4309-4321.

Fortin, A., Abel, L., Casanova, J.L. and Gros, P. **2007.** Host genetics of mycobacterial diseases in mice and men: forward genetic studies of BCG-osis and tuberculosis. *Annual Review of Genomics and Human Genetics,* **8:** 163-192.

Franciotta, D., Salvetti, M., Lolli, F., Serafini, B. and Aloisi, F. **2008.** B cells and multiple sclerosis. *Lancet Neurology,* **7:** 852-858.

Fratti, R.A., Backer, J.M., Gruenberg, J., Corvera, S. and Deretic, V. **2001.** Role of phosphatidylinositol 3-kinase and Rab5 effectors in phagosomal biogenesis and mycobacterial phagosome maturation arrest. *The Journal of Cell Biology,* **154(3):** 631-644.

Fratti, R.A., Chua, J. and Deretic, V. **2003.** Induction of p38 mitogen-activated protein kinase reduces early endosome autoantigen 1 (EEA1) recruitment to phagosomal membranes. *The Journal of Biological Chemistry,* **278(47):** 46961-46967.

Fremond, C., Allie, N., Dambuza, I.,Grivennikov, S., Yeremeev, V.,Quesniaux, V.F.J., Jacobs, M., Ryffel, B. **2005.** Membrane TNF confers protection to acute mycobacterial infection. *Respiratory Research*, **6:** 136.

Fremond, C.M., Yeremeev, V., Nicolle, D.M., Jacobs, M., Quesniaux, V.F. and Ryffel, B. **2004.** Fatal Mycobacterium tuberculosis infection despite adaptive immune response in the absence of MyD88. *Journal of Clinical Investigation,* **114(12):** 1790-1799.

Friberg, H., Bashyam, H., Toyosaki-Maeda, T., Potts, J.A., Greenough, T., Kalayanarooj, S., Gibbons, R.V., Nisalak, A., Srikiatkhachorn, A., Green, S., Stephens, H.A.F., Rothman, A.L. and Mathew, A. **2011.** Cross-Reactivity and Expansion of Dengue-Specific T cells During Acute Primary and Secondary Infections in Humans. *Scientific Reports,* **51:** 1-9.

Gabrilovich, D.I. and Nagaraj, S. **2009.** Myeloid-derived suppressor cells as regulators of the immune system. *Nature Reviews Immunology,* **9(3):** 162-174.

Gahring, L.C., Carlson, N.G., Kulmar, R.A. and Rogers, S.W. **1996.** Neuronal expression of tumor necrosis factor alpha in the murine brain. *Neuroimmunomodilation,* **3(5):** 289-303.

Galea, I., Bechmann, I. and Perry, V.H. **2007.** What is immune privilege? *Trends Immunology,* **28(1):** 12-18.

García de Vinuesa, C., Gulbranson-Judge, A., Khan, M., O'Leary, P., Cascalho, M., Wabl, M., Klaus, G.G.B., Owen,M.J. and MacLennan, I.C.M. **1999.** Dendritic cells associated with plasmablast survival. *European Journal of Immunology,* **29:** 3712-3721.

Garcia, I., Guler, R., Vesin, D., Olleros, M.L., Vassalli, P., Chvatchko, Y., Jacobs, M. and Ryffel, B. **2000.** Lethal Mycobacterium bovis Calmette Guerin infection in nitric oxide synthase 2-deficient mice: cell-mediated immunity requires nitric oxide synthase 2. *Laboratory Investigation,* **80(9):** 1385-97.

Garg, R.K., **1999.** Tuberculosis of the central nervous System. *Postgraduate Medical Journal,* **75:** 133-140.

Giacomini, E., Iona, E., Ferroni, L., Miettinen, M., Fattorini, L., Graziella Orefici, G., Julkunen, I. and Coccia, E.M. **2001.** Infection of Human Macrophages and Dendritic Cells with Mycobacterium tuberculosis Induces a Differential Cytokine Gene Expression That Modulates T Cell Response. *The Journal of Immunology,* **166:** 7033-7041.

Girard, M.P., Fruth, U. And Kiendy, M-P. **2005.** A review of vaccine research and development: tuberculosis. *Vaccine,* **23(50):** 5725-5731.

Girgis, N.I., Yassin, M.W., Laughlin, L.W., Edman, D.C., Farid, Z. and Watten, R.H. **1978.** Rifampicin in the treatment of tuberculous meningitis. *Journal of Tropical Medicine and Hygiene,* **81:** 246-247.

Girgis, N.I., Yassin, M.W., Sippel, J.E., Sorensen, K., Hassan, A., Miner, W.F., Farid, Z. and el Ella, A. **1976.** The value of ethambutol in the treatment of tuberculous meningitis. *Journal of Tropical Medicine and Hygiene,* **79:** 14-17.

Girgis, N.I., Farid, Z., Kilpatrick, M.E., Sultan, Y. and Mikhail, I.A. **1991.** Dexamethasone adjunctive treatment for tuberculous meningitis. *The Pediatric Infectious Disease Journal,* **10:** 179-183.

Glabinski, A.R., Tani, M., Tuohy, V.K., Tuthill, R.J. and Ransohoff, R.M. **1995.** Central nervous system chemokine mRNA accumulation follows initial leukocyte entry at the onset of acute murine experimental autoimmune encephalomyelitis. *Brain, Behavior, and Immunity,* **9:** 315-330.

Glass, C.K., Saijo, K., Winner, B., Marchetto, C.M. and Gage, F.H. **2011.** Mechanisms Underlying Inflammation in Neurodegeneration. *Cell,* **140:** 918-934.

Glass, W.G., Lim, J.K., Cholera, R., Alexander G. Pletnev, A.G., Gao, J-L. and Philip M. Murphy, P.M. **2005.** Chemokine receptor CCR5 promotes leukocyte trafficking to the brain and survival in West Nile virus infection. *Journal Experimental Medecine,* **202(8):** 1087-1098.

Gloor, S.M., Wachtel, M., Bolliger, M.F. and Ishihara, H. **2001.** Molecular and cellular permeability control at the blood–brain barrier. *Brain Research Reviews,* **36:** 258-264.

Godiska, R., Chantry, D., Dietsch, G.N. and Gray, P.W. **1995.** Chemokine expression in murine experimental allergic encephalomyelitis. *Journal of Neuroimmunology,* **58:** 167-176.

Gonzalez-Hernandez, J.A., Ehrhart-Bornstein, M., Spath-Schwalbe, E., Scherbaum, W.A. and Bornstein, S.R. **1996.** Human adrenal cells express tumor necrosis factor-alpha messenger ribonucleic acid: evidence for paracrine control of adrenal function. *The Journal of Clinical Endocrinology and Metabolism,* **81(2):** 807-13.

Gonzalez-Juarrero, M., Turner, O.C., Turner, J., Marietta, P., Brooks, J.V. and Orme, I.M. **2001.** Temporal and spatial arrangement of lymphocytes within lung granulomas induced by aerosol infection with Mycobacterium tuberculosis. *Infection and Immunity,* **69(3):** 1722-1728.

Gorelik, L. and Flavell, R.A. **2002.** Transforming growth factor-β in T-cell biology. *Nature Reviews Immunology,* **2(1):** 46-53.

Grech, A.P., Gardam, S., Chan, T., Quinn, R., Gonzales, R., Basten, A. and Brink, R. **2005.** Tumor Necrosis Factor Receptor 2 (TNFR2) Signaling Is Negatively Regulated by a Novel, Carboxyl-terminal TNFR-associated Factor 2 (TRAF2)-binding Site. *Journal of Biological Chemistry,* **280:** 31572-31581.

Green, J.A., Tran, C.T.H., Farrar, J.J., Nguyen, M.T.H., Nguyen, P.H., Dinh, S.X., Ho, N.D.T., Ly, C.V., Tran, H.T., Friedland, J.S. and Thwaites, G.E. **2009.** Dexamethasone, cerebrospinal fluid matrix metalloproteinase concentrations and clinical outcomes in tuberculous meningitis. *PLoS ONE,* **4(9):** e7277.

Gregersen, R., Lambertsen, K. and Finsen, B. **2000.** Microglia and macrophages are the major source of tumor necrosis factor in permanent middle cerebral artery occlusion in mice. *Journal of Cerebral Blood Flow & Metabolism,* **20:** 53-65.

Grell, M., Douni, E., Wajant, H., Löhden, M., Clauss, M., Maxeiner, B., Georgopoulos, S., Lesslauer, W., Kollias, G., Pfizenmaier, K. and Scheurich, P. **1995.** The transmembrane form of tumor necrosis factor is the prime activating ligand of the 80 kDa tumor necrosis factor receptor. *Cell,* **83:** 793-802.

Grell, M., Douni. E., Wajant, H., Löhden. M., Clauss, M., Maxeiner, B., Georgopoulos, S., Lesslauer, W., Kollias, G., Pfizenmaier, K. and Scheurich, P. **1995**. The transmembrane form of tumor necrosis factor is the prime activating ligand of the 80 kDa tumor necrosis factor receptor. *Cell,* **83(5):** 793-802.

Greten, F.R., Eckmann, L., Greten, T.F., Park, J.M., Li, Z.W., Egan, L.J., Kagnoff, M.F. and Karin, M. **2004.** KKbeta links inflammation and tumorigenesis in a mouse model of colitis-associated cancer. *Cell,* **118:** 285-296.

Grigg, E.R. **1958.** The arcane of tuberculosis. *American Review Tuberculosis,* **78:** 151-172.

Grivennikov, S.I., Tumanov, A.V., Liepinsh, D.J., Kruglov, A.A., Marakusha, B.I., Shakhov, A.N., Murakami, T., Drutskaya, L.N., Förster, I., Clausen, B.E., Tessarollo, L., Ryffel, B, Kuprash, D.V. and Nedospasov, S.A. **2005.** Distinct and nonredundant in vivo functions of TNF produced by t cells and macrophages/neutrophils: protective and deleterious effects. *Immunity,* **22(1):** 93-104.

Grzybowski, S., Styblo, K. and Dorken, E. **1976.** Tuberculosis in Eskimos. *Tubercle,* **57:** S1-S58.

Guez-Barber, D., Fanous, S., Harvey, B.K., Zhang, Y., Lehrmann, E., Becker, K.G., Picciotto, M.R. and Hope, B.T. **2012.** FACS purification of immunostained cell types from adult rat brain. *Journal of Neuroscience Methods,* **203(1):** 10-8.

Guicciardi, M.E., Deussing, J., Miyoshi, H., Bronk, S.F., Svingen, P.A., Peters, C., Kaufmann, S.H. and Gores, G.J. **2000.** Cathepsin B contributes to TNF-α-mediated hepatocyte apoptosis by promoting mitochondrial release of cytochrome c. *Journal of Clinical Investigation,* **106:** 1127-1137.

Gupta, S., Shenoy, V.P., Indira Bairy, I. and Muralidharan, S. **2010.** Diagnostic efficacy of Ziehl-Neelsen method against fluorescent microscopy in detection of acid fast bacilli. *Asian Pacific Journal of Tropical Medicine,* 328-329.

Gutcher, I. and Becher, B. **2007.** APC-derived cytokines and T cell polarization in autoimmune inflammation. *Journal of Clinical Investigation,* **117(5):** 1119-1127.

Haider, S and Knöfler, M. **2009.** Human tumour necrosis factor: physiological and pathological roles in placenta and endometrium. *Placenta,* **30(2):** 111-123.

Hamilton, D.L. and Abremski, K. **1984.** Site-specific recombination by the bacteriophage P1 lox-Cre system. Cre-mediated synapsis of two lox sites. *Journal of Molecular Biology,* **178:** 481-486.

Hansson, E and Rönnabäc, L. **2003.** Glial neuronal signaling in the central nervous system. *The FASEB Letters,* **17(3):** 341-348.

Hao, C., Richardson, A. and Fedoroff, S. **1991.** Macrophage-like cells originate from neuroepithelium in culture: characterization and properties of the macrophage-like cells. *International Journal of Development Neuroscience,* **9:** 1-14.

Harding, C.A. and Henry Boom, W. **2010.** Regulation of antigen presentation by Mycobacterium tuberculosis: a role for Toll-like receptors. *Nature Review of Microbiology,* **8(4):** 296-307.

Hargreaves, J.R., Boccia, D., Evans, C.A., Adato, M., Petticrew, M.and Porter, J.D.H. **2011.** The Social Determinants of Tuberculosis: From Evidence to Action. *American Journal of Public Health*, **101(4):** 654-662.

Harries, A.D., Nkhoma, W.A., Thompson, P.J., Nyangulu, D.S. and Wirima, J.J. **1988.** Nutritional status in Malawian patients with pulmonary tuberculosis and response to chemotherapy. *European Journal of Clinical Nutrition,* **42**: 445-450.

Harris, B. and Morris, T. **2007.** Central Nervous System Tuberculosis. *The Journal for Nurse Practitioners,* **3(5):** 319-325.

Harris, D.P., Haynes, L., Sayles, P.C., Duso, D.K., Eaton, S.M., Lepak, N.M., Johnson, L.L., Swain, S.L. and Lund, F.E. **2000.** Reciprocal regulation of polarized cytokine production by effector B and T cells. *Nature Immunology,* **1:** 475-482.

Hasan, Z., Zaidi, I., Jamil, B., Khan, M.A., Kanji, A. and Hussain. R. **2005.** Elevated ex vivo monocyte chemotactic protein-1 (CCL2) in pulmonary as compared with extra-pulmonary tuberculosis. *BMC Immunology,* **6:** 1-10.

Hashimoto, M., Ishikawa, Y., Goto, F., Bando, T., Sakakibara, Y. and Iriki, M. **1991.** Action site of circulating interleukin-1 on the rabbit brain. *Brain Research,* **540:** 217-223.

Hedlund, S., Persson, A., Vujic, A., Che, K. F., Stendahl, O. and Larsson, M. **2010.** Dendritic cell activation by sensing Mycobacterium tuberculosis-induced apoptotic neutrophils via DC-SIGN. *Human Immunology,* **71:** 535-540.

Hehlgans, T. and Pfeffer, K. **2005.** The intriguing biology of the tumour necrosis factor/tumour necrosis factor receptor superfamily: players, rules and the games. *Immunology*, **115(1):** 1-20.

Henderson, H.J., Dannenberg, A.M. Jr. and Lurie, M.B. **1963.** Phagocytosis of tubercle bacilli by rabbit pulmonary alveolar macrophages and its relation to native resistance to tuberculosis. *The Journal of Immunology,* **90:** 553-556.

Hesselgesser, J. and Horuk, R. **1999.** Chemokine and chemokine receptor expression in the central nervous system. *Journal of NeuroVirology,* **5:** 13-26.

Higuchi, M., Nagasawa, K., Horiuchi, T., Oike, M., Ito, Y., Yasukawa, M. and Niho, Y. **1997.** Membrane tumor necrosis factor-alpha (TNF-alpha) expressed on HTLV^{-I}-infected T cells mediates a costimulatory signal for B cell activation--characterization of membrane TNF-alpha. *Clinical Immunology and Immunopathology,* **82(2):** 133-140.

Hill, P.C., Jackson-Sillah, D., Donkor, S.A., Out, J., Adegbola, R.A. and Lienhardt, C. **2006.** Risk factors for pulmonary tuberculosis: a clinic-based case control study in The Gambia. *BMC Public Health,* **6(156):** 1-7.

Hirsch, C.S., Ellner, J.J., Russell, D.G. and Rich, E.A. **1994.** Complement receptormediated uptake and tumor necrosis factor-alpha-mediated growth inhibition of Mycobacterium tuberculosis by human alveolar macrophages. *The Journal of Immunology,* **152**: 743-753.

Hoesche, C., Sauerwald, A., Veh, R.W., Krippl, B. and Kilimann, M.W. **1993.** The 5"flanking region of the rat synapsin I gene directs neuron-specific and developmentally regulated reporter gene expression in transgenic mice. *Journal of Biological Chemistry,* **268:** 26494-26502.

Horiuchi, T., Mitoma, H., Harashima, S-i., Tsukamoto, H. and Shimoda, T. **2010.** Transmembrane TNF-α: structure, function and interaction with anti-TNF agents. *Rheumatology,* **49:** 1215-1228.

Horwitz, M.S., Evans, C.F., McGavern, D.B., Rodriguez, M. and Oldstone, M.B. **1997.** Primary demyelination in transgenic mice expressing interferon-gamma. *Nature Medicine,* **3(9):** 1037-41.

Hosoglu, S., Geyik, M.F., Balik, I., Aygen, B., Erol, S., Aygencel, T.G., Mert, A., Saltoglu, N., Dokmetas, I., Felek, S., Sunbul, M., Irmak, H., Aydin, K., Kokoglu, O.F., Ucmak, H., Altindis, M. and Loeb. M. **2002.** Predictors of outcome in patients with tuberculous meningitis. *International Journal of Tuberculosis and Lund Disease,* **6(1):** 64-70.

Hurwitz, A.A., Lyman, W.D., Guida, M.P., Calderon, T.M. and Berman, J.W. **1992.** Tumor Necrosis Factor ol Induces Adhesion Molecule Expression on Human Fetal Astrocytes. *Journal of Experimental Medicine,* **176:** 1631-1636.

Hutton, L.C., Castillo-Melendez, M., Smythe, G.A. and Walker, D.W. **2008.** Microglial activation, macrophage infiltration, and evidence of cell death in the fetal brain after uteroplacental administration of lipopolysaccharide in sheep in late gestation. *American journal of Obstetrics and Gynecology,* **198(1):** 117.e1-117.e11.

Huynh, K.K., Joshi, S.A. and Brown, E.J. **2011.** A delicate dance: host response to mycobacteria. *Current Opinion in Immunology,* **23(4):** 464-472.

Idris, Z.H., Sinno, A. and Kronfol. N.M. **1976.** Tuberculous meningitis in childhood: forty-three cases. *The American Journal of Disease of Children,* **130:** 364-367.

Iijima, N., Yanagawa, Y., Iwabuchi, K. and Onoé, K. **2003.** Selective regulation of CD40 expression in murine dendritic cells by thiol antioxidants. *Immunology,* **110(2):** 197-205.

Isaza, J.P., Duque, C., Gomez, V., Robledo, J., Barrera, L.F. and Alzate, J.F. **2012.** Whole genome shotgun sequencing of one Colombian clinical isolate of *Mycobacterium tuberculosis* reveals DosR regulon gene deletions. *Federation of European Microbiological Societies Microbiology Letters,* **330:** 113-120.

Ishikawa, F., Nakano, H., Seo, A., Okada, Y., Torihata, H., Tanaka, Y., Uchida, T., Miyake, H. and Kakiuchi, T. **2002.** Irradiation up-regulates CD80 expression through induction of tumour necrosis factor-α and CD40 ligand expression on B lymphoma cells. *Immunology,* **106:** 354-362.

Itai, T., Tanaka, M. and Nagata, S. **2001.** Processing of tumor necrosis factor by the membrane-bound TNF-alpha-converting enzyme, but not its truncated soluble form. European Journal of Biochemistry, **268(7):** 2074-2082.

Ito, H. and Seishima, M. **2010.** Regulation of the induction and function of cytotoxic T lymphocytes by natural killer T cell. *Journal of Biomedicine and Biotechnology*, **2010:** 1-8.

Jacobs, M., Brown, N., Allie, N. and Ryffel, B. **2000.** Fatal Mycobacterium bovis BCG Infection in TNF-LT-a-Deficient Mice. *Clinical Immunology,* **94(3):** 192-199.

Jacobsen, S.E., Jacobsen, F.W., Fahlman, C., Rusten, L.S. **1994.** TNF-alpha, the great imitator: role of p55 and p75 TNF receptors in hematopoiesis. *Stem cell,* **12(Suppl 1:111-26):** 126-128.

Janeway, C.A.Jr. and Bottomly, K. **1994.** Signals and signs for lymphocyte responses. *Cell,* **76:** 275-285.

Jiang, Y., Beller, D.I., Frendl, G. and Graves, D.T. **1992.** Monocyte chemoattractant protein-1 regulates adhesion molecule expression and cytokine production in human monocytes. *The Journal of Immunology,* **148:** 2423-2428.

Jiao, X.Y., Shen, Y.Q. and Li, K.S. **2008.** The correlation between cytokine production by cerebral cortical glial cells and brain lateralization in mice. *Neuromodulation,* **11(1):** 23-32.

Joosten, A.A., van der Valk, P.D., Geelen, J.A., Severin, W.P. and Jansen Steur, E.N. **2000.** Tuberculous meningitis: pitfalls in diagnosis. *Acta Neurologica Scandinavica,* **102:** 388-394.

Joosten, S.A. and Ottenhoff, T.H. **2008.** Human CD4 and CD8 regulatory T cells in infectious diseases and vaccination. *Human Immunology,* **69(11):** 760-770.

Jung, H.C., Eckmann, L., Yang, S.K., Panja, A., Fierer, J., Morzycka-Wroblewska, E. and Kagnoff, M.F. **1995.** A distinct array of proinflammatory cytokines is expressed in human colon epithelial cells in response to bacterial invasion. *Journal of Clinical Investigation,* **95(1):** 55-65.

Kadhim, H., Tabarki, B., De Prez, C. and Sebire, G. **2003.** Cytokine immunoreactivity in cortical and subcortical neurons in periventricular leukomalacia: are cytokines implicated in neuronal dysfunction in cerebral palsy? *Acta Neuropathology,* **105:** 209-216.

Kalergis, A.M. and Ravetch, J.V. **2002.** Inducing tumor immunity through the selective engagement of activating Fcgamma receptors on dendritic cells. *Journal of Experimental Medicine,* **195:** 1653-1659.

Kallfass, C., Ackerman, A., Lienenklaus, S., Weiss, S., Heimrich, B. and Staeheli, P. **2012.** Visualizing production of interferon-β by astrocytes and microglia in the brain of La Crosse virus-infected mice. *Journal of Virology,* **86(20):** 11223-11230.

Kaneko, H., Yamada, H., Mizuno, S., Udagawa, T., Kazumi, Y., Sekikawa, K. and Sugawara, I. **1999.** Role of tumor necrosis factor-alpha in Mycobacterium-induced granuloma formation in tumor necrosis factor-alpha-deficient mice. *Laboratory Investigation,* **79(4):** 379-86.

Karman, J., Ling, C., Sandor, M. and Fabry, Z. **2004.** Initiation of Immune Responses in Brain Is Promoted by Local Dendritic Cells. *The Journal of Immunology,* **173:** 2353-2361.

Karpus, J., and Kennedy, K. **1997.** MIP-1α and MCP-1 differentially regulate acute and relapsing autoimmune encephalomyelitis as well as Th1/Th2 lymphocyte differentiation. *Journal of Leukocyte Biology,* **62:** 681-687.

Karpus, J., Lukacs, N., Kennedy, K., Smith, W., Hurst, S. and Barrett, T. **1997.** Differential CC chemokine-induced enhancement of T helper cell cytokine production. *The Journal of Immunology,* **158:** 4129-4136.

Kartmann, B., Stenler, S. and Niederweis, M. **1999.** Porins in the cell wall of Mycobacterium tuberculosis. *Journal of Bacteriology,* **181(20):** 6543-6546.

Katti, M.K. **2004.** Pathogenesis, diagnosis, treatment, and outcome aspects of cerebral tuberculosis. *Medical Science Monitor,* **10:** RA215-29.

Kaufmann, S H E. **2002.** Protection against tuberculosis: cytokines, T cells, and macrophages. *Annals of the Rheumatic Diseases,* **61(Suppl II):** ii54-ii58.

Kaufmann, S.H.E. and Parida, S.K., **2008.** Tuberculosis in Africa: learning from pathogenesis for biomarker identification. *Cell Host and Microbe,* **4:** 219-228.

Kawanokuchi, J., Mizuno, T., Takeuchi, H., Kato, H., Wang, J., Mitsuma, N. and Suzumura, A. **2006.** Production of interferon-g by microglia. *Multiple Sclerosis,* 1**2:** 558-564.

Keane, J. **2005.** TNF-blocking agents and tuberculosis: new drugs illuminate an old topic. *Rheumatology,* **44(6):** 714-720.

Keane, J., Balcewicz-Sablinska, M.K., Remold, H.G., Chupp, G.L., Meek, B.B., Fenton, M.J. and Kornfeld, H. **1997.** Infection by *Mycobacterium tuberculosis* promotes human alveolar macrophage apoptosis. *Infection and Immunity,* **65(1):** 298-304.

Keller, C.W., Fokken, C., Turville, S.G., Lünemann, A., Schmidt, J., Münz, C., Lünemann, J.D. **2011.** TNF-alpha induces macroautophagy and regulates MHC class II expression in human skeletal muscle cells. *Journal of Biological Chemistry*, **286(5):** 3970-80.

Ken, P.A., M saghizadeh, M., Ong, J.M., Bosch, R.J., Deem, R. and Simsolo, R.B. **1995.** The expression of of Tumor necrosis factor in human adipose tissue regulation by obesity, weight loss and relationship to lipoprotein lipase. *Journal of Clinical Investigation,* **95:** 2111-2119.

Kerschensteiner, M., Gallmeier, E., Behrens, L., Leal, V.V., Misgeld, T., Klinkert, W.E., Kolbeck, R., Hoppe, E., Oropeza-Wekerle, R.L., Bartke, I., Stadelmann, C., Lassmann, H., Wekerle, H. and Hohlfeld, R. **1999.** Activated human T cells, B cells, and monocytes produce brain-derived neurotrophic factor in vitro and in inflammatory brain lesions: a neuroprotective role of inflammation? *Journal of Experimental Medicine,* **189:** 865-870.

Khanna, M., Srivastava, L.M. and Kumar, P. **2003.** Defective interleukin-2 production and interleukin-2 receptor expression in pulmonary tuberculosis. *Journal of Communicable Disease,* **35(2):** 65-70.

Kim, K.A., Kim, S., Chang, I., Kim, G.S., Min, Y.K., Lee, M.K., Kim, K.W. and Lee, M.S. **2002.** IFN gamma/TNF alpha synergism in MHC class II induction: effect of nicotinamide on MHC class II expression but not on islet-cell apoptosis. *Diabetology,* **45(3):** 385-393.

Kim, K.S., Wass, C.A., Cross, A.S. and Opal, S.M. **1992.** Modulation of blood-brain barrier permeability by tumor necrosis factor and antibody to tumor necrosis factor in the rat. *Lymphokine and Cytokine Research,* **11(6):** 293-298.

Kindler, V., Sappino, A.P., Grau, G.E., Piguet, P.F. and Vassalli, P. **1989.** The inducing role of tumor necrosis factor in the development of bactericidal granulomas during BCG infection. *Cell,* **56:** 731-740.

Kioussis, D. and Pachnis, V. **2009.** Immune and Nervous Systems: More Than Just a Superficial Similarity? *Immunity,* **31:** 705-710.

Kirby, E.D., Jensen, K., Goosens, K.A. and Kaufer, D. **2012.** Stereotaxic Surgery for Excitotoxic Lesion of Specific Brain Areas in the Adult Rat. *Journal of Visual Experiment,* **(65):** e4079.

Kitazawa, M., Yamasaki, T.R. and LaFerla, F.M. **2004.** Microglia as a potential bridge between the amyloid beta-peptide and tau. *Annals of the New York Academy of Sciences,* **1035:** 85-103.

Kivisäkk, P., Mahad, D., Callahan, M., Trebst, C., Tucky, B., Wei, T., Wu, L., Baekkevold, E., Lassmann, H., Staugaitis, S., Campbell, J. and Ransohoff, R. **2003.** Human cerebrospinal fluid central memory $CD4^+$ T cells: evidence for trafficking through choroid plexus and meninges via P-selectin. *Proceedings of the National Academy of Sciences,* **100:** 8389-8394.

Kleinnijenhuis, J., Oosting, M., Joosten, L.A.B., Netea, M.G. and Van Crevel, R. **2011.** Innate Immune Recognition of Mycobacterium tuberculosis. *Clinical and Developmental Immunology,* **2011**: 1-12.

Klopper, M., Warren, R.M., Hayes, H., Gey, N.C., Pittius, v., Streicher, E.M., Müller, B., Sirgel, F.A., Chabula-Nxiweni, M., Hoosain, E., Coetzee, G., van Helden, P.D., Victor, T.C. and Trollip, A.P. **2013.** Emergence and Spread of Extensively and Totally Drug-Resistant Tuberculosis, South Africa. *Emerging Infectious Diseases,* **19(3):** 449-455.

Korbel, D.S., Schneider, B.E. and Schaible, U.E. **2008.** Innate immunity in tuberculosis: myths and truth. *Microbes and Infection,* **10:** 995-1004.

Korhonen, R., Lahti, A., Kankaanranta, H. and Eeva Moilanen, E. **2005.** Nitric Oxide Production and Signaling in Inflammation. Current Drug Targets - *Inflammation & Allergy*, **4:** 471-479.

Korner, H., Riminton, D.S., Strickland, D.H., Lemckert, F.A., Pollard, J.D. and Sedgwick, J.D. **1997.** Critical points of tumor necrosis factor action in central nervous system autoimmune inflammation defined by gene targeting. *Journal of Experimental Medicine,* **186:** 1585.

Kozlowski, C. and Weimer, R.M. **2012.** An Automated Method to Quantify Microglia Morphology and Application to Monitor Activation State Longitudinally *In Vivo*. *PLoS ONE,* **7(2):** 1-9.

Kramer, K., Schaudien, D., Eisel, U.L.M., Herzog, S., Richt, J.A., Wolfgang Baumgärtner, W. and Herden, C. **2012.** TNF-Overexpression in Borna Disease Virus-Infected Mouse Brains Triggers Inflammatory Reaction and Epileptic Seizures. *PLoS ONE,* **7(7):** e41476 1-16.

Kratky, W., Reis e Sousa, C., Oxenius, A. and Spörri, R. **2011.** Direct activation of antigen-presenting cells is required for CD8+ T-cell priming and tumor vaccination. *Proceedings of the National Academy of Sciences,* **108(42):** 17414-17419.

Kriegler, M. **1990.** A nonsecretable cell surface mutant of tumor ne-crosis factor (TNF) kills by cell-to-cell contact. *Cell,* **63:** 251-258.

Kristensson, K. **2003.** Neuronal targeting and functional effects of infectious agents transmitted from animals to man. *Rendiconti Fisiche Accademia Lincei,* **14(9):** 281-292.

Kruglov, A.A., Lampropoulou, V., Fillatreau, S. And Nedospasov, S.A. **2011.** Pathogenic and protective functions of TNF in neuroinflammation are defined by its expression in T lymphocytes and myeloid cells. *The Journal of Immunology,* **187(11):** 5660-5670.

Krumbholz, M., Theil, D., Steinmeyer, F., Cepok, S., Hemmer, B., Hofbauer, M., Farina, C., Derfuss, T., Junker, A., Arzberger, T., Sinicina, I., Hartle, C., Newcombe, J., Hohlfeld, R. and Meinl E. **2007.** CCL19 is constitutively expressed in the CNS, up-regulated in neuroinflammation, active and also inactive multiple sclerosis lesions. *Journal of Neuroimmunology,* **190:** 72-79.

Kuang, Y., Lackay, S.N., Zhao, L. and Fu, Z.F. **2009.** Role of chemokines in the enhancement of BBB permeability and inflammatory infiltration after rabies virus infection. *Virus Research,* **144(1-2):** 18-26.

Kubota, K. **2009.** Innate IFN-c Production by Subsets of Natural Killer Cells, Natural Killer T Cells and cd T Cells in Response to Dying Bacterial-Infected Macrophages. *Scandinavian Journal of Immunology,* **71:** 199-209.

Kuhn, R. and Schwenk, F. **1997.** Advances in gene targeting methods. *Current Opinion in Immunology,* **9:** 183-188.

Kuprash, D.V., Tumanov, A.V., Liepinsh, D.J., Koroleva, E.P., Drutskaya, M.S., Kruglov, A.A., Shakhov, A.N., Eileen Southon, E., Murphy, W.J., Tessarollo, L., Grivennikov, S.I. and Nedospasov, S.A. **2005.** Novel tumor necrosis factor-knockout mice that lack Peyer's patches. *European Journal of Immunology*, **35:** 1592-1600.

Kuwahara, H., Miyamoto, Y., Akaike, T., Kubota, T. Tomohiro Sawa, T., Okamoto, S. and Maeda, H. **2000.** Helicobacter pylori Urease Suppresses Bactericidal Activity of Peroxynitrite via Carbon Dioxide Production. *Infection & Immunity,* **68(8):** 4378-4383.

Kwan, C.K. and Ernst, J.D. **2011.** HIV and tuberculosis: a deadly human syndemic. *Clinical Microbiology Review,* **24:** 351-376.

Kyrkanides, S., Olschowka, J.A., Williams, J.P., Hansen, J.T. and O'Banion, M.K. **1999.** TNF alpha and IL-1beta mediate intercellular adhesion molecule-1 induction via microglia-astrocyte interaction in CNS radiation injury. *Journal of Neuroimmunology,* **95(1-2):** 95-106.

Lawn, S.D. and Zumla, A.I. **2011.** Tuberculosis. *Lancet,* **378(9785):** 57-72.

Lawson, L.J., Perry, V.H., Dri, P. and Gordon, S. **1990.** Heterogeneity in the distribution and morphology of microglia in the normal adult mouse brain. *Neuroscience,* **39:** 151-170.

Lee, J.E., Ling, C., Kosmalski, M.M., Hulseberg, P., Schreiber, H.A., Sandor, M. and Fabry, S. **2009.** Intracerebral Mycobacterium bovis bacilli Calmette-Guerin infection-induced immune responses in the CNS. *Journal of Neuroimmunology,* **213(1-2):** 112-122.

Lee, S.C., Liu, W., Dickson, D.W., Brosnan, C.F. and Berman, J.W. **1993.** Cytokine production by human fetal microglia and astrocytes. Differential induction by lipopolysaccharide and IL-1 beta. *The Journal of Immunology,* **150(7):** 2659-6267.

Lenardo, M., Chan, F.K-M., Hornung, F., McFarland, H., Siegel, R., Wang, J. and Zheng, L. **1999.** Mature T Lymphocyte apoptosis-mmune Regulation in a Dynamic and Unpredictable Antigenic Environment. *Annual Review of Immunology,* **17:** 221-253.

Leonard, J.M., and Des Prez, R.M. **1990.** Tuberculous meningitis. *Infectious Disease Clinics of North America,* **4:** 769-787.

Letterio, J.J. **2000.** Murine models define the role of TGF-β as a master regulator of immune cell function. *Cytokine and Growth Factor Reviews,* **11(1-2):** 81-87.

Li, A.H., Waddell, S.J., Hinds, J., Malloff, C.A., Bains, M., Hancock, R.E., Lam, W.L., Butcher, P.D. and Stokes, R.W. **2010.** Contrasting transcriptional responses of a virulent and an attenuated strain of Mycobacterium tuberculosis infecting macrophages. 5(6): *PLoS ONE,* **5(6):** 1-14.

Li, R., Yang, L., Lindholm, K., Konishi, Y., Yue, X., Hampel, H., Zhang, D. and Shen, Y. **2004.** Tumor necrosis factor death receptor signaling cascade is required for amyloid-beta protein-induced neuron death. *Journal of Neuroscience,* **24:** 1760-1771.

Lieberman, A.P., Pitha, P.M., Shin, H.S. and Shin, M.L. **1989.** Production of tumor necrosis factor and other cytokines by astrocytes stimulated with lipopolysaccharide or a neurotropic virus. *Proceedings of the National Academy of Sciences,* **86:** 6348-6352.

Lima, M., Zhang, Y. and Villalta, F. **1997.** β-chemokines that inhibit HIV-1 infection of human macrophages stimulate uptake and promote destruction of *Trypanosoma cruzi* by human macrophages. *Cell Molecular Biology,* **43:** 1067-1076.

Lin, P.L., Plessner, H.L., Voitenok, N.N. and Flynn, J.L. **2007.** Tumor Necrosis Factor and Tuberculosis. *Journal of Investigative Dermatology Symposium Proceedings,* **12:** 22-25.

Lin, P.L., Myers, A., Smith, L., Bigbee, C., Bigbee, M., Fuhrman, C., Grieser, H., Chiosea, I., Voitenek, N.N., Capuano, S.V., Klein, E. and Flynn, J.L. **2010.** Tumor necrosis factor neutralization results in disseminated disease in acute and latent Mycobacterium tuberculosis infection with normal granuloma structure in a cynomolgus macaque model. *Arthritis Rheumatoid,* **62(2):** 340-350.

Lisby, S., Muller, K.M., Jongeneel, C.V., Saurat, J.H. and Hauser, C. **1995.** Nickel and skin irritants up-regulate tumor necrosis factor-alpha mRNA in keratinocytes by different but potentially synergistic mechanisms. *International Immunology,* **7(3):** 343-52.

Liu, P.T. and Modlin, R.L. **2008.** Human macrophage host defense against Mycobacterium tuberculosis. *Current Opinion in Immunology,* **20:** 371-376.

Liu, T., Clark, R.K., McDonnell, P.C., Young, P.R. White, R.F. Barone, F.C. and Feuerstein, G.Z. **1994.** Tumor Necrosis Factor-α Expression in Ischemic Neurons. *Stroke,* **25:** 1481-1488.

Liu, Y., Teige, I., Birnir, B. and Issazadeh-Navikas, S. **2006.** Neuron-mediated generation of regulatory T cells from encephalitogenic T cells suppresses EAE. *Nature Medicine,* **12(5):** 518-525.

Locati, M., Bonecchi, R. and Corsi, M.M. **2005.** Chemokines and Their Receptors Roles in Specific Clinical Conditions and Measurement in the Clinical Laboratory. *American Journal of Clinical Pathology* **123(Suppl 1):** S82-S95.

Locksley, R.M., Heinzel, F.P., Shepard, H.M., Agosti, J., Essalu, T. E., Aggarwal, B. B. and Harlan, J. M. **1987.** Tumors necrosis factors α and β differ in their capacities to generate interleuking 1 release from human endothelial cells. *The Journal of Immunology,* **139(6):** 1891-1895.

Lönnroth, K., Castro, K.G., Chakaya, J.M., Chauhan, S.L., Floyd, K., Glaziou, P. and Raviglione, M.C. **2010.** Tuberculosis control and elimination 2010-50: cure, care, and social development. *Lancet,* **375:** 1814-1829.

Lönnroth, K., Jaramillo, E., Williams, B.G., Dye, C. and Raviglione, M. **2009.** Drivers of tuberculosis epidemics: The role of risk factors and social determinants. *Social Science & Medicine,* **68:** 2240-2246.

Low, P.S., Lee, B.W., Yap, H.K., Tay, J.S., Lee, W.L., Seah, C.C. and Ramzan, M.M. **1995.** Inflammatory response in bacterial meningitis: cytokine levels in the cerebrospinal fluid. *Annals of Tropical Paediatrics*, **15(1):** 55-59.

Lu, T.H., Huang, R.M., Chang, T.D., Tsau, S.M. and Wu, T.C. **2005.** Tuberculosis mortality trends in Taiwan: a resurgence of non-respiratory tuberculosis. *International Journal of Tuberculosis and Lung Disease,* **9:** 105-10.

Lue, L.F., Rydel, R., Brigham, E.F., Yang, L.B., Hampel, H., Murphy, G.M.Jr., Brachova, L., Yan, S.D., Walker, D.G., Shen, Y. and Rogers, J. **2001.** Inflammatory repertoire of Alzheimer's disease and nondemented elderly microglia in vitro. *Glia,* **35:** 72-79.

Lukacs, N.W., Stricter, R. M., Warmington, K., Lincoln, P.L., Chensue, S.W. and Kunkel, S. **1997.** Differential Recruitment of Leukocyte Populations and Alteration of Airway Hyperreactivity by C-C Family Chemokines in Allergic Airway Inflammation. *The Journal of Immunology,* **158:** 4398-4404.

Luma, H.N., Tchaleu, B.C.N., Ngahane, B.H.M., Temfack, E., Doualla, M.S., Halle, M.P., Joko, H.A. and Koulla-Shiro, S. **2013.** Tuberculous meningitis: presentation, diagnosis and outcome in hiv-infected patients at the Douala general hospital, Cameroon: a cross sectional study. *AIDS Research and Therapy,* **10(16):** 1-6.

Lurie, M.B., Abramson, S. and Heppleston, A.G. **1952**. On the response of genetically resistant and susceptible rabbits to the quantitative inhalation of human type tubercle bacilli and the nature of resistance to tuberculosis. *Journal of Experimental Medicine,* **95:** 119-134.

Luther, S.A., Gulbranson-Judge, A., Acha-Orbea, H. and MacLennan, I.C.M. **1997.** Viral superantigen drives extrafollicular and follicular B cell differentiation leading to virus-specific antibody production. *Journal of Experimental Medicine,* **185:** 551-562.

MacMicking, J.D., North, R.J., LaCourse, R., Mudgett, J.S., Shah, S.K. and Nathan, C.F. **1997.** Identification of nitric oxide synthase as a protective locus against tuberculosis. *Proceedings of the National Academy of Sciences,* **94:** 5243-52438.

Maglione, P.J. and Chan, J. **2009.** How B cells shape the immune response against Mycobacterium tuberculosis. *European Journal of Immunology,* **39(3):** 676-86.

Maglione, P.J., Xu,J. and Chan, J.B. **2007.** Cells Moderate Inflammatory Progression and Enhance Bacterial Containment upon Pulmonary Challenge with Mycobacterium tuberculosis. *The Journal of Immunology,* **178:** 7222-7234.

Mak, T.W., Penninger, J.M. and Ohashi, P.S. **2001.** Knockout mice: a paradigm shift in modern immunology. *Nature Review Immunology,* **1:** 11-19.

Mäkelä, J., Koivuniemi, R., Korhonen, L. and Lindholm, D. **2010.** Interferon-γ Produced by Microglia and the Neuropeptide PACAP Have Opposite Effects on the Viability of Neural Progenitor Cells. *PLoSONE,* **5(6):** e11091.

Male, D., Cooke, A., Owen, M., Trowsdale, J. and Champion, B. **1996.** *Advanced Immunology.* 3rd ed. London, Mosby**. 6(2):** 1-156.

Mardh, P.A., Larsson, L., Hoiby, N., Engbaek, H.C. and G. Odham. **1983.** Tuberculostearic acid as a diagnostic marker in tuberculous meningitis. *Lancet,* **i:** 367.

Marques, C.P., Kapil, P., Hinton, D.R., Hindinger, C., Nutt, S.L., Ransohoff, R.M., Phares, T.W., Stohlman, S.A. and Bergmann, C.C. **2011.** CXCR3-Dependent Plasma Blast Migration to the Central Nervous System during Viral Encephalomyelitis. *Journal of Virology,* **85(13):** 6136-6147.

Mastroianni, C.M., Paoletti, F., Lichtner, M., D'Agostino, C., Vullo, V. and Delia. S. **1997.** Cerebrospinal fluid cytokines in patients with tuberculous meningitis. *Clinical Immunology and Immunopathology,* **84:** 171-176.

Mauri, C., Gray, D., Mushtaq, N. and Londei, M. **2003.** Prevention of arthritis by interleukin 10-producing B cells. *Journal of Experimental Medicine,* **197***:* 489-501.

Mazurek, G.H., Jereb, J., Vernon, A., LoBue, P., Goldberg, S. and Castro, K. **2010.** Updated guidelines for using interferon gamma release assays to detect Mycobacterium tuberculosis infection - United States. *Morbidity and Mortality Weekly Report,* **59/RR-5:** 1-26.

Mazzolla, R., Puliti, M., Barluzzi, R., Neglia, R., Bistoni, F., Barbolini, G. and Blasi. E. **2002.** Differential microbial clearance and immunoresponse of Balb/c (Nramp1 susceptible) and DBA2 (Nramp1 resistant) mice intracerebrally infected with *Mycobacterium bovis* BCG (BCG). *FEMS Immunology and Medical Microbiology*, **32:** 149-158.

McManus, C., Berman, J.W., Brett, F.M., Staunton, H, Farrell, M and Brosnan, C.F. **1998.** MCP-1, MCP-2 and MCP-3 expression in multiple sclerosis lesions: an immunohistochemical and in situ hybridization study. *Journal of Neuroimmunology,* **86:** 20-29.

McMicking, J.D., North, R.J., LaCourse, R., Mudgett, J.S., Shah, S.K. and Nathan, C.F. **1997.** Identification of nitric oxide synthase as a protective locus against tuberculosis. *Proceedings of the National Academy of Sciences,* **94:** 5243-5248.

Means, T.K., Wang, S., Lien, E., Yoshimura, A., Golenbock, D.T. and Fenton, M.J. **1999.** Human toll-like receptors mediate cellular activation by Mycobacterium tuberculosis. *The Journal of Immunology,* **163(7):** 3920-3927.

Medana, I., Li, Z., Flügel, A., Tschopp, J., Wekerle, H. and Neumann, H. **2001.** Fas ligand (CD95L) protects neurons against perforin-mediated T lymphocyte cytotoxicity. *The Journal of Immunology,* **167:** 674-681.

Medeiros, R., Prediger, R.D.S., Passos, G.F., Pandolfo, P., Duarte, F.S., Dafre, J.L., Giunta, G.D., Figueiredo, C.P., Takahashi, R.N., Campos, M.M. and Calixto, J.B. **2007.** Connecting TNF-α Signaling Pathways to iNOS Expression in a Mouse Model of Alzheimer's Disease: Relevance for the Behavioral and Synaptic Deficits Induced by Amyloid β Protein. *The Journal of Neuroscience,* **27(20):** 5394-5404.

Méndez-Samperio, P. **2010.** Role of interleukin-12 family cytokines in the cellular response to mycobacterial disease. *International Journal of Infectious Diseases,* 14: e366-e371.

Meuth, S.G., Herrmann, A.M., Simon, O.J., Siffrin, V., Melzer, N., Bittner, S., Meuth, P., Langer, H.F., Hallermann, S., Boldakowa, N., Herz, J., Munsch, T., Landgraf, P., Aktas, O., Heckmann, M., Lessmann, V., Budde, T., Kieseier, B.C., Zipp, F. and Wiendl, H. **2009.** Cytotoxic $CD8^+$ T cell-neuron interactions: perforin-dependent electrical silencing precedes but is not causally linked to neuronal cell death. *Journal of Neuroscience,* **29(49):** 15397-409.

Micheau, O. and Tschopp. J. **2003.** Induction of TNF receptor I-mediated apoptosis via two sequential signaling complexes. *Cell,* **114:** 181-190.

Mihret, A. **2012.** The role of dendritic cells in Mycobacterium tuberculosis infection. *Landes Bioscience,* **3(7):** 1-6.

Miller, E.A. and Ernst, J.D. **2009.** Anti-TNF immunotherapy and tuberculosis reactivation: another mechanism revealed. *Journal of Clinical Investigation,* **119:** 1079-1082.

Miranda, M.S., Breiman, A., Allain, S., Deknuydt, F. and Altare, F. **2012.** The Tuberculous Granuloma: An Unsuccessful Host Defence Mechanism Providing a Safety Shelter for the Bacteria? *Clinical and Developmental Immunology,* **2012:** 1-14.

Misra, U.K., Kalita, J. and Nair, P.P. **2010.** Role of aspirin in tuberculous meningitis: A randomized open label placebo controlled trial. *Journal of the Neurological Sciences,* **293:** 12-17.

Miyatake, Y., Ikeda, H., Ishizu, A., Baba, T., Ichihashi, T. Suzuki, A., Tomaru, U., Kasahara, M. and Yoshiki, T. **2006.** Role of Neuronal Interferon-γ in the Development of Myelopathy in Rats Infected with Human T-Cell Leukemia Virus Type 1. *American Journal of Pathology,* **169(1):** 189-194.

Miyazawa, M., Ito, Y., Kosaka, N., Nukada, Y., Sakagushi, H., Suzuki, H. and Nishiyama, N. **2008.** Role of TNF-a and extracellular ATP in THP-1 cell activation following allergen exposure. *The Journal of Toxicological Sciences,* **33(1):** 71-83.

Mizoguchi, A., Ogawa, A., Takedatsu, H., Sugimoto, K., Shimomura, Y., Shirane, K., Nagahama, K., Nagaishi, T., Mizoguchi, E., Blumberg, R.S. and Bhan, A.K. **2007.** Dependence of intestinal granuloma formation on unique myeloid DC-like cells. *Journal of Clinical Investigation,* **117:** 605-615.

Moalem, G., Leibowitz-Amit, R., Yoles, E., Mor, F., Cohen, I.R. and Schwartz, M. **1999.** Autoimmune T cells protect neurons from secondary degeneration after central nervous system axotomy. *Nature Medicine,* **5:** 49-55.

Modrowski, D., Godet, D. and Marie, P.J. **1995.** Involvement of interleukin 1 and tumour necrosis factor alpha as endogenous growth factors in human osteoblastic cells. *Cytokines,* **7(7):** 720-6.

Mogues, T., Goodrich, M.E., Ryan, L., LaCourse, R. and North, R.J. **2001.** The relative importance of T cell subsets in immunity and immunopathology of airborne Mycobacterium tuberculosis infection in mice. *Journal of Experimental Medicine,* **193:** 271-280.

Mohan, A.K., Coté, T.R., Block, J.A., Manadan, A.M., Siegel, J.N. and Braun, M.M. **2004.** Tuberculosis following the Use of Etanercept, a Tumor Necrosis Factor Inhibitor. *Clinical Infectious Diseases,* **39:** 295-299.

Mohan, M.J., Seaton, T., Mitchell, J., Howe, A., Blackburn, K., Burkhart, W., Moyer, M., Patel, I, Waitt, G.M., Becherer, J.D., Moss, M.L. and Milla, M.E. **2002.** The tumor necrosis factor-alpha converting enzyme (TACE): a unique metalloproteinase with highly defined substrate selectivity. *Biochemistry,* **41(30):** 9462-9469.

Moir, J.W. and Wood, N.J. **2001.** Nitrate and nitrite transport in bacteria. *Cellular and molecular life sciences,* **58:** 215-224.

Moll, H. **2003.** Dendritic cells and host resistance to infection. *Cell Microbiology,* **5:** 493-500.

Möller, M. and Hoal, E.G. **2010.** Current findings, challenges and novel approaches in human genetic susceptibility to tuberculosis. *Tuberculosis,* **90:** 71-83.

Moore, B.B., Moore, T.A. and Toews, G.B. **2001.** Role of T- and B-lymphocytes in pulmonary host defences. *European Respiratory Journal,* **18:** 846-856.

Moser, M. and Murphy, K.M. **2000.** Dendritic cell regulation of TH1-TH2 development. *Nature immunology,* **1(3):** 199-205.

Mossmann, T., Cherwinski, H., Bond, M., Giedlin, M. and Coffman, R.L. **1986.** Two types of murine helper T cell clone. I. Definition according to profiles of lymphokine activities and secreted proteins. *The Journal of Immunology,* **136:** 2348-2357.

Mustafa, M.M., Lebel, M.H., Ramilo, O., Olsen, K.D., Reisch, J.S., Beutler, B. and McCracken, G.H. Jr. **1989**. Correlation of interleukin- 1 beta and cachectin concentrations in cerebrospinal fluid and outcome from bacterial meningitis. *Journal of Pediatrics,* **115:** 208-213.

Babu, G.N., Kumar, A., Kalita, J. and Misra. U.K. **2008.** Proinflammatory cytokine levels in the serum and cerebrospinal fluid of tuberculous meningitis patients. *Neuroscience Letters,* **436(1):** 48-51.

Nagy, A. **2000.** Cre Recombinase: The Universal Reagent for Genome Tailoring. *Genesis,* **26:** 99-109.

Nahid, P., Bliven, E.E., Kim, E.Y., Mac Kenzie, W.R., Stout, J.E., Diem, L., Johnson, J.L., Gagneux, S., Philip C. Hopewell, P.C., Kato-Maeda, M. and the Tuberculosis Trials Consortium. **2010.** Influence of *M. tuberculosis* lineage variability within a clinical trial for pulmonary tuberculosis. *PLoS ONE,* **5(5):** e10753.

Nasu, K. and Narahara, H. **2010.** Pattern recognition via the toll-like receptor systemin the human female genital tract. *Mediators of Inflammation,* **2010:** 1-12.

Nathan, C. **1997.** Inducible nitric oxide synthase: what difference does it make? *The Journal of Clinical Investigation,* **100(10):** 2417-2423.

Nau, R., Prange, H.W., Menck, S., Kolenda, H., Visser, K. and Seydel, J.K.**1992.** Penetration of rifampicin into the cerebrospinal fluid of adults with uninflamed meninges. *Journal of Antimicrobiology and Chemotherapy,* **29:** 719-724.

Nelson, C.A. and. Zunt, J.R. **2011.** Tuberculosis of the Central Nervous System in Immunocompromised Patients: HIV Infection and Solid Organ Transplant Recipients. *Clinical Infectious Diseases,* **53(9):** 915-926.

Nelson, K.E. and Williams, C.M. **2007.** *Infectious disease epidemiology:* theory and practice. 2nd ed. Jones & Bartlett Learning, 1-1207.

Niederweis, M. **2008.** Nutrient acquisition by mycobacteria. *Microbiology,* **154:** 679-692.

Nikodemova, M. and Watters, J.J. **2012.** Efficient isolation of live microglia with preserved phenotypes from adult mouse brain. *Journal of Neuroinflammation*, **9(147):** 1-10.

Nimer, F.A., Lindblom, R., Ström, M., Guerreiro-Cacais, A.O., Parsa, R., Aeinehband, S., Mathiesen, T., Lidman, O. and Piehl, F. **2013.** Strain influences on inflammatory pathway activation, cell infiltration and complement cascade after traumatic brain injury in the rat. *Brain, Behavior, and Immunity,* **27(1):** 109-22.

Nussler, A. K., and T. R. Billiar. **1993.** Inflammation, immunoregulation, and inducible nitric oxide synthase. *Journal of Leukocyte Biology,* **54:** 171.

Nygårdas, P.T., Määttä, J.A. and Hinkkanen, A.E. **2000.** Chemokine expression by central nervous system resident cells and infiltrating neutrophils during experimental autoimmune encephalomyelitis in the BALB/c mouse. *The European Journal of Immunology,* **30:** 1911-1918.

Oberhelman, R.A., Soto-Castellares, G., Gilman, R.H., Caviedes, L., Castillo, M.E., Kolevic, L., Pino, T.D., Saito, M., Salazar-Lindo, E., Negron, E., Montenegro, S., Laguna-Torres, V. A., Moore, D.A.J. and Evans, C.A. **2010.** Diagnostic approaches for paediatric tuberculosis by use of diff erent specimen types, culture methods, and PCR: a prospective case-control study. *The Lancet Infectious Diseases,* **S1473-3099(10):** 70141-70149.

Oddo, M., Renno, T., Attinger, A., Bakker, T., Mac- Donald, H-R. and Meylan, P.R.A. **1998**. Fas ligand-induced apoptosis of infected human macrophages reduces the viability of intracellular *Mycobacterium tuberculosis*. *The Journal of Immunology*, **160(11):** 5448-5454.

Olin, M.R., Armién, A.G., Maxim C-J. Cheeran, M.C-J., Bryan Rock, R., Molitor, T.W. and Peterson, P.K. **2008.** Role of Nitric Oxide in Defense of the Central Nervous System against *Mycobacterium tuberculosis. The Journal of Infectious Diseases,* **198:** 886-889.

Onwubalili, J.K. **1988.** Malnutrition among tuberculosis patients in Harrow, England. *European Journal of Clinical Nutrition* **42**: 363-366.

O'Reilly, L.M. and Daborn, C.J. **1995.** The epidemiology of Mycobacterium bovis infections in animals and man: a review. *Tuberculosis and Lung Disease,* **76(Suppl 1):** 1-46.

Owens, G.P., Bennett, J.L., Gilden, D.H. and Burgoon, M.P. **2006.** The B-cell response in multiple sclerosis. *Neurological Research,* **28:** 236-244.

Pakasi, T.A., Karyadi, E., Dolmans, W.M., van der Meer, J.W. and van der Velden, K. **2009.** Malnutrition and socio-demographicfactors associated with pulmonary tuberculosis inTimor and Rote Islands, Indonesia. *International Journal of Tuberculosis and Lung Disease,* **13(6):** 755-759.

Pan, P.P., Santra, G., Khatua, D.K. and Pramanik, R. **2012.** Functional Outcome after Rehabilitation among Different Diagnostic Groups of Childhood Meningoencephalitis. *Indian Journal of Physical Medicine and Rehabilitation,* **23(2):** 57-61.

Park, J.H., and Shin, S.H. **1996.** Induction of IL-12 gene expression in the brain in septic shock. *Biochemical and Biophysical Research Communications,* **224:** 391-396.

Park, J.M., Greten, F.R., Li, Z.W. and Karin, M. **2002.** Macrophage apoptosis by anthrax lethal factor through p38 MAP kinase inhibition. *Science,* **297:** 2048-2051.

Pasparakis, M., Alexopoulou, L., Episkopou, V. and Kollias, G. **1996.** Immune and inflammatory responses in TNF α-deficient mice: A critical requirement for TNF α in the formation of primary B cell follicles, follicular dendritic cell networks and germinal centers, and in the maturation of the humoral immune response. *Journal of Experimental Medicine,* **184:** 1397-1411.

Pasparakis, M., Alexopoulou, L., Grell, M., Pfizenmaier, K., Bluethmann, H. and Kollias, G. **1997.** Peyer's patch organogenesis is intact yet formation of B lymphocyte follicles is defective in peripheral lymphoid organs of mice deficient for tumor necrosis factor and its 55-kDa receptor. *Proceedings of the National Academy of Sciences,* **94:** 6319-6323.

Pathak, S.K., Basu, S., Basu, K.K., Banerjee, A., Pathak, S., Bhattacharyya, A., Kaisho, T., Kundu, M. and Basu, J. **2007.** Direct extracellular interaction between the early secreted antigen ESAT-6 of Mycobacterium tuberculosis and TLR2 inhibits TLR signaling in macrophages. *Nature Immunology,* **8:** 610-618.

Pattacini, L., Boiardi, L., Casali, B. and Salvarani, C. **2010.** Differential effects of anti-TNF-α drugs on fibroblast-like synoviocyte apoptosis. *Rheumatology,* **49:** 480-489.

Pechhold, K., Patterson, N.B., Craighead, N., Lee, K.P., June, C.H. and Harlan, D.M. **1997.** Inflammatory Cytokines IFN-7 Plus TNF- Induce Regulated Expression of CD80 (B7-1) but Not CD86 (B7-2) on Murine Fibroblasts. *The Journal of Immunology,* **158:** 4921-4929.

Perlman, D.C., El-Sadr, W.M., Nelson, E.T., Matts, J.P., Telzak, E.E., Salomon, N., Chirgwin, K. and Hafner, R. **1997.** Variation of chest radiographic patterns in pulmonary tuberculosis by degree of human immunodeficiency virus-related immunosuppression. *Clinical Infectious Disease,* **25:** 242-246.

Perry, S.W., Dewhurst, S., Bellizzi, M.J. and Gelbard, H.A. **2002.** Tumor necrosis factor-alpha in normal and diseased brain: Conflicting effects via intraneuronal receptor crosstalk? *Journal of NeuroVirology,* **8:** 611-624.

Perry, V.H. and Gordon, S. **1991.** Macrophages and the nervous system. *International Review of Cytology,* **125:** 203-244.

Perry, V.H., Hume, D.A. and Gordon, S. **1985.** Immunohistochemical localization of macrophages and microglia in the adult and developing mouse brain. *Neuroscience,* **15:** 313-326.

Pessara, U. and Koch, N. **1990.** Tumor necrosis factor alpha regulates expression of the major histocompatibility complex class II-associated invariant chain by binding of an NF-kappa B-like factor to a promoter element. *Molecular Cell Biology,* **10(8):** 4146-4154.

Peterson, P.K., Gekker, G., Hu, S., Sheng, W.S., Anderson, W.R., Ulevitch, R.J., Tobias, P.S., Gustafson, K.V., Molitor, T.W. and Chao. C.C. **1995.** CD14 receptor-mediated uptake of nonopsonized Mycobacteria tuberculosis by human microglia. *Infection and Immunity,* **63:** 1598-1602.

Peterson, P.K., Hu, S., Sheng, W.S., Kravitz, F.H., Molitor, T.W., Chatterjee, D. and Chao, C. C., **1995.** Thalidomide inhibits tumor necrosis factor-alpha production by lipopolysaccharide- and lipoarabinomannan-stimulated human microglial cells. *Journal of Infectious Diseases,* **172(4):** 1137-1140.

Phuah, J.Y., Mattila, J.T., Lin, P.L. and Flynn, J.L. **2012.** Activated B cells in the granulomas of nonhuman primates infected with Mycobacterium tuberculosis. *The American Journal of Pathology,* **181(2):** 508-514.

Phuapradit, P., Supmonchai, K., Kaojarern, S. and Mokkhavesa, C. **1990.** The blood/cerebrospinal fluid partitioning of pyrazinamide: a study during the course of treatment of tuberculous meningitis. *Journal of Neurology and Neurosurgery Psychiatry*, **53:** 81-82.

Phypers, M.T., Harris, T. and Power, C. **2006.** CNS Tuberculosis: a longitudinal analysis of epidemiological and clinical features. *The International Journal of Tuberculosis and Lung Disease,* **10:** 99-103.

Prasad, K. and Singh, M.B. **2009.** Corticosteroids for managing tuberculous meningitis (Review). *Wiley,* 1-39.

Puissegur, M.P., Botanch, C., Duteyrat, J.L., Delsol, G., Caratero, C. and Altare, F. **2004.** An in vitro dual model of mycobacterial granulomas to investigate the molecular interactions between mycobacteria and human host cells. *Cellular Microbiology,* **6(5):** 423-433.

Radwanska, M., Guirnalda, P., De Trez, C., Ryffel, B., Black, S. and Magez, S. **2008.** Trypanosomiasis-Induced B Cell Apoptosis Results in Loss of Protective Anti-Parasite Antibody Responses and Abolishment of Vaccine-Induced Memory Responses. *PLoS Pathogens*, **4(5e1000078):** 1-11.

Rafiq, K., Bergtold, A. and Clynes, R. **2002.** Immune complex-mediated antigen presentation induces tumor immunity. *Journal of Clinical Investigation,* **110:** 71-79.

Ramakrishnan, L. **2012.** Revisiting the role of the granuloma in Tuberculosis. *Nature Reviews Immunology,* **12:** 352-366.

Ramesh, G., MacLean, A.G. and Philipp, M.T. **2013.** Cytokines and Chemokines at the Crossroads of Neuroinflammation, Neurodegeneration, and Neuropathic Pain. *Mediators of Inflammation,* **2013:** 1-20.

Ramilo, O., Saez-Llorens, X., Mertsola, J., Jafari, H., Olsen, K.D., Hansen, E.J., Yoshinaga, M., Ohkawara, S., Nariuchi, H. and McCracken Jr, G.H. **1990.** Tumor necrosis factor alpha/cachectin and interleukin 1 beta initiate meningeal inflammation. *The Journal of Experimental Medicine,* **172:** 497-507.

Randall, P.J., Hsu, N-J., Lang, D., Cooper, S., Sebesho, B., Allie, N., Keeton, R., Francisco, N.M., Salie, S., Labuschagné, A., Quesniaux, V., Ryffel, B., Kellaway, L. and Jacobs, M. **2014.** Neurons are host cells for *Mycobacterium tuberculosis*. *Infection and Immunity,* doi:10.1128/IAI.00474-13.

Ranheim, E.A. and Kipps, T.J. **1995.** Tumor Necrosis Factor-α Facilitates Induced of CD80 (B7-1) and CD54 on Human B cells by Activated T Cells: Complex Regulation by IL-4, IL-10, and CD40L. *Cellular Immunology,* **161:** 226-235.

Ransohoff, R,M. **2009.** Chemokines and chemokines receptors: Standing at the crossroads of Immunobiology and Neurobiology. *Immunity,* **31:** 711-721.

Ransohoff, R.M. and Brown, M.A. **2012.** Innate immunity in the central nervous system. *The Journal of Clinical Investigation,* **122(4):** 1164-1171.

Ransohoff, R.M. and Cardona, A.E. **2010.** The myeloid cells of the central nervous system parenchyma. *Nature,* **468:** 253-262.

Ransohoff, R.M. and Engelhardt, B. **2012.** The anatomical and cellular basis of immune surveillance in the central nervous system. *Nature Review Immunology,* **12:** 623-635.

Ransohoff, R.M., Kivisakk, P. and Kidd, G. **2003.** Three or more routes for leukocyte migration into the central nervous system. *Nature Review Immunology,* **3:** 569-581.

Ray, J.C., Flynn, J.L. and Kirschner, D.E. **2009.** Synergy between individual TNF-dependent functions determines granuloma performance for controlling *Mycobacterium tuberculosis* infection. *The Journal of Immunology,* **182(6):** 3706-3717.

Reiling, N., Holscher, C., Fehrenbach, A., Kroger, S., Kirschning, C.J., Goyert, S. and Ehlers, S. **2002.** Cutting edge: Toll-like receptor (TLR)2- and TLR4-mediated pathogen recognition in resistance to airborne infection with Mycobacterium tuberculosis. *The Journal of Immunology,* **169(7):** 3480-3484.

Reljic, R., Stylianou, E., Balu, S. and Ma, J.K. **2010.** Cytokine interactions that determine the outcome of mycobacterial infection of macrophages. *Cytokine,* **51:** 42-46.

Renno, T., Taupin, V., Bourbonnière, L., Verge, G., Tran, E., De Simone, R., Krakowski, M., Rodriguez, M., Peterson, A. and Owens T. **1998.** Interferon-gamma in progression to chronic demyelination and neurological deficit following acute EAE. *Molecular and Cellular Neuroscience*, **12(6):** 376-389.

Renno, T., Krakowski, M., Piccirillo, C., Lin, J.Y. and Owens, T. **1995.** TNF-alpha expression by resident microglia and infiltrating leukocytes in the central nervous system of mice with experimental allergic encephalomyelitis. Regulation by Th1 cytokines. *The Journal of Immunology,* **154(2):** 944-953.

Reynolds, H.Y. **1987.** Bronchoalveolar lavage. *American Review of Respiratory Disease,* **135:** 250-263.

Reyrat, J-M., Berthet, F-X. and Gicquel, B. **1995.** The urease locus of Mycobacterium tuberculosis and its utilization for the demonstration of allelic exchange in Mycobacterium bovis bacillus Calmette-Guerin. *Procedings of the National Academy of Sciences,* **92:** 8768-8772.

Rhoades, E.R., Frank, A.A. and Orme, I.M. **1997.** Progression of chronic pulmonary tuberculosis in mice aerogenically infected with virulent Mycobacterium tuberculosis. *Tuberculosis and Lung Disease,* **78:** 57-66.

Rich, A.R., and H.A. McCordock. **1933.** The pathogenesis of tuberculous meningitis. *Bulletin of Johns Hopkins Hospital,* **52:** 5-37.

Richter, C., Messerschmidt, S., Holeiter, G., Tepperink, J., Osswald, S., Zappe, A., Branschädel, M., Boschert, V., Mann, D.A., Scheurich, P. and Krippner-Heidenreich, A. **2012.** The Tumor Necrosis Factor Receptor Stalk Regions Define Responsiveness to Soluble versus Membrane-Bound Ligand. *Journal of Molecular Cell and Biology,* **32(13):** 2515-2529.

Riley, R.L. **1957.** Aerial dissemination of pulmonary tuberculosis. *American Review of Tuberculosis,* **76:** 931-941.

Riley, R.L., Mills, C.C., Nyka, W., Weinstock, N., Storey, P.B., Sultan, L.U., Riley, M.C. and Wells, W.F. **1959.** Aerial dissemination of pulmonary tuberculosis: a two- year study of contagion in a tuberculosis ward. *American Journal of Epidemiology*, **70(2):** 185-196.

Riminton, D.S., Korner, H., Strickland, D.H., Lemckert, F.A., Pollard, J.D. and Sedgwick, J.D. **1998.** Challenging cytokine redundancy: inflammatory cell movement and clinical course of experimental autoimmune encephalomyelitis are normal in lymphotoxin-deficient, but not tumor necrosis factor-deficient mice. *Journal of Experimental Medicine,* **187:** 1517.

Roach, D.R., Bean, A.G., Demangel, C., France, M.P., Briscoe, H. and Britton, W.J. **2002.** TNF regulates chemokine induction essential for cell recruitment, granuloma formation, and clearance of mycobacterial infection. *The Journal of Immunology,* **168(9):** 4620-4627.

Robinson, C.M. and Nau, G.J. **2008.** Interleukin-12 and interleukin-27 regulate macrophage control of Mycobacterium tuberculosis. *Journal of Infectious Disease,* **198(3):** 359-366.

Rock, R.B., Gekker, G., Hu, S., Sheng, W.S., Cheeran, M., Lokensgard, J.R. and Peterson, P.K. **2004.** Role of Microglia in Central Nervous System Infections. *Clinical Microbiology Reviews,* **20:** 942-964.

Rock, R.B., Hu, S., Gekker, G., Sheng, W.S., May, B., Kapur, V. and Peterson, P.K. **2005.** *Mycobacterium tuberculosis*-Induced Cytokine and Chemokine Expression by Human Microglia and Astrocytes: Effects of Dexamethasone. *The Journal of Infectious Diseases,* **192:** 2054-2058.

Rock, R.B., Olin, M., Baker, C.A., Molitor, T.W. and Peterson, P.K. **2008.** Central nervous system tuberculosis: Pathogenesis and clinical aspects. *Clinical Microbiology Reviews,* **21:** 243-261.

Romagnani, S. **1996.** Th1 and Th2 in human diseases. *Clinial Immunology and Immunopathology,* **80:** 225-235.

Rook, W. and Graham, A. **2007.** Th2 cytokines in susceptibility to tuberculosis. *Current Molecular Medicine,* **7(3):** 327-337.

Rossant, J. and McMahon, A. **1999.** "Cre"-ating mouse mutants-a meeting review on conditional mouse genetics. *Genes & Development,* **13:** 142-145.

Ryan, J.G. and Aksentijevich, I. **2009.** TNF Receptor-Associated Periodic Syndrome (TRAPS): Towards a Molecular Understanding of the Systemic Autoinflammatory Diseases. *Arthritis & Rheumatism,* **60(1):** 8-11.

Ryan, K.J., Rayn, Ray, C.G., Ahmad, N., Drew, W.L. and Plorde, J.J. **2010.** *Sherris medical microbiology.* 5th ed. McGraw Hill companies, 1-1026.

Saez-Llorens, X., Ramilo, O., Mustafa, M.M., Mertsola, J. and McCracken Jr,G.H. **1990.** Molecular pathophysiology of bacterial meningitis: current concepts and therapeutic implications. *The Journal of Pediatrics,* **116:** 671-684.

Saijo, K. and Glass, C.K. **2011.** Microglial cell origin and phenotypes in health and disease *Nature Reviews Immunology,* **11:** 775-787.

Saijo, K., Crottia, A. and Glass, C.K. **2013.** Regulation of Microglia Activation and Deactivation by Nuclear Receptors. *Glia,* **61:** 104-111.

Salgado, C.G., Nakamura, K., Sugaya, M., Tada, Y., Asahina, A., Fukuda, S., Koyama, Y., Irie S. and Tamaki, K. **1999.** Differential effects of cytokines and immunosuppressive drugs on CD40, B7-1, and B7-2 expression on purified epidermal Langerhans cells. *Journal of Investigation and Dermatology,* **113(6):** 1021-1027.

Saliba, E. and Henrot, A. **2001.** Inflammatory mediators and neonatal brain damage. *Biology of the Neonate*, **79:** 224-227.

Sánchez-Castañón, M., Baquero, I.C., Sánchez-Velasco, P., Fariñas, M.C., Ausín, F., Leyva-Cobián, F. and Ocejo-Vinyals, J.G. **2009.** Polymorphisms in CCL5 promoter are associated with pulmonary tuberculosis in northern Spain. *International Journal of Tuberculosis and Lung Disease,* **13:** 480-485.

Santello, M. and Volterra, A. **2012.** TNFa in synaptic function: switching gears. *Trends in Neurosciences,* **35(10):** 638-647.

Santello, M., Bezzi, P. and Volterra, A. **2011.** TNFalpha controls glutamatergic gliotransmission in the hippocampal dentate gyrus. *Neuron,* **69:** 988-1001.

Saukkonen, J.J., Bazydlo, B., Thomas, M., Strieter, R.M. Keane, J. and Kornfeld, H. **2002.** β-Chemokines Are Induced by *Mycobacterium tuberculosis* and Inhibit Its Growth. *Infection and Immunity,* 1684-1693.

Saukkonen, K., Sande, S., Cioffe, C., Wolpe, S., Sherry, B., Cerami, A. and Tuomanen, E. **1990.** The role of cytokines in the generation of inflammation and tissue damage in experimental gram-positive meningitis. *The Journal of Experimental Medicine,* **171:** 439-448.

Saunders, B.M., Frank, A.A. and Orme, I.M. **1999**. Granuloma formation is required to contain bacillus growth and delay mortality in mice chronically infected with *Mycobacterium tuberculosis. Immunology,* **98(3):** 324-328.

Saunders, B.M., Tran, S., Ruuls, S., Sedgwick, J.D., Briscoe, H. and Britton, W.J. **2005.** Transmembrane TNF is sufficient to initiate cell migration and granuloma formation and provide acute, but not long-term, control of *Mycobacterium tuberculosis* infection. *The Journal of Immunology,* **174(8):** 4852-4859.

Scanga, C.A., Mohan, V.P. Tanaka, K. Alland, D. Flynn, J.L. and Chan, J. **2001.** The inducible nitric oxide synthase locus confers protection against aerogenic challenge of both clinical and laboratory strains of Mycobacterium tuberculosis in mice. *Infection and Immunity,* **69(12):** 7711-7717.

Scanga, C.A., Mohan, V.P., Yu, K., Joseph, H., Tanaka, K., Chan, J. and Flynn, J.L. **2000.** Depletion of $Cd4^+$ T Cells Causes Reactivation of Murine Persistent Tuberculosis despite Continued Expression of Interferon-γ and Nitric Oxide Synthase. *Journal of Experimental Medicine,* **192(3):** 347-353.

Schmetterer, K.G., Haiderer, D., Leb-Reichl, V.M., Neunkirchner, A., Jahn-Schmid, B., Küng, H.J., Schuch, K., Steinberger, P., Bohle, B., Winfried, F. and Pickl, W.F.P. **2011.** Bet v 1–specific T-cell receptor/forkhead box protein 3 transgenic T cells suppress Bet v 1–specific T-cell effector function in an activation-dependent manner. *Journal of Allergy and Clinical Immunology,* **127(1):** 38-245.e3.

Schneemann, M. and Schoeden, G. **2007.** Macrophage biology and immunology: man is not a mouse. *Journal of Leukocyte Biology,* **81(3):** 579.

Schoeman, J.F., Springer, P., van Rensburg, A.J., Swanevelder, S., Hanekom, W.A., Haslett, P.A.J. and Kaplan, G. **2004.** Adjunctive thalidomide therapy for childhood tuberculous meningitis: results of a randomized study. *Journal of Child Neurology,* **19(4):** 250-257.

Schroeter, M.L., Mertsch, K., Giese, H., Müller, S., Sporbert, A., Hickel, B. and Blasig, I.E. **1999.** Astrocytes enhance radical defence in capillary endothelial cells constituting the blood brain barrier. *Federation of European Biochemical Societies letters,* **449(2-3):** 241-244.

Scott-Browne, J.P., Shafiani, S., Tucker-Heard, G., Ishida-Tsubota, K., Fontenot, J.D., Rudensky, A.Y., Bevan, M.J. and Urdahl, K.B. **2007.** Expansion and function of Foxp3-expressing T regulatory cells during tuberculosis*. Journal of Experimental Medicine,* **204:** 2159-2169.

Sedgwick, J.D., Schwender, S., Imrich, H., Dorries, R., Butcher, G.W., and ter Meulen, V. **1991.** Isolation and direct characterization of resident microglial cells from the normal and inflamed central nervous system. *Proceedings of the National Academy of Sciences,* **88:** 7438-7442.

Selwyn, P.A., Hartel, D., Lewis, V.A., Schoenbaum, E.E., Vermund, S.H., Klein, R.S., Walker, A.T. and Friedland, G.H. **1989.** A prospective study of the risk of tuberculosis among intravenous drug users withhuman immunodefi ciency virus infection. *The New England Journal of Medicine,* **320(9):** 545-550.

Senaldi, G., Yin, S., Shaklee, C.L., Piguet, P.F., Mak, T.W. and Ulich, T.R. **1996.** Corynebacterium parvum- and Mycobacterium bovis bacillus Calmette-Guerin-induced granuloma formation is inhibited in TNF receptor I (TNF-RI) knockout mice and by treatment with soluble TNF-RI. *The Journal of Immunology,* **157:** 5022-5026.

Serafini, B., Rosicarelli, B., Magliozzi, R., Stigliano, E. and Aloisi, F. **2004.** Detection of ectopic B-cell follicles with germinal centers in the meninges of patients with secondary progressive multiple sclerosis. *Brain Pathology,* **14(2):** 164-174.

Shafiani, S., Tucker-Heard, G., Kariyone, A., Takatsu, K. and Urdahl, K.B. **2010.** Pathogen-specific regulatory T cells delay the arrival of effector T cells in the lung during early tuberculosis. *Journal of Experimental Medicine,* **207(7):** 1409-1420.

Sharief, M.K., Ciardi, M. and Thompson, E.J. **1992.** Blood-brain barrier damage in patients with bacterial meningitis: association with tumor necrosis factor-alpha but not interleukin-1 beta. *Journal of Infectious Diseases,* **166(2):** 350-358.

Sharma, S. and Bose, M. **2001.** Role of Cytokines in Immune Response to Pulmonary Tuberculosis. *Asian Pacific Journal of Allergy and Immunology,* **19:** 213-219.

Sharma, S., Sharma, M., Roy, S., Kumar, P. and Bose, M. **2004.** *Mycobacterium tuberculosis* induces high production of nitric oxide in coordination with production of tumour necrosis factor-α in patients with fresh active tuberculosis but not in MDR tuberculosis. *Immunology and Cell Biology*, **82:** 377-382.

Sharma, S.K., Mohanan, S. and Sharma, A. **2012**. Relevance of Latent TB Infection in Areas of High TB Prevalence. *CHEST,* **142(3):** 761-773.

Sharpe, A.H. and Freeman, G.J. **2002.** The B7-CD28 superfamily. *Nature Review Immunology,* **2:** 116-126.

Shaul, P.W. **2002.** Regulation of endothelial nitric oxide synthase: location, location, location. *Annual Review Physiology,* **64:** 749.

Shen, Y., He, P., Zhong, Z., McAllister, C. and Lindholm, K. **2006.** Distinct destructive signal pathways of neuronal death in Alzheimer's disease. *Trends in Molecular Medicine,* **12:** 574-579.

Shin, A-R., Lee, K-S., Lee, J-S., Kim, S-Y., Song, C-H., Jung, S-B., Yang, C-S., Jo, E-K., Park, J-K., Paik, T.H. and Kim, H-J. *Mycobacterium tuberculosis* HBHA. **2006.** Protein Reacts Strongly with the Serum Immunoglobulin M of Tuberculosis Patients. *Clinical Vaccine Immunology,* **13(8):** 869-875.

Shin, S.G., Roh, J.K., Lee, N.S., Shin, J.G., Jang, I.J., Park, C.W. and Myung, H.J. **1990.** Kinetics of isoniazid transfer into cerebrospinal fluid in patients with tuberculous meningitis. *Journal of Korean Medical Science,* **5:** 39-45.

Shrikant, P. and Benveniste, E.N. **1996.** The central nervous system as an immunocompetent organ: role of glial cells in antigen presentation. *The Journal of Immunology,* **157:** 1819-1822.

Simmons, R.D. and Willenborg, D.O. **1990.** Direct injection of cytokines into the spinal cord causes autoimmune encephalomyelitis-like inflammation. *Journal of the Neurological Sciences*, **100:** 37-42.

Simpson, J.E., Newcombe, J., Cuzner, M.L. and Woodroofe, M.N. **1998.** Expression of monocyte chemoattractant protein-1 and other beta-chemokines by resident glia and inflammatory cells in multiple sclerosis lesions. *The Journal of Neuroimmunology,* **84:** 238-249.

Simpson, J.E., Newcombe, J., Cuzner, M.L. and Woodroofe, M.N. **2000.** Expression of the interferon-gamma-inducible chemokines IP-10 and Mig and their receptor, CXCR3, in multiple sclerosis lesions. *Neuropathology and Applied Neurobiology***, 26:** 133-142.

Sinha, A., Salam, N., Gupta, S. and Natarajan, K. **2007.** Mycobacterium tuberculosis and dendritic cells: recognition, activation and functional implications. *Indian Journal of Biochemistry and biophysics,* **44(5):** 279-288.

Smith, N.H., Hewinson, R.G., Kremer, K., Brosch, R. and Gordon, S.V. **2009.** Myths and misconceptions: the origin and evolution of Mycobacterium tuberculosis. *Nature Review Microbiology,* **7:** 537-544.

Smookler, D.S., Mohammed, F.F., Kassiri, Z., Duncan, G.S., Mak, T.W. and Khokha, R. **2006.** Cutting edge: Tissue inhibitor of metalloproteinase 3 regulates TNF-dependent systemic inflammation. *The Journal of Immunology,* **176:** 721-725.

Sohaskey, C.D. and Wayne, L.G. **2003.** Role of narK2X and narGHJI in hypoxic upregulation of nitrate reduction by Mycobacterium tuberculosis. *Journal of Bacteriology,* **185:** 7247-7256.

Solodova, E., Jablonska, J., Weiss, S. and Lienenklaus, S. **2011.** Production of IFN-beta during Listeria monocytogenes infection is restricted to monocyte/macrophage lineage. *PLoS ONE,* **446(6):** e18543.

Sorensen, T.L., Tani, M., Jensen, J., Pierce, V., Lucchinetti, C., Folcik, V.A., Qin, S., Rottman, J., Sellebjerg, F., Strieter, R.M., Frederiksen, J.L. and Ransohoff, R.M. **1999.** Expression of specific chemokines and chemokine receptors in the central nervous system of multiple sclerosis patients. *Journal of Clinical Investigation,* **103:** 807-815.

Sorensen, T.L., Trebst, C., Kivisakk, P., Klaege, K.L., Majmudar, A., Ravid, R., Lassmann, H., Olsen, D.B., Strieter, R.M., Ransohoff, R.M. and Sellebjerg, F. **2002.** Multiple sclerosis: a study of CXCL10 and CXCR3 co-localization in the inflamed central nervous system. *The Journal of Neuroimmunology,* **127:** 59-68.

Sousa, A.O., Wargnier, A., Poinsignon, Y., Simonney, N., Gerber, F., Lavergne, F. Herrmann, J.L. and Lagrange, P.H. **2000.** Kinetics of circulating antibodies,immune complex and specific antibody-secreting cells in tuberculosis patients during 6 months of antimicrobial therapy. *Tubercle and Lung Disease*, **80(1):** 27-33.

Springer, B., Master, S., Sander, P., Zahrt, T., McFalone, M., Song, J., Papavinasasundaram, K. G., Colston, M. J., Boettger, E. and Deretic, V. **2001.** Silencing of oxidative stress response in Mycobacterium tuberculosis: Expression patterns of ahpC in virulent and avirulent strains and effect of ahpC inactivation. *Infection and Immunity,* **69(10):** 5967-5973.

Sredni-Kenigsbuch, D. **2002.** TH1/TH2 cytokines in the central nervous system. *International Journal of Neuroscience,* **112(6):** 665-703.

Stalder, A.K., Pagenstecher, A., Yu, N.C., Kincaid, C., Chiang, C.-S., Hobbs, M.V., Bloom, F.E. and Campbell, I.L. **1997.** Lipopolysaccharide-induced IL-12 expression in the central nervous system and cultured astrocytes and microglia. *The Journal of Immunology,* **159:** 1344-1351.

Stellwagen, D. and Malenka, R.C. **2006.** Synaptic scaling mediated by glial TNF-alpha. *Nature,* **440:** 1054-1059.

Sugimoto, K., Ogawa, A., Shimomura, Y., Nagahama, K., Mizoguchi, A. and Bhan, A.K. **2007.** Inducible IL-12- producing B cells regulate Th2-mediated intestinal inflammation. *Gastroenterology,* **133:** 124-136.

Sze, D.M., Toellner, K.M., García de Vinuesa, C., Taylor, D.R. and MacLennan, I.C. **2000.** Intrinsic constraint on plasmablast growth and extrinsic limits of plasma cell survival. *Journal of Experimental Medicine,* **192(6):** 813-821.

Takano, H., Ohtsuka, M., Akazawa, H., Toko, H., Harada, M., Hasegawa, H., Nagai, T. and Komuro, I. **2003.** Pleiotropic effects of cytokines on acute myocardial infarction: G-CSF as a novel therapy for acute myocardial infarction. *Current Pharmaceutical Design,* **9(14):** 1121-1127.

Takeda, K., Kaisho, T. and Akira, S. **2003.** Toll-like receptors. *Annual Review of Immunology,* **21:** 335-376.

Takeshita, Y. and Ransohoff, R.M. **2012.** Inflammatory cell trafficking across the blood-brain barrier: chemokine regulation and in vitro models. *Immunological Reviews*, **248:** 228-239.

Tang, C., Xue, H.-L., Bai, C.I. and Fu, R. **2011.** Regulation of Adhesion Molecules Expression in TNF-a-stimulated Brain Microvascular Endothelial Cells by Tanshinone IIA: Involvement of NF-kB and ROS Generation. *Phytotherapy Research,* **25:** 376-380.

Taoufik, Y., de Goër de Herve, M.G., Giron-Michel, J., Durali, D., Cazes, E., Tardieu, M., Azzarone, B. and Delfraissy J.F. **2001.** Human microglial cells express a functional IL-12 receptor and produce IL-12 following IL-12 stimulation. *European Journal of Immunology,* **31(11):** 3228-3239.

Tartaglia, L.A. and Goeddel, D.V. **1992.** Two TNF receptors. *Immunology Today,* **13:** 151-153.

Taub, D., Turcovski-Corrales, S., Key, M., Longo, D. and Murphy, W. **1996.** Chemokines and T lymphocyte activation: β-chemokines costimulate human T lymphocyte activation in vitro. *The Journal of Immunology,* **156:** 2095-2103.

Tchelingerian, J.-L., Le Saux, F. and Jacque, C. **1996.** Identification and Topography of Neuronal Cell Populations Expressing TNFa and IL-1a in Response to Hippocampal Lesion. *Journal of Neuroscience Research,* **43:** 99-106.

Teitelbaum, R., Schubert, W., Gunther, L., Kress, Y., Macaluso, K., Pollard, J.W., McMurray, D. N. and Bloom, B.R. **1999.** The M Cell as a portal of entry to the lung for the bacterial pathogen *Mycobacterium tuberculosis*. *Immunity,* **10:** 641-650.

Thwaites, G.E. and Hien, T.T. **2005.** Tuberculous meningitis: many questions, too few answers. *The Lancet Neurology,* **4(3):** 160-170.

Thwaites, G.E., Bang, N.D., Dung, H.N., Quy, T.H., Oanh, D.T.T., Thoa, N.T.C., Hien, N.Q., Thuc, N.T., Hai, N.N., Lan, N.T.N., Lan, N.N., Duc, N.H., Tuan, V.N., Hiep, H.C., Chau, T.T.H., Mai, P., Dung, N.T., Stepniewska, K., White, N.J., Hien, T.T. and Farrar, J.J. **2004.** Dexamethasone for the Treatment of Tuberculous Meningitis in Adolescents and Adults. *The New England Journal of Medicine*, **351:** 1741-1751.

Thwaites, G.E., Fisher, M., Hemingway, C., Scott, G., Solomon, T. and Innes, J. **2009.** British Infection Society guidelines for the diagnosis and treatment of tuberculosis of the central nervous system in adults and children. *Journal of Infection,* **59:** 167-187.

Thwaites, G.E., Simmons, C.P., Than, Quyen, N.T.H., Chau, T.T.H., Mai, P.P., Dung, N.T., Phu, N.H., White, N.P., Hien, T.T. and Farrar, J.J. **2003.** Pathophysiology and prognosis in Vietnamese adults with tuberculous meningitis. *Journal of Infectious Diseases,* **188:** 1105-1015.

Thye, T., Nejentsev, S., Intemann, C.D., Browne, E.N., Chinbuah, M.A., Gyapong, J., Osei, I., Owusu-Dabo, E., Zeitels, L.R., Herb, F., Horstmann, R.D. and Meyer, C.G. **2009.** MCP-1 promoter variant -362C associated with protection from pulmonary tuberculosis in Ghana, West Africa. *Human Molecular Genetics,* **18:** 381-388.

Tobin, D.M., Roca, F.J., Oh, S.F., McFarland, R., Vickery, T.W., Ray, J.P., Ko, D.C., Zou, Y., Bang, N.D., Chau, T.T.H., Vary, J.C., Hawn, T.R., Dunstan, S.J., Farrar, J.J., Guy E. Thwaites, G.E., King, M-C., Serhan, C.N. and Ramakrishnan, L. **2012.** Host Genotype-Specific Therapies Can Optimize the Inflammatory Response to Mycobacterial Infections. *Cell,* **148:** 434-446.

Tobin, D.M., Vary, J.C.Jr, Ray, J.P., Walsh, G.S., Dunstan, S.J., Bang, N.D., Hagge, D.A., Khadge, S., King, M.C., Hawn, T.R., Moens, C.B. and Ramakrishnan, L. **2010.** The lta4h locus modulates susceptibility to mycobacterial infection in zebrafish and humans. *Cell,* **140(5):** 717-730.

Toellner, K.-M., Gulbranson-Judge, A., Taylor, D.R., Sze, D.M.-Y. and MacLennan, I.C.M. **1996.** Immunoglobulin switch transcript production in vivo related to the site and time of antigen-specific B cell activation. *Journal of Experimental Medicine,* **183:** 2303-2312.

Toossi, Z., Kleinhens, M.E. and Ellner, J.J. **1986.** Defective interleukin 2 production and responsiveness in human pulmonary tuberculosis. *Journal of Experimental Medicine,* **163:** 1162-1172.

Török, M.E., Yen, N.T., Chau, T.T., Mai, N.T., Phu, N.H., Mai, P.P., Dung, N.T., Chau, N.V,, Bang, N.D., Tien, N.A., Minh, N.H., Hien, N.Q., Thai, P.V., Dong, D.T., Anh do, T.T., Thoa, N.T., Hai, N.N., Lan, N.N., Lan, N.T., Quy, H.T., Dung, N.H., Hien, T.T., Chinh, N.T., Simmons, C.P., de Jong, M., Wolbers, M. and Farrar, J.J. **2011.** Timing of initiation of antiretroviral therapy in human immunodeficiency virus (HIV)-associated tuberculous meningitis. *Clinical Infection Disease,* **52(11):** 1374-1383.

Torrelles, J.B. and Schlesinger, L.S. **2010.** Diversity in *Mycobacterium tuberculosis* mannosylated cell wall determinants impacts adaptation to the host. *Tuberculosis,* **90:** 84-93.

Torres, D., Janot, L., Quesniaux, V.F.J., Grivennikov, S.I., Maillet, I., Sedgwick, J.D., Ryffel, B. and Erard, F. **2005.** Membrane Tumor Necrosis Factor Confers Partial Protection to Listeria Infection. *American Journal of Pathology,* **167(6):** 167:1677-1687.

Torres, M., Ramachandra, L., Rojas, R.E., Bobadilla, K., Thomas, J., Canaday, D.H., Harding, C.V. and Boom, W.H. **2006.** Role of Phagosomes and Major Histocompatibility Complex Class II (MHC-II) Compartment in MHC-II Antigen Processing of *Mycobacterium tuberculosis* in Human Macrophages. *Infection and Immunity,* **74(3):** 1621-1630.

Townsend, S.E. and Goodnow, C.C. **1998.** Abortive proliferation of rare T cells induced by direct or indirect antigen presentation by rare B cells in vivo. *Journal of Experimental Medicine*, **187:** 1611-1621.

Tracey, D., Klareskog, L., Sasso, E.H., Salfeld, J.G. and Tak, P.P. **2008**. Tumor necrosis factor antagonist mechanisms of action: A comprehensive review. *Pharmacology and Therapeutics,* **117:** 244-279.

Tracey, K.J. and Cerami, A. **1993.** Tumor necrosis factor, other cytokines and disease. *Annual Review of Cell Biology,* **9:** 317-343.

Tran, E.H., Hardin-Pouzet, H., Verge, G. and Owens, T. **1997.** Astrocytes and microglia express inducible nitric oxide synthase in mice with experimental allergic encephalomyelitis. *Journal of Neuroimmunology,* **74(1-2):** 121-129.

Trivedi, R., Sona Saksena, S. and Gupta, R.K. **2009.** Magnetic resonance imaging in central nervous system tuberculosis. *Indian Journal of Radiology and Imaging,* **19(4):** 256-265.

Tsai, M.C., Chakravarty, S., Zhu, G., Xu, J., Tanaka, K., Koch, C., Tufariello, J., Flynn, J. and Chan, J. **2006.** Characterization of the tuberculous granuloma in murine and human lungs: cellular composition and relative tissue oxygen tension. *Cellular Microbiology,* **8(2):** 218-232.

Tsenova, L., Bergtold, A., Freedman, V.H., Young, R.A. and Kaplan, G. **1999.** Tumor necrosis factor alpha is a determinant of pathogenesis and disease progression in mycobacterial infection in the central nervous system. *Proceedings of the National Academy of Sciences,* **96:** 5657-5662.

Tsenova, L., Ellison, E., Harbacheuski, R., Moreira, A.L., Kurepina, N., Reed, M.B., Mathema, B.M., Barry III, C.E. and Kaplan, G. **2005.** Virulence of Selected Mycobacterium tuberculosis Clinical Isolates in the Rabbit Model of Meningitis Is Dependent on Phenolic Glycolipid Produced by the Bacilli. *The Journal of Infectious Diseases,* **192:** 98-106.

Tsenova, L., Sokol, K., Freedman, V.H. and Kaplan, G. **1998.** A combination of thalidomide plus antibiotics protects rabbits from mycobacterial meningitis-associated death. *The Journal of Infectious Diseases,* **177:** 1563-1572.

Tsolaki, A.G, Nagy, J., Leiva, S., Kishore, U., Rosenkrands, I. and Robertson, B.D. **2013.** Mycobacterium tuberculosis antigen 85B and ESAT-6 expressed as a recombinant fusion protein in Mycobacterium smegmatiselicits cell-mediated immune response in a murine vaccination model. *Molecular Immunology,* **54(3-4):** 278-283.

Ulrichs, T., Kosmiadi ,G.A., Trusov, V., Jörg, S., Pradl, L., Titukhina, M., Mishenko, V., Gushina, N., Kaufmann, S.H. **2004.** Human tuberculous granulomas induce peripheral lymphoid follicle-like structures to orchestrate local host defence in the lung. *Journal of Pathology,* **204:** 217-228.

Valway, S.E., Sanchez, M.P., Shinnick, T.F., Orme, I., Agerton, T., Hoy, D., Jones, J.S., Westmoreland, H. and Onorato, I.M. **1998.** An outbreak involving extensive transmission of a virulent strain of Mycobacterium tuberculosis. *New England Journal of Medicine,* **338:** 633-639.

Van Der Voorn, P., Tekstra, J., Beelen, R.H., Tensen, C.P., Van Der Valk, P. and De Groot, C.J. **1999.** Expression of MCP-1 by reactive astrocytes in demyelinating multiple sclerosis lesions. *American Journal of Pathology,* **154:** 45-51.

Van Lettow, M., Kumwenda, J.J., Harries, A.D., Whalen, C.C., Taha, T.E., Kumwenda, N., Kang'ombe, C. and Semba, R.D. **2004.** Malnutrition and the severity of lung disease in adults with pulmonary tuberculosis in Malawi. *International Journal of Tuberculosis and Lung Disease,* **8(2):** 211-217.

van Well, G.T.J., Paes, B.F., Terwee, C.B., Springer, P., Roord, J.J., Donald, P.R., van Furth, A.M. and Schoeman, J. **2009.** Twenty Years of Pediatric Tuberculous Meningitis: A Retrospective Cohort Study in the Western Cape of South Africa. *Pediatrics,* **123(1):** e1-e8.

van Well, G.T.J., Wieland, C.W., Florquin, S., Roord, J.J., der Poll, T. and van Furth, A.M. **2007.** A New Murine Model to Study the Pathogenesis of Tuberculous Meningitis. *The Journal of Infectious Diseases,* **195(5):** 694-697.

Varela, L.M. and Ip, M.M. **1996.** Tumor necrosis factor-alpha: a multifunctional regulator of mammary gland development. *Endocrinology,* **137:** 4915-4924.

Varfolomeev, E. E. and Ashkenazi. A. **2004.** Tumor necrosis factor: an apoptosis JuNKie? *Cell,* **116:** 491-497.

Vascotto, F., Le Roux, D., Lankar, D., Faure-Andre, G., Vargas, P., Guermonprez, P. and Lennon-Dumenil, A.M. **2007.** Antigen presentation by B lymphocytes: how receptor signaling directs membrane trafficking. *Current Opinion in Immunology*, **19:** 93-98.

Velasco-Velázqueza, M. A., Barrerab, D., González-Arenasb, A., Rosalesc, C. and Agramonte-Hevia. J. **2003.** Macrophage-Mycobacterium tuberculosis interactions: role of complement receptor 3. *Microbial Pathogenesis,* **35:** 125-131.

Vezzani, A., Moneta, D., Richichi, C., Aliprandi, M., Burrows, S.J., Ravizza, T., Perego, C. and De Simoni, M.G. **2002.** Functional role of inflammatory cytokines and antiinflammatory molecules in seizures and epileptogenesis. *Epilepsia,* **43:** 30-35.

Vinnard, C. and Macgregor, R.R. **2009.** Tuberculosis meningitis in HIV infected individuals. *Current HIV/AIDS Rep,* **6(3):** 139-145.

Voziyanov, Y., Pathania, S. and Jayaram, M. **1999.** A general model for sitespecific recombination by the integrase family recombinases. *Nucleic Acids Research,* **27:** 930-941.

Wajant, H., Pfizenmaier, K. and Scheurich, P. **2003.** Tumor necrosis factor signaling. *Cell Death and Differentiation,* **10(1):** 45-65.

Wallach, D., Varfolomeev, E.E., Malinin, N.L., Goltsev, Y.V., Kovalenko, A.V. and Boldin, M.P. **1999.** Tumor necrosis factor receptor and Fas signaling mechanisms. *Annual Review of Immunology,* **17:** 331-367.

Wang, Y., Wu, T.R., Cai, S., Welte, T. and Chin, Y.E. **2000.** Stat1 as a Component of Tumor Necrosis Factor Alpha Receptor 1-TRADD Signaling Complex To Inhibit NF-κB Activation. *Molecular and Cellular Biology,* **20(13):** 4505-4512.

Ware, C.F., Vanarsdale, T.L., Crowe, P.D. and Browning, J.L. **1995.** The ligands and receptors of the lymphotoxin system. *Current Topics in Microbiology and Immunology,* **198:** 175-218.

Ware, C.F., Crowe, P.D., Grayson, M.H., Androlewicz, M.J. and Browning, J.L. **1992.** Expression of surface lymphotoxin and tumor necrosis factor on activated T, B, and natural killer cells. *The Journal Immunology,* **149(12):** 3881-388.

Watanabe, E., Buchman, T.G., Hirasawa, H., Zehnbauer, B.A. **2010.** Association between lymphotoxin-alpha (tumor necrosis factor-beta) intron polymorphism and predisposition to severe sepsis is modified by gender and age. *Critical Care Medicine,* **38(1):** 181-193.

Weekkrdenburg, E.M., Peters, P.J. and van der Wel, N.N. **2009.** How do mycobacteria activate CD8+ T cells? *Trends in Microbiology,* **18(1):** 1-9.

Weiergräber, M., Henrya, M., Hescheler, J., Smyth, N. and Schneider, T. **2005.** Electrocorticographic and deep intracerebral EEG recording in mice using a telemetry system. *Brain Research Protocols,* **14(2005):** 154-164.

Weisman, M.H. **2002.** What are the risks of biologic therapy in rheumatoid arthritis? An update on safety. *Journal of Rheumatology,* **Suppl 65:** 33-38.

Wells, C.D, Cegielski, J.P., Nelson, L.J., Laserson, K.F., Holtz, T.H., Finlay, A., Castro, K.G. and Weyer, K. **2007.** HIV infection and multidrug-resistant tuberculosis—The perfect storm. *Journal of Infectious Diseases,* **196(1):** S86-S107.

Welser-Alves, J.V. and Milner, R. **2013.** Microglia are the major source of TNF-α and TGF-β1 in postnatal glial cultures; regulation by cytokines, lipopolysaccharide, and vitronectin. *Neurochemistry International,* **63(1):** 47-53.

Wenner, C.A., Güler, M.L., Macatonia, S.E., O'Garra, A. and Murphy, K.M. **1996.** Roles of IFN-γ and IFN-α in IL-12-induced T helper cell-1 development. *The Journal of Immunology,* **156:** 1442-1447.

Wiggley, S.C. **1991.** Tuberculosis in Papua New Guinea. In: Proust, A.J. History of tuberculosis in Australia, New Zealand and Papua New Guinea. (ed). Canberra: Brogla, 103-118.

Wildenberg, M.E., Welzen-Coppens J.M.C., van Helden-Meeuwsen C.G., Bootsma, H., Vissink, A., van Rooijen, N., van de Merwe, J.P., Drexhage, H.A. and Versnel, M.A. **2009.** Increased frequency of $CD16^{+}$ monocytes and the presence of activated dendritic cells in salivary glands in primary Sjögren syndrome. *Annals of the Rheumatic Diseases,* **68:** 420-426.

Wilson, E.H., Weninger, W. and Hunter, C.A. **2010.** Trafficking of immune cells in the central nervous system. *The Journal of Clinical Investigation,* **120(5):** 1368-1379.

Wolf, A.J., Desvignes, L., Linas, B., Banaiee, N., Tamura, T., Takatsu, K. and Ernst, J.D. **2008.** Initiation of the adaptive immune response to Mycobacterium tuberculosis depends on antigen production in the local lymph node, not the lungs. *Journal of Experimental Medicine,* **205(1):** 105-115.

Wolf, A.J., Linas, B., Trevejo-Nuñez, G.J., Kincaid, E., Tamura, T., Takatsum, K. and Ernst, J.D. **2007.** *Mycobacterium tuberculosis* Infects Dendritic Cells with High Frequency and Impairs Their Function In Vivo. *The Journal of Immunology,* **179:** 2509-2519.

Wollebo, H.S., Safak, M., Del Valle, L., Khalili, K. and White, M.K. **2011.** Role for tumor necrosis factor-α in JC virus reactivation and progressive multifocal leukoencephalopathy. *Journal of Neuroimmunology,* **233(1-2):** 46-53.

Woodworth, J. and Behar, S.M. **2006.** Mycobacterium tuberculosis specific CD8+ T cells and their role in immunity. *Critical Review in Immunology,* **26:** 317-352.

World Health Organization. **2009.** Global tuberculosis control: surveillance, planning and financing, WHO/HTM/TB/2009.411, WHO, Geneva, Switzerland.

World Health Organization. **2009.** Global tuberculosis control, WHO/HTM/TB/2009.411. Geneva: World Health Organization.

World Health Organization. Global Tuberculosis Control: WHO Report **2010.** Geneva: WHO, 2010. Available from: http://whqlibdoc. who.int/publications/ 2010/9789241564069_eng.pdf.

World Health Organization. Global tuberculosis report 2012. Geneva: WHO, **2012.** Available from: http://whqlibdoc. http://www.who.int/tb/publications/global_report/en/index.html.

World Health Organization. WHO Report **2011:** Global Tuberculosis Control. World Health Organization.website:http://www.who.int/tb/publications/global_report/2011/gtbr11_ main.pdf. Accessed February 06, 2014.

Wright, A., Zignol, M., Van Deun, A., Falzon, D., Gerdes, S.R., Feldman, K., Hoffner, S., Drobniewski, F., Barrera, L., van Soolingen, D., Boulabhal, F., Paramasivan, C.N., Kam, K.M., Mitarai, S., Nunn, P., Raviglione, M and Global project on anti-tuberculosis drug resistance surveillance. **2009.** Epidemiology of antituberculosis drug resistance 2002-07: an updated analysis of the global project on anti-tuberculosis drug resistance surveillance. *Lancet,* **373(9678):** 1861-1873.

Xia, M.Q., Qin, S.X., Wu, L.J., Mackay, C.R. and Hyman, B.T. **1998.** Immunohistochemical study of the beta-chemokine receptors CCR3 and CCR5 and their ligands in normal and Alzheimer's disease brains. *American Journal of Pathology,* **153(1):** 31-37.

Xin, G., Su, Y., Gao, Y.L., Zhang, H., Wang, G.F. and Li, K.S. **2011.** Lipopolysaccharide enhances asymmetrical production of cytokines and nitric oxide by left and right cerebral cortical microglial cells in BALB/C mice. *Cell Biochemistry & Function,* **29(1):** 50-54.

Yahagi, A., Umemura, M., Tamura, T., Kariyone, A., Begum, M.D., Kawakami, K., Okamoto, Y., Hamada, S., Oshiro, K., Kohama, H., Arakawa, T., Ohara, N., Takatsu, K. and Matsuzaki, G. **2010.** Suppressed induction of mycobacterial antigenspecific Th1-type $CD4^+$ T cells in the lung after pulmonary mycobacterial infection. *International Immunology,* **22(4):** 307-318.

Yamada, K., Takane, N., Otabe, S., Inada, C., Inoue, M. and Nonaka, K. **1993.** Pancreatic p-Cell-Selective Production of Tumor Necrosis Factor-cx Induced by Interleukin-1. *Diabetes,* **42:** 1026-1031.

Young, J.M., Adetifa, I.M.O., Ota, M.O.C. and Sutherland, J.S. **2010.** Expanded polyfunctional T cell response to mycobacterial antigens in TB disease and contraction post-treatment. *PLoS ONE,* **5(6):** 1-7.

Yu, X. and Xie, J. **2012.** Roles and underlying mechanisms of ESAT-6 in the context of Mycobacterium tuberculosis–host interaction from a systems biology perspective. *Cellular Signalling,* **24(9):** 1841-1846.

Yuan, Z., Wang, R., Lee, Y., Chen, C.Y., Yu, X., Wu, Z., Huang, D., Shen, L. and Chen, Z.W. **2009.** Tuberculosis-induced variant IL-4 mRNA encodes a cytokine functioning as growth factor for (E)-4-hydroxy-3-methyl-but-2-enyl pyrophosphate-specific Vγ2Vδ2 T cells1. *The Journal of Immunology,* **182:** 811-819.

Zevallos, K., Vergara, K.C., Vergara, A., Vidal, C., Garcia, H.H. and Evans, C.A. **2010.** Tuberculin skin-test reactions are unaffected by the severity of hyperendemic intestinal helminth Infections and co-infections. *American Journal of Tropical Medicine and Hygiene,* **83(2):** 319-325.

Zhang, B., Patel, J., Croyle, M., Diamonda, M.S. and Klein, R.S. **2010.** TNF-α-dependent regulation of CXCR3 expression modulates neuronal survival during West Nile virus encephalitis. *Journal of Neuroimmunology,* **224:** 28-38.

Zhang, D.W., Shao, J., Lin, J., Zhang, N., Lu, B.-L., Lin, S.-C., Dong, M.-Q. and Han, J. **2009.** RIP3, an energy metabolism regulator that switches TNF-induced cell death from apoptosis to necrosis. *Science,* **325:** 332-336.

Zhang, Y., Chen, C., Liu, J., Deng, H., Pan, A., Zhang, L., Zhao, X., Huang, M., Lu, B., Dong, H., Du, P., Chen, W. and Wan, K. **2011.** Complete Genome Sequences of *Mycobacterium tuberculosis* Strains CCDC5079 and CCDC5080, Which Belong to the Beijing Family. *Journal of Bacteriology,* **193(19):** 5591-5592.

Zheng, B., Sage, M., Sheppeard, E.A., Jurecic, V. and Bradley, A. **2000.** Engineering Mouse Chromosomes with Cre-loxP: Range, Efficiency, and Somatic Applications. *Molecular and Cellular Biology,* 648-655.

Zhou, L.J. and Tedder, T.F. **1995.** A distinct pattern of cytokine gene expression by human $CD83^+$ blood dendritic cells. *Blood,* **86(9):** 3295-3301.

Zhu, Y., Romero, M.I., Ghosh, P., Ye, Z., Charnay, P., Rushing, E.J., Marth, J.D. and Parada, L.F. **2001.** Ablation of NF1 function in neurons induces abnormal development of cerebral cortex and reactive gliosis in the brain. *Genes Development,* **15(7):** 859-876.

Zucchi, F.C., Pelegrini-da-Silva, A., Neder, L., Silva, C.L., Tsanaclis, A.M.C. and Takayanagui, O.M. **2012.** The contribution of a murine CNS-TB model for the understanding of the host-pathogen interactions in the formation of granulomas. *Journal of Neuroscience Methods,* **206(1):** 88-93.

Zucker-Franklin, D., Warfel, A., Grusky, G., Frangione, B. and Teitel, D. **1987.** Novel monocyte-like properties of microglial/astroglial cells. Constitutive secretion of lysozyme and cystatin-C. *Laboratory Investigation,* **57:** 176-185.

Zumla, A., Raviglione, M., Hafner, R. and von Reyn, C.F. **2013.** Tuberculosis. *The New England Journal of Medicine,* **368:** 745-755.

APPENDICES

APPENDIX A

Polymerase Chain Reaction (PCR) reagents

1. **1000 mM Tris-HCl (Stock solution):**

15.76g was dissolved in 100ml of distilled H_2O (pH 8) and then autoclaved at 121°C for 30 minutes. The solution was thereafter filtered through a 0.45µm filter (Millipore Corporation, Bedford, USA) and stored at room temperature.

2. **500 mM EDTA (Stock solution):**

18.612g was dissolved in 100ml of distilled H_2O (pH8) and then autoclaved at 121°C for 30 minutes. The solution was thereafter filtered through a 0.45µm filter (Millipore Corporation, Bedford, USA) and stored at room temperature.

3. **6000 mM NaCl (Stock solution):**

35.064g was dissolved in 100ml of distilled H_2O and then autoclaved at 121°C for 30 minutes. The solution was thereafter filtered through a 0.45µm filter (Millipore Corporation, Bedford, USA) and stored at room temperature.

4. **10% SDS (Stock solution):**

10g was dissolved in 100ml of distilled H_2O and then autoclaved at 121°C for 30 minutes. The solution was thereafter filtered through a 0.45µm filter (Millipore Corporation, Bedford, USA) and stored at room temperature.

5. **10x TBE (Running buffer):**

108g Tris Base

55g Boric acid

40 ml of 500mM EDTA was dissolved in 1 liter distilled H_2O and autoclaved for 30 minutes at 121°C. The solution was stored at room temperature.

6. Tissue (Tail biopsies) lysis buffer:

50mM Tris-HCl, pH8
100mM EDTA, pH 8
100mM NaCl,
1% SDS and
0.5mg/ml Proteinase K (Roche, Germany) was made up to the required volume with distilled H_2O.

7. 6x Gel Loading Buffer:

0.25% Bromophenol blue
0.25% Xylene cyanol and
50% Glucose was dissolved in 100 ml distilled H_2O and autoclaved for 30 minutes at 121°C. The solution was stored at room temperature.

8. 6x Agarose Gel:

1.5g Agarose (1.5%) and
100ml 0.5 x TBE was boiled in microwave then cooled slightly and 450ng/ml ethidium bromide was added.

APPENDIX B

Bacteriological reagents

1. Difco Middlebrook 7H10 Agar (M7H10):

19g M7H10 agar
5ml glycerol was made up to 900ml with distilled H_2O and autoclaved at 121°C for 10 minutes. The solution was allowed to cool to 55°C and 100ml of oleic acid albumin dextrose catalase (OADC) was added. An agar solution of 7ml was pipetted and poured per side in sterile duplicate petridishes (Sterilin). And allowed to set, the plates were sealed with a platic bag and stored inverted at 4°C.

2. 0.9% Saline solution:

0.9g NaCl was dissolved in 100ml of distilled H_2O and then autoclaved at 121°C for 30 minutes. The solution was stored at room temperature. The solution was thereafter filtered through a 0.45µm filter (Millipore Corporation, Bedford, USA) and stored at room temperature.

APPENDIX C

Anaesthetic reagents

1. Lethal anaesthetic:

500µl Xylazine and 2ml Ketamine were added to 9 ml of 0.9% of saline solution. The solution was filtered through a 0.45µm filter (Millipore Corporation, Bedford, USA) and was prepared daily.

2. General anaesthetic:

0.66 ml of Ketamine (100 mg/ml) (Bayer Pty Ltd, Germany) and 0.22 ml of Xylazine (20mg/ml) (Intervet, Zurich, Switzerland) were added in 9.13 ml of sterile isotonic saline (0.9%). The solution was filtered through a 0.45µm filter (Millipore Corporation, Bedford, USA) and was prepared daily.

APPENDIX D

Histology reagents

1. Mayers haemotoxylin:

1g Haemotoxylin 50g,
Ammonium alum (Aluminium ammonium sulphate)
or potassium alum (Aluminium potassium sulphate) were first dissolved, then after
0.2g Sodium iodate
1g Citric acid
50g Chloral hydrate we added in H_2O. Filter through Whatmann filter paper no 1 and the solution was stored at room temperature.

2. **Eosin:**

150ml of 1% Eosin in distilled H_2O (2 parts)
75ml of 1% Phloxine in distilled H_2O (1 part) in
225ml distilled H_2O. One drop formalin or thymol was added to the 1% eosin for preservation. Filter through Whatmann filter paper no. 1 and the solution was stored at room temperature.

3. **Carbol fuchsin:**

10ml of 6% Basic fuchsin in absolute alcohol and 90ml of 5% carbolic acid, the solution was filtered through Whatmann filter paper no.1 and stored at room temperature.

4. **Buffered formalin (Tissues fixative):**

100ml formaldehyde (40% w/v formaldehyde solution) in 900ml 1x PBS (pH 7.4). The solution was stored at room temperature.

5. **Loeffers' Methylene blue:**

1ml of 1% KOH was added to
99ml distilled H_2O and
3ml of 0.8% Methylene blue (in absolute alcohol) was thereafter added. The solution was filtered through Whatmann filter paper no.1 and stored at room temperature.

APPENDIX E

Fluorescent activated cell sorting (FACS) reagents

1. **10% NaN_3 (Sodium Azide):**

10g NaN_3 was dissolved in 100ml of distilled H_2O. The solution was filtered through a 0.45µm millipore filter (Millipore Corporation, Bedford,USA) and stored at 4°C.

2. **FACS buffer:**

0.1% BSA and 0.01% NaN_3 were added in 1 x PBS (pH 7.4). The solution was sterilised with a 0.45µm millipore filter (Millipore Corporation, Bedford, USA) and stored at 4°C.

3. FACS blocking solution:

0.9375µl αFcyRIII (CD32/CD16c)
3.75µl Normal rat serum (heat inactivated)
3.75µl Normal mouse serum (heat inactivated) were diluted in
141.56µl of FACS buffer.

4. Fixation buffer:

2% paraformaldehyde (PFA) in 1 x PBS
4g NaOH was dissolved in 100ml distilled H_2O.
20g PFA and 600ml 1 x PBS was then added. The pH was adjusted to pH 7.2 with concentrated HCl and the volume adjusted to 1000ml. The solution was sterilised through a 0.45µm millipore filter (Millipore Corporation, Bedford, USA). The bottle was covered with aluminum foil and stored at 4°C.

5. Permeabilisation buffer containing saponin:

0.1% Saponin
1mM $CaCl_2$
1mM $MgSO_4$ and
10mM HEPES were dissolved in 1x PBS containing 0.05% NaN_3 and 0.1% BSA. The solution was sterilised through a 0.45µm filter (Millipore Corporation, Bedford, USA) and stored at 4°C.

APPENDIX F

General reagents

1. 10 x Phosphate-Buffered Saline (PBS):

80g NaCl (1.37 M),
2.4g KH_2PO4
2g KCl (0.03M) and
14.4g Na_2HPO_4 $2H_2O$ were dissolved in 900ml distilled H_2O. The pH adjusted to 7.4 and the solution made up to 1 liter with distilled H_2O. The solution was sterilised through a 0.45µm millipore filter (Millipore Corporation, Bedford, USA) and stored at room temperature.

2. Homogenising buffer:

0.9% NaCl
0.04% Tween 80 was dissolved in distilled H_2O and autoclaved for 30 minutes at 121°C. The solution was stored at room temperature.

3. Saline solution (0.9%):

0.9g of NaCl was dissolved in 100ml of distilled H_2O. The solution was autoclaved for 30 minutes at 121°C and stored at room temperature.

APPENDIX G

Enzyme-linked Immunosorbent Assay (ELISA) reagents as per manufacturer (R&D) recommandation

1. Coating buffer:

0.2g NaN_3 was dissolved in 800ml 1 x PBS. The pH was adjusted to 7.4 and the solution made up to 1 liter. The solution was sterilised through a 0.45µm millipore filter and stored at 4°C.

2. Sodium azide (NaN_3) 10%:

10g NaN_3 was dissolved in 100ml of distilled H_2O. The solution was sterilised through a 0.45µm millipore filter and stored at 4°C.

3. Dilution buffer:

10g (1%) BSA (Roche, Germany)was dissolved in 1 x PBS (pH 7.4) and made up to 1 liter, The solution was sterilised through a 0.45µm millipore filter (Millipore Corporation, Bedford, USA) and stored at 4°C.

4. Blocking buffer:

1% BSA (Roche, Germany)
5% Sucrose and
0.05% NaN_3 was dissolved in 1 x PBS. The pH was adjusted to 7.4 and the solution made up to

1 liter. The solution was sterilised through a 0.45µm millipore filter (Millipore Corporation, Bedford, USA) and stored at 4°C.

5. 10 x Washing buffer:

0.5% Tween 20 in 10x PBS, pH 7.4

6. Substrate buffer:

0.2g NaN_3,
97ml Di-ethanolamine (liquefy in 37°C water-bath), and 0.8g $MgCl_26H_2O$ were dissolved in 700ml distilled H_2O. The pH was adjusted to 9.8 and the volume was made up to 1 liter with distilled H_2O. The solution was sterilised through a 0.45µm millipore filter (Millipore Corporation, Bedford, USA) and stored at 4°C.

APPENDIX H

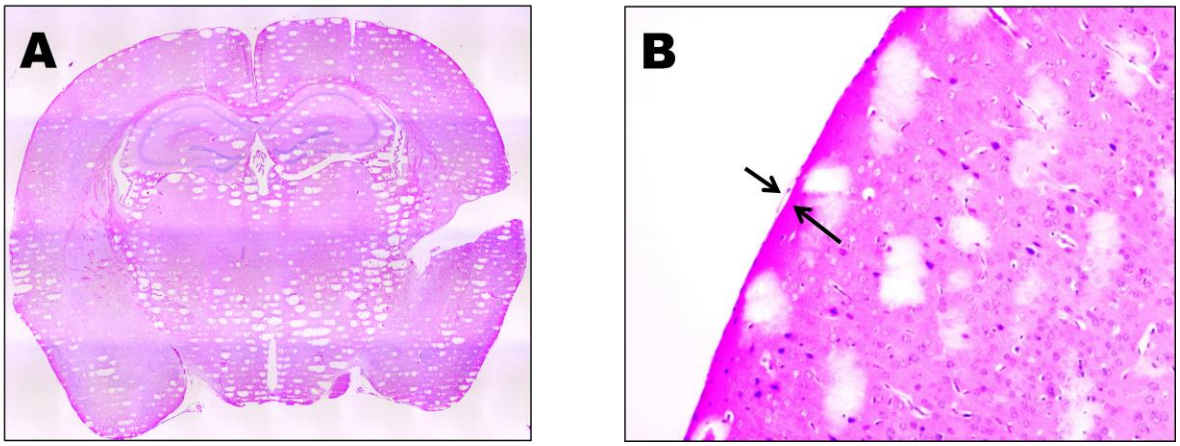

Figure A1: Representative of hematoxylin-eosin-stained section of murine brain after 3 weeks post saline injection. $TNF^{f/f}$, $NsTNF^{-/-}$, $M\text{-}TNF^{-/-}$, $MT\text{-}TNF^{-/-}$ and $TNF^{-/-}$ mice were intracerebrally injected with 3µl of saline at each time point of experimental infection. The results (*n*= 5 mice/group) represent one of three similar experiments. Morphology of 2µm brain sections (magnification= 40x) (A), and meningeal lymphocytic infiltration (magnification= 100x), arrows indicate no meningeal lymphocytic infiltration (B).

APPENDIX I

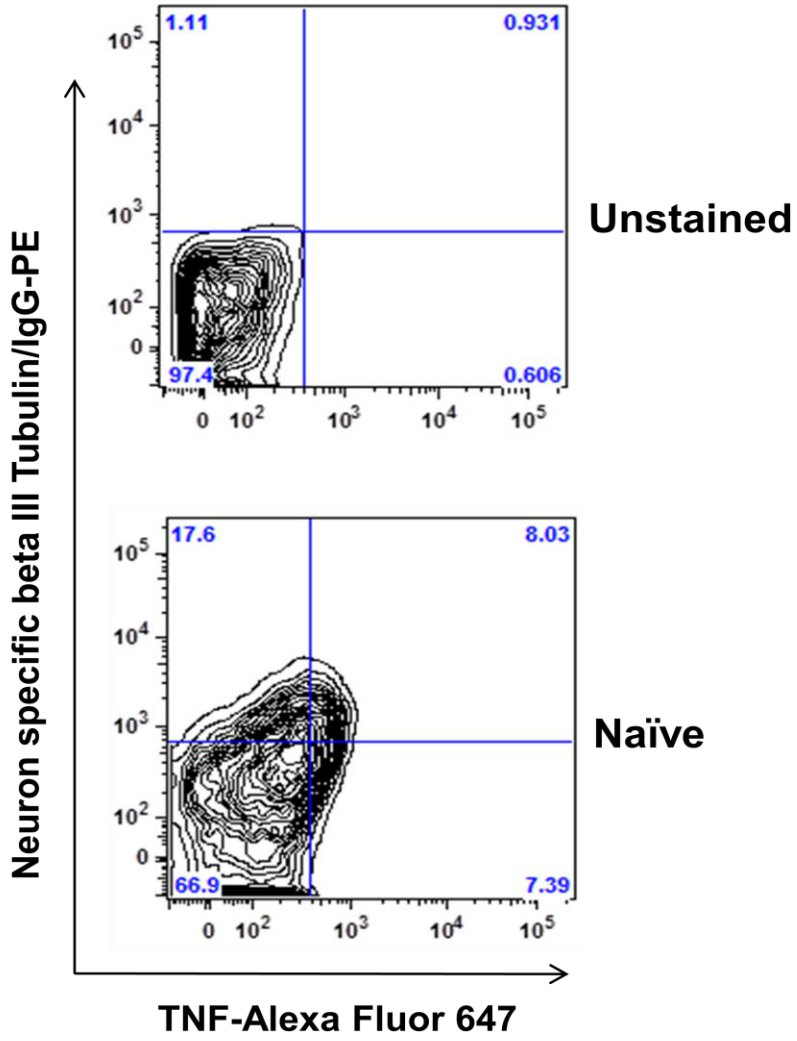

Figure A2: Representative of TNF expression in naïve neurons following intracerebal stimulation with LPS: Representative FACS plots of Beta III Tubulin/IgG-PE versus TNF-Alexa Fluor 647; numbers represent the percentage of gated cells. The data represent one of at least three experiments with similar results (*n*= 5 mice/group). Unstained (top) and naïve (bottom). Naïve = unifected mice.